VIRGINIA COMMONWEALTH UNIVERSITY

Virginia Commonwealth University
VCU Scholars Compass

Theses and Dissertations | Graduate School

2009

Automated Methods for Fiber Diameter Measurement of Fibrous Scaffolds

Anna Bulysheva
Virginia Commonwealth University

Follow this and additional works at: http://scholarscompass.vcu.edu/etd

Part of the Biomedical Engineering and Bioengineering Commons

© The Author

Downloaded from
http://scholarscompass.vcu.edu/etd/1996

This Thesis is brought to you for free and open access by the Graduate School at VCU Scholars Compass. It has been accepted for inclusion in Theses and Dissertations by an authorized administrator of VCU Scholars Compass. For more information, please contact libcompass@vcu.edu.

School of Engineering
Virginia Commonwealth University

This is to certify that the thesis prepared by Anna Alexandra Bulysheva entitled AUTOMATED METHODS FOR FIBER DIAMETER MEASUREMENT OF FIBROUS SCAFFOLDS has been approved by her committee as satisfactory completion of the thesis requirement for the degree of Master of Science in Biomedical Engineering

Gary L. Bowlin, Ph.D., School of Engineering

Gary Tepper, Ph.D., Chair of Mechanical Engineering, School of Engineering

Gerald E. Miller, Ph.D., Chair of Biomedical Engineering, School of Engineering

Rosalyn Hobson, Ph.D., Associate Dean of Graduate Studies

Russell D. Jamison, Ph.D., Dean, School of Engineering

F. Douglas Boudinot, Ph.D., Dean of the Graduate School

December 10, 2009
Date

© Anna Alexandra Bulysheva 2009

All Rights Reserved

AUTOMATED METHODS FOR FIBER DIAMETER MEASUREMENT OF FIBROUS SCAFFOLDS

A thesis submitted in partial fulfillment of the requirements for the degree of Master of Science in Biomedical Engineering at Virginia Commonwealth University.

by

ANNA ALEXANDRA BULYSHEVA
B.S., University of North Carolina at Chapel Hill, 2006

Director: GARY L. BOWLIN, PH.D
PROFESSOR, BIOMEDICAL ENGINEERING

Virginia Commonwealth University
Richmond, Virginia
December 2009

Acknowledgements

I would like to thank the many people who have helped me advance through this laborious process. Although at times it was a lonely road, I could not have accomplished this without the support and advice from my family, advisor, friends, and lab-mates.

I am dedicating this work to my parents, Drs. Larissa and Alexander Bulyshev as a tribute to your unconditional guidance, love and support. I would not be here today; if it was not for the many daily sacrifices that you have made on my behalf. I cannot thank you enough for a life and education that you have made possible. Your faith in my abilities has made me strive to achieve more than I thought possible. Thank you.

I would like to thank my advisor, Dr. Gary Bowlin for providing the motivation to initiate and complete this work.

My lab-mates have started out as guides and many became close friends in the process. Thank you for providing support with kind words and technical advice. I especially would like to thank Koyal Garg and Yas Maghdouri, for the many stimulating and insightful end-of-the-day discussions that have brought joy and laughter during the good and better grad-school days.

To all who are not mentioned by name, you have brought me closer to this day in small and large ways, which are all remembered and highly valued.

Table of Contents

Page

Acknowledgements ii

Table of Contents iii

List of Tables vi

List of Figures viii

List of Abbreviations xvii

Introduction 1

Project Synopsis 3

Background Information 5

Fibrous ECM Analogues in Tissue Engineering 5

Manual Method for Fiber Diameter Measurement 8

Automated Method for Fiber Diameter Measurement 9

Edge Detection Methods in Image Processing 11

Hough Transform 12

Materials and Methods 14

Test Images 14

Human Data 15

Overview of Automated Fiber Diameter Measurements 16

Skeleton Slopes Fiber Diameter Measurement 17

Canny Slopes Fiber Diameter Measurement 18

Canny Hough Fiber Diameter Measurement 19

Custom Canny Slopes Fiber Diameter Measurement 20

Custom Canny Hough Fiber Diameter Measurement 21

Statistical Analysis 22

Results and Discussion **37**
Overview 37
Manual Method Results 37
Skeleton Slopes Fiber Diameter Measurement Results 39
Canny Slopes Fiber Diameter Measurement Results 40
Canny Hough Fiber Diameter Measurement Results 40
Custom Canny Slopes Fiber Diameter Measurement Results 41
Custom Canny Hough Fiber Diameter Measurement Results 42
Conclusion **76**

Literature Cited 78

APPENDIX A: Statistical Analysis 80

ANOVA Tables for all data sets per image for all test images 80
Tukey-Kramer Multiple comparison of Means for all ANOVA tables 84

APPENDIX B: Resulting Images for Skeleton Slopes Method 95

CSkS edges superimposed over the narrow distribution simulated images. 95
CSkS edges superimposed over the wide distribution simulated images 99
CSkS edges superimposed over real SEM images 103

APPENDIX C: Resulting Images for Canny Slopes Method 108

DCS edges superimposed over the narrow distribution simulated images 108
DCS edges superimposed over the wide distribution simulated images 112
DCS edges superimposed over real SEM images 116
APPENDIX D: Resulting Images for Canny Hough Method 121

DCH edges superimposed over the narrow distribution simulated images 121

DCH edges superimposed over the wide distribution simulated images ... 125
DCH edges superimposed over real SEM images ... 129

APPENDIX E: Resulting Images for Custom Canny Slopes Method ... 134

CCS edges superimposed over the narrow distribution simulated images 134
CCS edges superimposed over the wide distribution simulated images ... 138
CCS edges superimposed over real SEM images ... 142

APPENDIX F: Resulting Images for Custom Canny Hough Method ... 147

CCH edges superimposed over the narrow distribution simulated images 147
CCH edges superimposed over the wide distribution simulated images ... 152
CCH edges superimposed over real SEM images ... 156

VITA ... 160

List of Tables

Page

Table 1 Multiple comparison of means for narrow distribution test images 73

Table 2 Multiple comparison of mean for wide distribution test images 74

Table 3 Multiple comparison of the means for real SEM images.....75

Table 4 ANOVA Table for narrow10 80

Table 5 ANOVA Table for narrow15 80

Table 6 ANOVA Table for narrow20 80

Table 7 ANOVA Table for narrow25 80

Table 8 ANOVA Table for narrow30 81

Table 9 ANOVA Table for narrow35 81

Table 10 ANOVA Table for wide10.....81

Table 11 ANOVA Table for wide15.....81

Table 12 ANOVA Table for wide20.....81

Table 13 ANOVA Table for wide25.....82

Table 14 ANOVA Table for wide30.....82

Table 15 ANOVA Table for wide35.....82

Table 16 ANOVA Table for SEM1 82

Table 17 ANOVA Table for SEM2 82

Table 18 ANOVA Table for SEM3 83

Table 19 ANOVA Table for SEM4 83

Table 20 ANOVA Table for SEM5 83

Table 21 ANOVA Table for SEM6 83

Table 22 ANOVA Table for SEM7 83

Table 23 ANOVA Table for SEM8 84

List of Figures

Page

Figure 1 Sequence of image processing steps of the Ziabari method 10

Figure 2 Image neighborhood representation 11

Figure 3 Algorithm used for generating test images 23

Figure 4 Test images with wide distribution of fiber diameters 24

Figure 5 Test images with narrow distribution of fiber diameters 25

Figure 6 SEM images of real electrospun webs used in this study 26

Figure 7 Skeleton Slopes Fiber Diameter Measurement Algorithm 27

Figure 8 Image processing steps of the Skeleton Slopes fiber diameter measurement method 28

Figure 9 Canny Slopes Fiber Diameter Measurement Algorithm 29

Figure 10 Image processing steps of the Canny Slopes fiber diameter measurement method 30

Figure 11 Canny Hough Fiber Diameter Measurement Algorithm 31

Figure 12 Image processing steps of the Canny Hough fiber diameter measurement method 32

Figure 13 Custom Canny Slopes Fiber Diameter Measurement Algorithm 33

Figure 14 Image processing steps of the Custom Canny Slopes fiber diameter measurement method 34

Figure 15 Custom Canny Hough Fiber Diameter Measurement Algorithm 35

Figure 16 Image processing steps of the Custom Canny Hough fiber diameter measurement method 36
Figure 17 Average fiber diameters for narrow10....43
Figure 18 Average fiber diameters for narrow15....43
Figure 19 Average fiber diameters for narrow20....44
Figure 20 Average fiber diameters for narrow25....44
Figure 21 Average fiber diameters for narrow30....45
Figure 22 Average fiber diameters for narrow35....45
Figure 23 Average fiber diameters for wide10....46
Figure 24 Average fiber diameters for wide15....46
Figure 25 Average fiber diameters for wide20....47
Figure 26 Average fiber diameters for wide25....47
Figure 27 Average fiber diameters for wide30....48
Figure 28 Average fiber diameters for wide35....48
Figure 29 Average fiber diameters for SEM1....49
Figure 30 Average fiber diameters for SEM2....49
Figure 31 Average fiber diameters for SEM3....50
Figure 32 Average fiber diameters for SEM4....50
Figure 33 Average fiber diameters for SEM5....51
Figure 34 Average fiber diameters for SEM6....51
Figure 35 Average fiber diameters for SEM7....52
Figure 36 Average fiber diameters for SEM8....52

Figure 37 Histograms for all fiber diameter measurements of image narrow10 53

Figure 38 Histograms for all fiber diameter measurements of image narrow15 54

Figure 39 Histograms for all fiber diameter measurements of image narrow20 55

Figure 40 Histograms for all fiber diameter measurements of image narrow25 56

Figure 41 Histograms for all fiber diameter measurements of image narrow30 57

Figure 42 Histograms for all fiber diameter measurements of image narro35 58

Figure 43 Histograms for all fiber diameter measurements of image wide10.....59

Figure 44 Histograms for all fiber diameter measurements of image wide15.....60

Figure 45 Histograms for all fiber diameter measurements of image wide20.....61

Figure 46 Histograms for all fiber diameter measurements of image wide25.....62

Figure 47 Histograms for all fiber diameter measurements of image wide30.....63

Figure 48 Histograms for all fiber diameter measurements of image wide35.....64

Figure 49 Histograms for all fiber diameter measurements of image SEM1 65

Figure 50 Histograms for all fiber diameter measurements of image SEM2 66

Figure 51 Histograms for all fiber diameter measurements of image SEM3 67

Figure 52 Histograms for all fiber diameter measurements of image SEM4 68

Figure 53 Histograms for all fiber diameter measurements of image SEM5 69

Figure 54 Histograms for all fiber diameter measurements of image SEM6 70

Figure 55 Histograms for all fiber diameter measurements of image SEM7 71

Figure 56 Histograms for all fiber diameter measurements of image SEM8 72

Figure 57 Tukey-Kramer Multiple Comparison of Means for narrow10 84

Figure 58 Tukey-Kramer Multiple Comparison of Means for narrow15 85

Figure 59 Tukey-Kramer Multiple Comparison of Means for narrow20 85
Figure 60 Tukey-Kramer Multiple Comparison of Means for narrow25 86
Figure 61 Tukey-Kramer Multiple Comparison of Means for narrow30 86
Figure 62 Tukey-Kramer Multiple Comparison of Means for narrow35 87
Figure 63 Tukey-Kramer Multiple Comparison of Means for wide10.....87
Figure 64 Tukey-Kramer Multiple Comparison of Means for wide15.....88
Figure 65 Tukey-Kramer Multiple Comparison of Means for wide20.....88
Figure 66 Tukey-Kramer Multiple Comparison of Means for wide25.....89
Figure 67 Tukey-Kramer Multiple Comparison of Means for wide30.....89
Figure 68 Tukey-Kramer Multiple Comparison of Means for wide35.....90
Figure 69 Tukey-Kramer Multiple Comparison of Means for SEM1 90
Figure 70 Tukey-Kramer Multiple Comparison of Means for SEM2 91
Figure 71 Tukey-Kramer Multiple Comparison of Means for SEM3 91
Figure 72 Tukey-Kramer Multiple Comparison of Means for SEM4 92
Figure 73 Tukey-Kramer Multiple Comparison of Means for SEM5 92
Figure 74 Tukey-Kramer Multiple Comparison of Means for SEM6 93
Figure 75 Tukey-Kramer Multiple Comparison of Means for SEM7 93
Figure 76 Tukey-Kramer Multiple Comparison of Means for SEM8 94
Figure 77 Image narrow10 with CSkS valid edges.....95
Figure 78 Image narrow15 with CSkS valid edges.....96
Figure 79 Image narrow20 with CSkS valid edges.....96
Figure 80 Image narrow25 with CSkS valid edges.....97

Figure 81 Image narrow30 with CSkS valid edges....97
Figure 82 Image narrow35 with CSkS valid edges....98
Figure 83 Image wide10 with CSkS valid edges....99
Figure 84 Image wide15 with CSkS valid edges....100
Figure 85 Image wide20 with CSkS valid edges....100
Figure 86 Image wide25 with CSkS valid edges....101
Figure 87 Image wide30 with CSkS valid edges....101
Figure 88 Image wide35 with CSkS valid edges....102
Figure 89 Image SEM1 with CSkS valid edges....103
Figure 90 Image SEM2 with CSkS valid edges....104
Figure 91 Image SEM3 with CSkS valid edges....104
Figure 92 Image SEM4 with CSkS valid edges....105
Figure 93 Image SEM5 with CSkS valid edges....105
Figure 94 Image SEM6 with CSkS valid edges....106
Figure 95 SEM7 with CSkS valid edges....106
Figure 96 Image SEM8 with CSkS valid edges....107
Figure 97 Image narrow10 with DCS valid edges....108
Figure 98 Image narrow15 with DCS valid edges....109
Figure 99 Image narrow20 with DCS valid edges....109
Figure 100 Image narrow25 with DCS valid edges....110
Figure 101 Image narrow30 with DCS valid edges....110
Figure 102 Image narrow35 with DCS valid edges....111

Figure 103 Image wide10 with DCS valid edges 112
Figure 104 Image wide15 with DCS valid edges 113
Figure 105 Image wide20 with DCS valid edges 114
Figure 106 Image wide25 with DCS valid edges 114
Figure 107 Image wide30 with DCS valid edges 115
Figure 108 Image wide35 with DCS valid edges 115
Figure 109 Image SEM1 with DCS valid edges 116
Figure 110 Image SEM2 with DCS valid edges 117
Figure 111 Image SEM3 with DCS valid edges 117
Figure 112 Image SEM4 with DCS valid edges 118
Figure 113 Image SEM5 with DCS valid edges 118
Figure 114 Image SEM6 with DCS valid edges 119
Figure 115 Image SEM7 with DCS valid edges 119
Figure 116 Image SEM8 with DCS valid edges 120
Figure 117 Image narrow10 with DCH valid edges 121
Figure 118 Image narrow15 with DCH valid edges 122
Figure 119 Image narrow20 with DCH valid edges 122
Figure 120 Image narrow25 with DCH valid edges 123
Figure 121 Image narrow30 with DCH valid edges 123
Figure 122 Image narrow35 with DCH valid edges 124
Figure 123 Image wide10 with DCH valid edges 125
Figure 124 Image wide15 with DCH valid edges 126

Figure 125 Image wide20 with DCH valid edges....126
Figure 126 Image wide25 with DCH valid edges....127
Figure 127 Image wide30 with DCH valid edges....127
Figure 128 Image wide35 with DCH valid edges....128
Figure 129 Image SEM1 with DCH valid edges....129
Figure 130 Image SEM2 with DCH valid edges....130
Figure 131 Image SEM3 with DCH valid edges....130
Figure 132 Image SEM4 with DCH valid edges....131
Figure 133 Image SEM5 with DCH valid edges....131
Figure 134 Image SEM6 with DCH valid edges....132
Figure 135 Image SEM7 with DCH valid edges....132
Figure 136 Image SEM8 with DCH valid edges....133
Figure 137 Image narrow10 with CCS valid edges....134
Figure 138 Image narrow15 with CCS valid edges....135
Figure 139 Image narrow20 with CCS valid edges....135
Figure 140 Image narrow25 with CCS valid edges....136
Figure 141 Image narrow30 with CCS valid edges....136
Figure 142 Image narrow35 with CCS valid edges....137
Figure 143 Image wide10 with CCS valid edges....138
Figure 144 Image wide15 with CCS valid edges....139
Figure 145 Image wide20 with CCS valid edges....139
Figure 146 Image wide25 with CCS valid edges....140

Figure 147 Image wide30 with CCS valid edges....140
Figure 148 Image wide35 with CCS valid edges....141
Figure 149 Image SEM1 with CCS valid edges....142
Figure 150 Image SEM2 with CCS valid edges....143
Figure 151 Image SEM3 with CCS valid edges....143
Figure 152 Image SEM4 with CCS valid edges....144
Figure 153 Image SEM5 with CCS valid edges....144
Figure 154 Image SEM6 with CCS valid edges....145
Figure 155 Image SEM7 with CCS valid edges....145
Figure 156 Image SEM8 with CCS valid edges....146
Figure 157 Image narrow10 with CCH valid edges....147
Figure 158 Image narrow15 with CCH valid edges....148
Figure 159 Image narrow20 with CCH valid edges....149
Figure 160 Image narrow25 with CCH valid edges....149
Figure 161 Image narrow30 with CCH valid edges....150
Figure 162 Image narrow35 with CCH valid edges....151
Figure 163 Image wide10 with CCH valid edges....152
Figure 164 Image wide15 with CCH valid edges....153
Figure 165 Image wide20 with CCH valid edges....153
Figure 166 Image wide25 with CCH valid edges....154
Figure 167 Image wide30 with CCH valid edges....154
Figure 168 Image wide35 with CCH valid edges....155

Figure 169 Image SEM1 with CCH valid edges.....156
Figure 170 Image SEM2 with CCH valid edges.....157
Figure 171 Image SEM3 with CCH valid edges.....157
Figure 172 Image SEM4 with CCH valid edges.....158
Figure 173 Image SEM5 with CCH valid edges.....158
Figure 174 Image SEM6 with CCH valid edges.....159
Figure 175 Image SEM8 with CCH valid edges.....159

List of Abbreviations

CCH ..... Custom Canny Hough

CCS ..... Custom Canny Slopes

CSkS..... Canny Skeleton Slopes, also referred to as Skeleton Slopes

DCH ..... Default Canny Hough, also referred to as Canny Hough

DCS ..... Default Canny Slopes, also referred to as Canny Slopes

ECM ..... Extracellular Matrix

P1 ..... Person One

P2 ..... Person Two

P3 ..... Person Three

P4 ..... Person Four

P5 ..... Person Five

SEM ..... Scanning Electron Microscopy

Abstract

AUTOMATED METHODS FOR FIBER DIAMETER MEASUREMENT OF FIBROUS SCAFFOLDS

By Anna Alexandra Bulysheva, B.S.

A Thesis submitted in partial fulfillment of the requirements for the degree of Master of Science in Biomedical Engineering at Virginia Commonwealth University.

Virginia Commonwealth University, 2009

Major Director: Gary L. Bowlin, Ph.D.
Professor, Biomedical Engineering

The purpose of this work was to develop an automated method of measuring fiber diameters of electrospun scaffolds from scanning electron microscopy images of these scaffolds. Several automated methods were developed and evaluated by comparison to known values and data obtained via the standard manual method. Simulated images with known diameters were used as test images to evaluate the accuracy of each measurement technique. Eight scanning electron microscopy images were also used for the evaluation of the automated methods compared to the standard manual method. All diameter measurements were made in pixels. Five new automated methods coded in MATLAB were developed. The five methods varied the approach of identifying edges of fibers as well as assigning edges to single fibers and calculating the distance between edges assigned to the

same fiber. One-way analysis of variance and the Tukey-Kramer tests were performed for comparison of all methods per image. The Custom Canny Slopes automated method was shown to accurately approximate the mean diameters in ten simulated images as well as microscopy image of real scaffolds ($p<0.05$)

Introduction

Tissue engineering is a rapidly evolving field with the main goal of constructing living tissues *in vitro* for *in vivo* applications. One area of research towards this goal is the development of scaffolds for mimicking micro-cellular environments for cell proliferation outside of the body. Such scaffolds are carefully characterized based on cell-scaffold interactions, mechanical strength of the scaffolds, topography, immune-compatibility, diffusion permeability, etc. Depending on the manufacturing techniques, the characterization parameters can vary. One popular manufacturing technique of scaffolds is electrospinning. Electrospinning is a technique for creating non-woven mats of fibers on a nano to micro-scale in terms of fiber diameters. This technique closely simulates the natural fibrous three-dimensional morphology of the extra-cellular matrix, which normally supports cells within various tissues. This technique can be applied to a large variety of natural and synthetic polymers in order to create a favorable scaffold. The versatility in terms of materials and morphological similarity to natural extra-cellular matrices makes electrospinning a highly promising area of research. A very fundamental characteristic of electrospun scaffolds is the mean fiber diameter. It has influence over many other properties the scaffold may exhibit, such as allowing cell adhesion, cell migration and diffusion of nutrients. Therefore, average fiber diameter is always measured and reported for electrospun scaffolds. Various parameters for a given polymer or even blends of

polymers can be altered in order to produce favorable fiber dimensions for cellular proliferation (1-3).

Fiber diameter measurement is usually performed manually by measuring the diameters of multiple fibers within one microscopy image. This is a laborious process which requires the operator to draw a segment orthogonal to the direction of each fiber approximating its borders. Specialized software calculates the distance between the endpoints of the segment, the operator then draws the next segment and the process is repeated 20-100 times. An automated, operator independent method can significantly reduce the time and effort spent on characterization of electrospun scaffolds especially for processing multiple scaffolds as well as reducing variability in results.

Project Synopsis

The focus of this study is to develop an automated method for measuring the fiber diameters of electrospun scaffolds. This work employs image processing techniques to extract diameter information from the Scanning Electron Microscopy (SEM) images of the scaffolds. The goal is to develop an operator independent method which can process the images and accurately measure fiber diameters. Two different implementations of Canny edge detection method were used to determine the location of the fiber borders. The Canny method was chosen for its superior accuracy compared to other edge detection methods (4,5). Once the edges were found, three different approaches were used to assign two edges to single fibers. The distance between the selected edges was then computed for each recognized fiber.

The author has found no literature regarding validation studies of a standard method compared to known values; therefore test images were created to simulate scanning electron microscopy images of electrospun scaffolds. The diameter of each fiber within these images was predetermined and known. Images with a narrow distribution of fiber diameters, and a wide distribution of fiber diameters with approximately 100 fibers per image were created.

Data was collected from five volunteers processing each image using the conventional manual method. Each image was displayed in image processing software such as ImageJ or UTHSCSA ImageTool, and the distance measurement tool of the

software was used to measure one hundred diameters. Every image was also processed with each of the five developed automated techniques.

Background Information

Fibrous ECM Analogues in Tissue Engineering

Tissue engineering is a growing field involving a diverse set of disciplines ranging from biological sciences, to engineering and physical sciences. Engineering tissues *in vitro* can have either therapeutic applications for *in vivo* implantation or treatment development applications for *in vitro* disease models. Developing tissues *in vitro* entails mimicking the micro and macro-scale cellular environment to allow for native cells of the tissues to perform their usual functions. There are various factors to be considered for manipulating cellular environment. Soluble cell-cell signals, nutrients, oxygen and carbon dioxide exchange, temperature, salinity and pH balance are all vital aspects of tissue culturing. Another critical aspect to closely mimicking the micro-environment of tissues is mimicking the extra-cellular matrix (ECM). The ECM not only functions to physically support the cells via cell adhesion, but it also regulates their proliferation and migration rates as well as other vital metabolic functions. The cell-matrix interactions occur in all three dimensions, which is difficult to replicate outside of the body. An ideal ECM analogue would provide cells of a particular tissue with the same cues that they would receive from their native ECM *in vivo*, but would do so *in vitro*.

The natural ECM of various tissues is often fibrous in nature with nano-scale diameters. Although this fibrous structure is very complex and is composed of numerous types of macromolecules and varies in structure and composition from tissue to tissue, the idea of creating fibrous scaffolds for the ECM analogues has gained tremendous momentum. The morphology of native ECM is primarily a network of long protein nano-fibers linked together with various glycoproteins. This fibrous morphology is the driving factor for creating fibrous scaffolds for ECM analogues (6-8). It has been experimentally determined that compared to two-dimensional smooth surfaces and three-dimensional porous films, fibrous networks of the same material provide better support for adhesion and migration of various cells (9).

Common methods for creating small fiber diameter webs include self-assembly, phase separation and electrospinning. Amphiphilic peptides with a hydrophobic and hydrophilic regions are known to self assemble into structures such as vesicles, micelles and tubules when dissolved in an aqueous solution. The structure of these peptides dictates the shape of the three-dimensional network formed in solution depending on temperature, pH and salinity of the aqueous solution. Various peptides have been fabricated to exploit their properties for self-assembling into three-dimensional nanofibrous networks with usage in tissue engineering and drug delivery applications. The fiber diameters for scaffolds created with this method are on the order of 30-50 nm (7,10,11).

Phase separation can either be non-solvent induced separation or thermally induced separation. Non-solvent induced separation can be accomplished by dissolving the polymer in a solvent and then introducing a non-solvent to the surface of the solution. The non-

solvent displaces the solvent in the solution making the solution unstable and causing the polymer to precipitate out of solution and therefore forming a porous scaffold (7,12). Thermally induced phase separation is more common and involves dissolving the polymer in a solvent at high temperatures, and then quickly lowering the temperature to cause rapid precipitation, at which point the scaffold forms and the solvent is removed via sublimation or extraction (7,12,13). The fiber diameters fall into the range of 50-500 nm, when this method is implemented (7).

The most well studied method for preparation of fibrous scaffolds is electrospinning. This is a fairly simple process of utilizing electrostatic forces to produce non-woven fibrous mats. As one example, a polymer solution is drawn up into a syringe with a blunt needle. The needle is positively charged and a negatively charged collecting plate is placed at a predetermined distance from the needle. The resulting electrostatic field between the needle and the collecting plate causes a force to act on the polymer solution in the direction of the collecting plate. If the force is sufficiently high, the surface tension of the solution breaks and a jet of polymer solution moves from the tip of the needle to the collecting plate. While the jet travels to the collecting plate, the solvent evaporates leaving only the polymer fibers in the newly generated scaffold. This method can be use for a large range of natural and synthetic polymers and a large range of solvents. The fiber diameters for this method fall into the range of 200nm-10μm, depending on the polymer and solvent chosen as well as parameters such as concentration, air gap distance, and electric field strength (2,3,6,7,11).

It has been experimentally determined that scaffold diameters of the same material have a great impact on cell migration and proliferation. Smaller fiber diameter scaffolds have been shown to promote better cellular adhesion and migration than larger diameter scaffolds (1). It is therefore important to be able to measure the fiber diameter in an efficient accurate way. This measurement would become even more important if any of these scaffolds reach clinical applications and mass production. It is unlikely that a manual measurement can be performed efficiently on a large scale. The author is therefore proposing automated methods for performing fiber diameter measurements from SEM images of fibrous scaffolds.

Manual Method for Fiber Diameter Measurement

Although there is no validated standard manual method for measurement of fiber diameters from SEM images of scaffolds, there is a generally excepted manual method, which is frequently used to quantify fiber diameters. The image of the scaffold is opened in image processing software such as ImageJ (NIH) or UTHSCSA ImageTool. The scale is set based on the pixel/scale bar ratio, which is obtained by measuring the scale bar in pixels and providing length of the scale bar in metric units. The distance tool of the software is then used to acquire 20-100 measurements of fiber widths. In each measurement, an orthogonal segment is drawn beginning and ending on the edges of the fiber. The angle of the segment is determined qualitatively by visual inspection. The placement of the end points on the edges of the fibers is also determined by visual

inspection. The software then calculates the distance between the endpoints in pixels and converts it to metric units previously specified. The average diameter and the standard deviation from that average are reported for each scaffold (2,14-16).

Automated Method for Fiber Diameter Measurement

There is one published, image processing based method for fiber diameter measurement of electrospun scaffolds by Ziabari and coworkers. The grey scale images are converted to black and white images via local thresholding. A distance transform image is constructed from the black and white image with intensity values indicating the distance each white pixel is from the nearest edge. The distance transform image is then thinned and pruned to produce a skeleton of the fiber network with white lines corresponding to the location of the center of each fiber. The intersections of these skeletons are then removed. The four images can be seen consecutively in Figure 1. The new skeleton is used with correlation to the distance transform image to choose only the diameters from the distance transform matrix that do not correspond to intersections. This method was tested on a simulated image with known fiber distribution and an image of a micrograph of the real electrospun web (17).

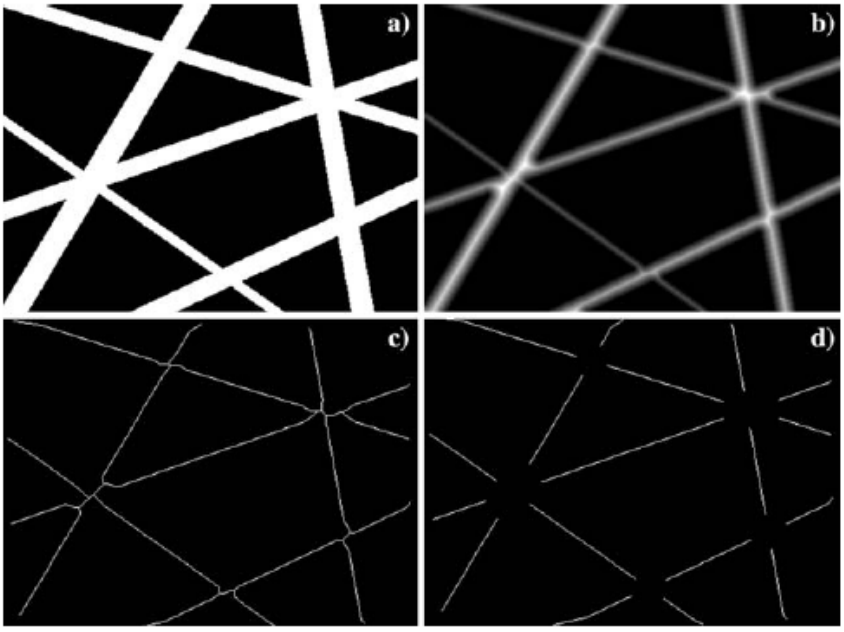

Figure 1 Sequence of image processing steps of the Ziabari method. a) black and white simulated image, b) distance transform image, c) skeleton, d) skeleton with intersections removed (17)

The main drawback of this method is the difficulty of obtaining a black and white image that accurately represents the boundaries of the fibers when the background in not very well defined or cluttered with more fibers, which is often the case for real fibrous scaffolds. This method works well for networks that do not have many overlapping fibers. The black and white conversion, even with local thresholding, does not work accurately for densely sited fibers in scaffolds. The black and white image ends up with some fibers fused together into one wide fiber, or the border region is placed well outside of the actual edge of the fiber. Therefore the remaining manipulations introduced with this method result in inaccurate measurements of the fiber size from the original grey scale image.

Edge Detection Methods in Image Processing

Edge detection can be accomplished by first or second order derivatives in order to extract meaningful information from changes in intensity values in images. The first order gradient equation is most commonly used for convenience.

$$\nabla F = \begin{bmatrix} G_x \\ G_y \end{bmatrix} = \begin{bmatrix} \frac{\partial F}{\partial x} \\ \frac{\partial F}{\partial y} \end{bmatrix}$$

Since images are discrete sets of values, the derivatives must be approximated by numerical solution. There are many different approaches to finding a numerical solution in order to identify a meaningful discontinuity in an image, which can be labeled as an edge. The most commonly used methods are methods developed by Sobel, Prewitt, Roberts and Canny (4,5). For an image neighborhood in Figure 2, the Sobel approximation is

$$G_x = (a_7 + 2a_8 + a_9) - (a_1 + 2a_2 + a_3)$$

$$G_y = (a_3 + 2a_6 + a_9) - (a_1 + 2a_4 + a_7)$$

a_1	a_2	a_3
a_4	a_5	a_6
a_7	a_8	a_9

Figure 2 Image neighborhood representation (4)

The Prewitt approximation of the gradient is:

$$G_x = (a_7 + a_8 + a_9) - (a_1 + 2a_2 + a_3)$$

$$G_y = (a_3 + a_6 + a_9) - (a_1 + 2a_4 + a_7)$$

The Roberts approximation is simply:

$$G_x = a_9 - a_5$$

$$G_y = a_8 - a_6$$

The Canny method is more complex than taking a maximum gradient as a meaningful edge. A Gaussian filter is employed in order to make method less sensitive to noise. Once the noise is minimized, a derivative in the form of a numerical approximation of the gradient is generated with the local maxima taken as the possible edges. A high and low threshold value is used to determine the strong and weak discontinuities which can be edges. The weak edges are only used if they are connected to a strong edge. Of the above methods, the Canny method is considered to be the most accurate and is often used for various image processing applications (4,5).

Hough Transform

It is often desired not only to identify edges, but also to detect line segments within the image. This can be accomplished by first detecting edges with the methods above and then using the Hough transform to identify lines. The Hough transform can be used to link a set of points to a meaningful segment. A straight line is the simplest of the possible

equations that can be represented using the Hough transform. The familiar equation of a line $y_i = mx_i + b$ can be represented parametrically in the form of $b = -x_i m + y_i$, where in the parameter space (*m*-*b* space), there is only one line that corresponds to the specific pair (x_i, y_i). Therefore, intersections of lines in the *m*-*b* space signify that pairs (x_i, y_i) and (x_j, y_j) are on the same line in the *x*-*y* plane. Parametric representation in the *m*-*b* space can be useful in counting the number of intersections in the *m*-*b* plane to represent lines in the original image, however it becomes computationally difficult, when *m* approaches infinity with vertically sloped lines (4,5).

The linear Hough transform allows for a finite representation of lines in the parametric space. The following equation can be used

$$x\cos\theta + y\sin\theta = \rho$$

where θ is the angle between the *x*-axis and a normal segment to the line in *x*-*y* space passing through the origin, ρ is the length of that segment, or the distance the line is away from the origin in the *x*-*y* space. In the θ-ρ space each (θ_i, ρ_i) pair corresponds to a single line the *x*-*y* space. The intensity value in the θ-ρ space corresponds to how many points fall on that line from the *x*-*y* space. The local maxima in the θ-ρ space can then be used to identify meaningful lines in the original image by setting a reasonable threshold for how many points should be on a line in order to detect a line (4,5).

Materials and Methods

Test Images

There were multiple types of test images generated for evaluating the accuracy of various methods of fiber diameter measurements. All test images were created via code written in MATLAB. The images have randomly oriented fibers with 10% white noise incorporated into the fiber intensities and into the background intensities. The orientation of the fiber is also random. Each fiber has intensity values increasing towards the central axis of the fiber and decreasing intensity towards the edges. The peak intensity varies randomly from fiber to fiber within a specified range. The flowchart in Figure 3 illustrates the algorithm used to create the test images. The algorithm was implemented in MATLAB.

There were two possible fiber diameter distributions. Narrow distribution restricted the fiber diameters from 0.85-1% of the maximum fiber diameter for that image. Wide distribution restricted the fiber diameters from 2 pixels to the maximum fiber diameter for that image. The maximum diameters ranged from 10-35 pixels. For each fiber the width was calculated randomly within the specified range. There were six images generated with a narrow distribution of fiber diameters and six images with a wide distribution of fiber diameters. The diameters of each fiber in every image were recorded.

Figure 4 shows the wide fiber diameter distribution test images used for testing with maximum fiber diameters ranging from 10-35 pixels. Figure 5 shows the narrow fiber diameter distribution test images, with maximum fiber diameters ranging from 10-35 pixels. The size of each image was set to 1020×650 pixels which is the typical image size used for creating real SEM images of electrospun scaffolds. Magnification and pixel resolution is usually adjusted so the fiber diameter is within the range chosen for test images in this study.

The real SEM images were generously donated by Koyal Garg and Scott Sell from their own research on electrospun scaffolds. Figure 6 shows the eight SEM images used for this study.

Human Data

Five volunteers measured each test image using the conventional manual technique. One hundred diameters were measured per image. Each volunteer was provided with all electronic test images and was directed to use either ImageJ or ImageTool software to view the images and employ the provided distance tool to measure diameters. The data was then collected from each volunteer and used for comparison with other measurement methods. No personal information about the volunteers was collected or recorded.

Overview of Automated Fiber Diameter Measurements

The main challenges in utilizing automated methods for fiber diameter measurement are identifying the boundaries or edges of individual fibers and correctly pairing two edges from the same fiber. Alternate solutions to the identification and pairing problems are presented in each of the five automated methods.

There are two methods that were explored for identifying edges. Both methods are implementations of the Canny edge detection method. The default MATLAB Canny edges detection was used initially, but was then replaced by a custom Canny implementation for improved accuracy of edge detection.

There are three methods that were explored for pairing edges. The first method creates a skeleton of the electrospun web in the image. This skeleton is compared with the edges that were found independently using the edge detection method to identify individual fiber segments. The fiber segments are considered valid if the skeleton and two edges around the skeleton have the exact same slope. The second method uses the sign of gradient to the original picture to assign left or right edges from independently found edges. The left and right edges are then paired if their slope is identical. The final method for pairing valid edges uses the sign of the gradient to assign left and right edges as in the previous method. However, in order to address the existence of numerous discontinuities in fiber edges due to intersections, the Hough transform is used. The descriptions of each complete measurement algorithm are presented in the following sections.

Skeleton Slopes Fiber Diameter Measurement

The first method developed by the author uses elements from the previously described Ziabari method, but varies in the determination of valid fiber edges portion of the method. In order to identify fibers from the background, a black and white image is created via a local threshold algorithm. A skeleton of the black and white image is created by thinning the white/fiber areas of the images and removing the intersections. The skeleton is used to define fibers, but the black and white image is not used to calculate the actual diameters. The binary image does not accurately represent the location of the edges of the fibers; therefore a distance transform would only perpetuate the error. Therefore a standard MATLAB Canny edge detection function was used to determine the location of the edges. Once a fiber is defined with a skeleton and two edges with identical slopes the distance between the two edges is recorded taking into account the inclination of the fiber. Figure 7 illustrates the algorithm developed for this portion of the experiments. The algorithm was implemented in MATLAB. All test images were processed with this method, and the collected data was compared to data from the manual measurements, as well as known diameters for the synthesized images. A simple sample image has been processed with this method to demonstrate the various steps involved. Figure 8 illustrates the various stages of processing this image.

Canny Slopes Fiber Diameter Measurement

This method uses a different principle to define valid left and right edges than the previous method, but uses a similar idea of slope determination to define valid pairs of edges to determine diameters of fibers. The original image is first filtered with a Gaussian filter to minimize noise. A numerical gradient is then taken of the filtered image and used to determine the approximate left and right borders of the fibers in the image, while the MATLAB Canny edge function was used to determine the edges. Positive gradient signifies a left border, while a negative gradient signifies a right border. This combined information is used to define single pixel wide left and right edges of fibers inside the images. Slopes of the left and right edges and their proximity were used to determine corresponding left and right edges of single fibers. The distance between them was calculated using their calculated inclination. Figure 9 illustrates the different stages of this algorithm. The sample image was processed with this method, and the various stages of processing this image with this method are shown in Figure 10. All test images were processed with this method and the resulting data was compared to the know diameters (when possible) and to the data collected from manual measurements as well as the other developed methods. The algorithm was implemented in MATLAB.

.

Canny Hough Fiber Diameter Measurement

This method uses the same strategy as the previous method to determine where the left and right edges are located, but uses the linear Hough transform to identify individual fibers to calculate their diameters. The left and right edge matrices are created as in the previous method. The Hough transform is applied to each edge matrix. The left edges are not necessarily visible in the same part of the fiber as are the corresponding right edges. Performing the Hough transform allows to choose left and right pairs of edges from the same fiber, without having the pairs to be in the exact same horizontal position as is required by the Slopes method. This method assumes that the fibers are linear and that edges found along the same line in left edges matrix belong to the same edge of the same fiber. Lines with identical inclination from the left and right edges matrices with no lines between them are assumed to belong to the two edges of the same fiber. The diameters are then measured once for each fiber found. Intersections of fibers do not introduce limitations to fiber diameter measurement when this method is applied.

The algorithm for this method, illustrated in Figure 11, was implemented in MATLAB. All test images were processed with this method. The collected data was compared to data from the manual measurements, as well as known diameters for the synthesized images. The sample image was processed with this method. Figure 12 shows the different image processing stages. The gradient images were omitted in this figure since they already appear in Figure 10 (c-d).

Custom Canny Slopes Fiber Diameter Measurement

Determining the location for the edges of each fiber is the most critical element in accurately measuring the fiber diameters. A custom edge function based on the Canny method was written in MATLAB for the purpose of accurate fiber diameter determination. A Gaussian filter is applied to the original image. The gradient is taken of the filtered image. The magnitude of the gradient is thinned to only contain one local maximum, effectively making the edges one pixel wide. The left and right edges are defined by existence of an edge and positive x-direction gradient or existence of an edge and negative x-direction gradient respectively. The pairs of edge segments from the same fiber are then determined. The following steps are the same as in the Canny Slopes fiber diameter measurement algorithm. Moving along each row of the left edges matrix, an edge is paired with a corresponding right edge. The slopes of both are calculated and if identical, a diameter measurement is taken from that segment of the fiber. Figure 13 illustrates the various stages of this algorithm.

This algorithm was implemented in MATLAB and all test images were processed with this method. Recorded data for each image was compared to the known diameters for the simulated images and to human data when known diameters were not available. A sample image was also processed to demonstrate the various stages of this method. Figure 14 shows the resulting stages of processing the sample image with this method.

Custom Canny Hough Fiber Diameter Measurement

This method combines the custom edge detection of the previous method with Hough transform for defining valid fibers and their diameters. The original image is filtered with a Gaussian filter. The numerical gradient approximation is taken of the filtered image. The magnitude of the gradient matrix is thinned to one pixel width by suppressing all non-maxima points. The left and right edges are determined by using the thinned matrix of edges and the x-direction gradient matrix. Every edge corresponding to a positive gradient defines the left edge, while every edge corresponding to a negative gradient defines the right edge.

The linear Hough transform is taken of each edge image. The local peaks within the Hough transform space are taken to define edge lines within the original image. Corresponding line pairs from left and right edges with the same slope are taken to define a fiber if there are no other lines of the same inclination in between the lines of the selected pair. The diameters are calculated between the selected edges.

The algorithm for this method is shown in Figure 15. The method was implemented in MATLAB. All test images were processed with this method and resulting fiber diameters were compared to known and manually measured diameters. Figure 16 shows the various outputs of this method on the sample image, the gradient pictures are not included in this figure since they already appear in Figure 14 (c-d).

Statistical Analysis

Data sets from different methods for each image were compared to determine if differences existed between the different methods and if so which methods were statistically different. One-way analysis of variance (ANOVA) was performed on all data sets from each image to determine whether there were differences. If statistically significant differences existed, the Tukey-Kramer test was performed on data from images with statistical differences between data sets ($\alpha = 0.05$). The MATLAB statistical package was used to perform the statistical analysis. Statistical analysis results such as ANOVA tables and multiple comparison figures can be found in Appendix A.

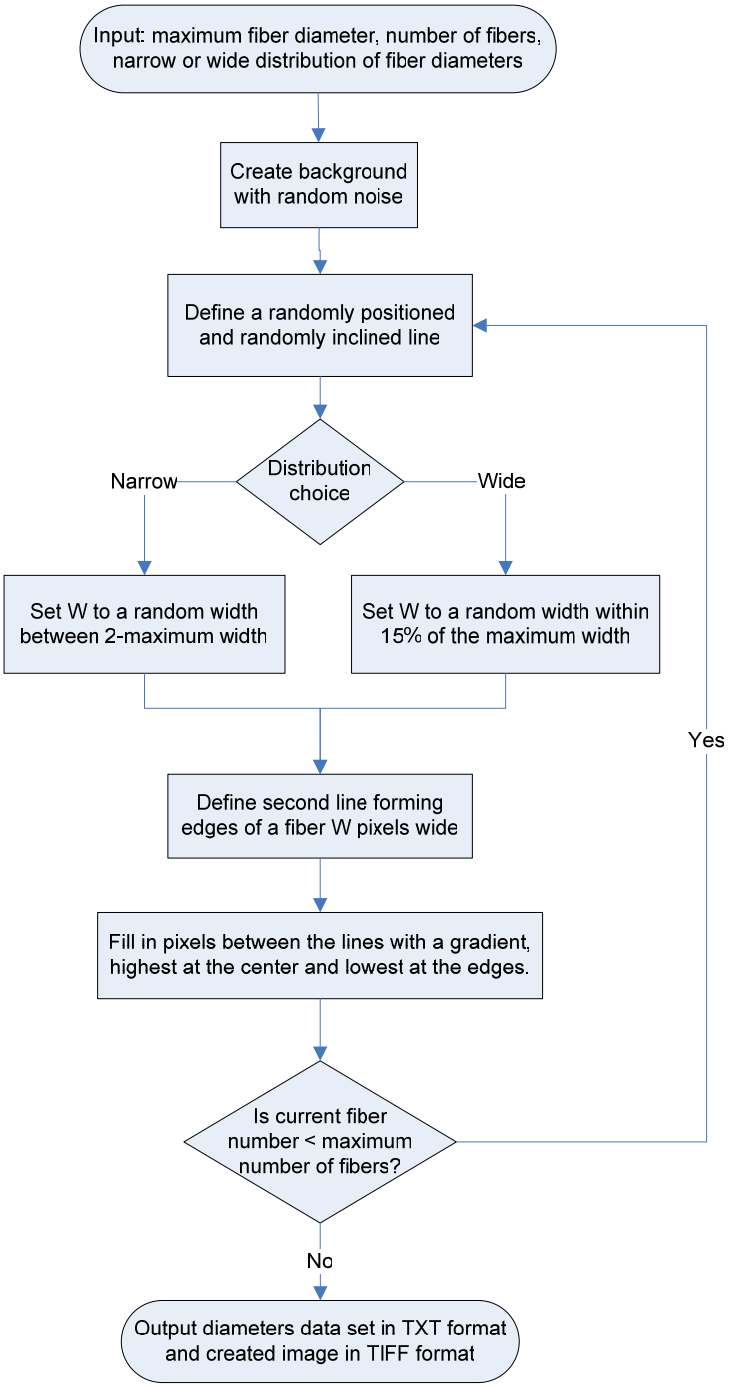

Figure 3 Algorithm used for generating test images

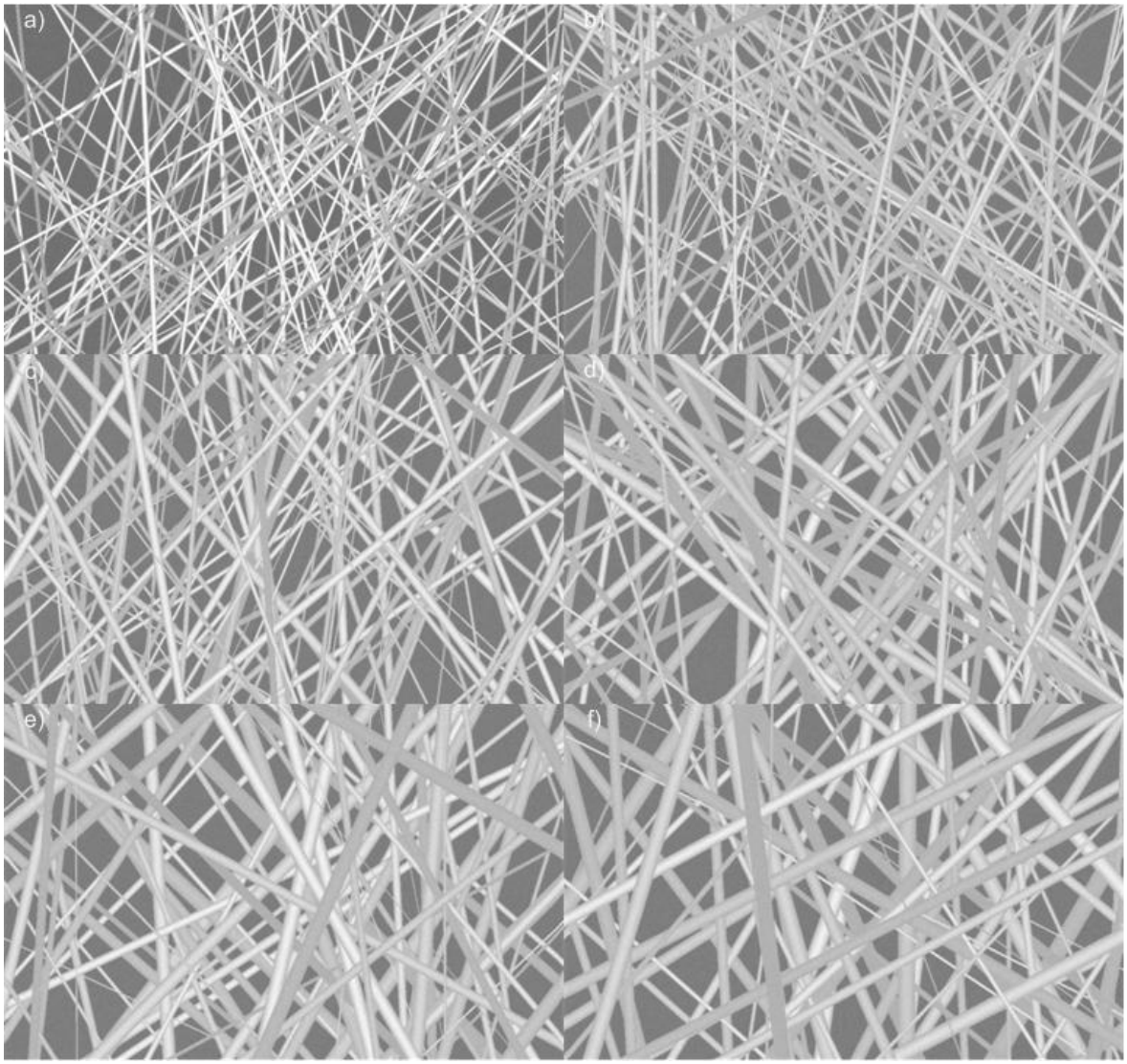

Figure 4 Test images with wide distribution of fiber diameters. The maximum diameter is a) 10, b) 15, c) 20, d) 25, e) 30, f) 35 pixels

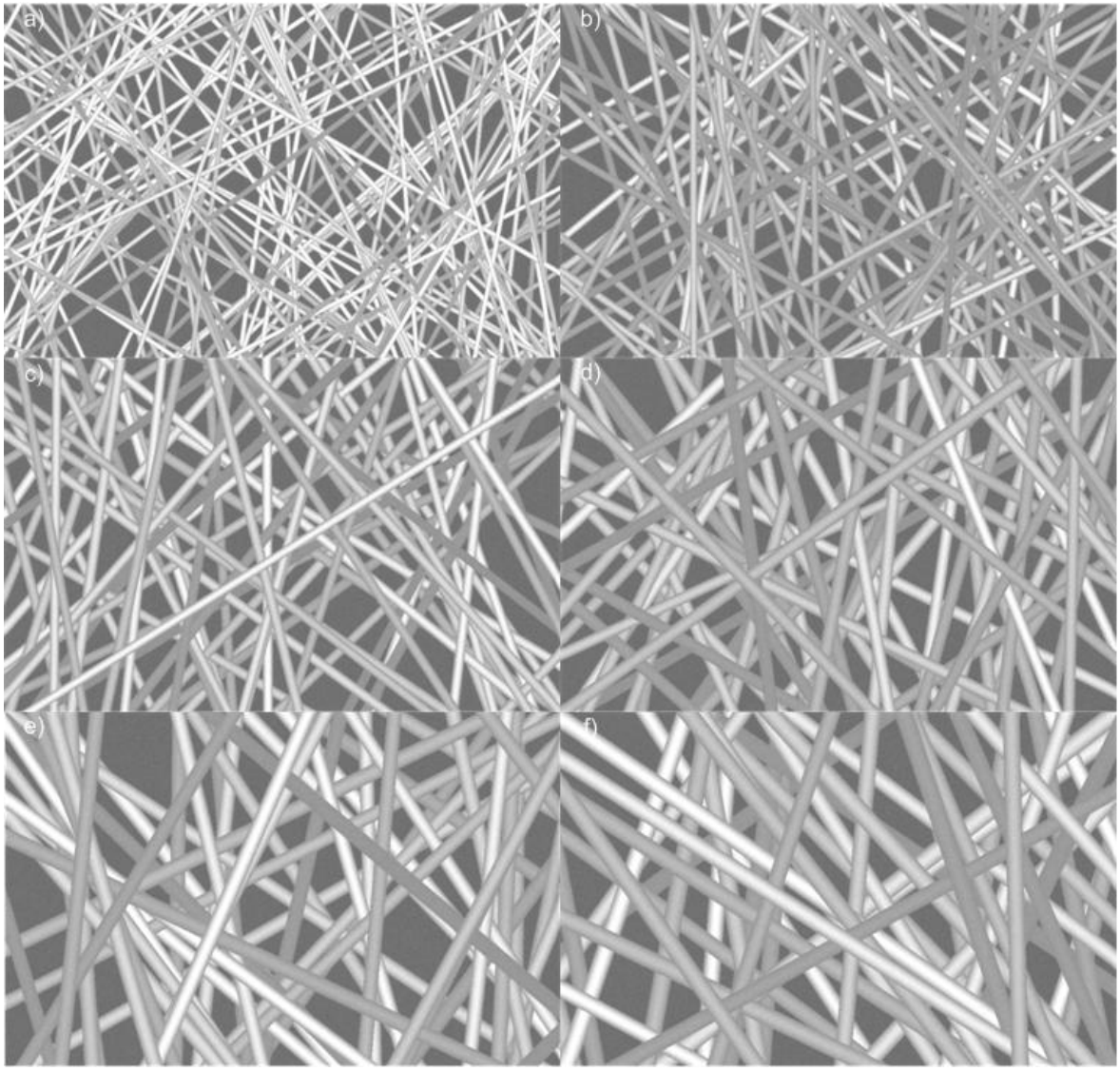

Figure 5 Test images with narrow distribution of fiber diameters. The maximum diameter is a) 10, b) 15, c) 20, d) 25, e) 30, f) 35 pixels

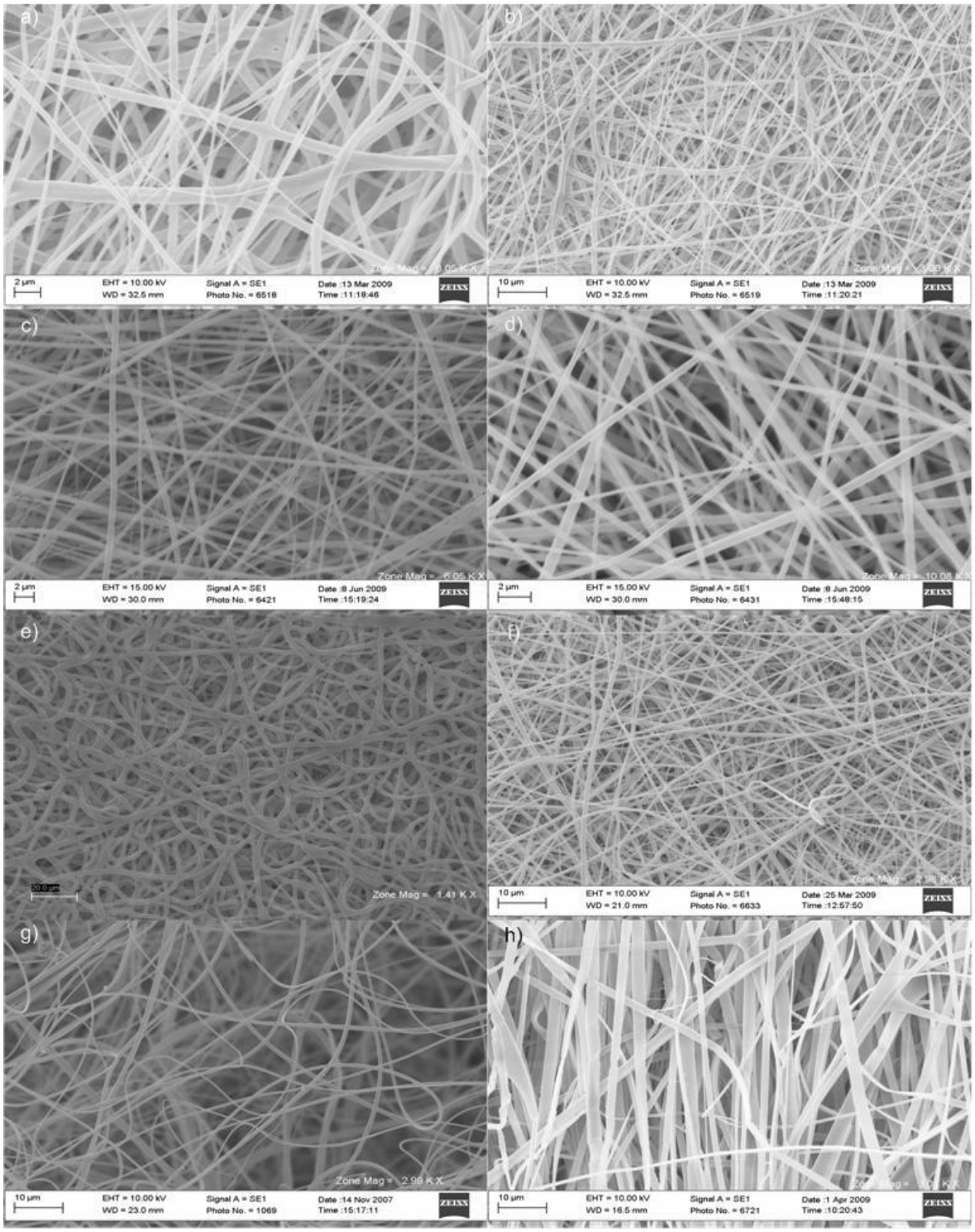

Figure 6 SEM images of real electrospun webs used in this study

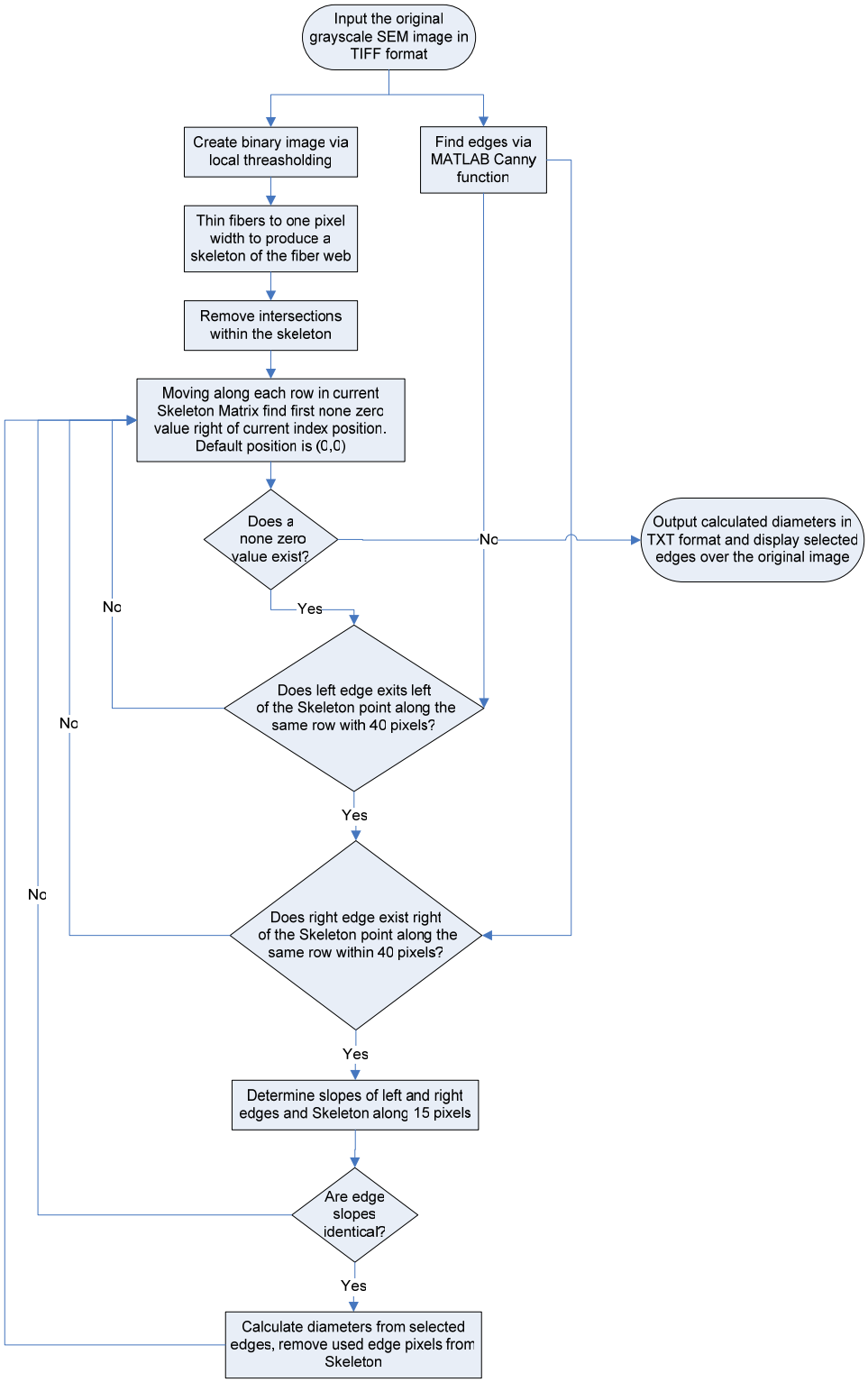

Figure 7 Skeleton Slopes Fiber Diameter Measurement Algorithm

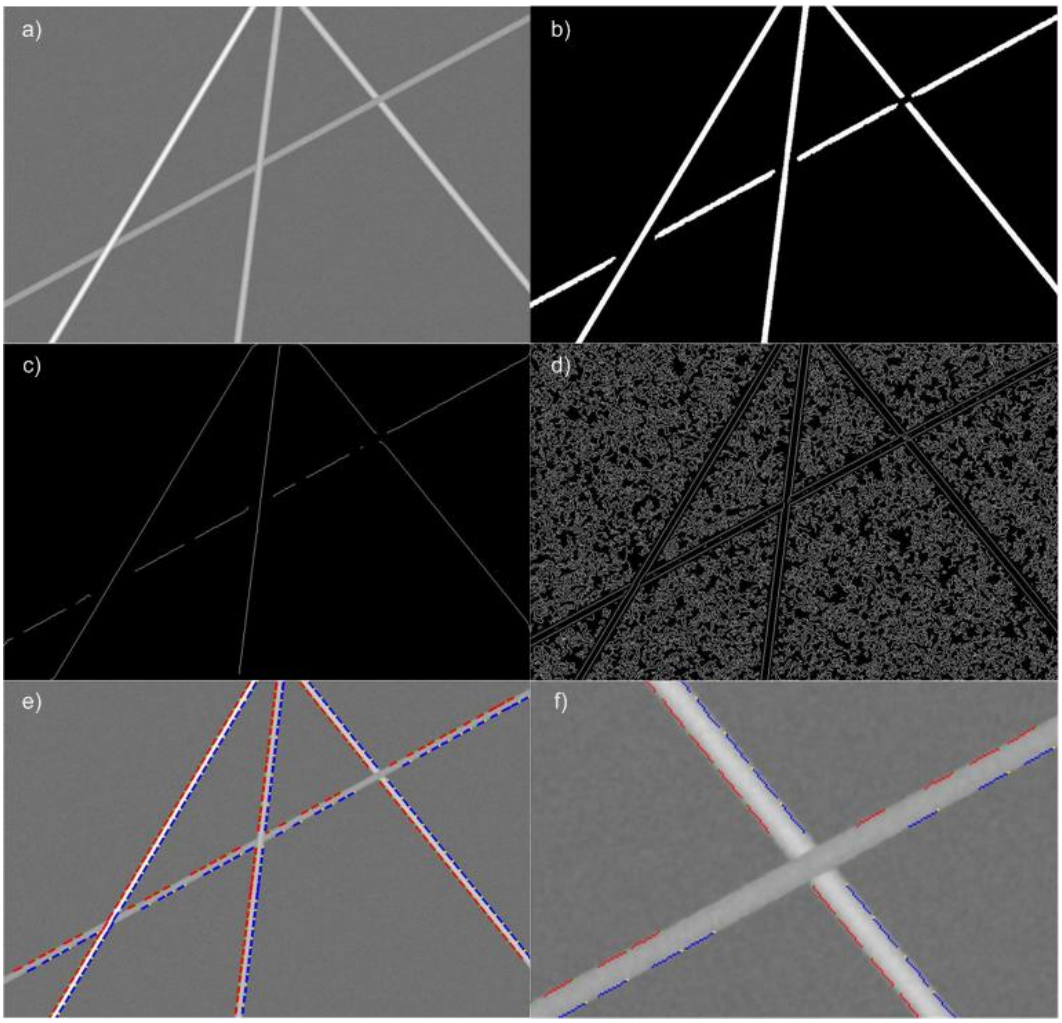

Figure 8 Image processing steps of the Skeleton Slopes fiber diameter measurement method. a) Original simulated image, b) original image converted to black and white, c) Skeleton without intersections, d) Edges from MATLAB Canny edge function, e) selected edges

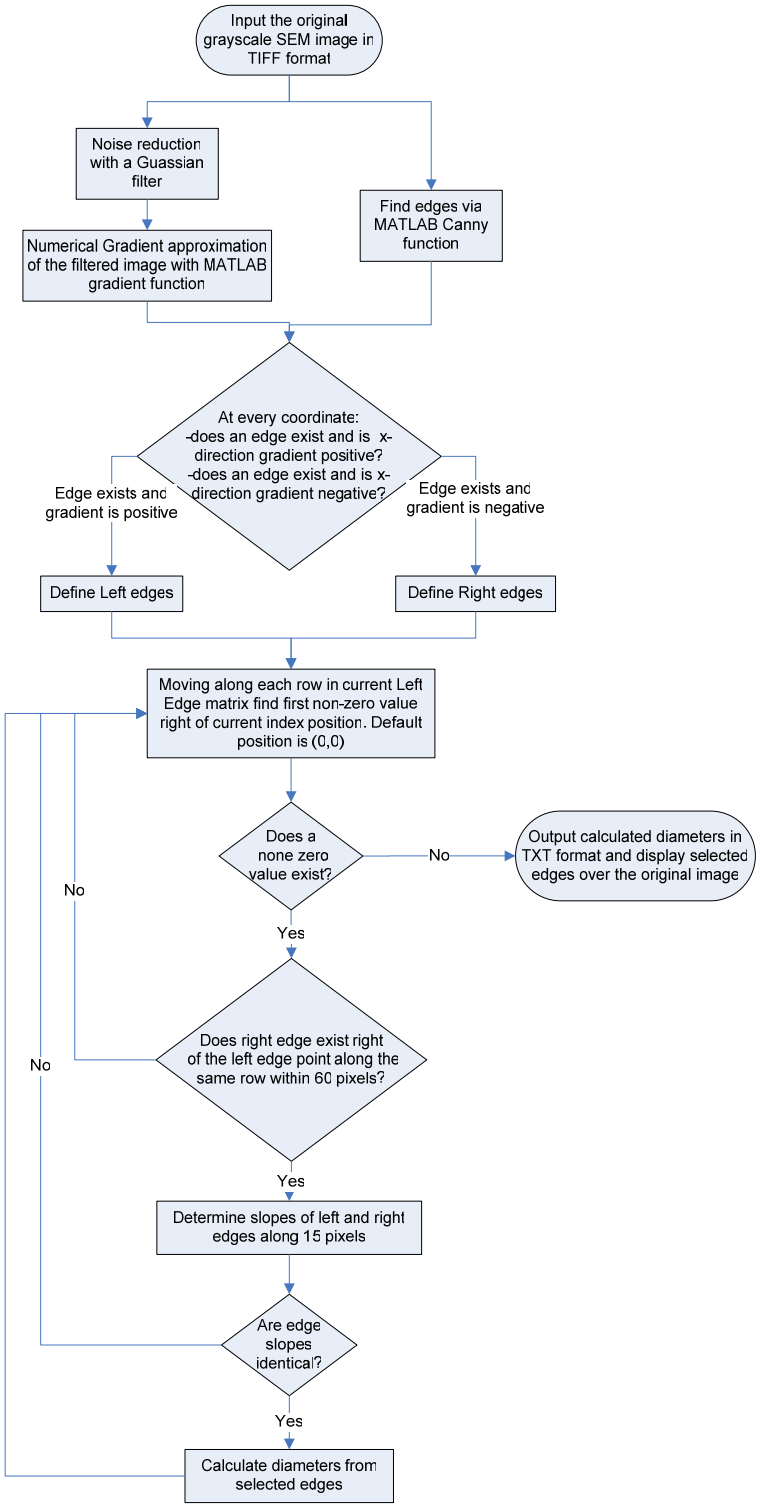

Figure 9 Canny Slopes Fiber Diameter Measurement Algorithm

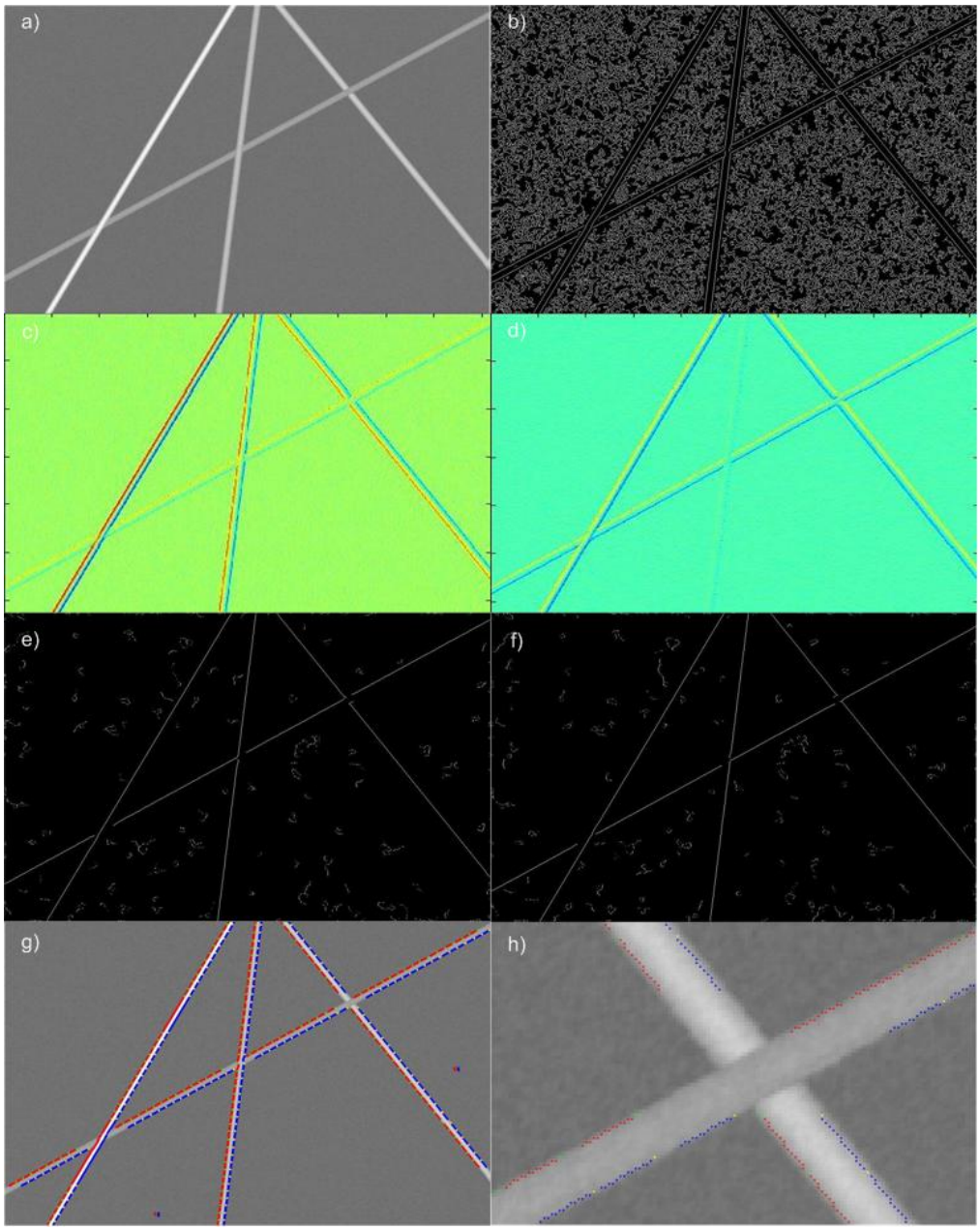

Figure 10 Image processing steps of the Canny Slopes fiber diameter measurement method. a) Original simulated image, b) Edges from MATLAB Canny edge function, c) gradient in x-direction, d), gradient in y-direction, e) left edges, f) right edges, g) selected edge

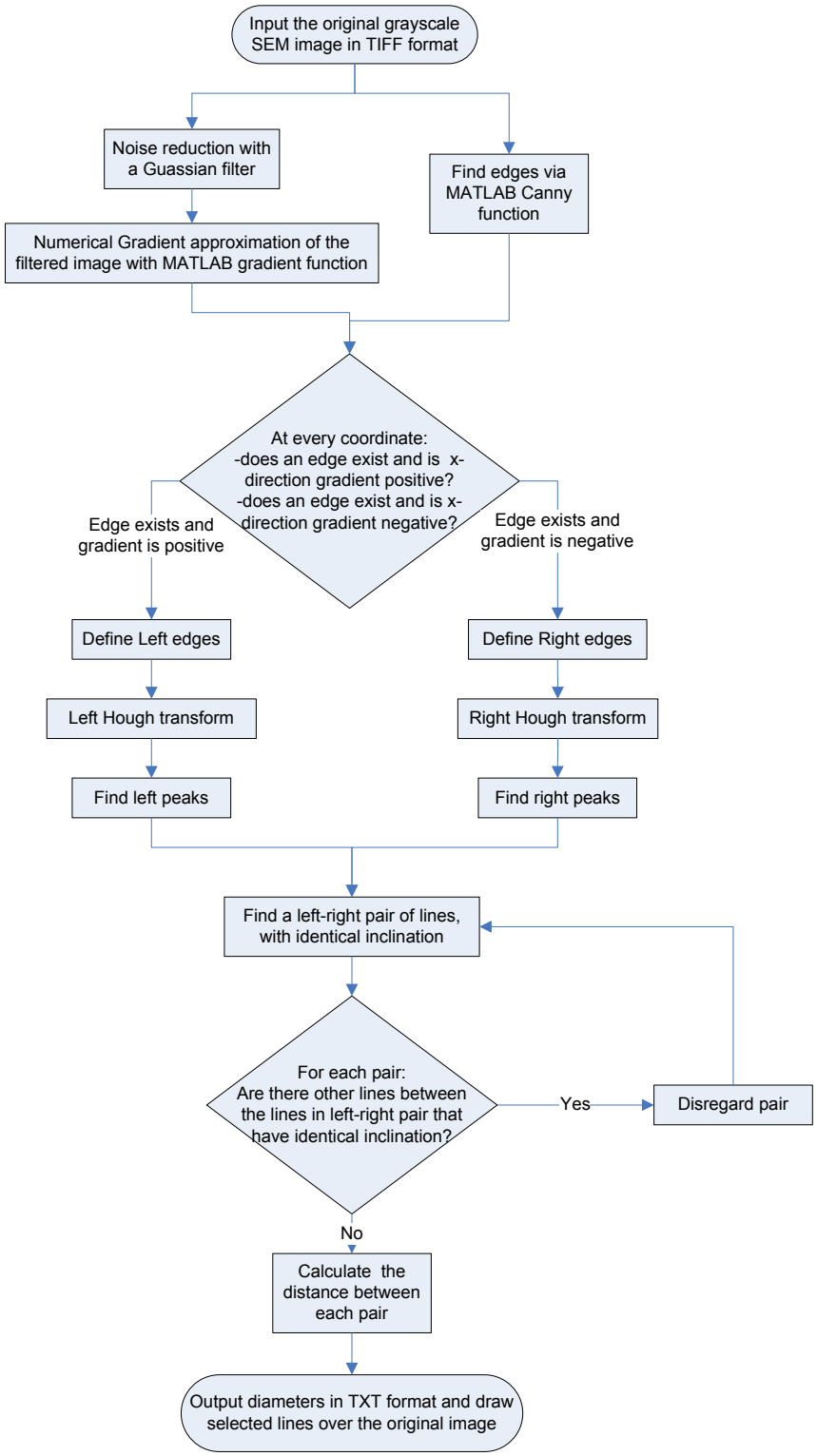

Figure 11 Canny Hough Fiber Diameter Measurement Algorithm

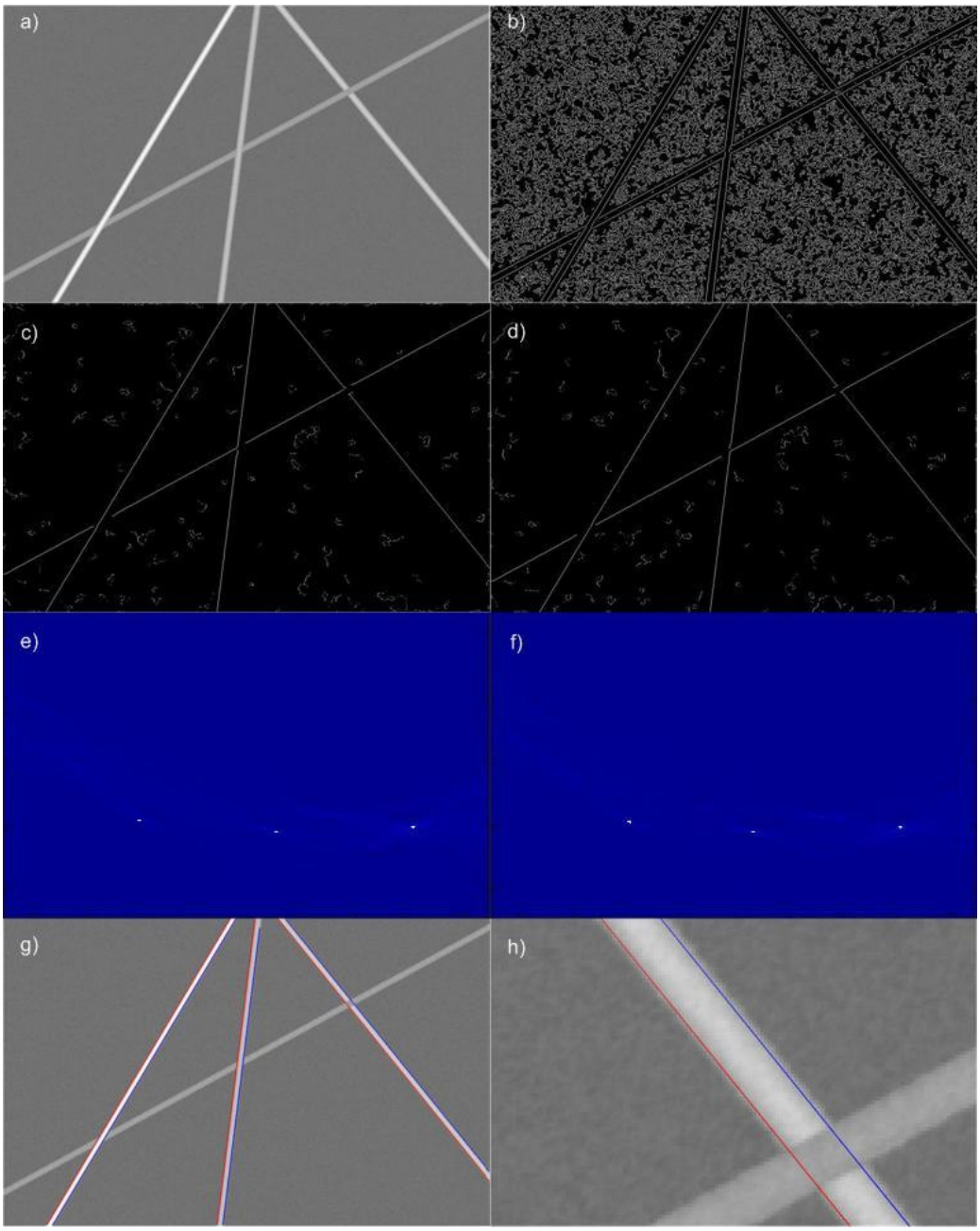

Figure 12 Image processing steps of the Canny Hough fiber diameter measurement method. a) Original simulated image, b) Edges from MATLAB Canny edge function, c) left edges, d), right edges, e) Hough transform of (c), f) Hough transform of (d), g) selected edges superimposed over the original image, h) high magnification of (g)

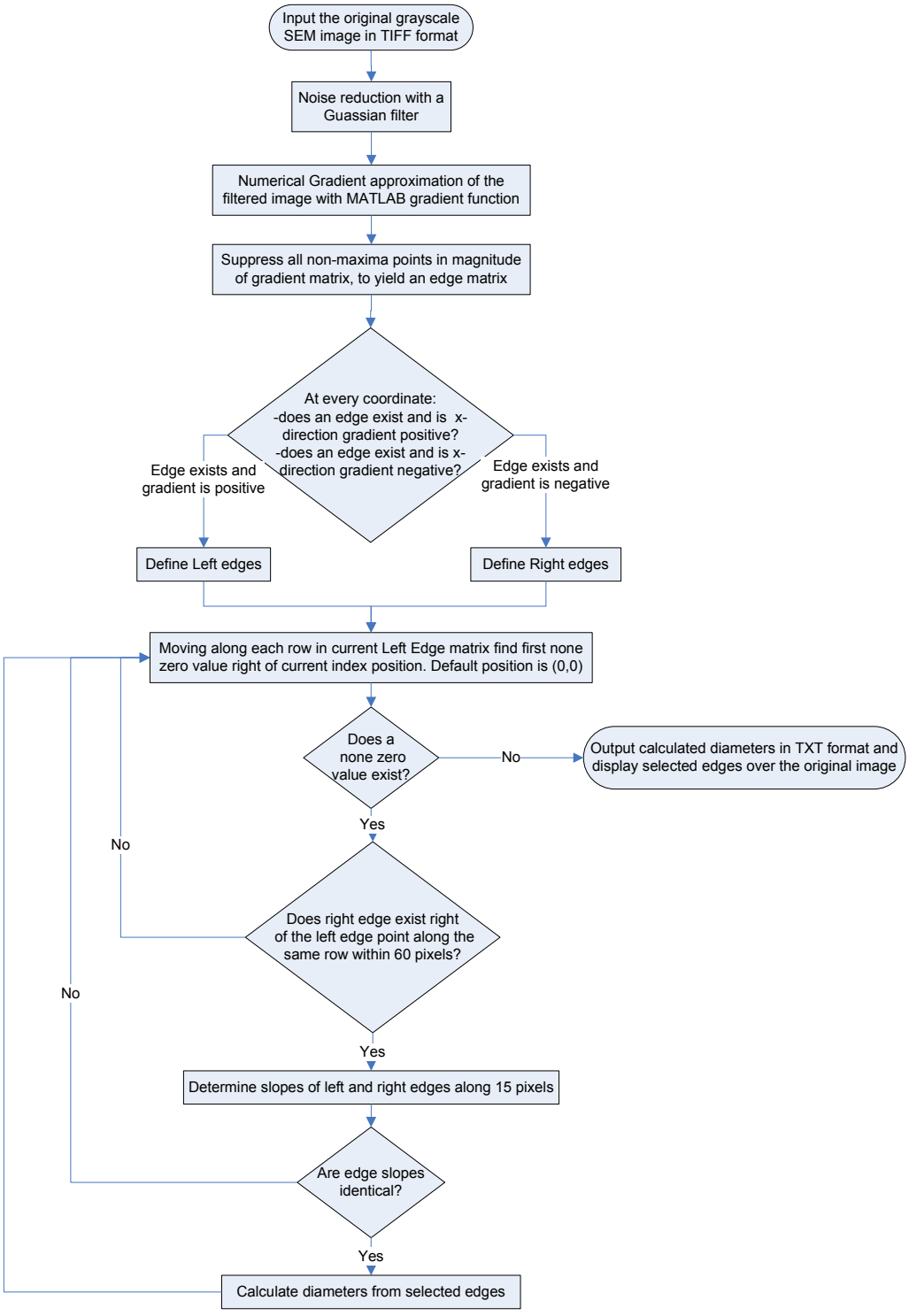

Figure 13 Custom Canny Slopes Fiber Diameter Measurement Algorithm

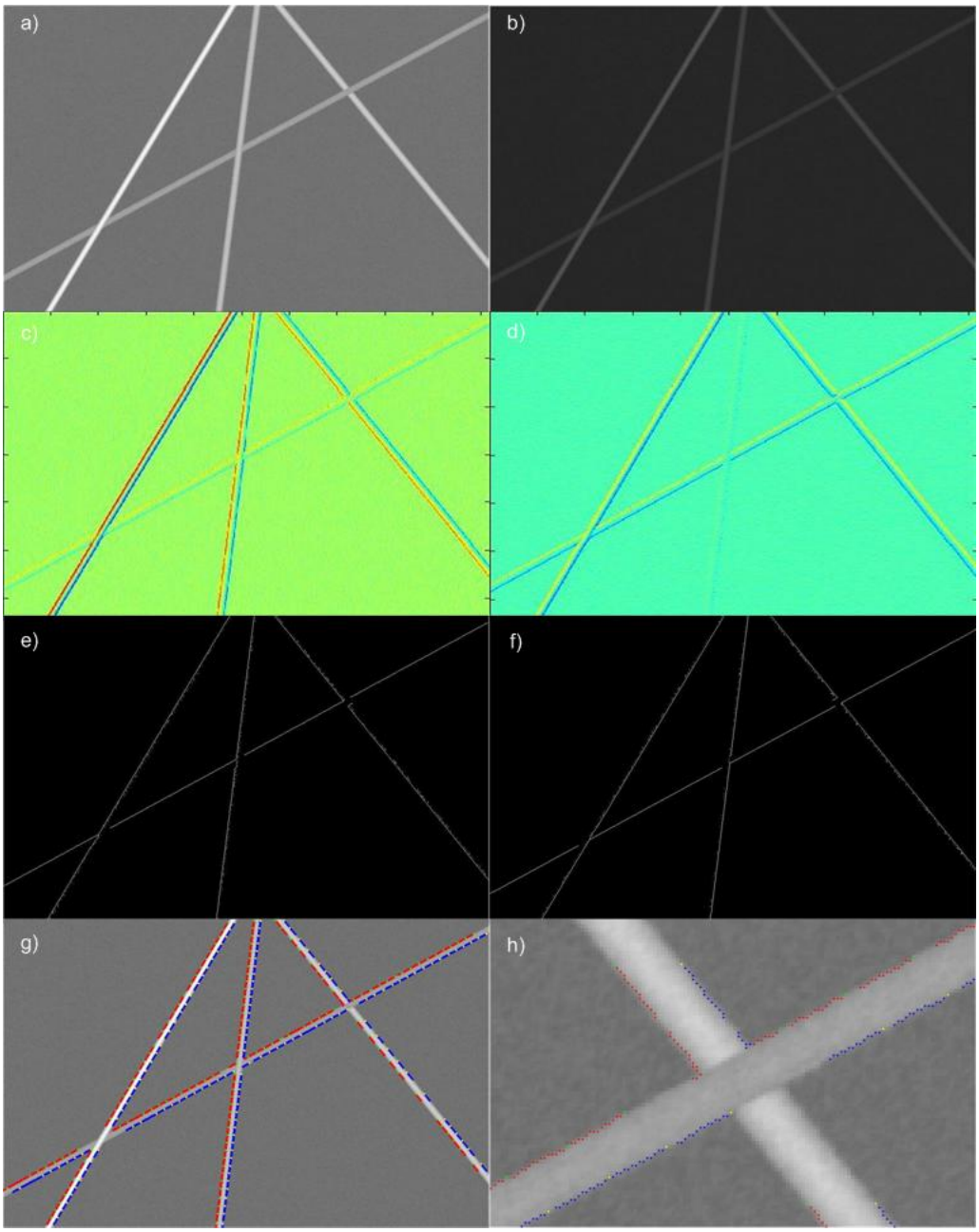

Figure 14 Image processing steps of the Custom Canny Slopes fiber diameter measurement method. a) Original simulated image, b) Filtered image c) gradient in x-direction, d), gradient in y-direction, e) left edges, f) right edges, g) selected edges superimposed over the original image, h) high magnification of (g)

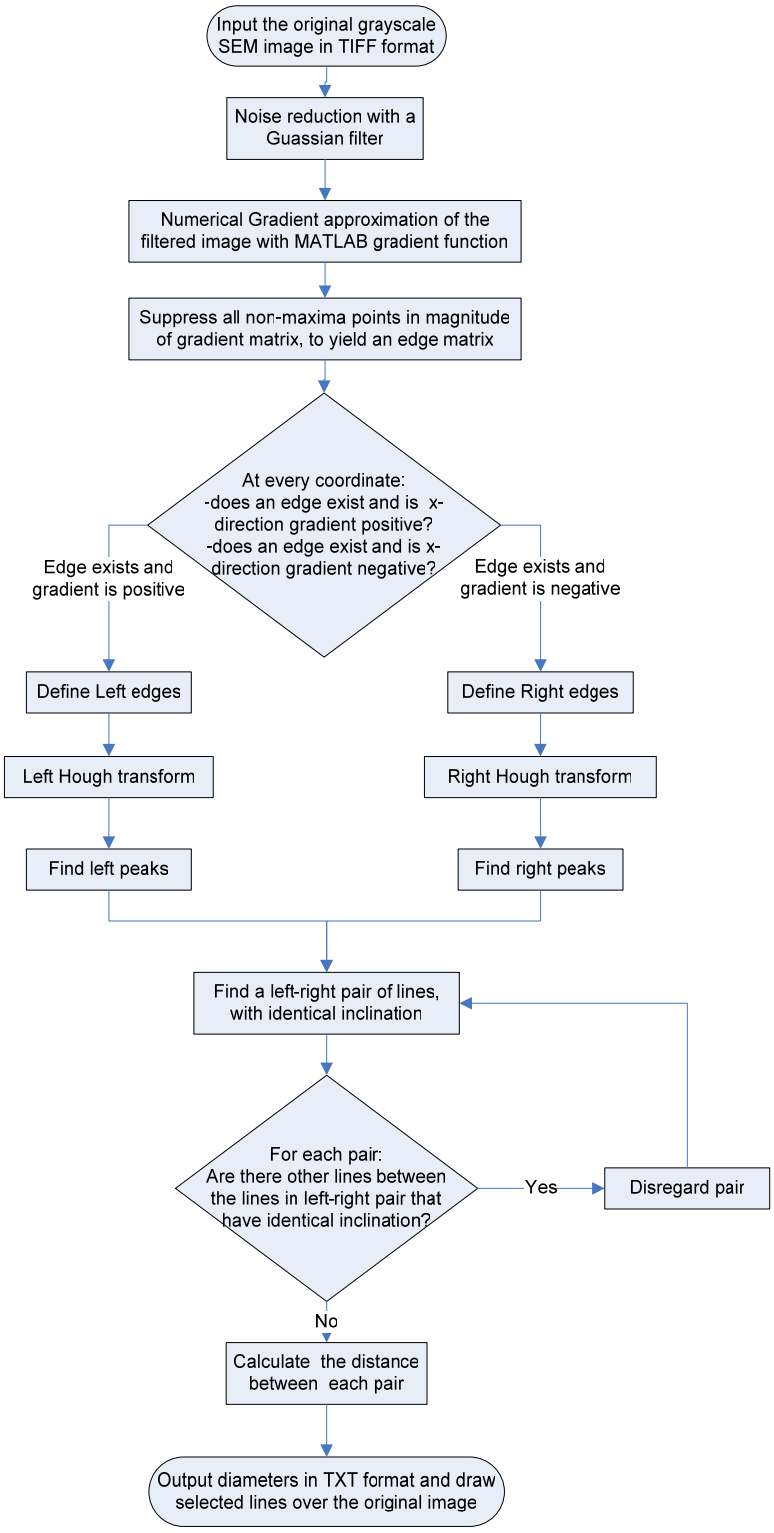

Figure 15 Custom Canny Hough Fiber Diameter Measurement Algorithm

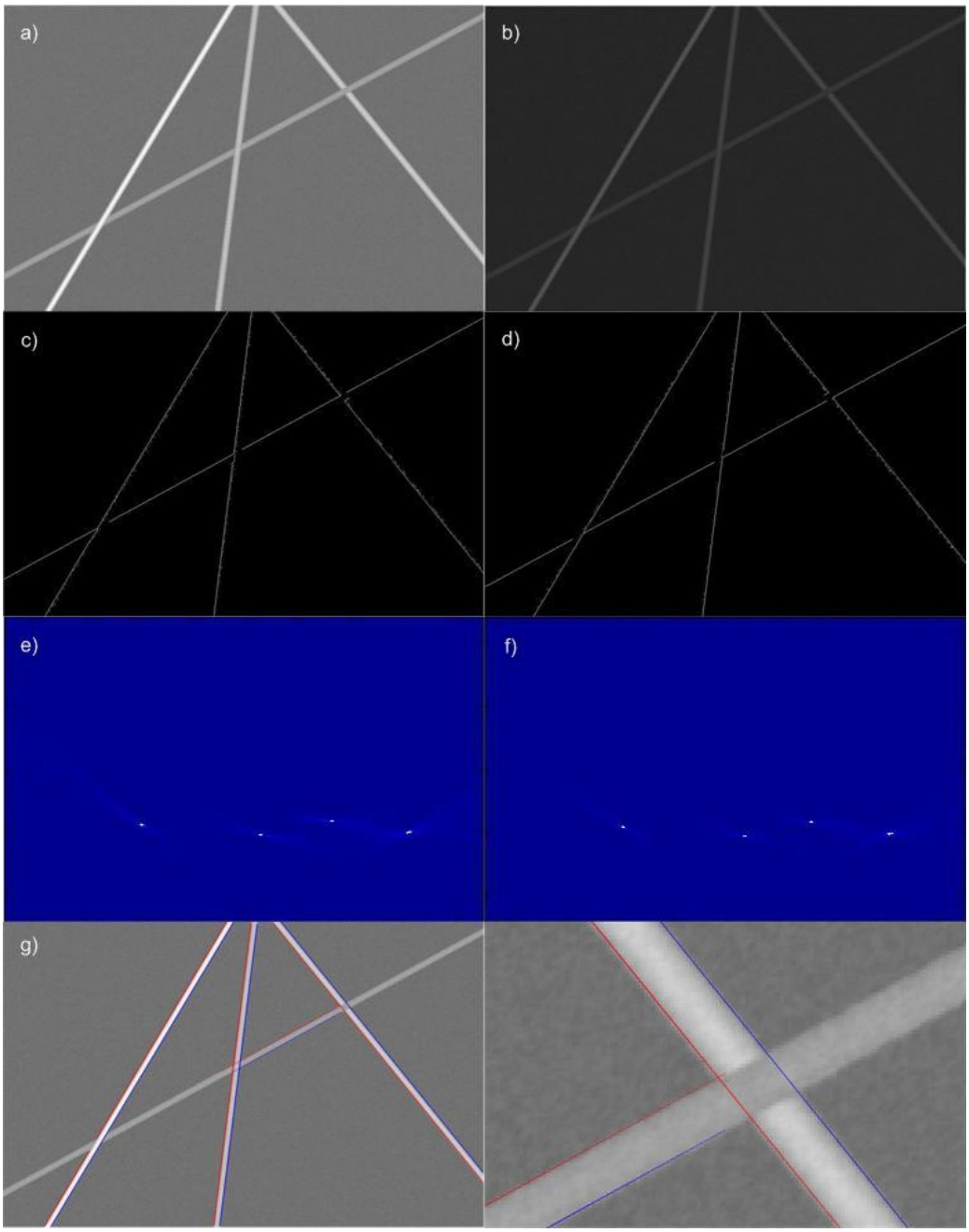

Figure 16 Image processing steps of the Custom Canny Hough fiber diameter measurement method. a) Original simulated image, b) filtered image, c) left edges, d), right edges, e) Hough transform of (c), f) Hough transform of (d), g) selected edges superimposed over the original image, h) high magnification of (g)

Results and Discussion

Overview

The graphs in Figures 17-36 demonstrate the resulting average fiber diameters ± standard deviation for all data sets per each image. Figures 37-55 show the histograms for each data set per test image. One-way ANOVA and Tukey-Kramer multiple comparison test results are summarized in Table 1, Table 2 and Table 3 for narrow fiber diameter distribution, wide fiber diameter distribution and real SEM images respectively. The names of images indicate a statistically significant difference for the pair of data acquisition methods when both methods were applied to that test image.

Manual Method Results

The accuracy of the manual method was quantitatively evaluated by manually measuring fiber diameters of simulated SEM images with known fiber diameters. As can be seen in Table 1, data sets acquired by person 1, 3, 4 and 5 were not statistically different from the known fiber diameters for any of the narrow fiber diameter distribution images. Person 2 collected data sets that were statistically different from the known fiber diameters

for images narrow10 and narrow30. For wide fiber diameter distribution, variation from the known fiber diameters was more notable, since only person 1 and person 5 collected data sets with no statistically significant differences from the known mean diameters. Persons 2 and 4 collected data sets that varied from the known for images wide15 and wide30 respectively, while person 3 collected data varying from the known for images wide10, wide25, and wide20. The variation between the accuracy of the manual method for narrow distribution fibers as opposed to wide distribution fibers can be related to the larger variation in available fiber dimensions to measure. Personal preference plays a role in which fibers are chosen for measurement, and it is possible that different people choose different fibers for measurement, resulting in differences in mean fiber diameter. This difference is not observed while processing the narrow distribution fibers due to a relative lack of choice in fiber diameters. Other sources of error include qualitatively assessing the angle of the fiber and the edges of the fiber via visual inspection instead of quantitative measures.

Tables 1, 2 and 3 also demonstrate that there are considerable statistically significant differences between measurements made by different people of the same test images. Tables 1 and 2 show that although data collected by different people may be statistically accurate compared to the known diameters, it does not mean that there is no significant difference between measurements by different people. For example person 3 and person 4 have both accurately measured the mean fiber diameters from all narrow distribution test images, but their data sets have a statistically different means for narrow15, narrow20 and narrow25.

Skeleton Slopes Fiber Diameter Measurement Results

This method showed consistent underestimation of the fiber diameters for the narrow distribution images as can be seen in Figures 17-22. It is also considerably inconsistent with the known diameters for those images as can be seen in Table 1. This method was more successful at processing the wide distribution test images than the narrow distribution images as can be seen in Table 2. Only images wide10 and wide30 were not accurately measured with this method. The sources of error for this method include the creation of the skeleton to identify the relative position of the fibers, and the accuracy of the location of the edges found for each fiber. Due to the conversion to a binary image, some fibers fuse into one, and the skeleton only reflects the position of one of the fibers, therefore some fibers are not measured even if their edges were found during edge detection. This method is very sensitive to accurate conversion to a binary image, which cannot be accurately standardized for all images. The binary conversion parameters can vary from image to image increasing the need for user input and rendering this method impractical.

When compared to the manually obtained data for real SEM images, this method yielded some statistically significant differences. It is difficult to asses the validity of such comparison, since there are no known fiber diameters for these images, and inconsistencies with some of the people data does not necessarily translate to inaccurate measurements.

Canny Slopes Fiber Diameter Measurement Results

This method was shown to process a larger number of fibers compared to the previous method. However the accuracy of this measurement does not appear to surpass the accuracy of the previous method as can be seen in Table 1 and Table 2, when comparing this method (DCS) with the known (act) diameters. Table 2 does show a considerable reduction in error, since there was a significant error in processing only two images. The major source of error is therefore the detection of the location of the edges of the fibers as opposed to fiber selection bias. As can be seen in Table 3, this method found statistically different mean fiber diameters from all manually acquired measurements of almost all real SEM images. This result in combination with the inaccurate measurements of known fiber diameter data, indicates that this method is not ideal for fiber diameter measurement of electrospun scaffolds.

Canny Hough Fiber Diameter Measurement Results

The results of this method also show significant inaccuracies based on comparison to known fiber diameters with narrow distribution, which is illustrated in Table 1 while comparing this method (DCH) with known (act) diameters. This measurement method applied to wide fiber diameter distribution test images yielded only two statistically

different results for wide10 and wide15. The differences between this method and manually acquired data for real SEM images can be seen in Table 3. It is highly likely that this method produced an inaccurate measurement for SEM5, SEM6 and SEM7 since it did not agree with any of the manually acquired data sets for these images. It is unlikely that all manually acquired data sets for these images are inaccurate. Since the previous two methods and this method differ in the way they find pairs of valid edges, but are the same in the way they determine the edge locations, the major source of error for this method is the same as the previous two methods. The edge location it appears to be inaccurate, rendering any methods using this edge location technique, impractical. An added source of error for this method is the requirement that the fibers a linear, since a straight line equation is fitted to the points on edges found. The real SEM images that had many curved fibers yielded fewer measurements with this method, since fewer long straight segments existed in the image.

Custom Canny Slopes Fiber Diameter Measurement Results

The accuracy of the Custom Canny Slopes (CCS) method has been validated by comparison to the known mean diameters, which can be seen in Table 1 and Table 2. The mean diameters acquired with this method were not statistically different from any of known diameters for the narrow and wide distribution test images. As can be observed in Table 3, when this method was applied to real SEM images of electrospun scaffolds, the

mean diameters measured with this method were consistent with at least one or more manually obtained fiber diameter means for the corresponding images. This method is therefore considered to be an equivalent alternative to the manual measurement of fiber diameters form processing of SEM images.

Custom Canny Hough Fiber Diameter Measurement Results

This method performed in a similar way to the Custom Canny Slopes Method, as can be see in Table 1 and Table 2 when comparing this method (CCH) to the know fiber diameters (act). There was a considerable drawback to this method, when it was applied to real SEM images. It performed reasonably well, when processing images with straight fibers, however due to its inherent feature of linear fit to edges for the selection of valid edge pairs; it was not able to process SEM images with a large proportion of curved fibers as can be seen in Table 3 for SEM5 and SEM7. The SEM images that had relatively straight fibers were processed with statistically equivalent results to three or more manually obtained fiber diameter means for corresponding images. This method is therefore considered to be equivalent to the manual measurement of fiber diameters of electrospun scaffolds with straight fibers.

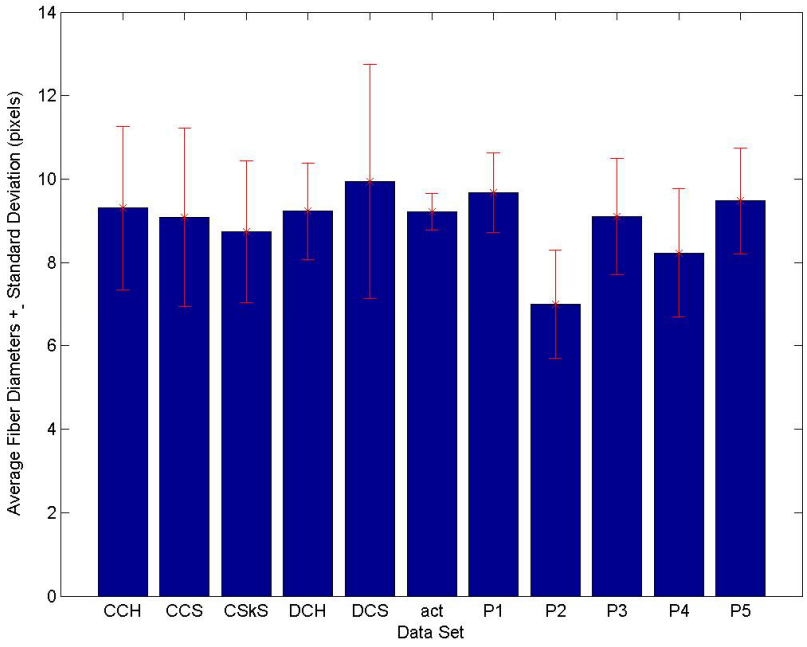

Figure 17 Average fiber diameters for narrow10

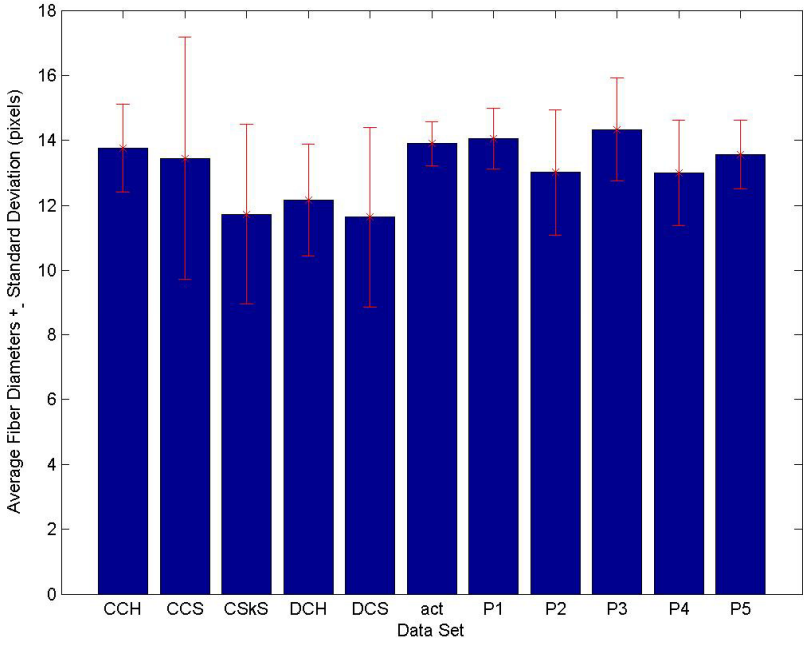

Figure 18 Average fiber diameters for narrow15

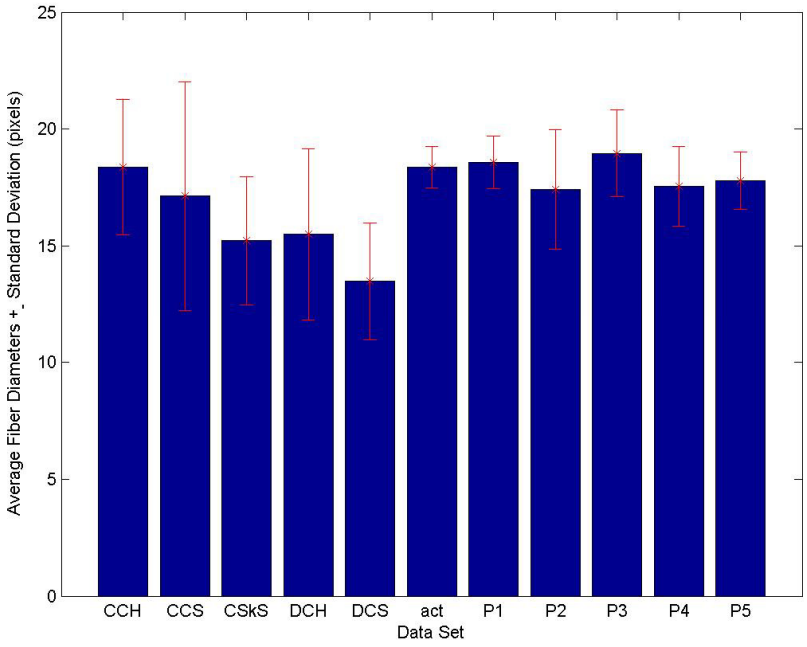

Figure 19 Average fiber diameters for narrow20

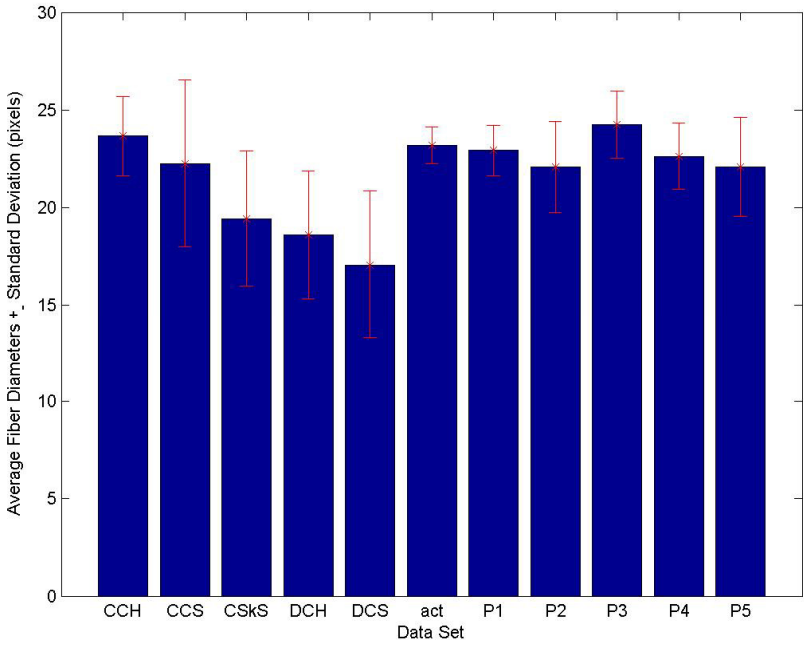

Figure 20 Average fiber diameters for narrow25

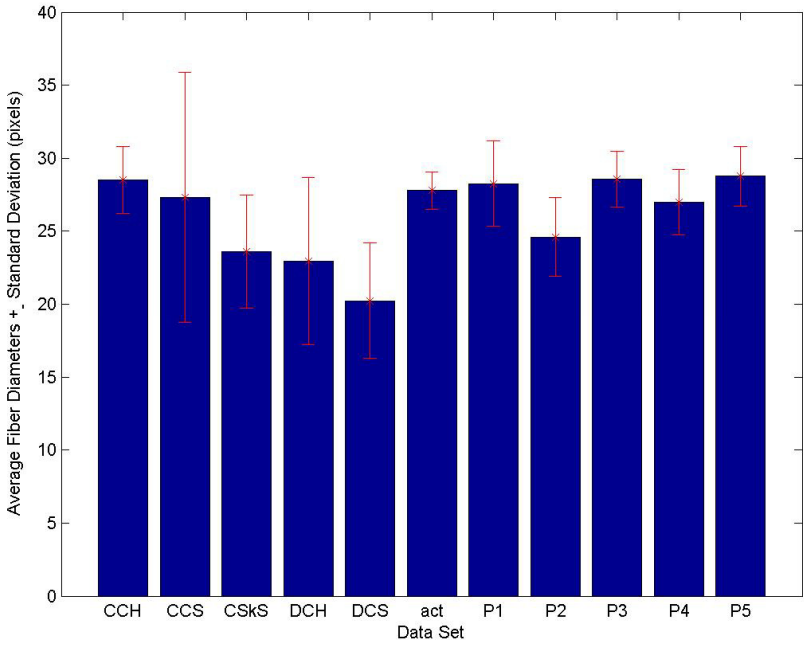

Figure 21 Average fiber diameters for narrow30

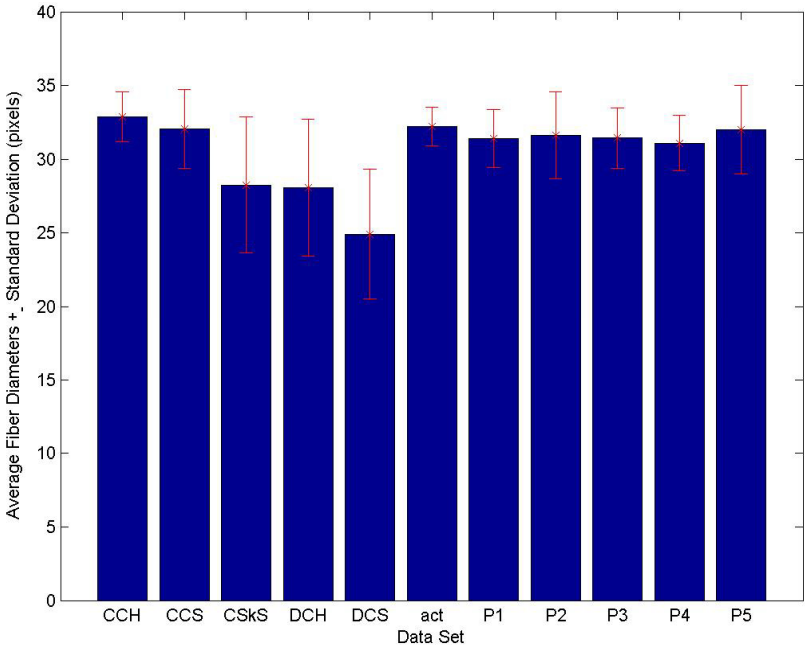

Figure 22 Average fiber diameters for narrow35

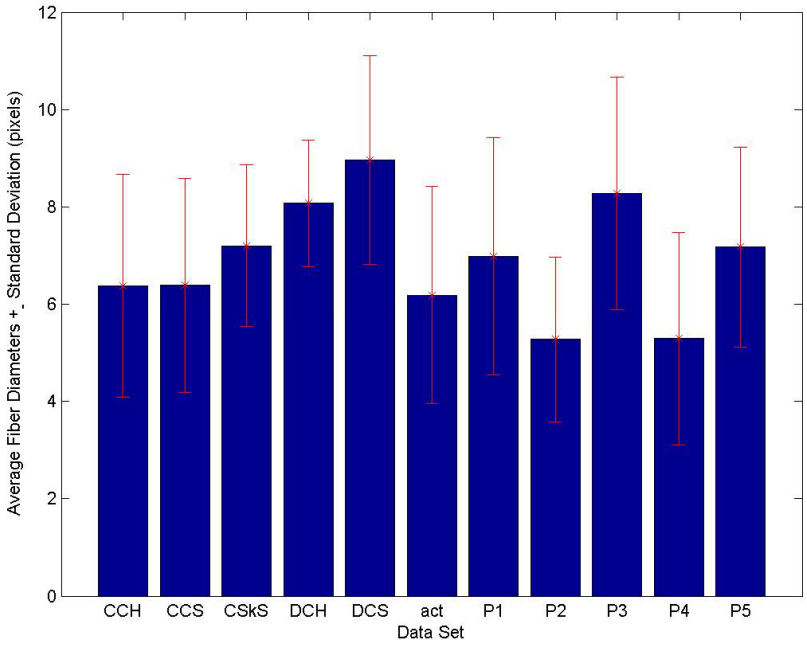

Figure 23 Average fiber diameters for wide10

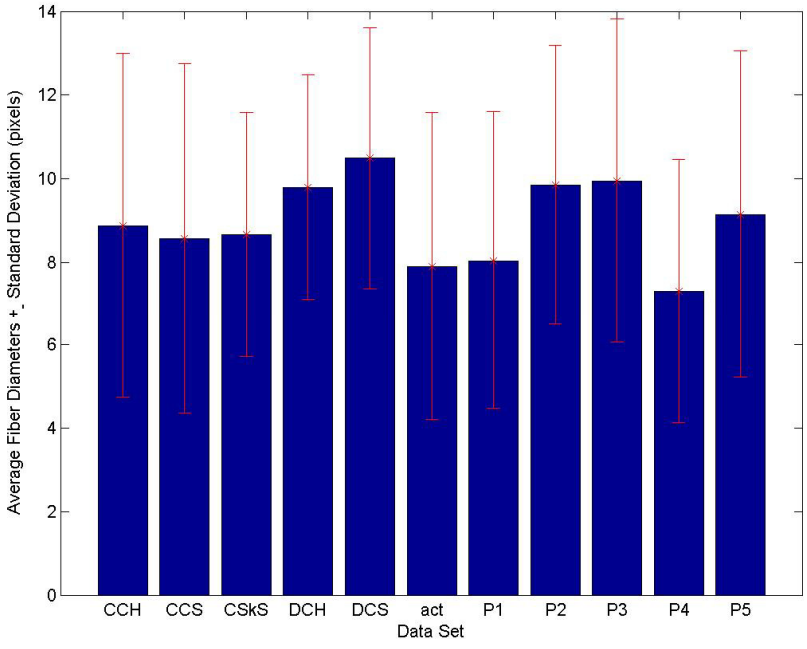

Figure 24 Average fiber diameters for wide15

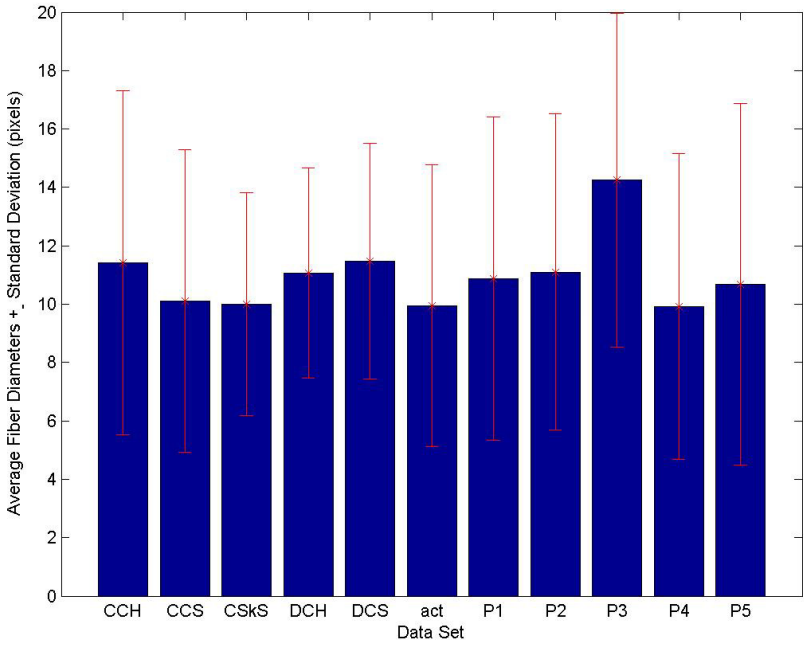

Figure 25 Average fiber diameters for wide20

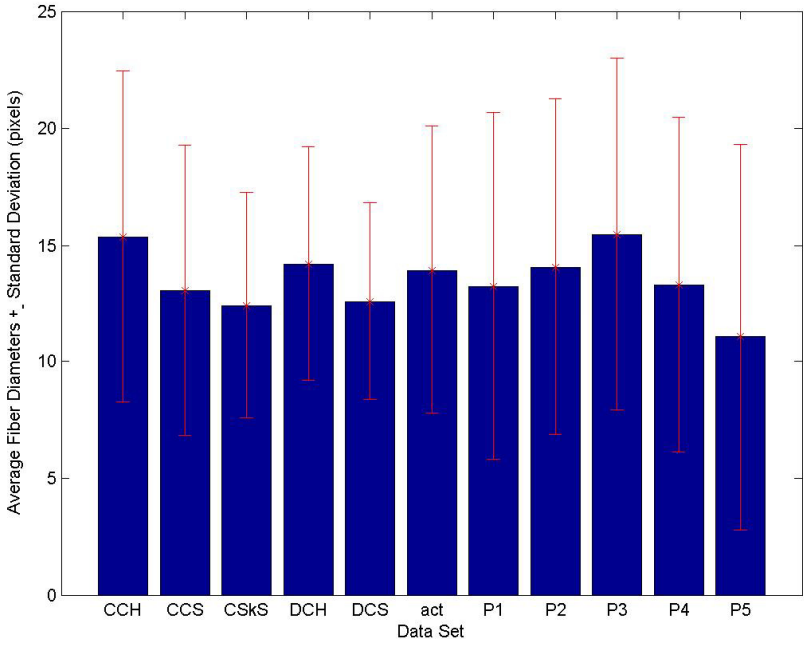

Figure 26 Average fiber diameters for wide25

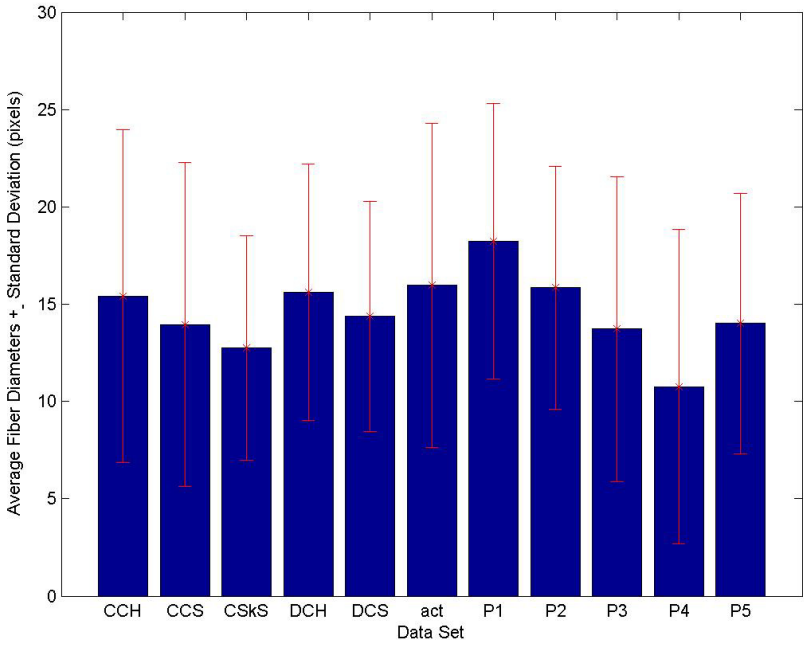

Figure 27 Average fiber diameters for wide30

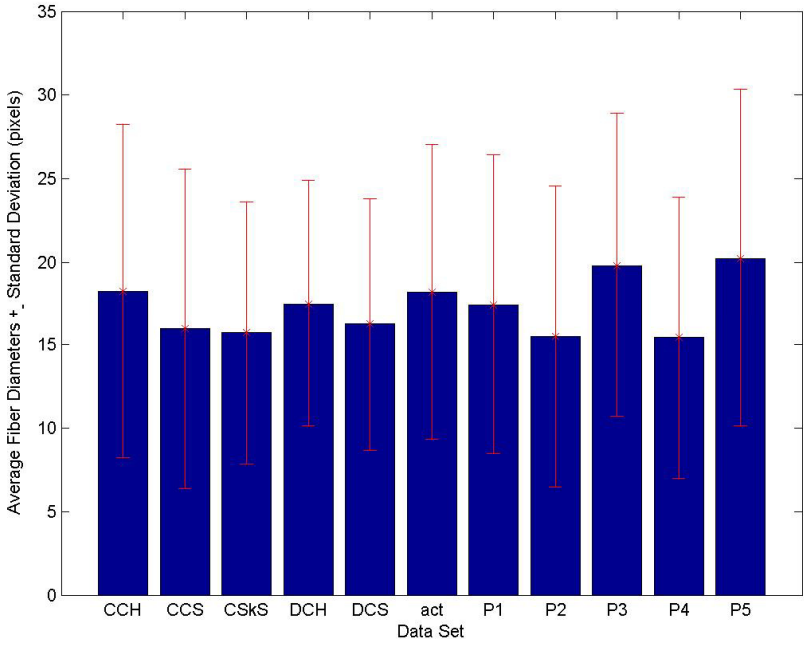

Figure 28 Average fiber diameters for wide35

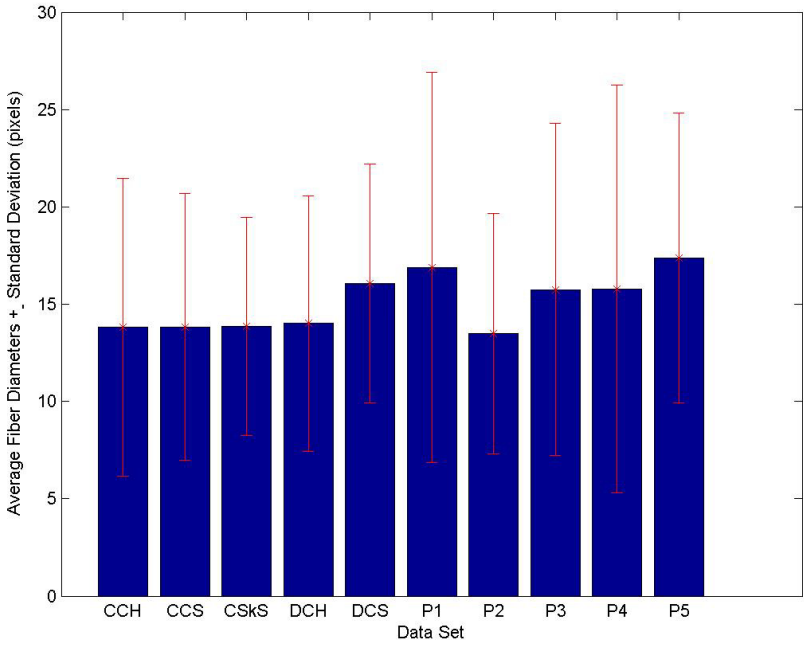

Figure 29 Average fiber diameters for SEM1

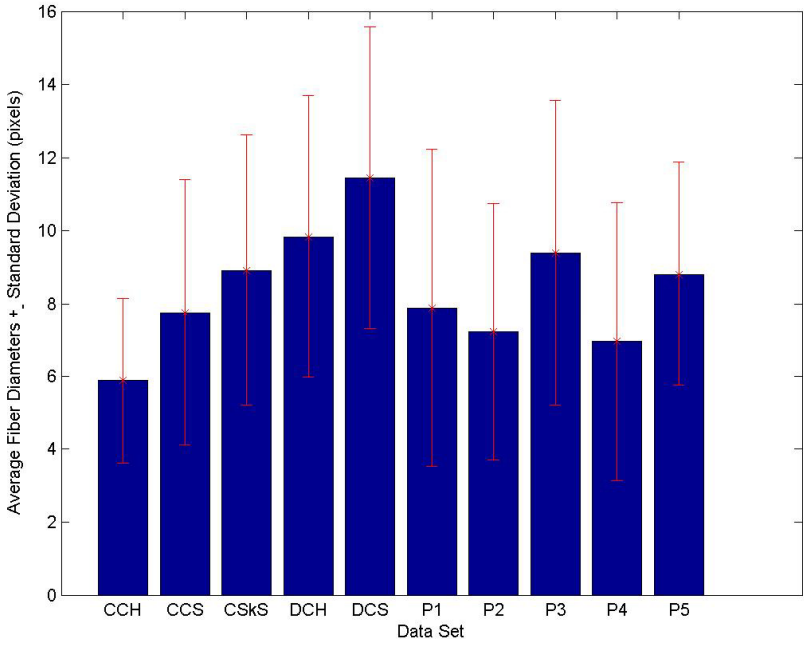

Figure 30 Average fiber diameters for SEM2

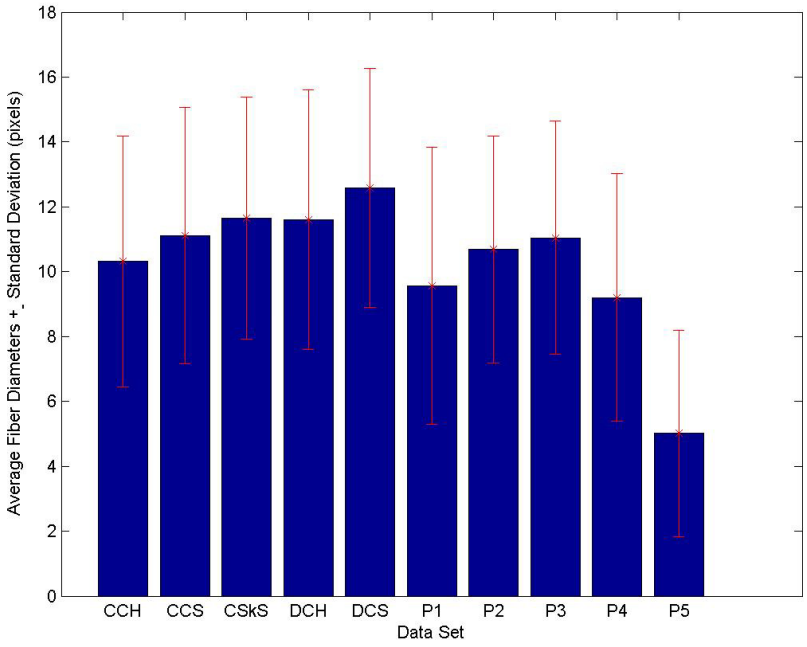

Figure 31 Average fiber diameters for SEM3

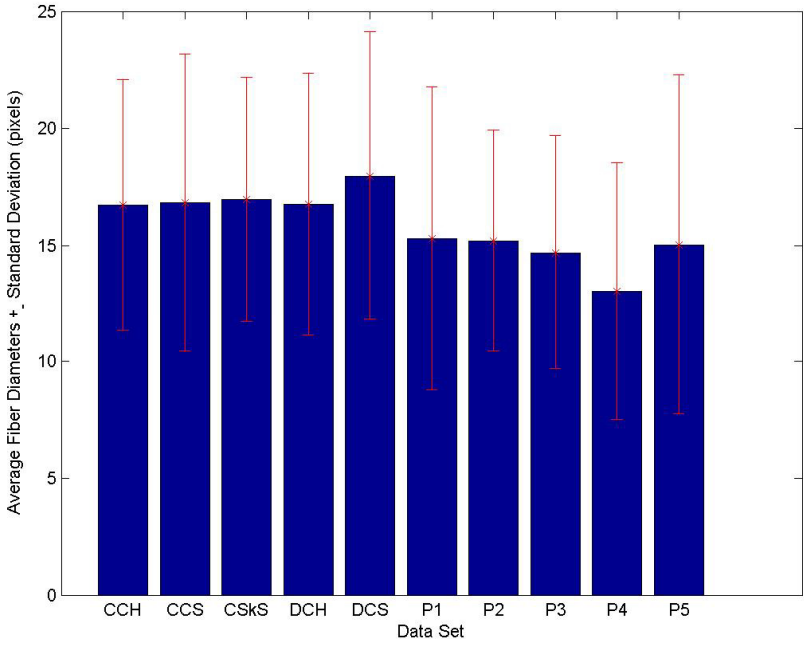

Figure 32 Average fiber diameters for SEM4

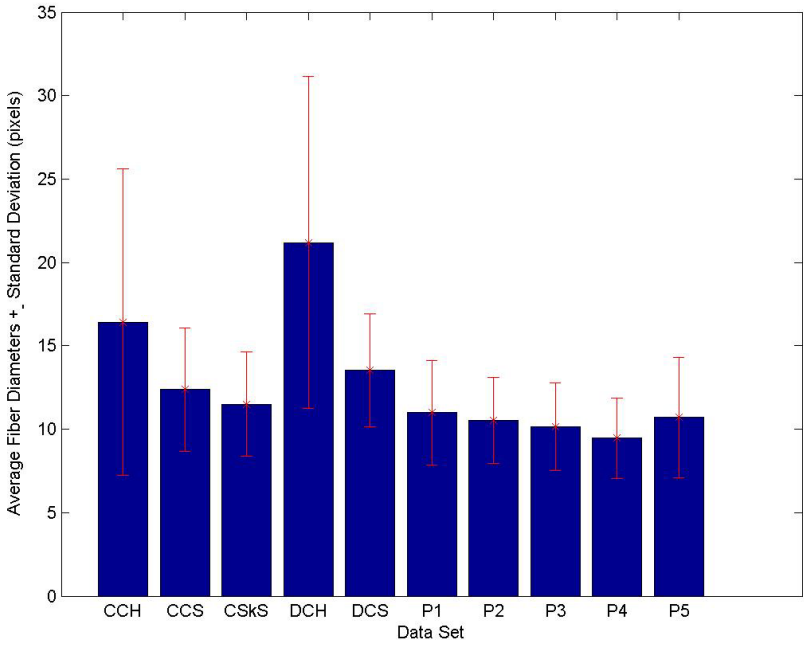

Figure 33 Average fiber diameters for SEM5

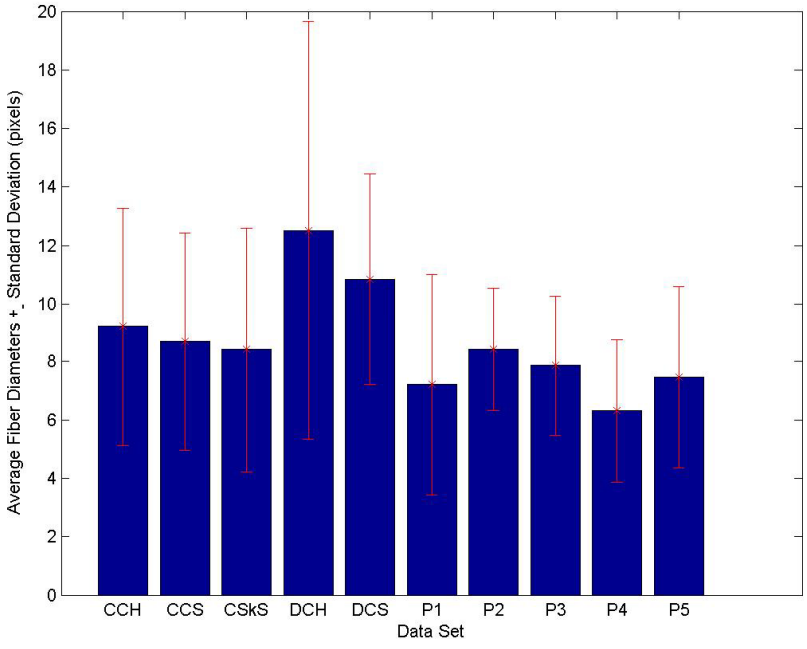

Figure 34 Average fiber diameters for SEM6

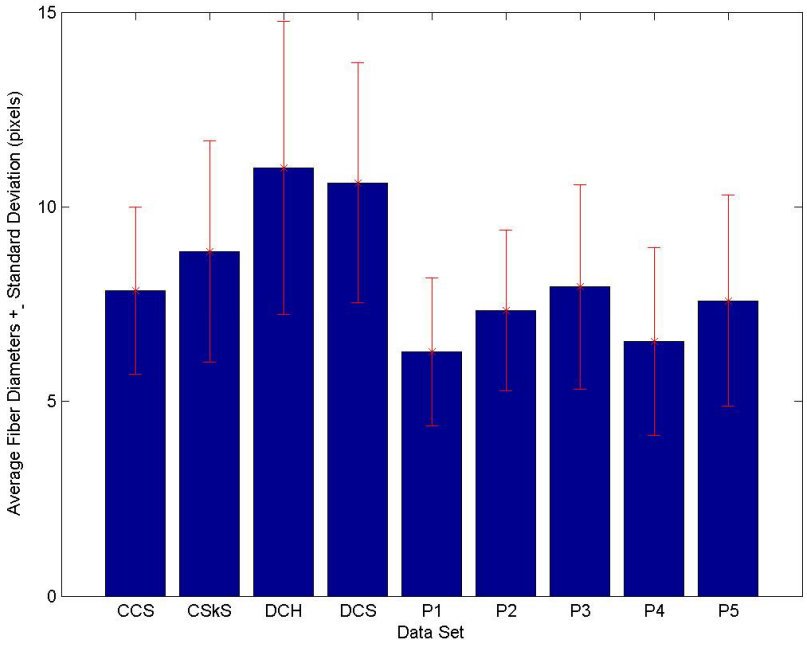

Figure 35 Average fiber diameters for SEM7

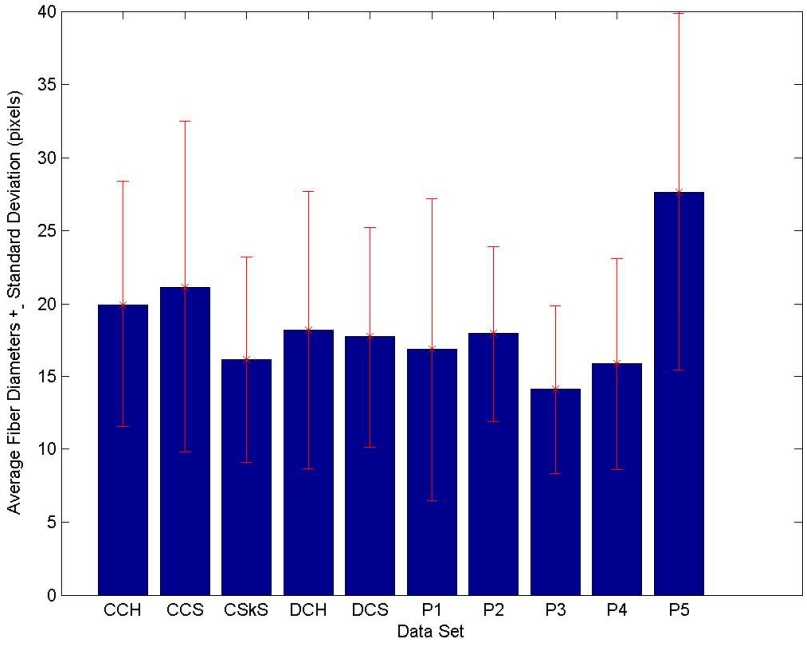

Figure 36 Average fiber diameters for SEM8

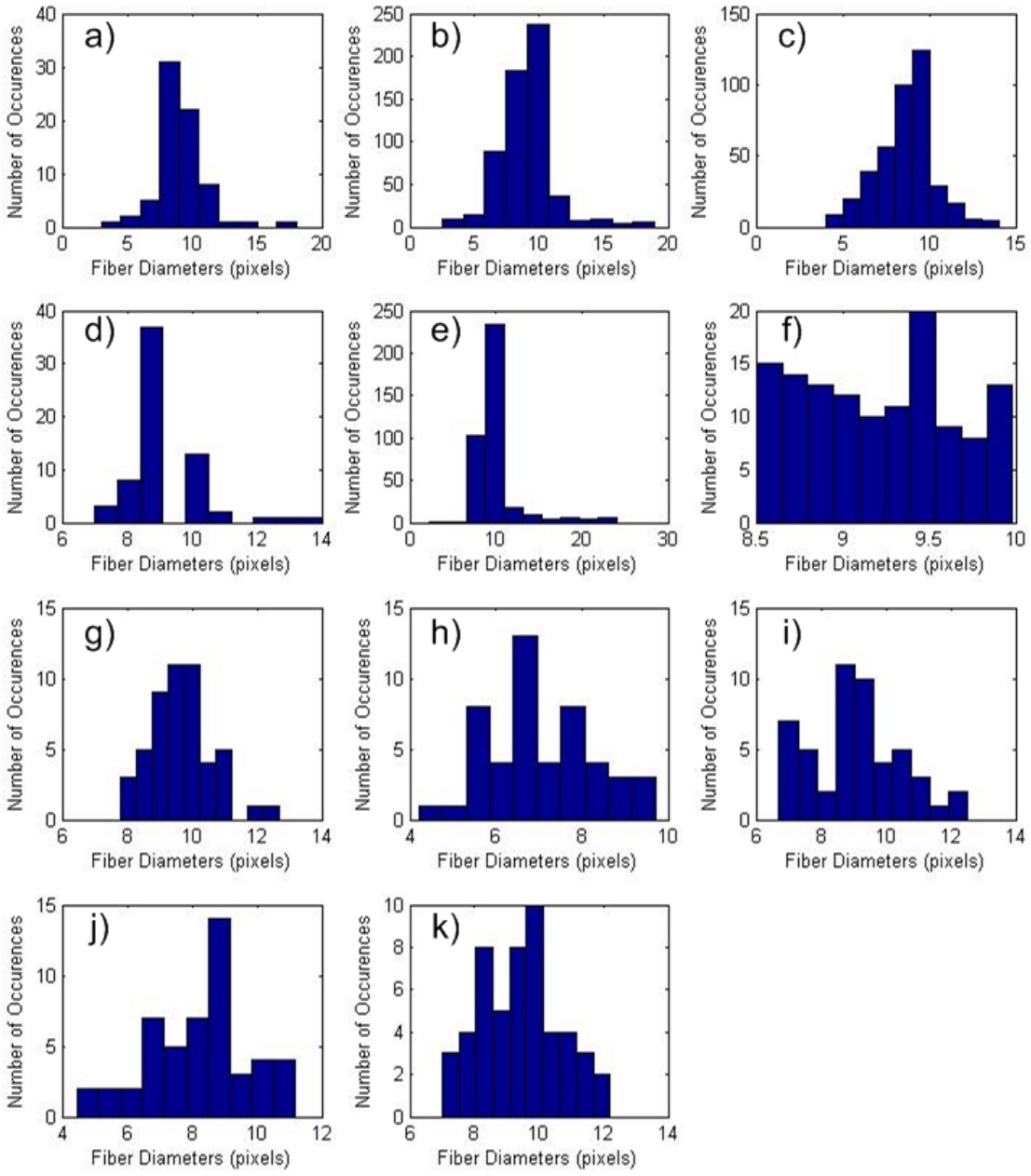

Figure 37 Histograms for all fiber diameter measurements of image narrow10. a) Custom Canny Hough measurement, b) Custom Canny Slopes measurement, c) Skeleton Slopes measurement, d) Canny Hough measurement, e) Canny Slopes Measurement, f) known fiber diameters, g) Person 1 measurement, h) Person 2 measurement, i) Person 3 measurement, j) Person 4 measurement, k) Person 5 measurement

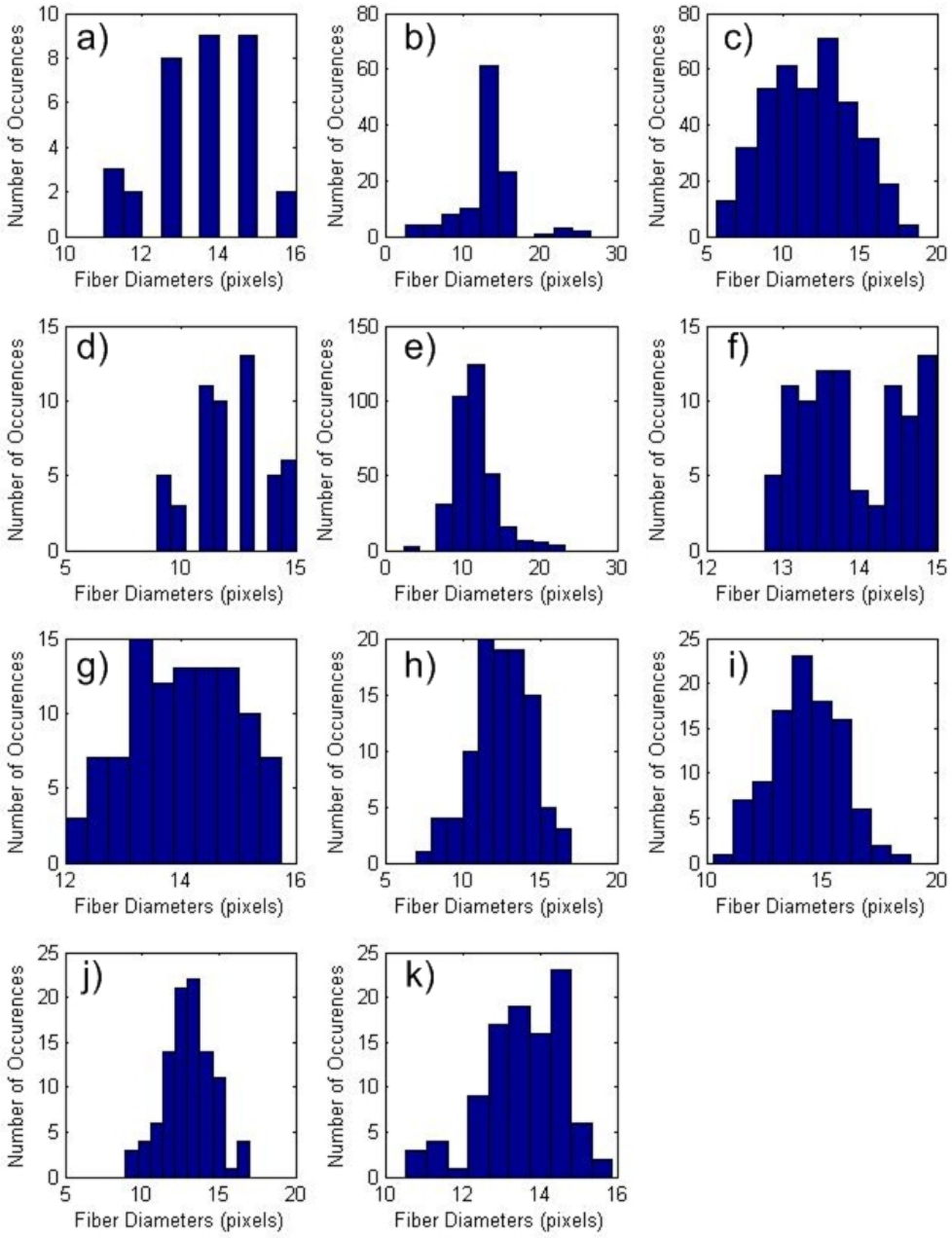

Figure 38 Histograms for all fiber diameter measurements of image narrow15. a) Custom Canny Hough measurement, b) Custom Canny Slopes measurement, c) Skeleton Slopes measurement, d) Canny Hough measurement, e) Canny Slopes Measurement, f) known fiber diameters, g) Person 1 measurement, h) Person 2 measurement, i) Person 3 measurement, j) Person 4 measurement, k) Person 5 measurement

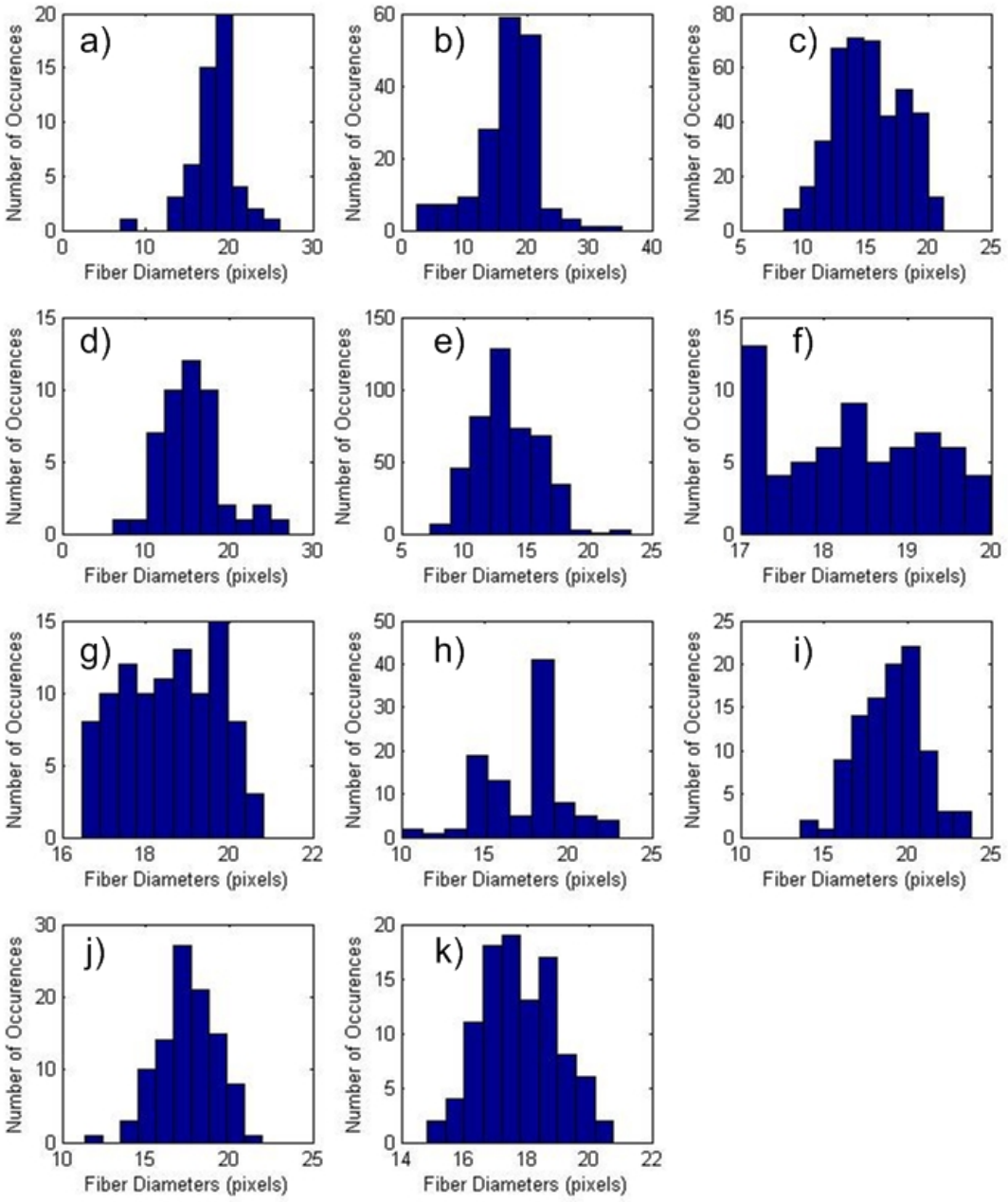

Figure 39 Histograms for all fiber diameter measurements of image narrow20. a) Custom Canny Hough measurement, b) Custom Canny Slopes measurement, c) Skeleton Slopes measurement, d) Canny Hough measurement, e) Canny Slopes Measurement, f) known fiber diameters, g) Person 1 measurement, h) Person 2 measurement, i) Person 3 measurement, j) Person 4 measurement, k) Person 5 measurement

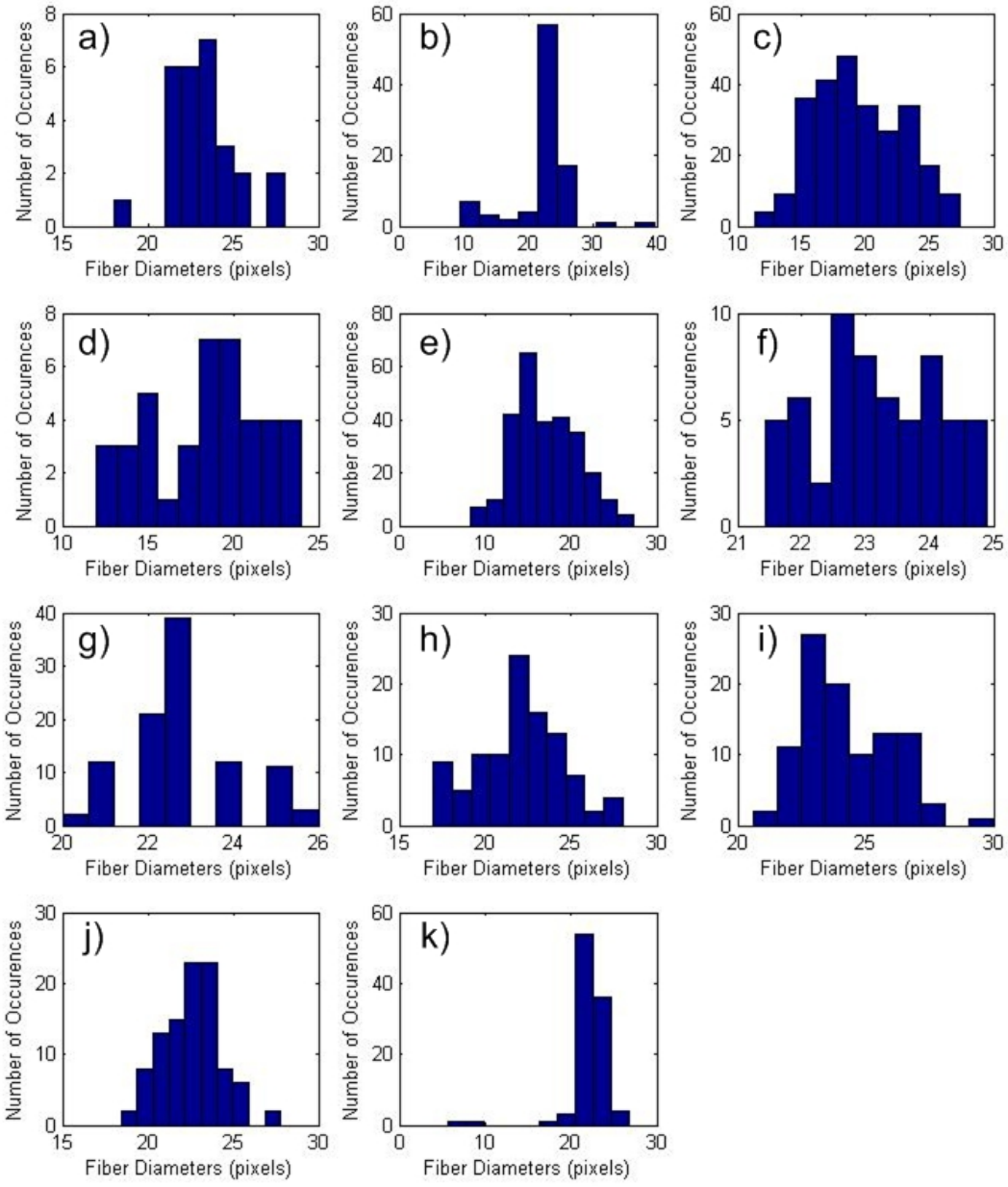

Figure 40 Histograms for all fiber diameter measurements of image narrow25. a) Custom Canny Hough measurement, b) Custom Canny Slopes measurement, c) Skeleton Slopes measurement, d) Canny Hough measurement, e) Canny Slopes Measurement, f) known fiber diameters, g) Person 1 measurement, h) Person 2 measurement, i) Person 3 measurement, j) Person 4 measurement, k) Person 5 measurement

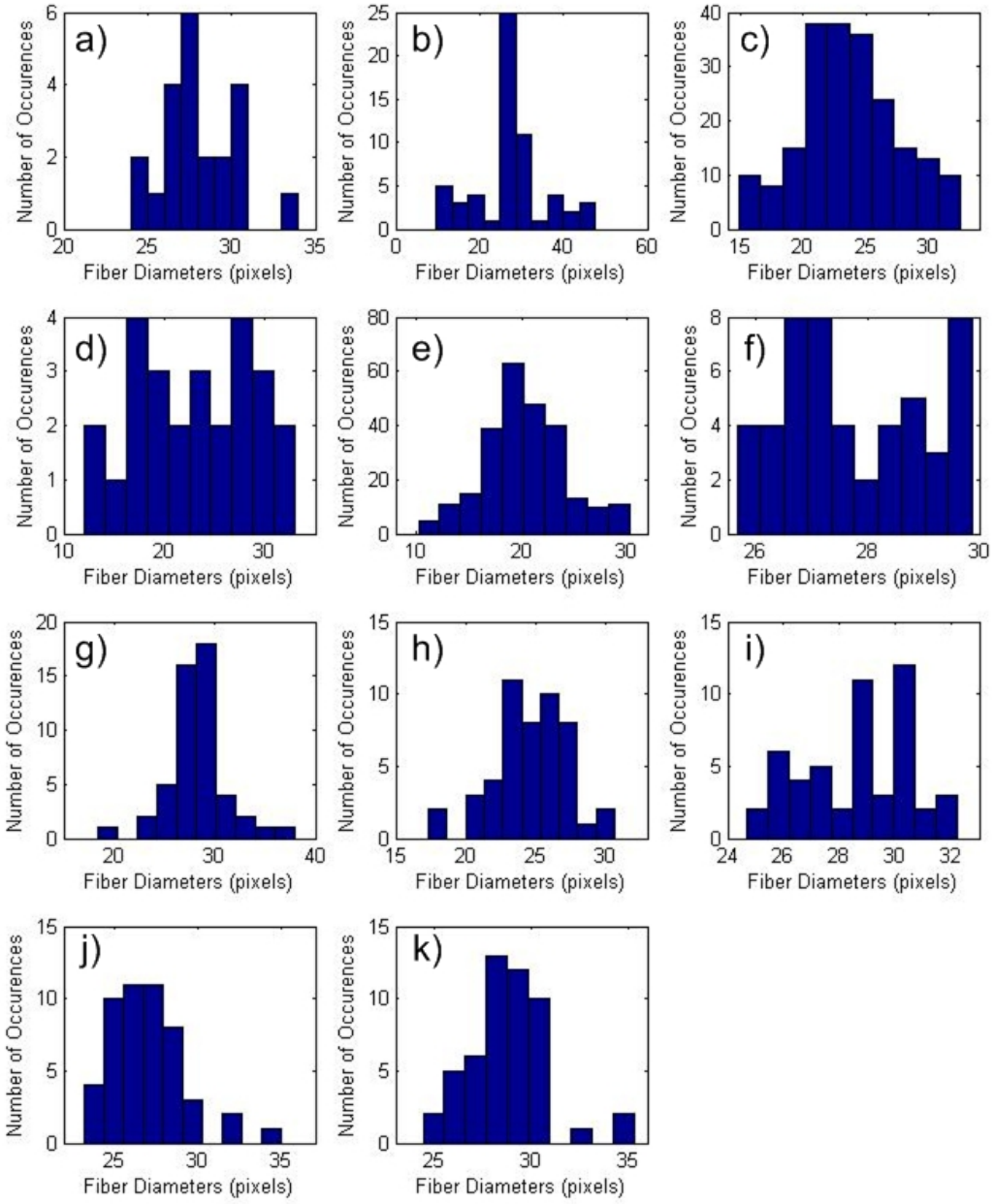

Figure 41 Histograms for all fiber diameter measurements of image narrow30. a) Custom Canny Hough measurement, b) Custom Canny Slopes measurement, c) Skeleton Slopes measurement, d) Canny Hough measurement, e) Canny Slopes Measurement, f) known fiber diameters, g) Person 1 measurement, h) Person 2 measurement, i) Person 3 measurement, j) Person 4 measurement, k) Person 5 measurement

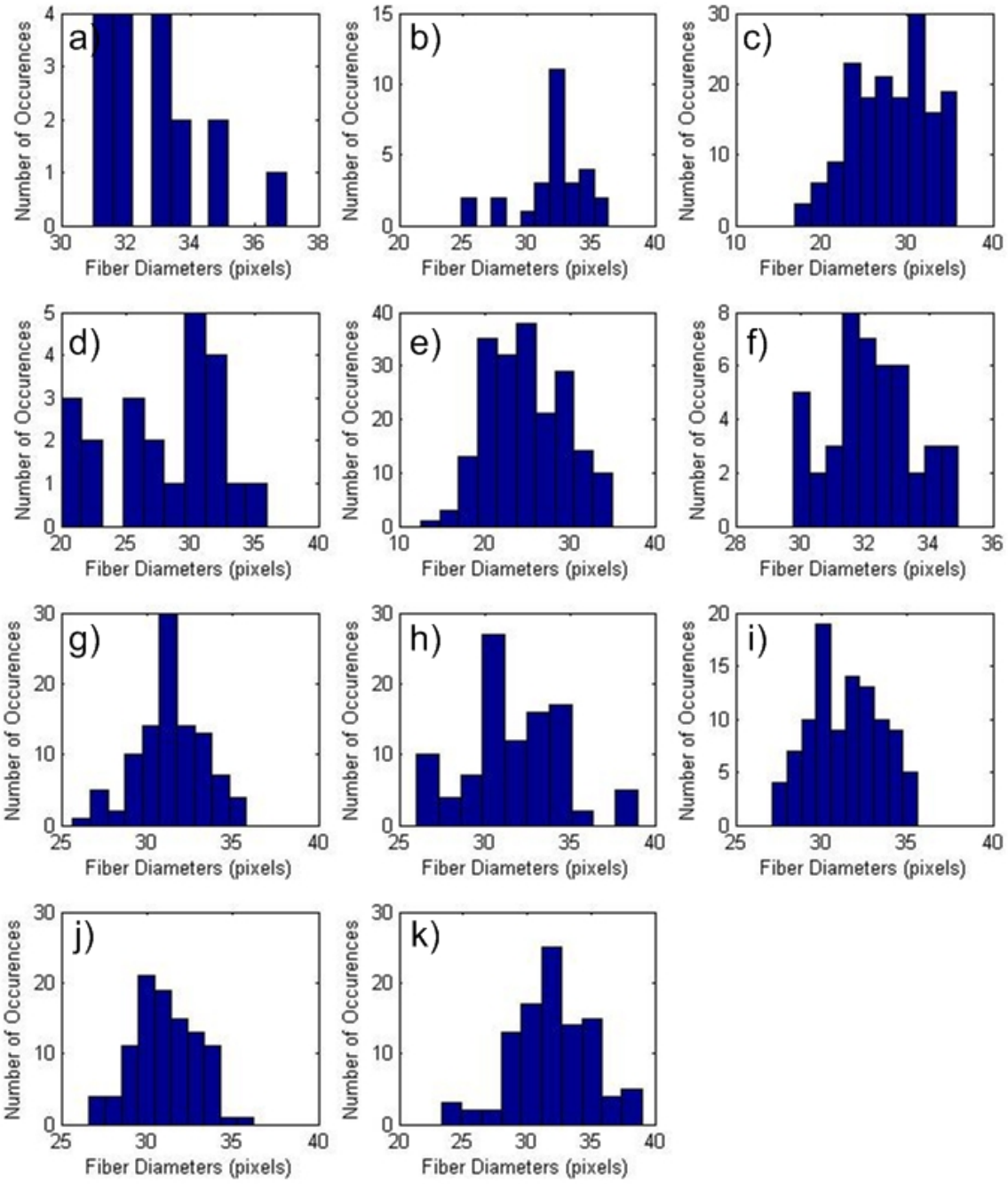

Figure 42 Histograms for all fiber diameter measurements of image narro35. a) Custom Canny Hough measurement, b) Custom Canny Slopes measurement, c) Skeleton Slopes measurement, d) Canny Hough measurement, e) Canny Slopes Measurement, f) known fiber diameters, g) Person 1 measurement, h) Person 2 measurement, i) Person 3 measurement, j) Person 4 measurement, k) Person 5 measurement

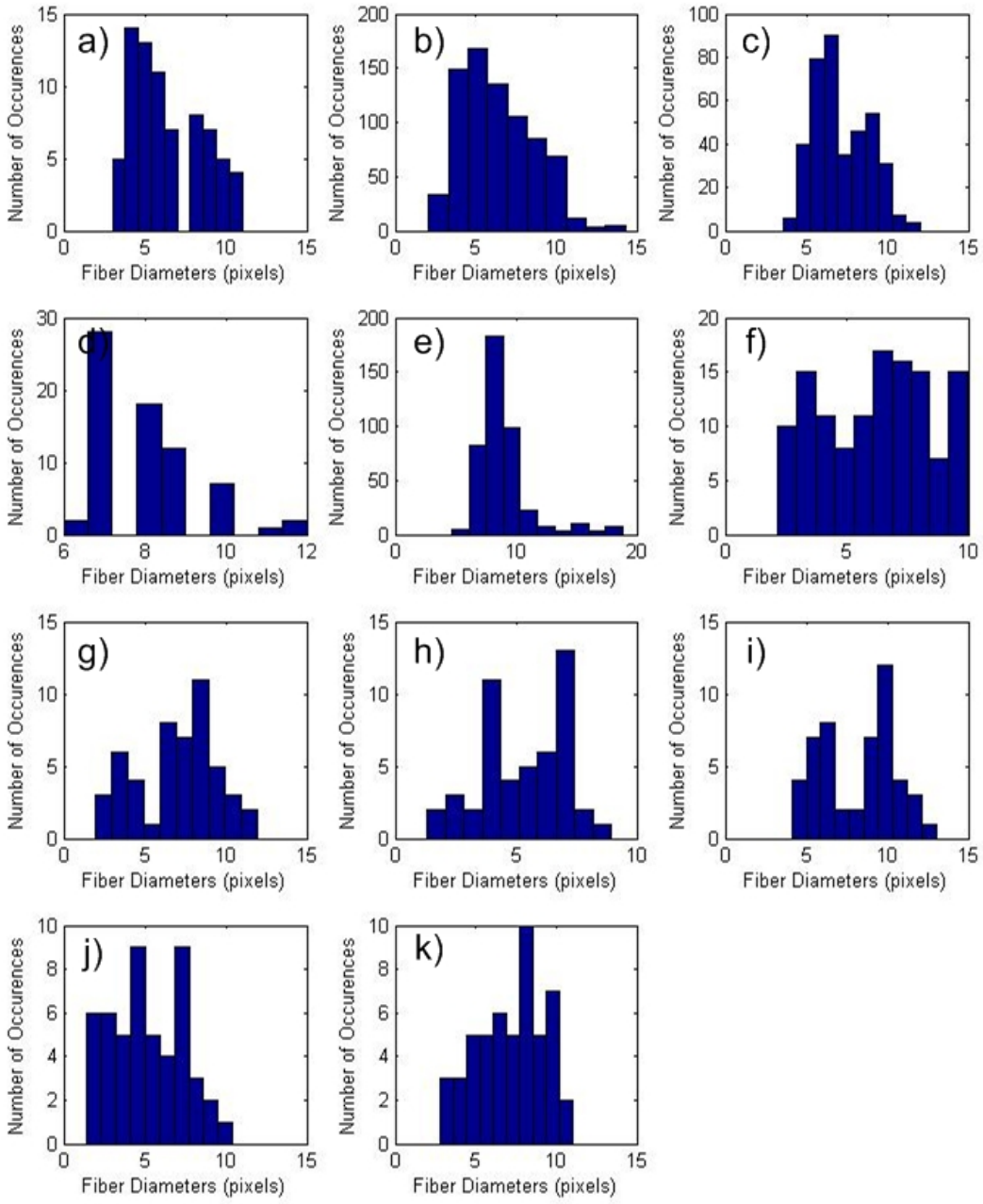

Figure 43 Histograms for all fiber diameter measurements of image wide10. a) Custom Canny Hough measurement, b) Custom Canny Slopes measurement, c) Skeleton Slopes measurement, d) Canny Hough measurement, e) Canny Slopes Measurement, f) known fiber diameters, g) Person 1 measurement, h) Person 2 measurement, i) Person 3 measurement, j) Person 4 measurement, k) Person 5 measurement

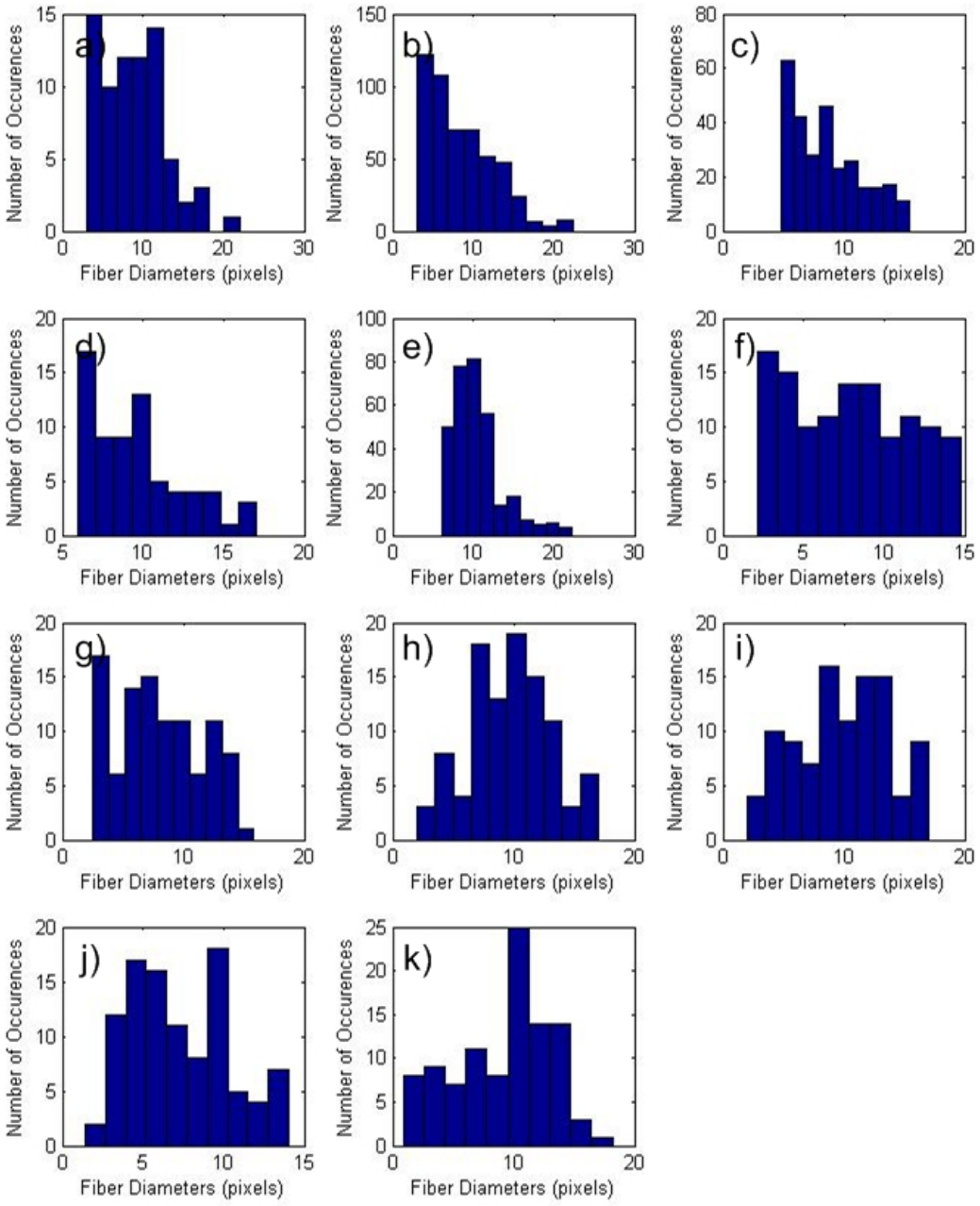

Figure 44 Histograms for all fiber diameter measurements of image wide15. a) Custom Canny Hough measurement, b) Custom Canny Slopes measurement, c) Skeleton Slopes measurement, d) Canny Hough measurement, e) Canny Slopes Measurement, f) known fiber diameters, g) Person 1 measurement, h) Person 2 measurement, i) Person 3 measurement, j) Person 4 measurement, k) Person 5 measurement

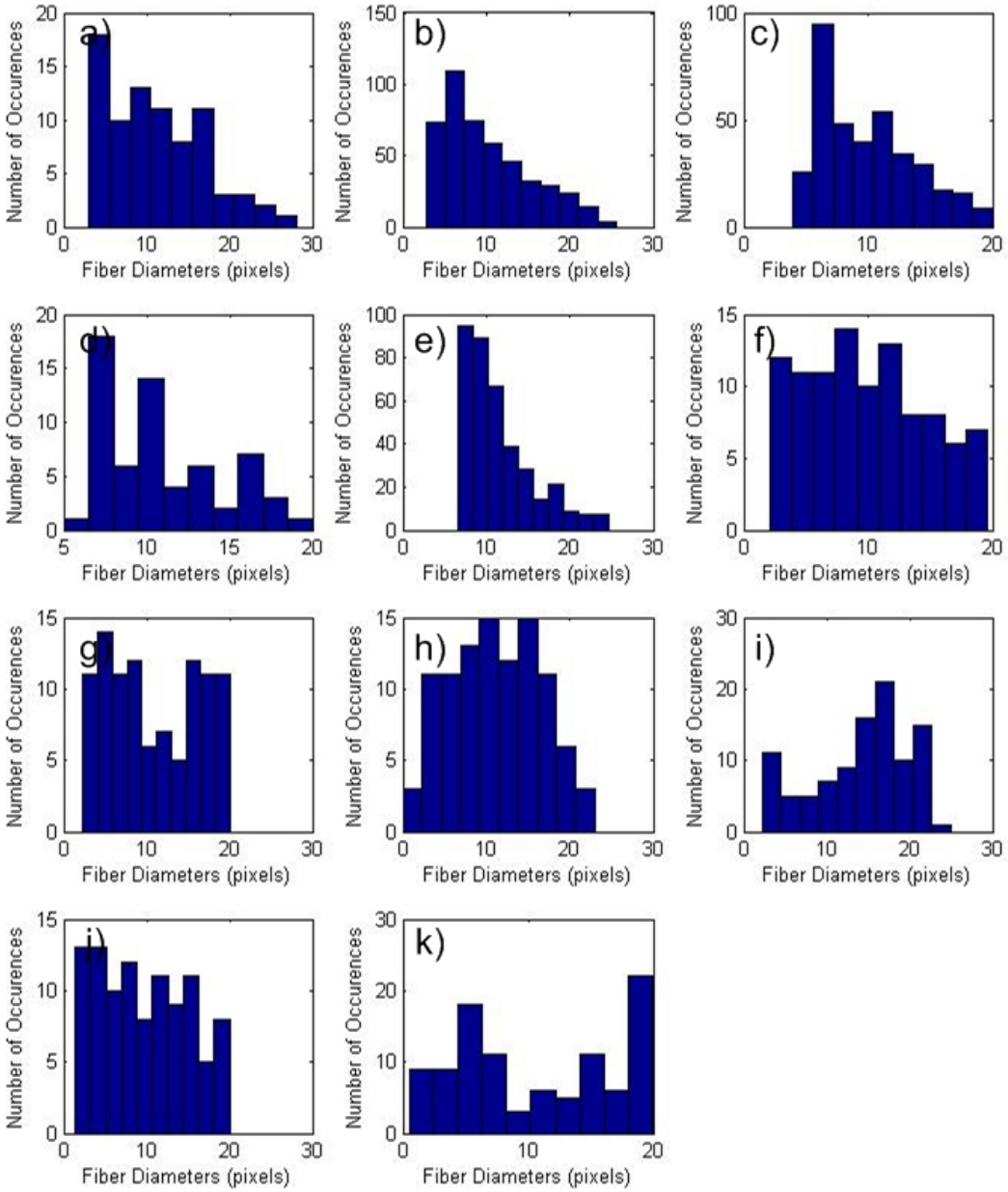

Figure 45 Histograms for all fiber diameter measurements of image wide20. a) Custom Canny Hough measurement, b) Custom Canny Slopes measurement, c) Skeleton Slopes measurement, d) Canny Hough measurement, e) Canny Slopes Measurement, f) known fiber diameters, g) Person 1 measurement, h) Person 2 measurement, i) Person 3 measurement, j) Person 4 measurement, k) Person 5 measurement

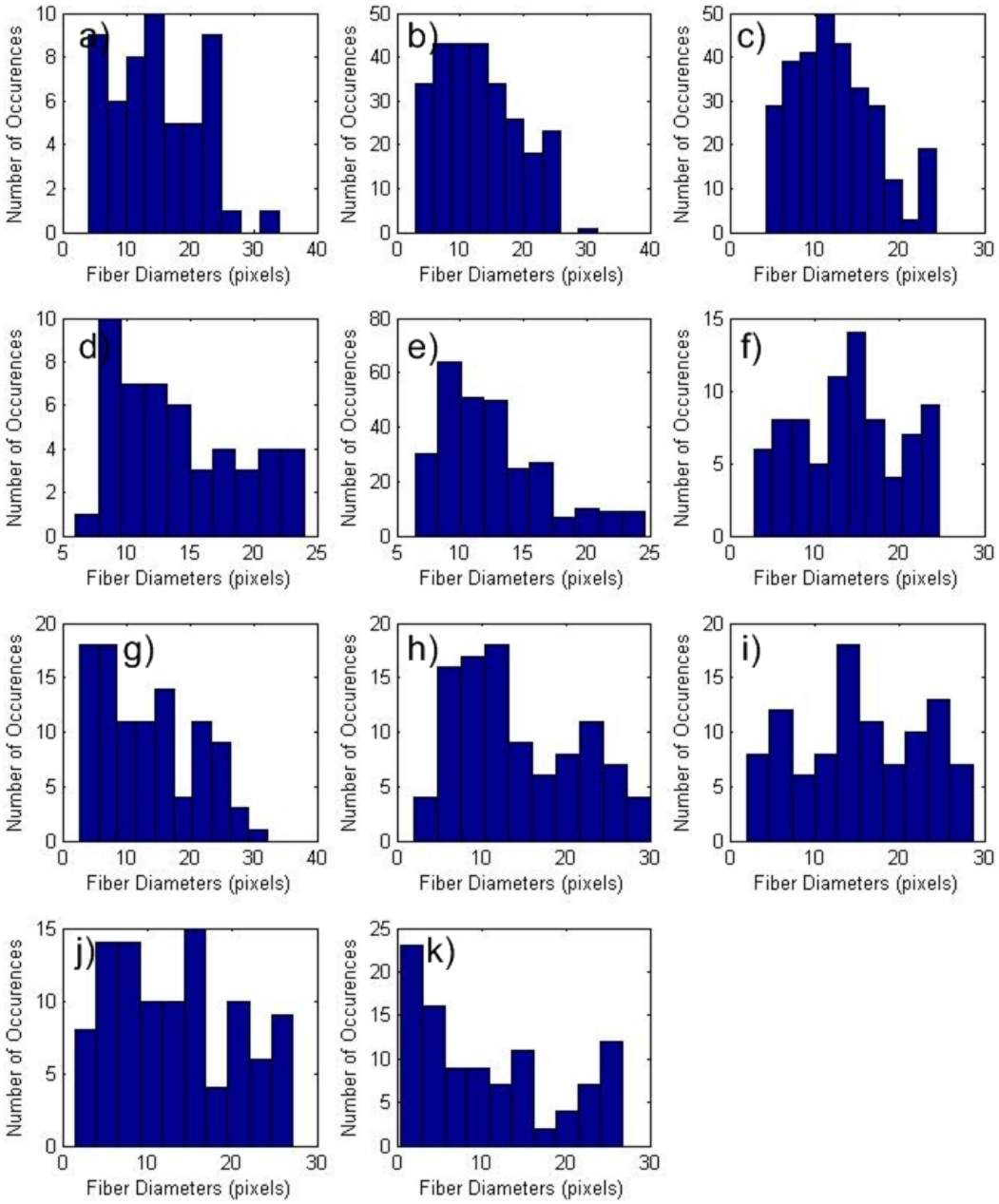

Figure 46 Histograms for all fiber diameter measurements of image wide25. a) Custom Canny Hough measurement, b) Custom Canny Slopes measurement, c) Skeleton Slopes measurement, d) Canny Hough measurement, e) Canny Slopes Measurement, f) known fiber diameters, g) Person 1 measurement, h) Person 2 measurement, i) Person 3 measurement, j) Person 4 measurement, k) Person 5 measurement

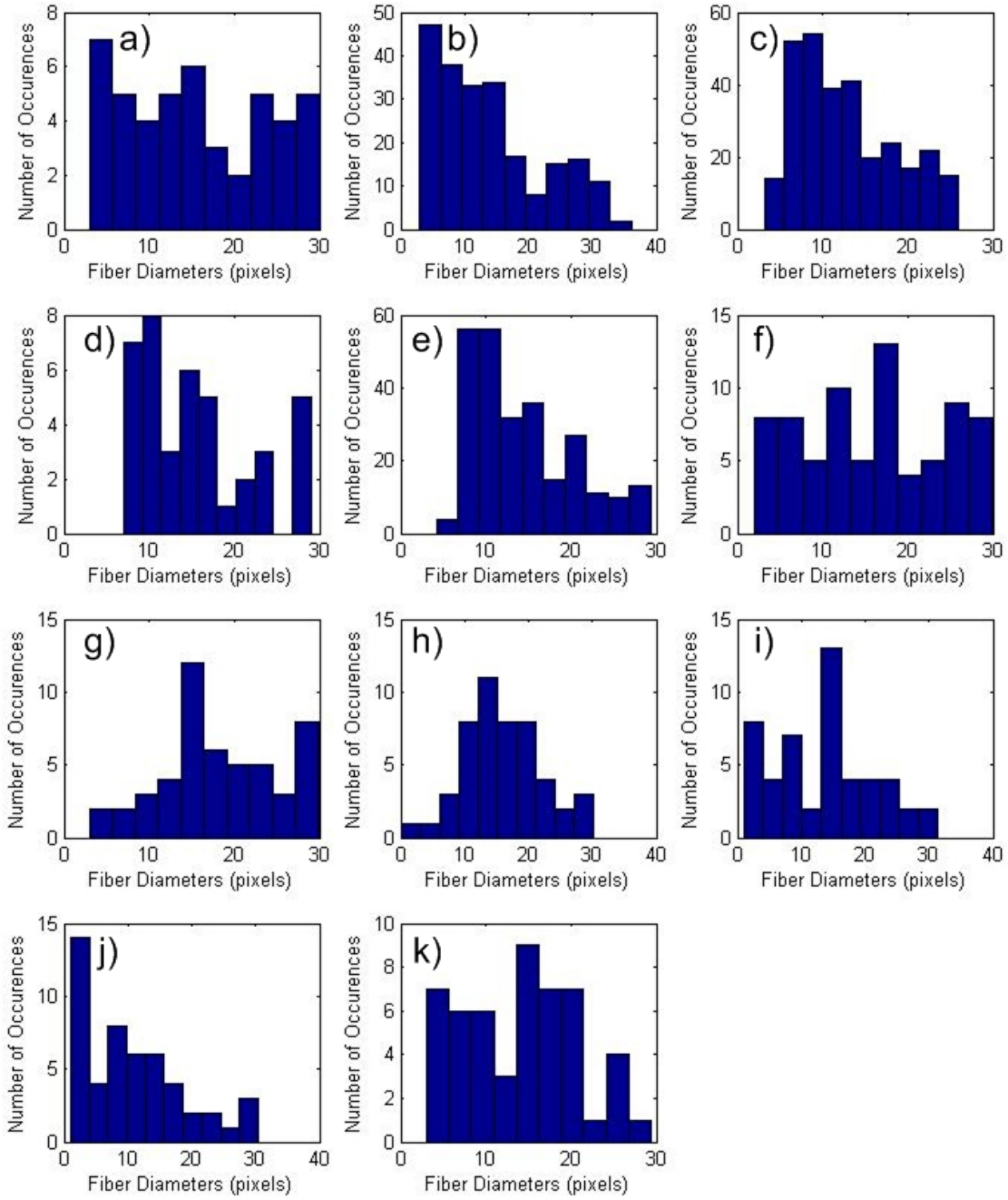

Figure 47 Histograms for all fiber diameter measurements of image wide30. a) Custom Canny Hough measurement, b) Custom Canny Slopes measurement, c) Skeleton Slopes measurement, d) Canny Hough measurement, e) Canny Slopes Measurement, f) known fiber diameters, g) Person 1 measurement, h) Person 2 measurement, i) Person 3 measurement, j) Person 4 measurement, k) Person 5 measurement

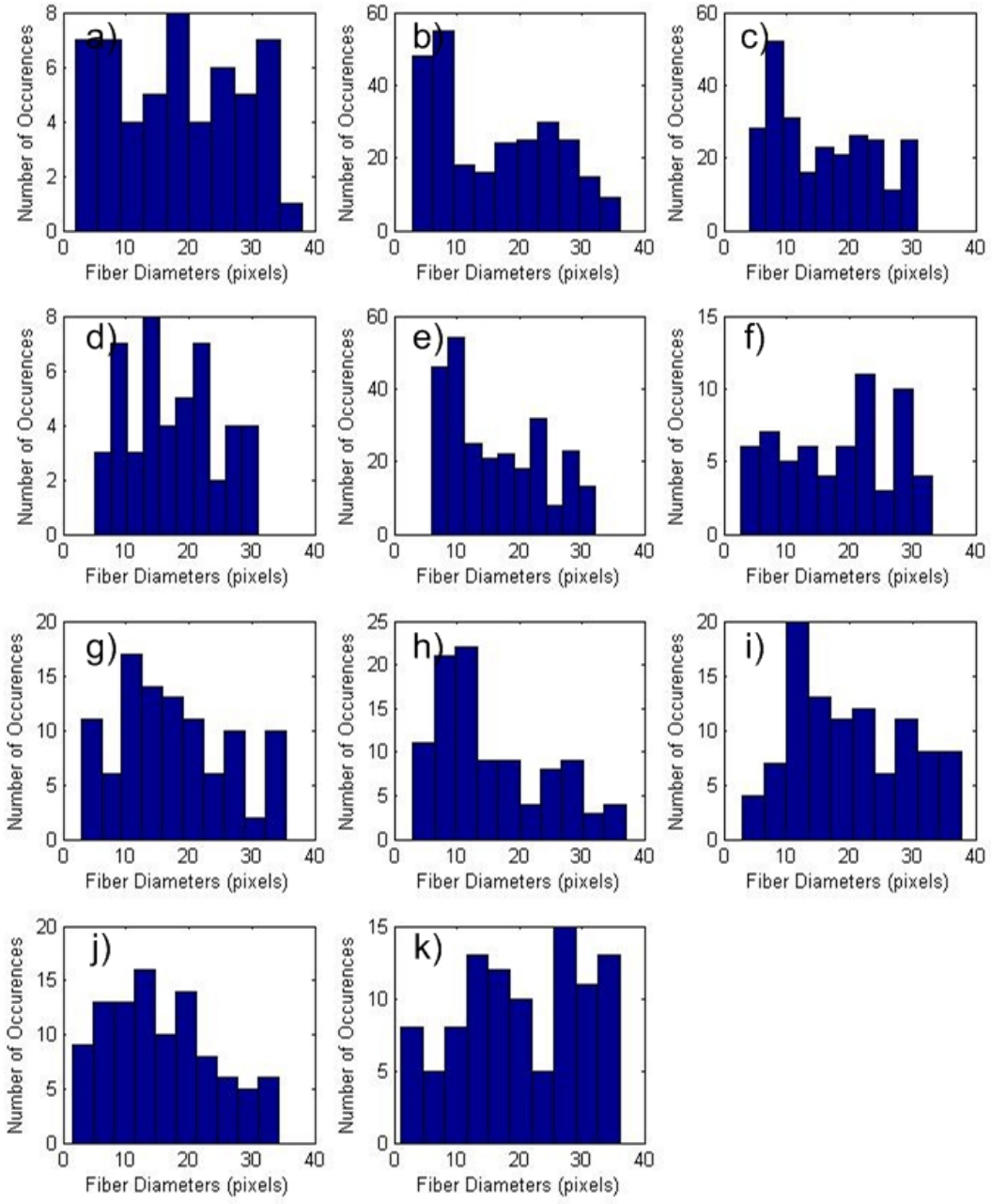

Figure 48 Histograms for all fiber diameter measurements of image wide35. a) Custom Canny Hough measurement, b) Custom Canny Slopes measurement, c) Skeleton Slopes measurement, d) Canny Hough measurement, e) Canny Slopes Measurement, f) known fiber diameters, g) Person 1 measurement, h) Person 2 measurement, i) Person 3 measurement, j) Person 4 measurement, k) Person 5 measurement

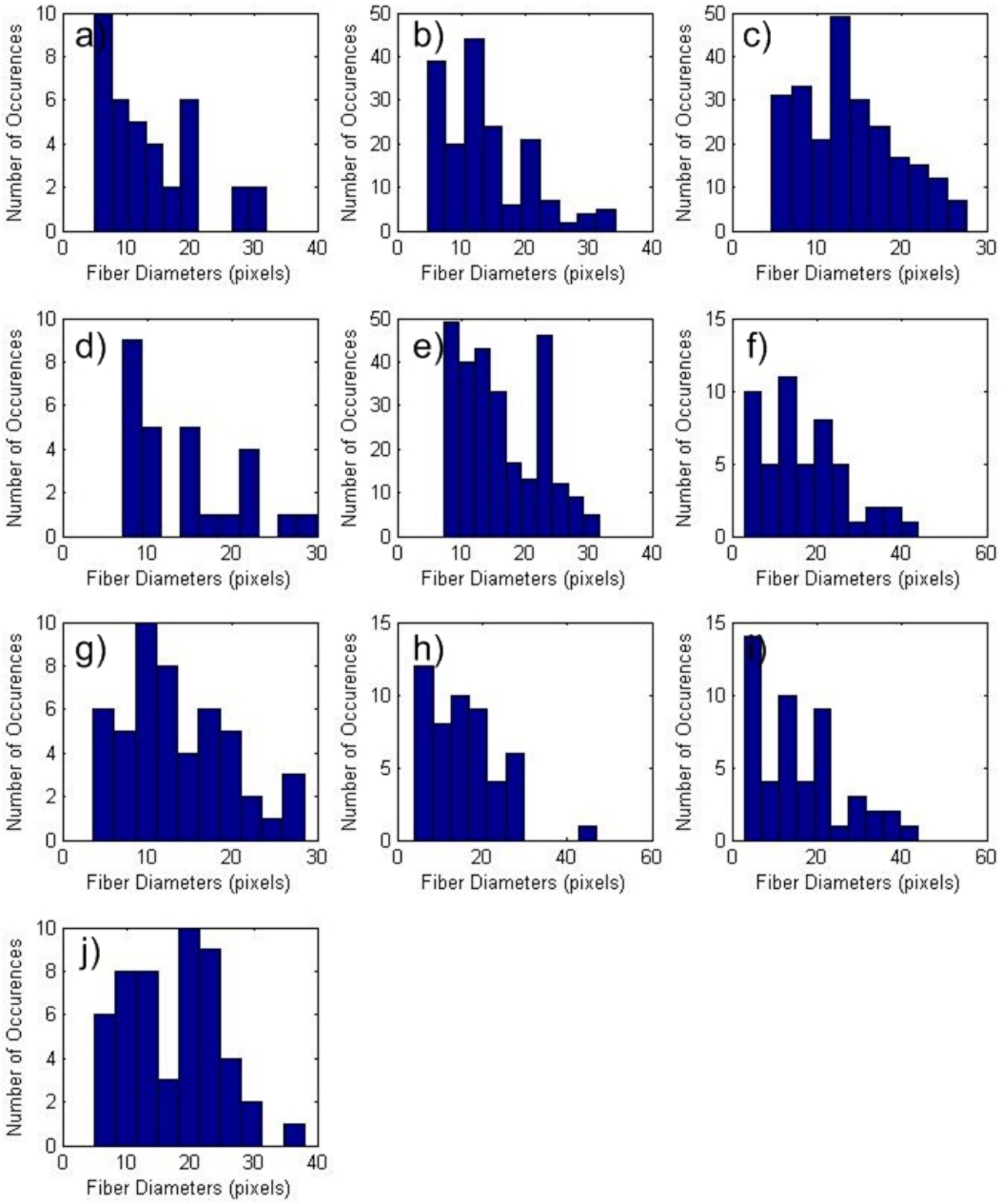

Figure 49 Histograms for all fiber diameter measurements of image SEM1. a) Custom Canny Hough measurement, b) Custom Canny Slopes measurement, c) Skeleton Slopes measurement, d) Canny Hough measurement, e) Canny Slopes Measurement, f) Person 1 measurement, g) Person 2 measurement, h) Person 3 measurement, i) Person 4 measurement, j) Person 5 measurement

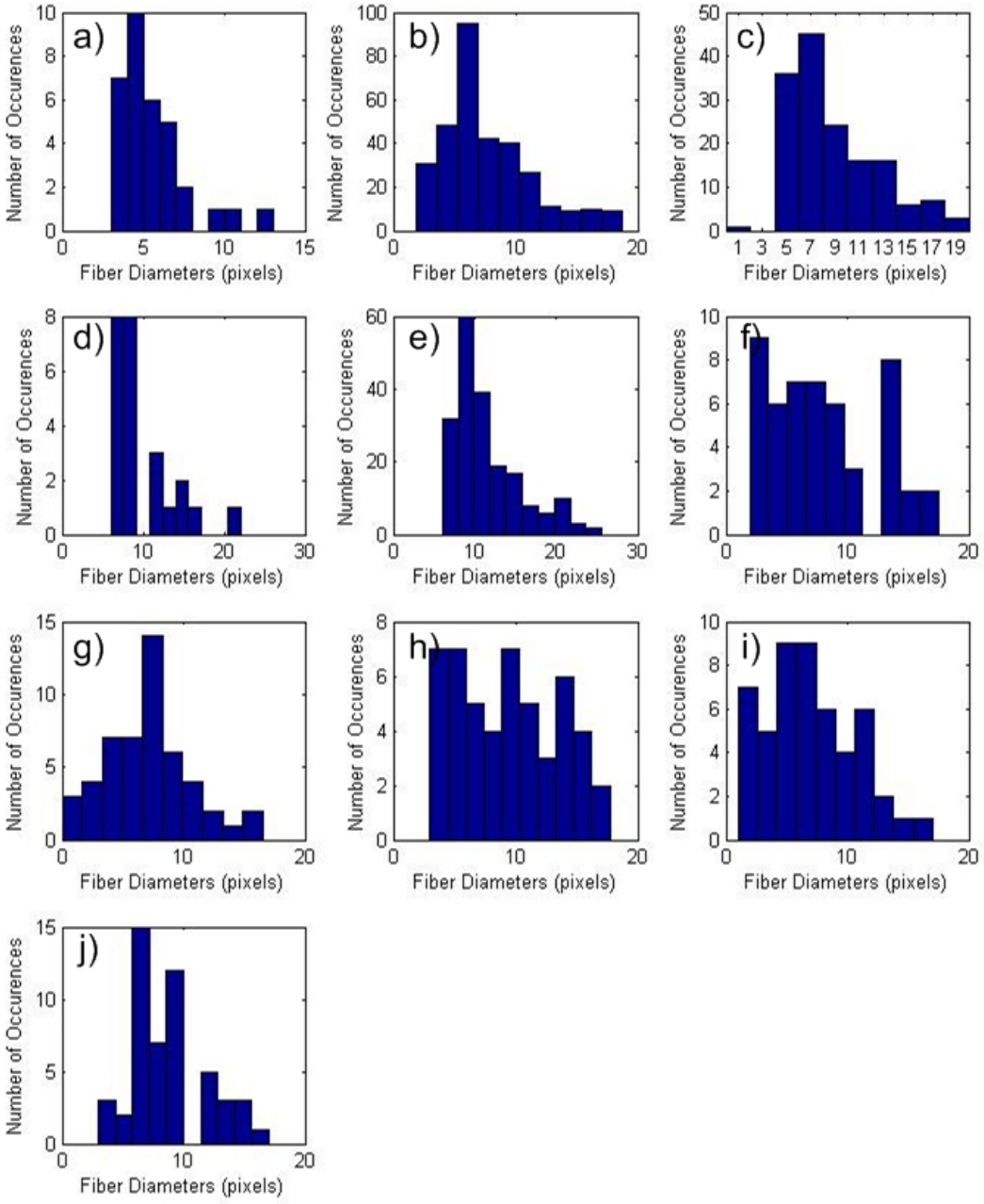

Figure 50 Histograms for all fiber diameter measurements of image SEM2. a) Custom Canny Hough measurement, b) Custom Canny Slopes measurement, c) Skeleton Slopes measurement, d) Canny Hough measurement, e) Canny Slopes Measurement, f) Person 1 measurement, g) Person 2 measurement, h) Person 3 measurement, i) Person 4 measurement, j) Person 5 measurement

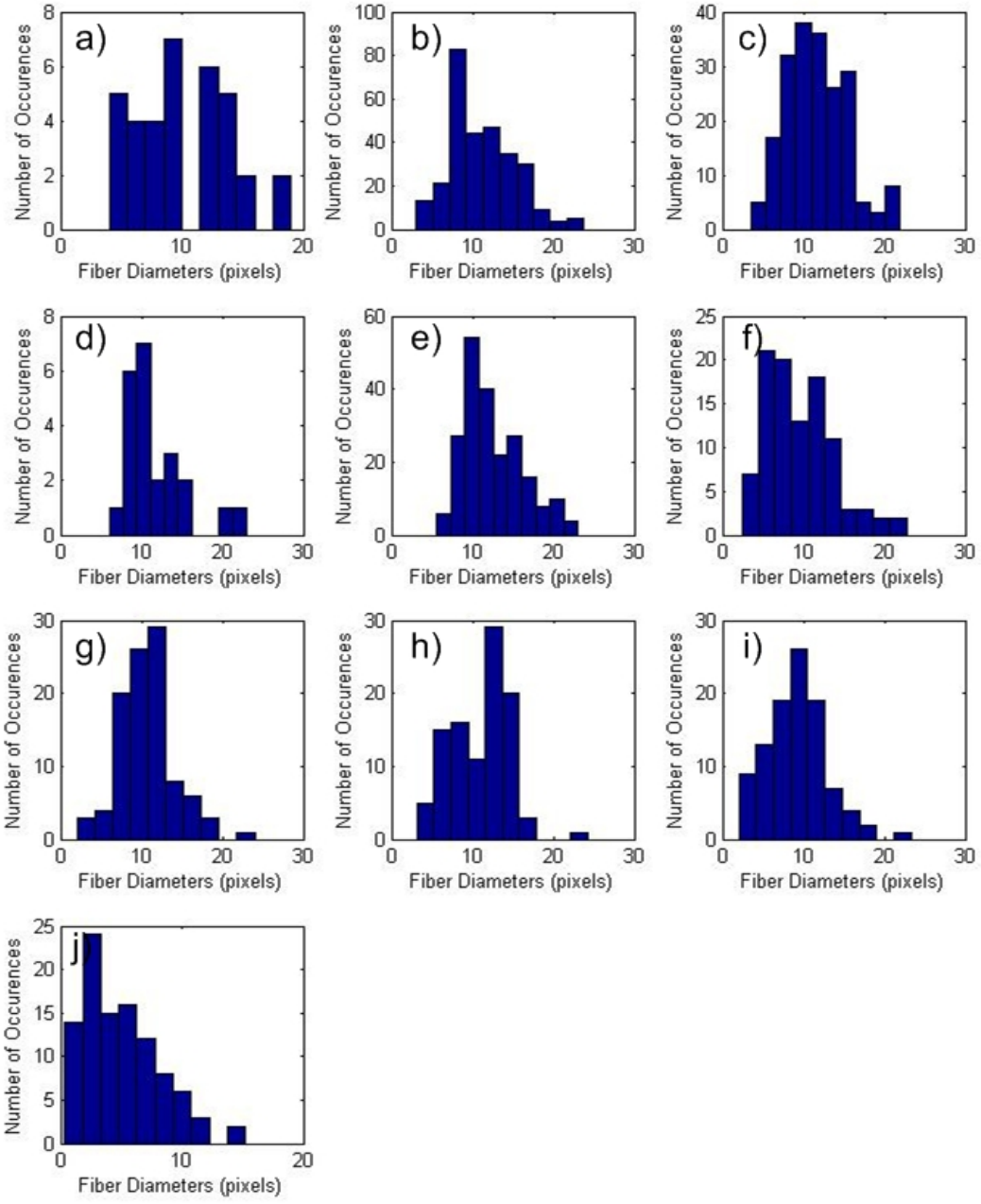

Figure 51 Histograms for all fiber diameter measurements of image SEM3. a) Custom Canny Hough measurement, b) Custom Canny Slopes measurement, c) Skeleton Slopes measurement, d) Canny Hough measurement, e) Canny Slopes Measurement, f) Person 1 measurement, g) Person 2 measurement, h) Person 3 measurement, i) Person 4 measurement, j) Person 5 measurement

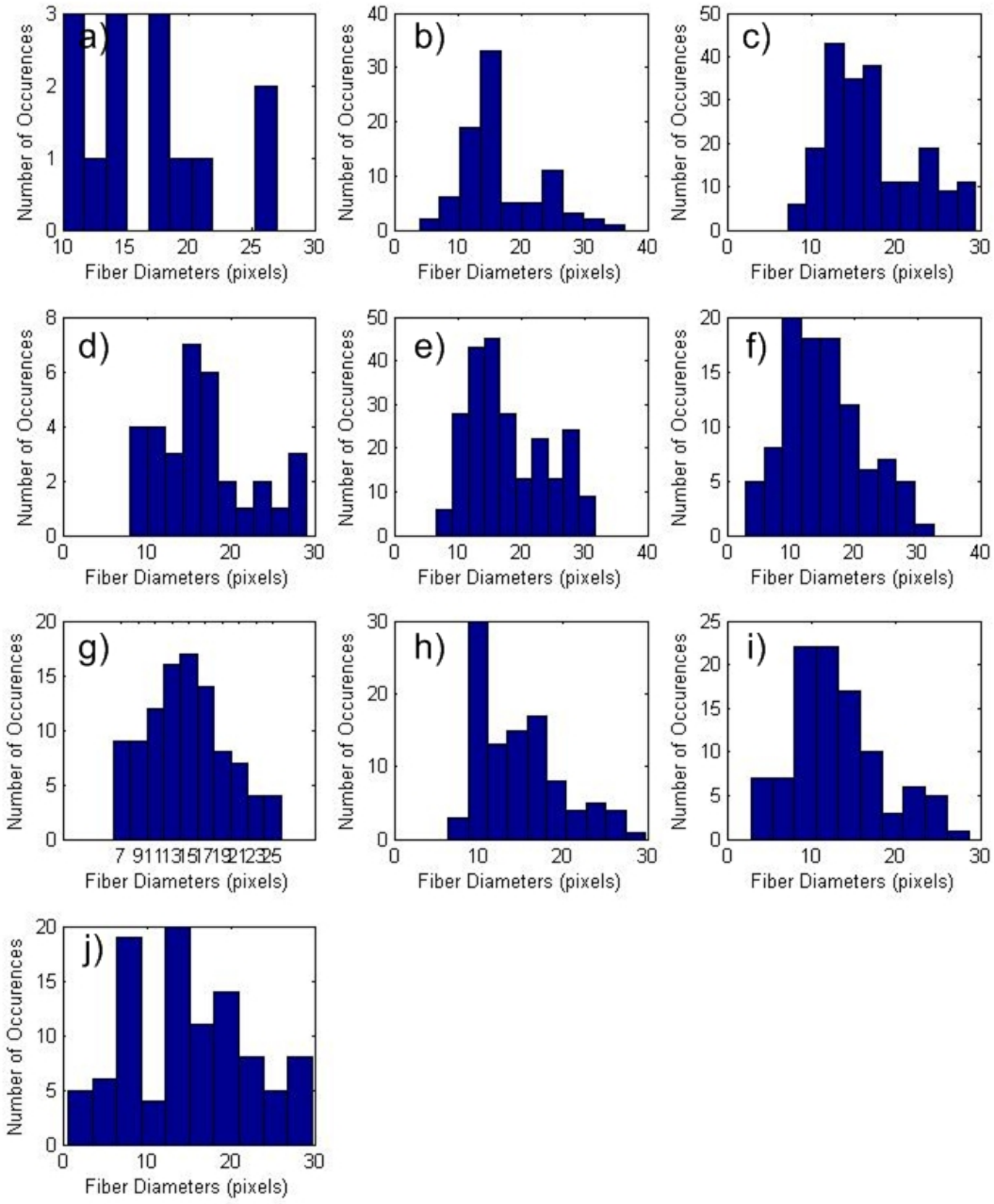

Figure 52 Histograms for all fiber diameter measurements of image SEM4. a) Custom Canny Hough measurement, b) Custom Canny Slopes measurement, c) Skeleton Slopes measurement, d) Canny Hough measurement, e) Canny Slopes Measurement, f) Person 1 measurement, g) Person 2 measurement, h) Person 3 measurement, i) Person 4 measurement, j) Person 5 measurement

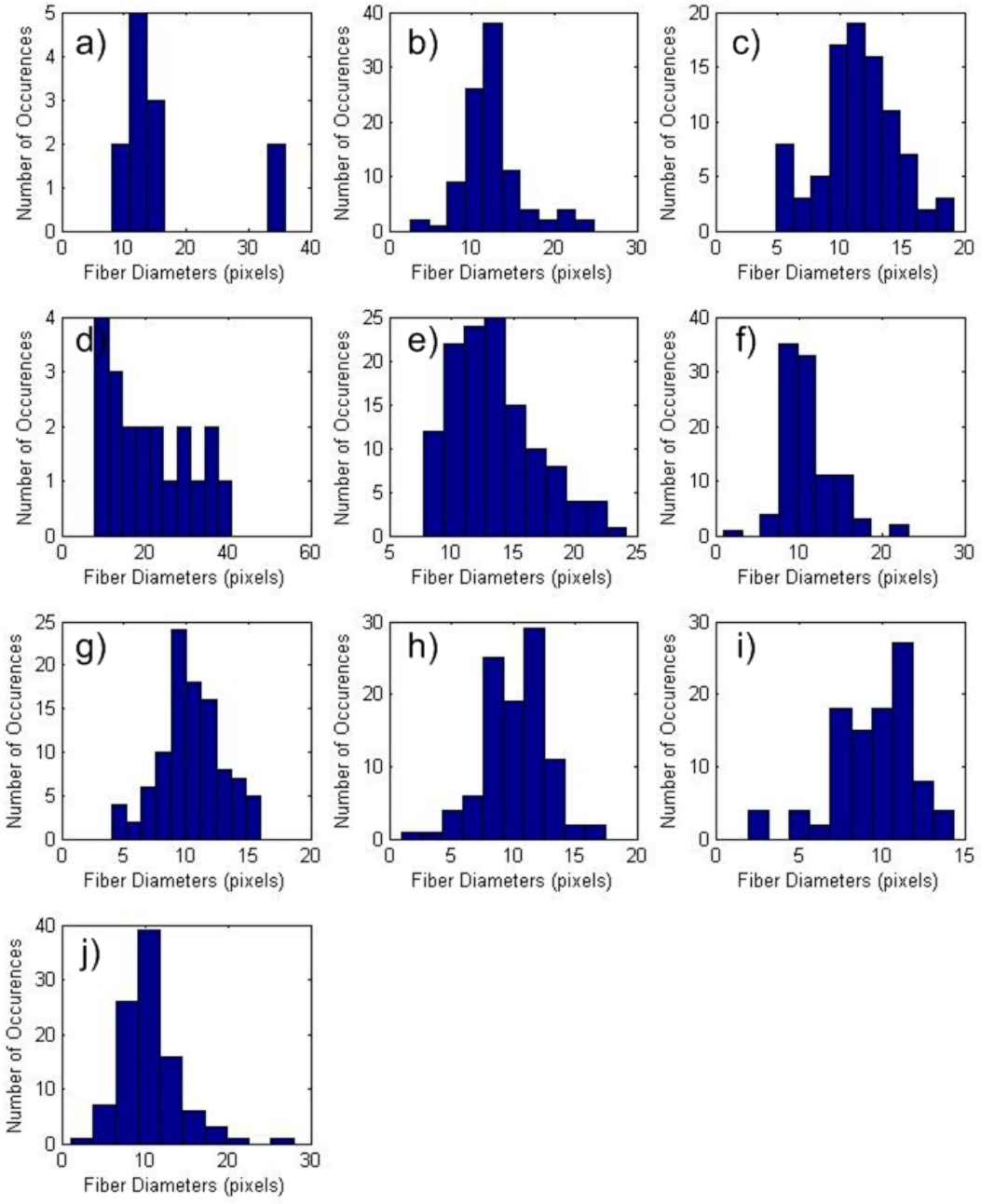

Figure 53 Histograms for all fiber diameter measurements of image SEM5. a) Custom Canny Hough measurement, b) Custom Canny Slopes measurement, c) Skeleton Slopes measurement, d) Canny Hough measurement, e) Canny Slopes Measurement, f) Person 1 measurement, g) Person 2 measurement, h) Person 3 measurement, i) Person 4 measurement, j) Person 5 measurement

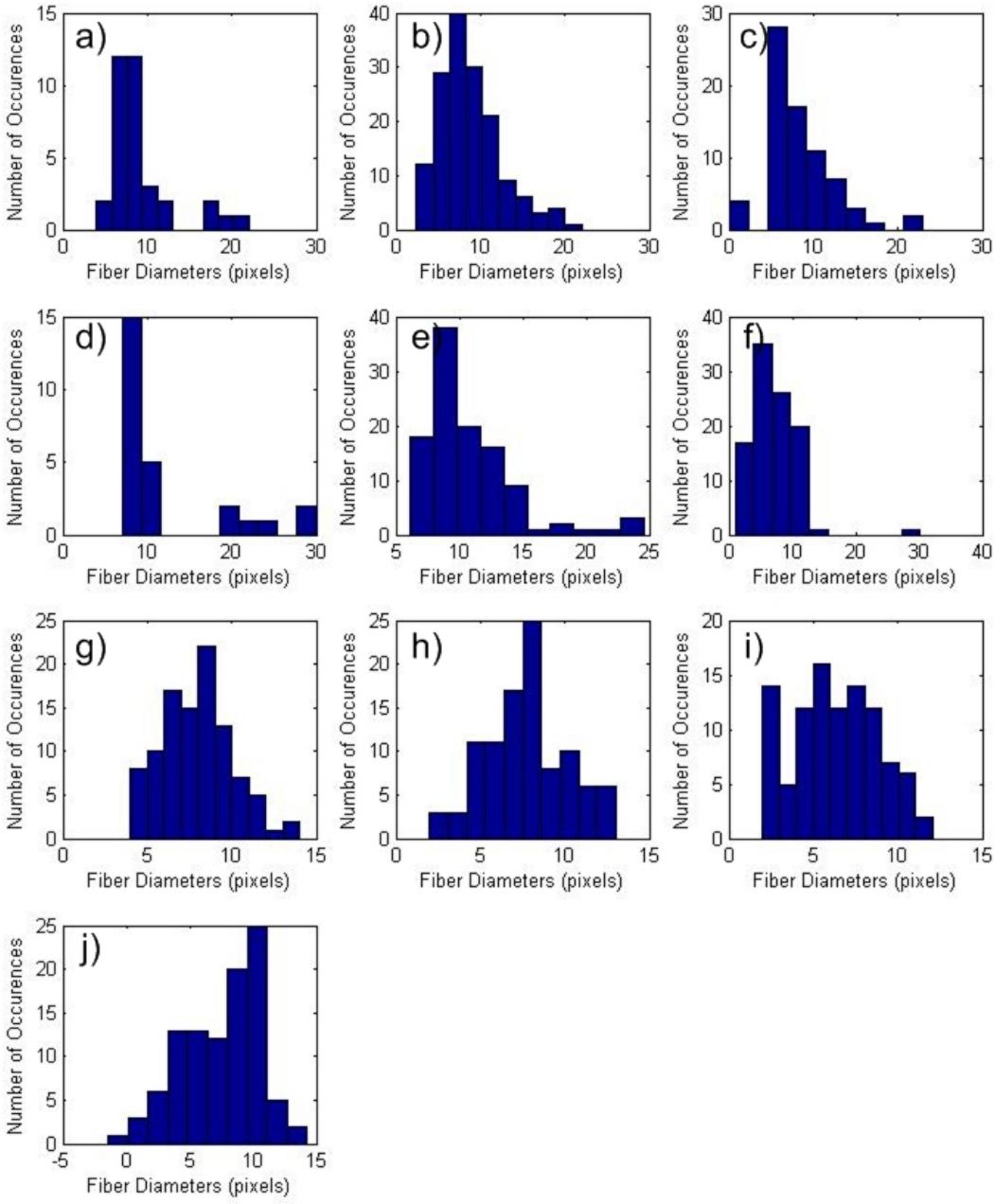

Figure 54 Histograms for all fiber diameter measurements of image SEM6. a) Custom Canny Hough measurement, b) Custom Canny Slopes measurement, c) Skeleton Slopes measurement, d) Canny Hough measurement, e) Canny Slopes Measurement, f) Person 1 measurement, g) Person 2 measurement, h) Person 3 measurement, i) Person 4 measurement, j) Person 5 measurement

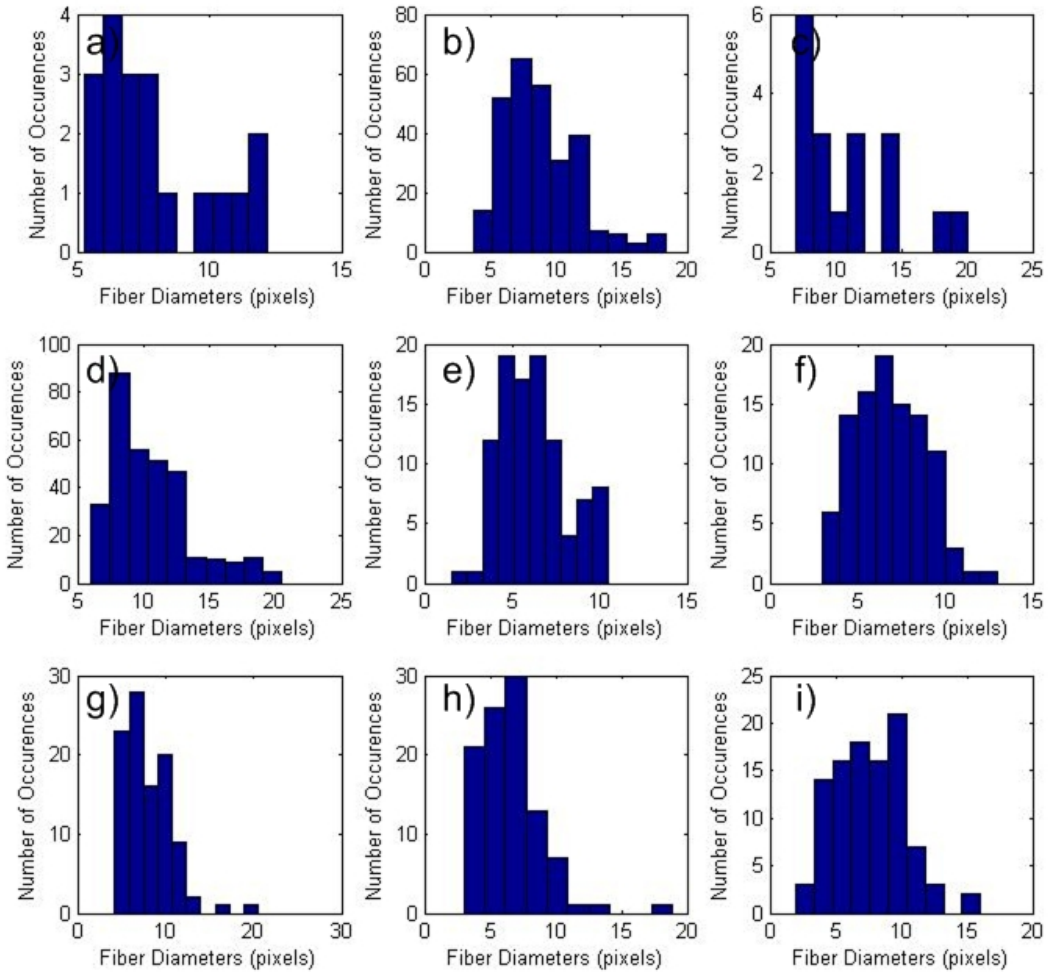

Figure 55 Histograms for all fiber diameter measurements of image SEM7. a) Custom Canny Slopes measurement, b) Skeleton Slopes measurement, c) Canny Hough measurement, d) Canny Slopes Measurement, e) Person 1 measurement, f) Person 2 measurement, g) Person 3 measurement, h) Person 4 measurement, i) Person 5 measurement

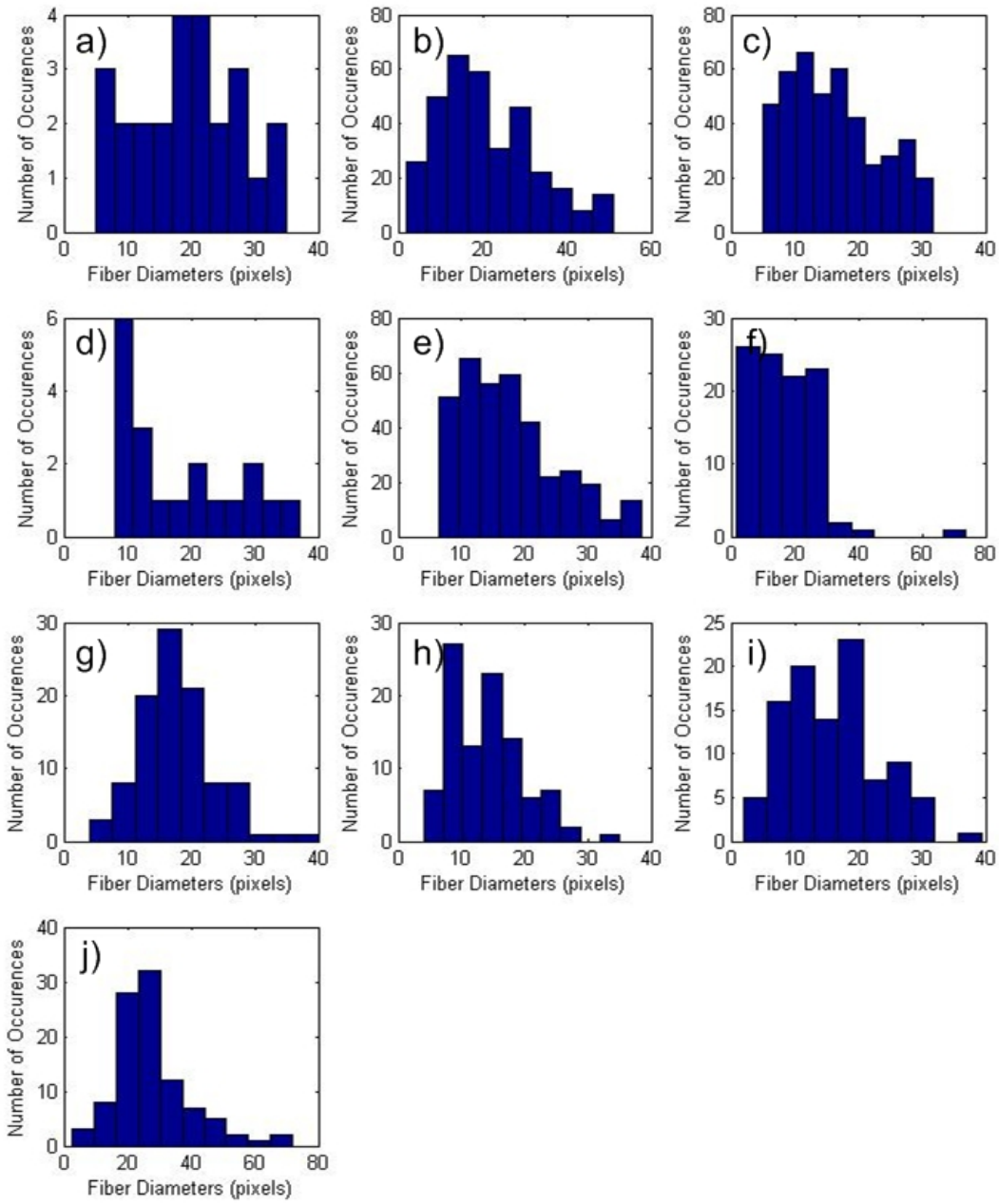

Figure 56 Histograms for all fiber diameter measurements of image SEM8. a) Custom Canny Hough measurement, b) Custom Canny Slopes measurement, c) Skeleton Slopes measurement, d) Canny Hough measurement, e) Canny Slopes Measurement, f) Person 1 measurement, g) Person 2 measurement, h) Person 3 measurement, i) Person 4 measurement, j) Person 5 measurement

	Data Sets											
Data Sets	CCH	CCH	CCS	CSkS	DCH	DCS	act	P1	P2	P3	P4	P5
	CCS			narrow15 narrow20 narrow25 narrow30 narrow35	narrow20 narrow25 narrow30 narrow35	narrow15 narrow20 narrow25 narrow30 narrow35			narrow10 narrow30			
	CSkS			narrow15 narrow20 narrow25 narrow30 narrow35	narrow15 narrow20 narrow25 narrow30 narrow35	narrow10 narrow15 narrow20 narrow25 narrow30 narrow35		narrow20	narrow10 narrow30	narrow20 narrow25		
	DCH	narrow15 narrow20 narrow25 narrow30 narrow35	narrow15 narrow20 narrow25 narrow30 narrow35			narrow10 narrow20 narrow25 narrow30 narrow35	narrow15 narrow20 narrow25 narrow30 narrow35	narrow15 narrow20 narrow25 narrow30 narrow35	narrow10 narrow15 narrow20 narrow25 narrow35	narrow15 narrow20 narrow25 narrow30 narrow35	narrow15 narrow20 narrow25 narrow30 narrow35	narrow15 narrow20 narrow25 narrow30 narrow35
	DCS	narrow20 narrow25 narrow30 narrow35	narrow15 narrow20 narrow25 narrow30 narrow35			narrow20 narrow25 narrow30 narrow35	narrow15 narrow20 narrow25 narrow30 narrow35	narrow15 narrow20 narrow25 narrow30 narrow35	narrow10 narrow20 narrow25 narrow35	narrow15 narrow20 narrow25 narrow30 narrow35	narrow20 narrow25 narrow30 narrow35	narrow15 narrow20 narrow25 narrow30 narrow35
	act	narrow15 narrow20 narrow25 narrow30 narrow35	narrow10 narrow15 narrow20 narrow25 narrow30 narrow35	narrow10 narrow20 narrow25 narrow30 narrow35	narrow20 narrow25 narrow30 narrow35		narrow10 narrow15 narrow20 narrow25 narrow30 narrow35	narrow15 narrow20 narrow25 narrow30 narrow35	narrow10 narrow15 narrow20 narrow25 narrow30 narrow35	narrow15 narrow20 narrow25 narrow30 narrow35	narrow10 narrow15 narrow20 narrow25 narrow30 narrow35	narrow15 narrow20 narrow25 narrow30 narrow35
	P1			narrow15 narrow20 narrow25 narrow30 narrow35	narrow15 narrow20 narrow25 narrow30 narrow35	narrow10 narrow15 narrow20 narrow25 narrow30 narrow35			narrow10 narrow30			
	P2		narrow20	narrow15 narrow20 narrow25 narrow30 narrow35	narrow15 narrow20 narrow25 narrow30 narrow35	narrow15 narrow20 narrow25 narrow30 narrow35			narrow10 narrow30		narrow10	
	P3	narrow10 narrow30	narrow10 narrow30	narrow10 narrow15 narrow20 narrow25 narrow35	narrow10 narrow20 narrow25 narrow35	narrow10 narrow15 narrow20 narrow25 narrow30 narrow35	narrow10 narrow30	narrow10 narrow30		narrow10 narrow15 narrow20 narrow25 narrow30		narrow10 narrow30
	P4		narrow20 narrow25	narrow15 narrow20 narrow25 narrow30 narrow35	narrow15 narrow20 narrow25 narrow30 narrow35	narrow15 narrow20 narrow25 narrow30 narrow35			narrow10 narrow15 narrow20 narrow25 narrow30		narrow15 narrow20 narrow25	narrow25
	P5			narrow15 narrow20 narrow25 narrow30 narrow35	narrow20 narrow25 narrow30 narrow35	narrow10 narrow15 narrow20 narrow25 narrow30 narrow35		narrow10		narrow15 narrow20 narrow25		

Table 1 Multiple comparison of means for narrow distribution test images (α=0.05)

	Data Sets											
Data Sets		CCH	CCS	CSkS	DCH	DCS	act	P1	P2	P3	P4	P5
	CCH			wide25	wide10	wide10 wide15				wide10 wide20	wide30	wide25
	CCS			wide10	wide10	wide10 wide15 wide20		wide30	wide10 wide15	wide10 wide15 wide20 wide25 wide35	wide10 wide15	wide35
	CSkS	wide25	wide10		wide10	wide10 wide15 wide20	wide10 wide30	wide30	wide10	wide10 wide20 wide25 wide35	wide10 wide15	wide35
	DCH	wide10	wide10	wide10		wide10	wide10 wide15		wide10	wide20	wide10 wide15 wide30	
	DCS	wide10 wide15	wide10 wide15 wide20	wide10 wide15 wide20	wide10 wide15		wide10 wide15	wide10 wide15 wide30	wide10	wide20 wide25 wide35	wide10 wide15 wide30	wide10 wide15 wide35
	act			wide10 wide30	wide10 wide15	wide10 wide15			wide15	wide10 wide15 wide20	wide30	
	P1		wide30	wide30		wide10 wide15			wide10 wide15	wide15 wide20	wide10 wide30	
	P2		wide10 wide15	wide10	wide10	wide10	wide15	wide10 wide15		wide10 wide20 wide35	wide15 wide30	wide10 wide25 wide35
	P3	wide10 wide20	wide10 wide15 wide20 wide25 wide35	wide10 wide20 wide25 wide35	wide20	wide20 wide25 wide35	wide10 wide15 wide20	wide15 wide20	wide10 wide20 wide35		wide10 wide15 wide20 wide35	wide20 wide25
	P4	wide30	wide10 wide15	wide10 wide15	wide10 wide15 wide30	wide10 wide15 wide30	wide30	wide10 wide30	wide15 wide30	wide10 wide15 wide20 wide35		wide10 wide15 wide35
	P5	wide25	wide35	wide35		wide10 wide15 wide35			wide10 wide25 wide35	wide20 wide25	wide10 wide15 wide35	

Table 2 Multiple comparison of mean for wide distribution test images (α=0.05)

		Data Sets									
Data Sets		CCH	CCS	CSkS	DCH	DCS	P1	P2	P3	P4	P5
	CCH		SEM5 SEM7	SEM2 SEM5 SEM7	SEM2 SEM5 SEM6 SEM7	SEM2 SEM3 SEM7	SEM5 SEM7	SEM5 SEM7	SEM2 SEM5 SEM7	SEM5 SEM6 SEM7	SEM2 SEM3 SEM5 SEM7 SEM8
	CCS	SEM5 SEM7		SEM8	SEM5 SEM6 SEM7	SEM2 SEM3 SEM6 SEM7 SEM8	SEM3 SEM6 SEM8	SEM5	SEM5 SEM8	SEM3 SEM4 SEM5 SEM6 SEM8	SEM1 SEM3 SEM5 SEM8
	CSkS	SEM2 SEM5 SEM7	SEM8		SEM5 SEM6 SEM7	SEM2 SEM5 SEM6 SEM7	SEM3 SEM7	SEM7		SEM2 SEM3 SEM4 SEM5 SEM6 SEM7	SEM1 SEM3 SEM7 SEM8
	DCH	SEM2 SEM5 SEM6 SEM7	SEM5 SEM6 SEM7	SEM5 SEM6 SEM7		SEM5	SEM5 SEM6 SEM7	SEM5 SEM6 SEM7	SEM5 SEM6 SEM7	SEM4 SEM5 SEM6 SEM7	SEM3 SEM5 SEM6 SEM7 SEM8
	DCS	SEM2 SEM3 SEM7	SEM2 SEM3 SEM6 SEM7 SEM8	SEM2 SEM5 SEM6 SEM7	SEM5		SEM2 SEM3 SEM4 SEM5 SEM6 SEM7	SEM2 SEM3 SEM4 SEM5 SEM6 SEM7	SEM2 SEM3 SEM4 SEM5 SEM6 SEM7	SEM2 SEM3 SEM4 SEM5 SEM6 SEM7	SEM2 SEM3 SEM4 SEM5 SEM6 SEM7 SEM8
	P1	SEM5 SEM7	SEM3 SEM6 SEM8	SEM3 SEM7	SEM5 SEM6 SEM7	SEM2 SEM3 SEM4 SEM5 SEM6 SEM7			SEM7		SEM3 SEM7 SEM8
	P2	SEM5 SEM7	SEM5	SEM7	SEM5 SEM6 SEM7	SEM2 SEM3 SEM4 SEM5 SEM6 SEM7				SEM6	SEM3 SEM8
	P3	SEM2 SEM5 SEM7	SEM5 SEM8		SEM5 SEM6 SEM7	SEM2 SEM3 SEM4 SEM5 SEM6 SEM7	SEM7			SEM2 SEM3 SEM6 SEM7	SEM3 SEM8
	P4	SEM5 SEM6 SEM7	SEM3 SEM4 SEM5 SEM6 SEM8	SEM2 SEM3 SEM4 SEM5 SEM6 SEM7	SEM4 SEM5 SEM6 SEM7	SEM2 SEM3 SEM4 SEM5 SEM6 SEM7		SEM6	SEM2 SEM3 SEM6 SEM7		SEM3 SEM8
	P5	SEM2 SEM3 SEM5 SEM7 SEM8	SEM1 SEM3 SEM5 SEM8	SEM1 SEM3 SEM7 SEM8	SEM3 SEM5 SEM6 SEM7 SEM8	SEM2 SEM3 SEM4 SEM5 SEM6 SEM7 SEM8	SEM3 SEM7 SEM8	SEM3 SEM8	SEM3 SEM8	SEM3 SEM8	

Table 3 Multiple comparison of the means for real SEMs (α=0.05)

Conclusion

Five automated methods and the manual method for measuring fiber diameters of electrospun scaffolds were evaluated for accuracy by processing simulated images with known fiber diameters via all methods. It was determined that the manual method does provide accurate measurements of the mean fiber diameter with $p<0.05$. The Skeleton Canny Slopes, Default Canny Slopes, and Default Canny Hough methods were shown to provide inaccurate measurements. The primary reason for these inaccuracies was determined to be the inaccurate determination of fiber edge locations. All three methods use the default Canny function to determine the fiber edge location. The methods vary in terms of identifying valid pairs of edges, however there did not appear to be an appreciable instance of wrong pairs of left and right edges, therefore the only appreciable source of error is the edge detection.

The Custom Canny methods did not show the same inaccuracies. The Custom Canny Slopes method was found to be accurate when applied to the simulated images ($p<0.05$), and it was also determined to be equivalent to the manual method when applied to real SEM images of electrospun webs. The Custom Canny Hough method produced statistically equivalent mean fiber diameters to known values when applied to the simulated images. It also provided statistically equivalent mean fiber diameters to the manual method values for real SEM images of scaffolds with straight fibers. This method is not applicable for scaffolds with curved fibers. The optimal method is the Custom Canny

method, since it produced statistically accurate measurements, which are equivalent to the manual method

Future work will focus on improvements in the implementation of the Custom Canny Slopes method, potentially using C or C++ for coding the program, since MATLAB is not ideal for speedy computational tasks. Another direction that can be pursued is developing a non-linear generalized Hough transform to choose individual fibers. Fitting a curve to a fiber edge would eliminate the problem of the Custom Canny Hough method, since non-linear stretches of fibers could be identified. It would also eliminate the problem of counting the same fiber multiple times as is done in the Custom Canny Slopes method. Parametrically expressing a non-linear curve equation is a very difficult computational problem. Each additional parameter to the Hough transform, adds another dimension to the parametric representation of Hough space. For example the equation of the circle would have three parameters (center coordinates and radius) and therefore three-dimensional Hough Space. Ideally a generalized Hough transform would be used with different parameters, but even with just four parameters (for example a parabola) the computational problem becomes overwhelming for practical applications at this time.

Literature Cited

(1) Hsu YM, Chen CN, Chiu JJ, Chang SH, Wang YJ. The effects of fiber size on MG63 cells cultured with collagen based matrices. Journal of biomedical materials research.Part B, Applied biomaterials 2009.
(2) Carlberg B, Axell MZ, Nannmark U, Liu J, Kuhn HG. Electrospun polyurethane scaffolds for proliferation and neuronal differentiation of human embryonic stem cells. Biomedical materials 2009;4(4):45004.
(3) Barnes CP, Sell SA, Boland ED, Simpson DG, Bowlin GL. Nanofiber technology: designing the next generation of tissue engineering scaffolds. Advanced Drug Delivery Reviews 2007;59(14):1413.
(4) Gonzalez RC, Eddins SL, Woods RE. Digital Image processing using MATLAB. Upper Saddle River, N. J.: Pearson Prentice Hall; 2004.
(5) Gonzalez RC, Woods RE. Digital image processing. 3rd ed. Upper Saddle River, NJ: Pearson/Prentice Hall; 2008.
(6) Li W, Tuan R. Fabrication and application of nanofibrous scaffolds in tissue engineering. Current protocols in cell biology 2009;Chapter 25:Unit 25.
(7) Vasita R, Katti D. Nanofibers and their applications in tissue engineering. International journal of nanomedicine 2006;1(1):15.
(8) Venugopal J, Ramakrishna S. Applications of polymer nanofibers in biomedicine and biotechnology. Appl.Biochem.Biotechnol. 2005;125(3):147.
(9) Finne-Wistrand A, Albertsson A, Kwon O, Kawazoe N, Chen G, Kang I, et al. Resorbable scaffolds from three different techniques: electrospun fabrics, salt-leaching porous films, and smooth flat surfaces. Macromolecular bioscience 2008;8(10):951.
(10) Kyle S, Aggeli A, Ingham E, McPherson M. Production of self-assembling biomaterials for tissue engineering. Trends Biotechnol. 2009;27(7):423.
(11) Zhang S, Marini D, Hwang W, Santoso S. Design of nanostructured biological materials through self-assembly of peptides and proteins. Curr.Opin.Chem.Biol. 2002;6(6):865.
(12) Weigel T, Schinkel G, Lendlein A. Design and preparation of polymeric scaffolds for tissue engineering. Expert Review of Medical Devices 2006;3(6):835.
(13) Budyanto L, Goh YQ, Ooi CP. Fabrication of porous poly(L-lactide) (PLLA) scaffolds for tissue engineering using liquid-liquid phase separation and freeze extraction. Journal of materials science.Materials in medicine 2009;20(1):105.
(14) Neal RA, McClugage SG, Link MC, Sefcik LS, Ogle RC, Botchwey EA. Laminin nanofiber meshes that mimic morphological properties and bioactivity of basement membranes. Tissue Engineering Part C: Methods 2009;15(1):11.

(15) Patlolla A, Collins G, Arinzeh TL. Solvent-dependent properties of electrospun fibrous composites for bone tissue regeneration. Acta Biomaterialia 2009.
(16) Desai K, Kit K, Li J, Zivanovic S. Morphological and surface properties of electrospun chitosan nanofibers. Biomacromolecules 2008;9(3):1000.
(17) Ziabari M, Mottaghitalab V, McGovern ST, Haghi AK. A New Image Analysis Based Method for Measuring Electrospun
Nanofiber Diameter. Nanoscale Res Lett 2007;2(12):597-600.

APPENDIX A: Statistical Analysis

ANOVA Tables for all data sets per image for all test images

Source	SS	df	MS	F	Prob>F
Groups	604.51	10.00	60.45	14.71	0.00
Error	7780.04	1893.00	4.11		
Total	8384.55	1903.00			

Table 4 ANOVA Table for narrow10

Source	SS	df	MS	F	Prob>F
Groups	1536.79	10.00	153.68	27.32	0.00
Error	8522.49	1515.00	5.63		
Total	10059.28	1525.00			

Table 5 ANOVA Table for narrow15

Source	SS	df	MS	F	Prob>F
Groups	6251.70	10.00	625.17	83.11	0.00
Error	12674.53	1685.00	7.52		
Total	18926.23	1695.00			

Table 6 ANOVA Table for narrow20

Source	SS	df	MS	F	Prob>F
Groups	7564.51	10.00	756.45	84.24	0.00
Error	11143.86	1241.00	8.98		
Total	18708.37	1251.00			

Table 7 ANOVA Table for narrow25

Source	SS	df	MS	F	Prob>F
Groups	8962.79	10.00	896.28	55.65	0.00
Error	13818.78	858.00	16.11		
Total	22781.58	868.00			

Table 8 ANOVA Table for narrow30

Source	SS	df	MS	F	Prob>F
Groups	7143.55	10.00	714.36	63.14	0.00
Error	10861.56	960.00	11.31		
Total	18005.11	970.00			

Table 9 ANOVA Table for narrow35

Source	SS	df	MS	F	Prob>F
Groups	2460.51	10.00	246.05	56.98	0.00
Error	9012.69	2087.00	4.32		
Total	11473.20	2097.00			

Table 10 ANOVA Table for wide10

Source	SS	df	MS	F	Prob>F
Groups	1572.39	10.00	157.24	12.12	0.00
Error	24265.16	1871.00	12.97		
Total	25837.55	1881.00			

Table 11 ANOVA Table for wide15

Source	SS	df	MS	F	Prob>F
Groups	2006.09	10.00	200.61	8.56	0.00
Error	45441.44	1939.00	23.44		
Total	47447.53	1949.00			

Table 12 ANOVA Table for wide20

Source	SS	df	MS	F	Prob>F
Groups	1682.98	10.00	168.30	4.47	0.00
Error	57167.90	1517.00	37.68		
Total	58850.88	1527.00			

Table 13 ANOVA Table for wide25

Source	SS	df	MS	F	Prob>F
Groups	2574.84	10.00	257.48	5.32	0.00
Error	57094.47	1179.00	48.43		
Total	59669.31	1189.00			

Table 14 ANOVA Table for wide30

Source	SS	df	MS	F	Prob>F
Groups	3302.61	10.00	330.26	4.35	0.00
Error	109153.47	1437.00	75.96		
Total	112456.07	1447.00			

Table 15 ANOVA Table for wide35

Source	SS	df	MS	F	Prob>F
Groups	1565.08	9.00	173.90	3.61	0.00
Error	47305.91	983.00	48.12		
Total	48870.99	992.00			

Table 16 ANOVA Table for SEM1

Source	SS	df	MS	F	Prob>F
Groups	2378.31	9.00	264.26	18.57	0.00
Error	13800.03	970.00	14.23		
Total	16178.34	979.00			

Table 17 ANOVA Table for SEM2

Source	SS	df	MS	F	Prob>F
Groups	4612.40	9.00	512.49	36.07	0.00
Error	17788.48	1252.00	14.21		
Total	22400.88	1261.00			

Table 18 ANOVA Table for SEM3

Source	SS	df	MS	F	Prob>F
Groups	2427.57	9.00	269.73	7.87	0.00
Error	36205.59	1057.00	3 4.25		
Total	38633.16	1066.00			

Table 19 ANOVA Table for SEM4

Source	SS	df	MS	F	Prob>F
Groups	3554.55	9.00	394.95	31.05	0.00
Error	10646.25	837.00	12.72		
Total	14200.79	846.00			

Table 20 ANOVA Table for SEM5

Source	SS	df	MS	F	Prob>F
Groups	1809.60	9.00	201.07	16.71	0.00
Error	10683.36	888.00	12.03		
Total	12492.96	897.00			

Table 21 ANOVA Table for SEM6

Source	SS	df	MS	F	Prob>F
Groups	2711.61	8.00	338.95	45.72	0.00
Error	8361.86	1128.00	7.41		
Total	11073.47	1136.00			

Table 22 ANOVA Table for SEM7

Source	SS	df	MS	F	Prob>F
Groups	16282.23	9.00	1809.14	23.77	0.00
Error	126343.14	1660.00	76.11		
Total	142625.36	1669.00			

Table 23 ANOVA Table for SEM8

Tukey-Kramer Multiple comparison of Means for all ANOVA tables

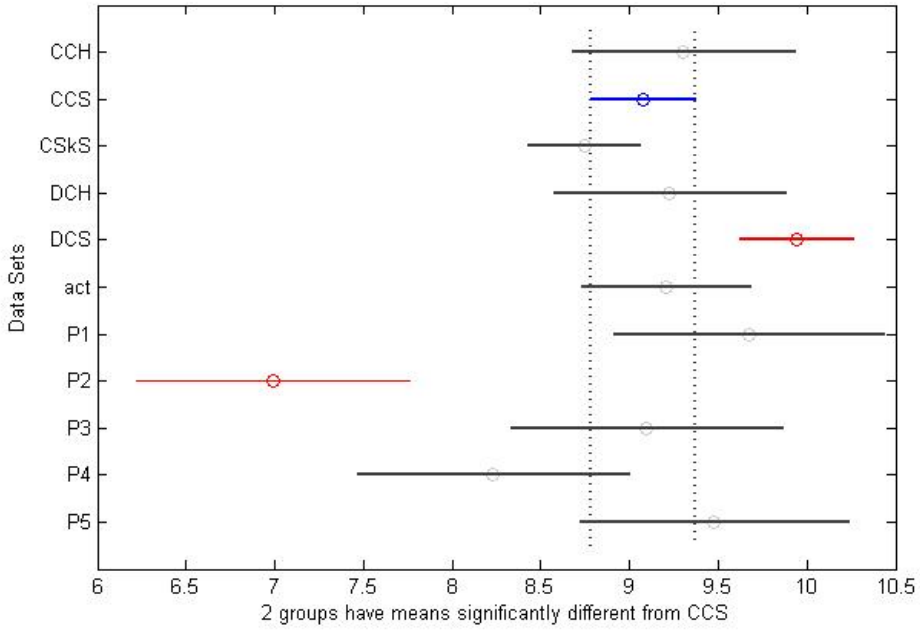

Figure 57 Tukey-Kramer Multiple Comparison of Means for narrow10 (α=0.05)

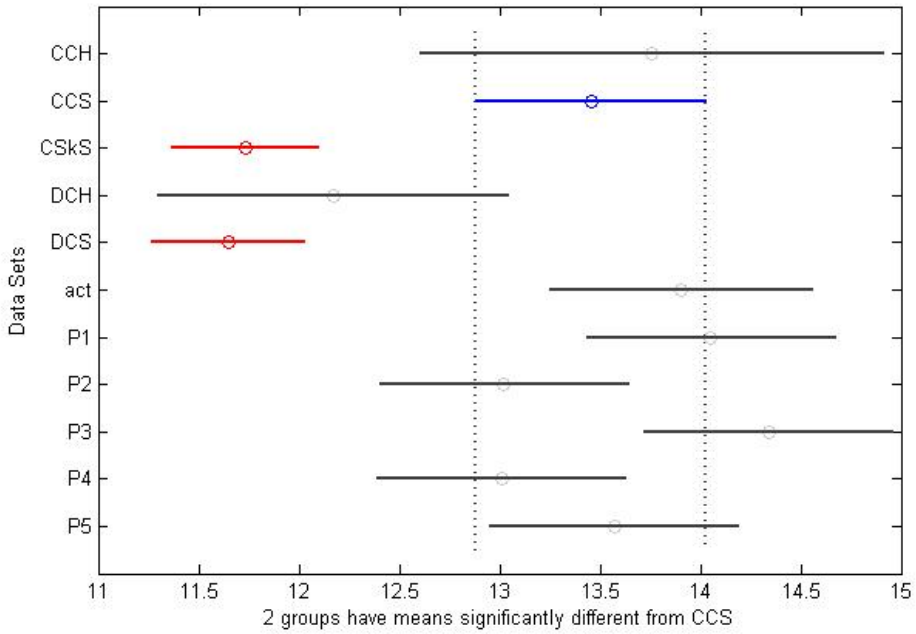

Figure 58 Tukey-Kramer Multiple Comparison of Means for narrow15 (α=0.05)

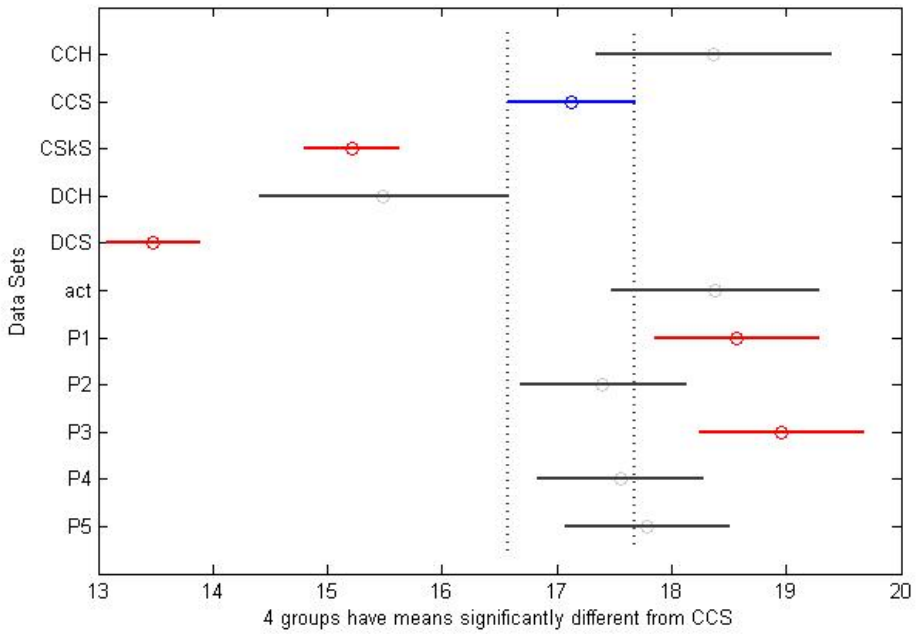

Figure 59 Tukey-Kramer Multiple Comparison of Means for narrow20 (α=0.05)

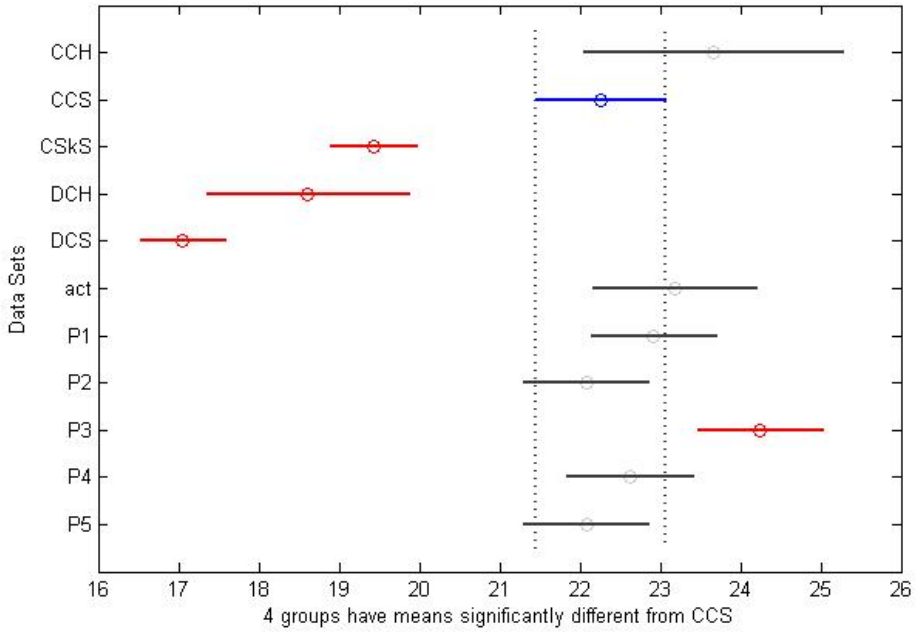

Figure 60 Tukey-Kramer Multiple Comparison of Means for narrow25 (α=0.05)

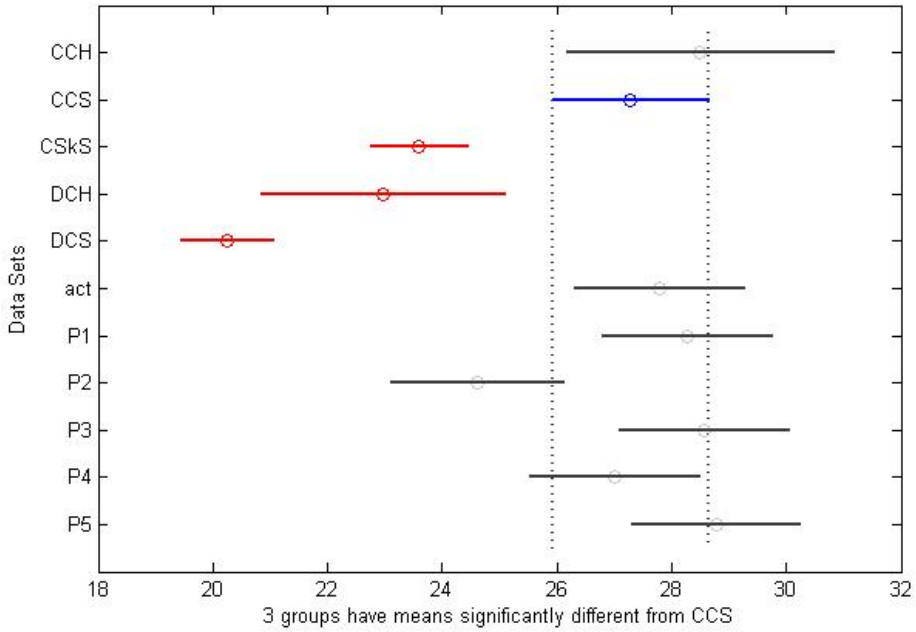

Figure 61 Tukey-Kramer Multiple Comparison of Means for narrow30 (α=0.05)

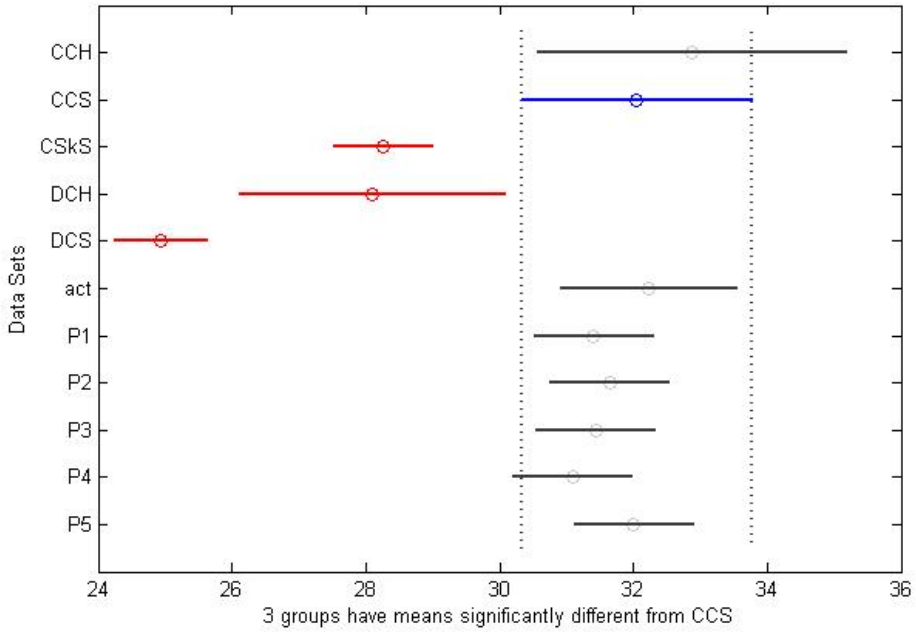

Figure 62 Tukey-Kramer Multiple Comparison of Means for narrow35 (α=0.05)

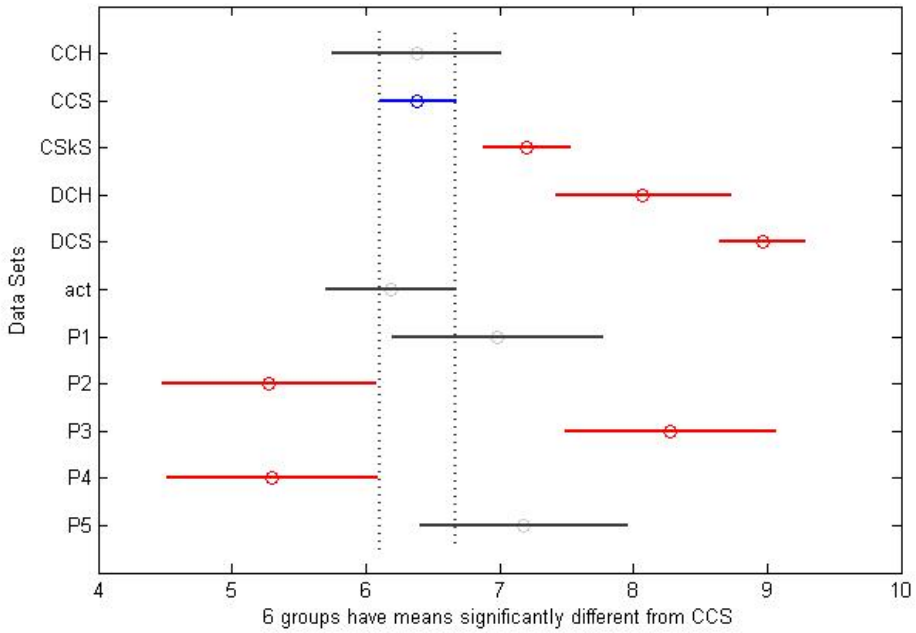

Figure 63 Tukey-Kramer Multiple Comparison of Means for wide10 (α=0.05)

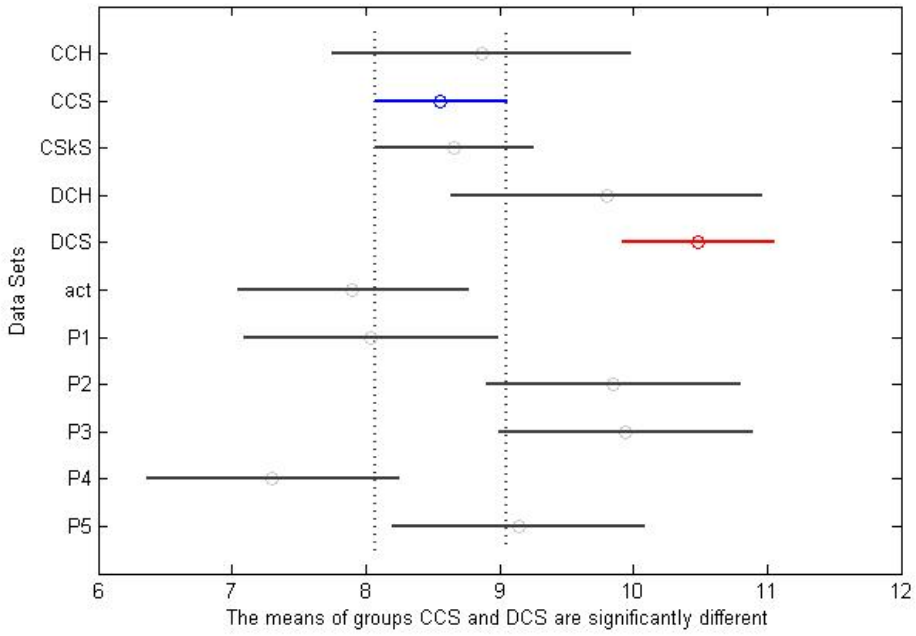

Figure 64 Tukey-Kramer Multiple Comparison of Means for wide15 (α=0.05)

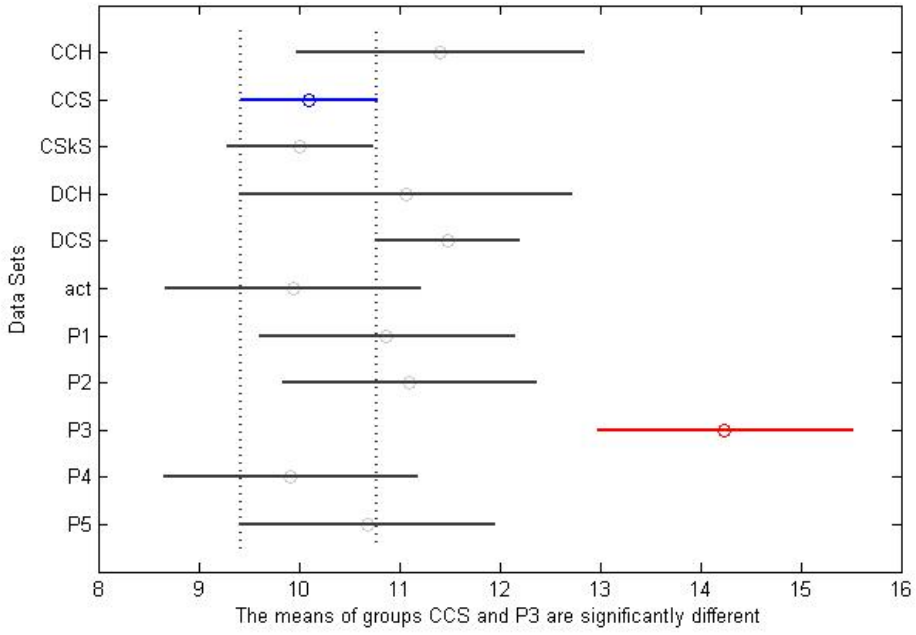

Figure 65 Tukey-Kramer Multiple Comparison of Means for wide20 (α=0.05)

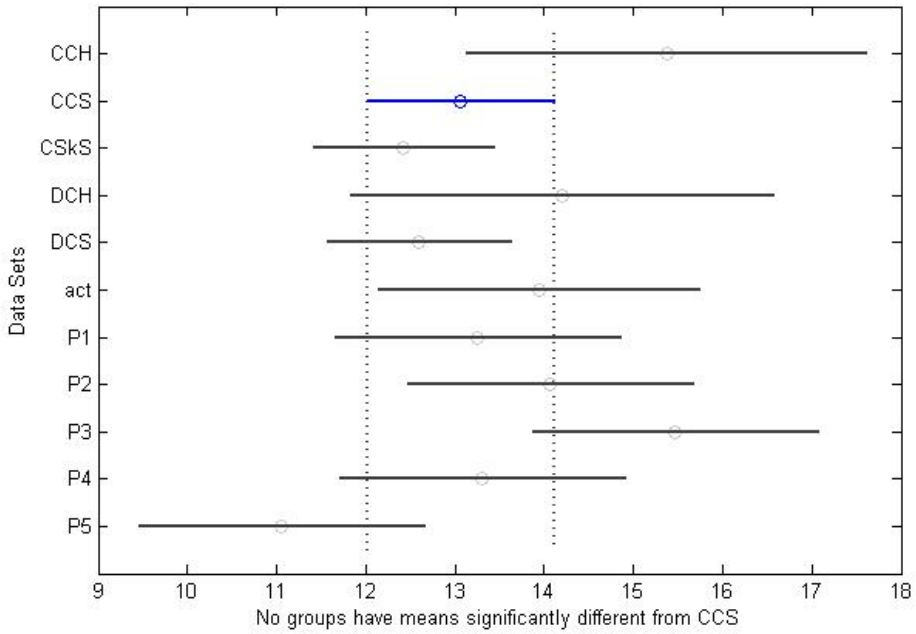

Figure 66 Tukey-Kramer Multiple Comparison of Means for wide25 (α=0.05)

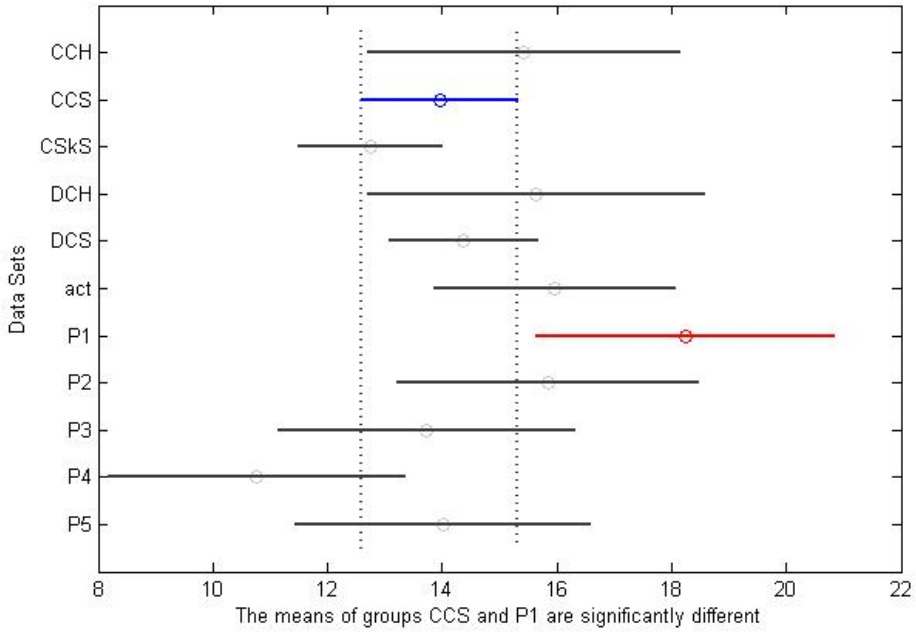

Figure 67 Tukey-Kramer Multiple Comparison of Means for wide30 (α=0.05)

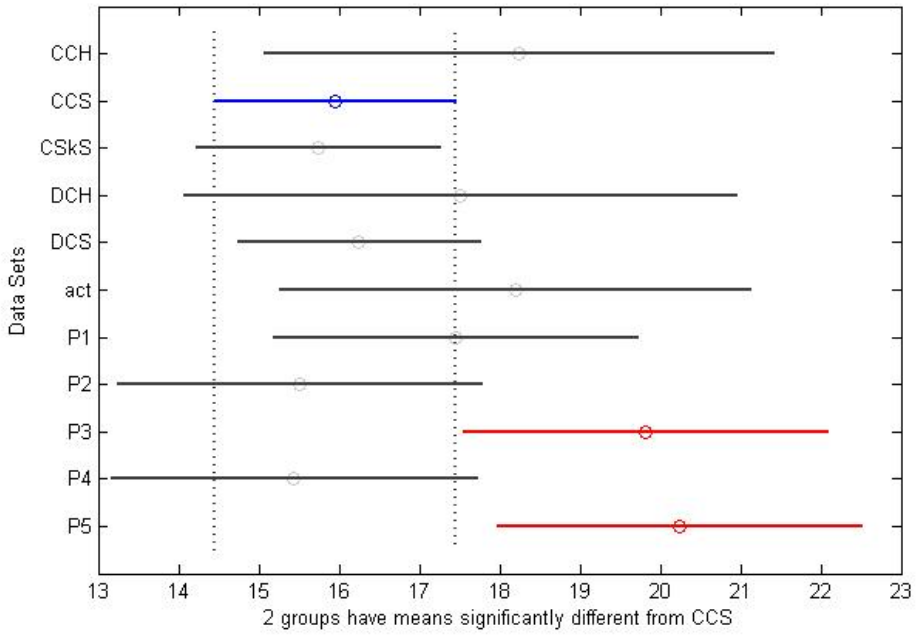

Figure 68 Tukey-Kramer Multiple Comparison of Means for wide35 (α=0.05)

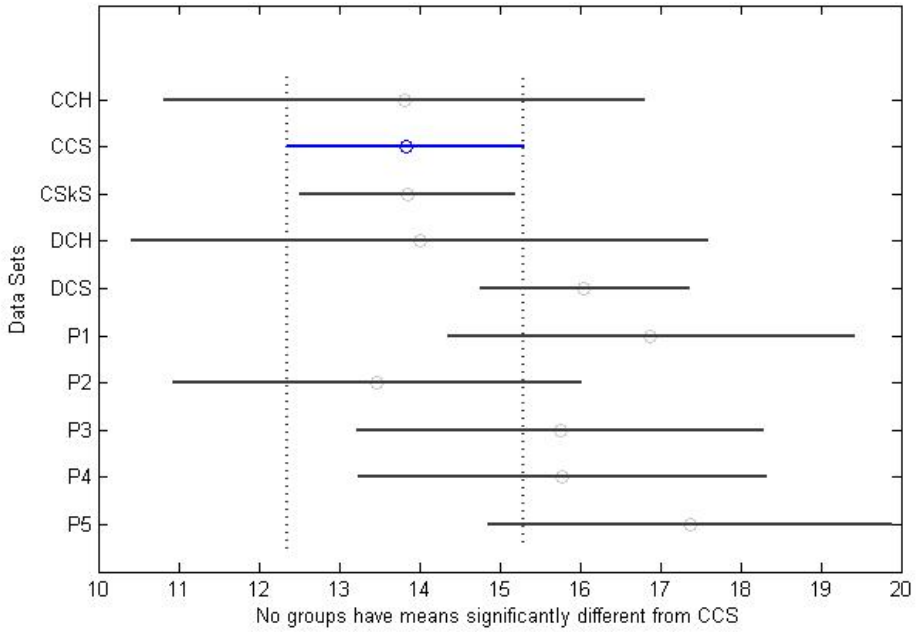

Figure 69 Tukey-Kramer Multiple Comparison of Means for SEM1 (α=0.05)

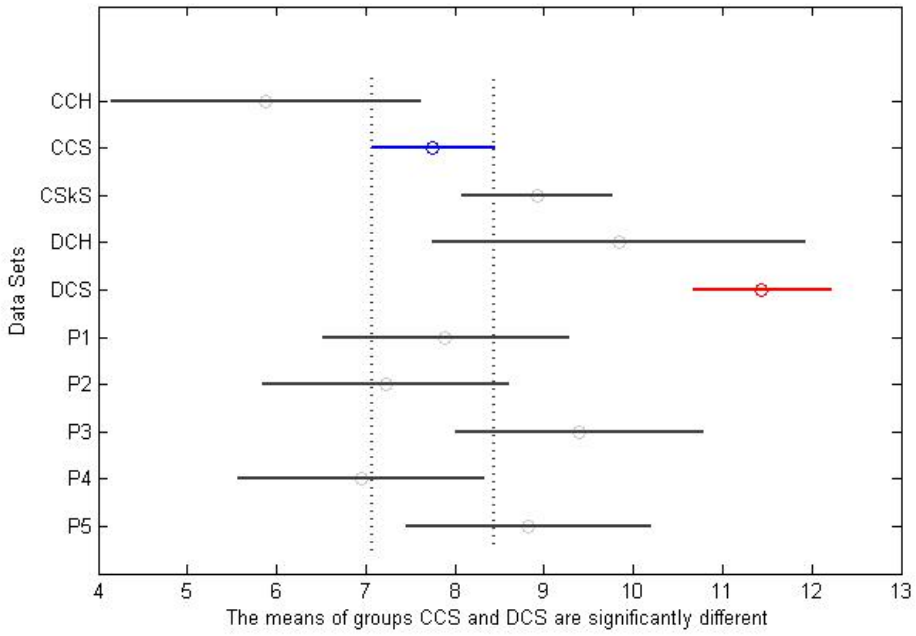

Figure 70 Tukey-Kramer Multiple Comparison of Means for SEM2 (α=0.05)

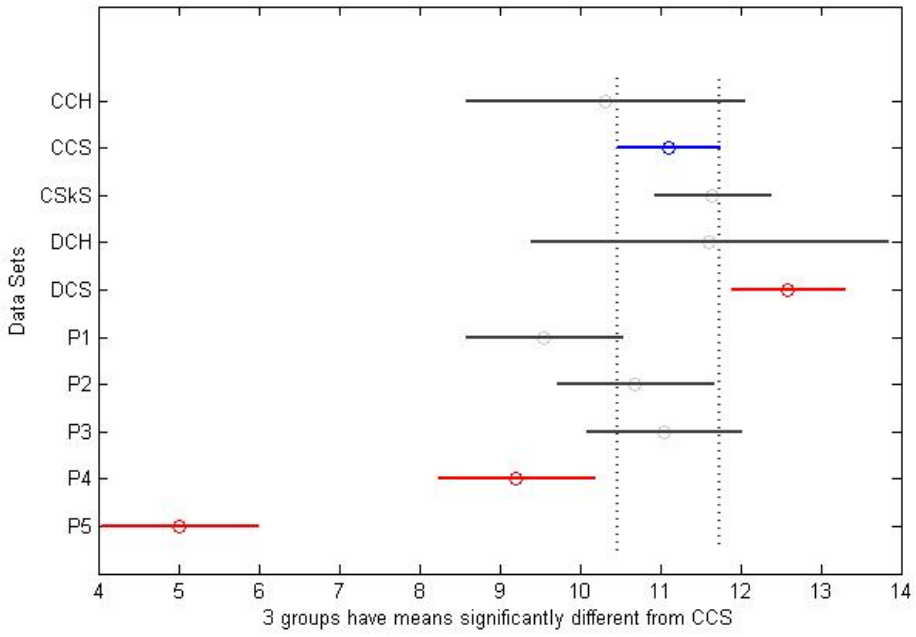

Figure 71 Tukey-Kramer Multiple Comparison of Means for SEM3 (α=0.05)

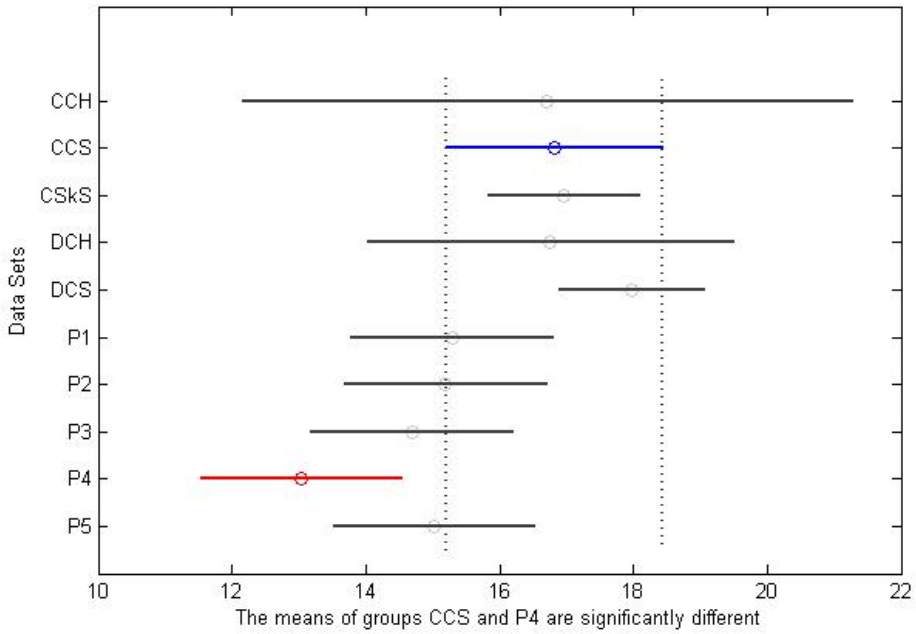

Figure 72 Tukey-Kramer Multiple Comparison of Means for SEM4 (α=0.05)

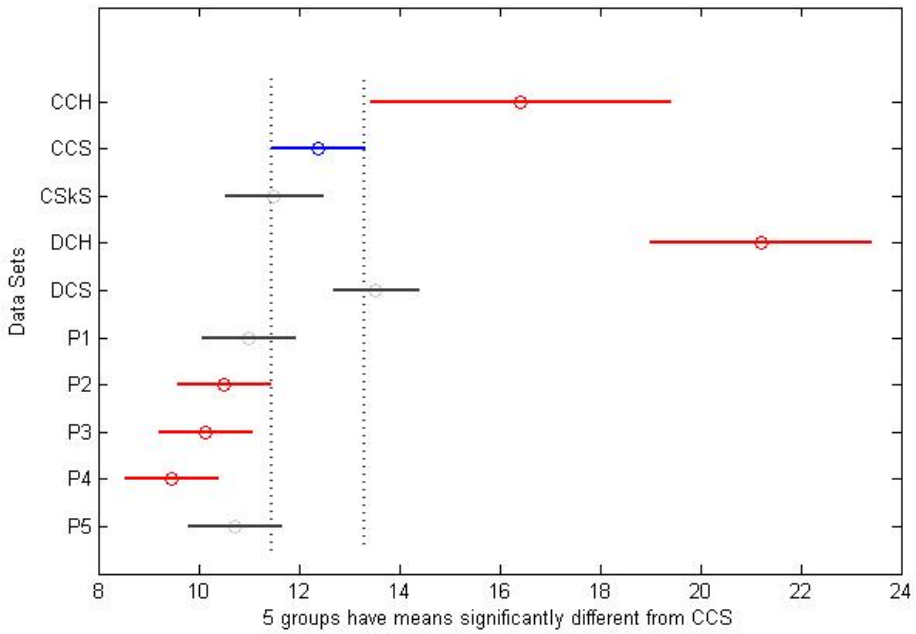

Figure 73 Tukey-Kramer Multiple Comparison of Means for SEM5 (α=0.05)

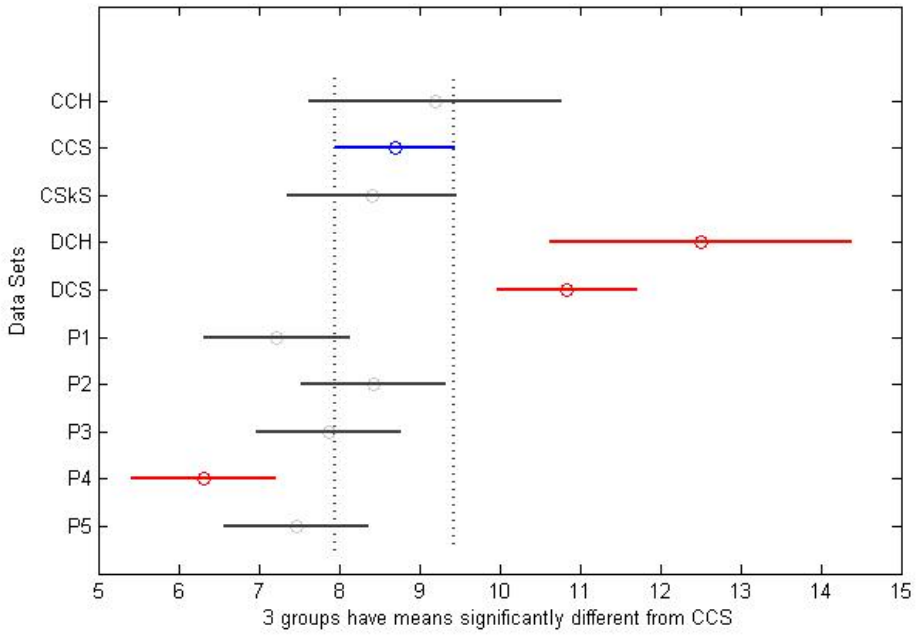

Figure 74 Tukey-Kramer Multiple Comparison of Means for SEM6 (α=0.05)

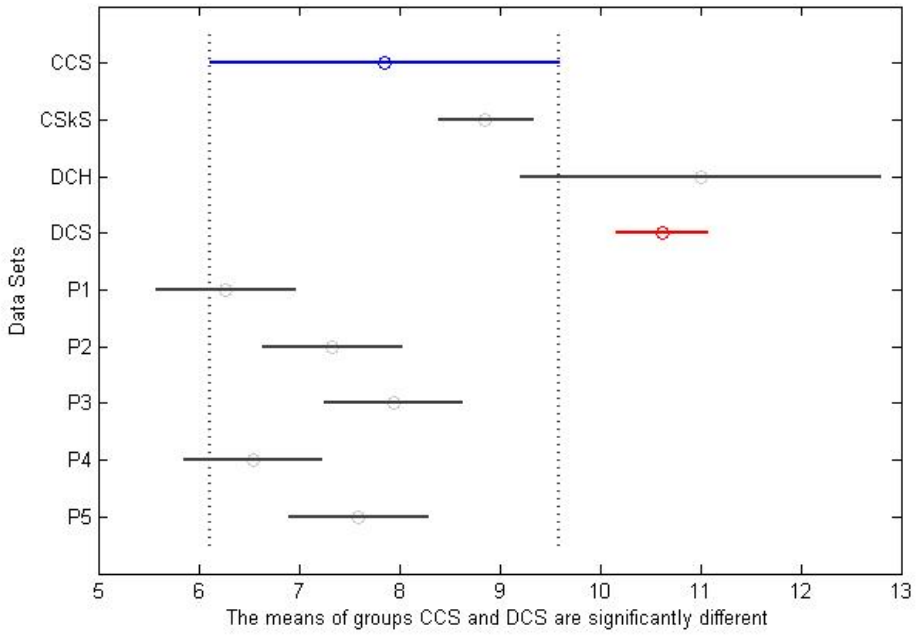

Figure 75 Tukey-Kramer Multiple Comparison of Means for SEM7 (α=0.05)

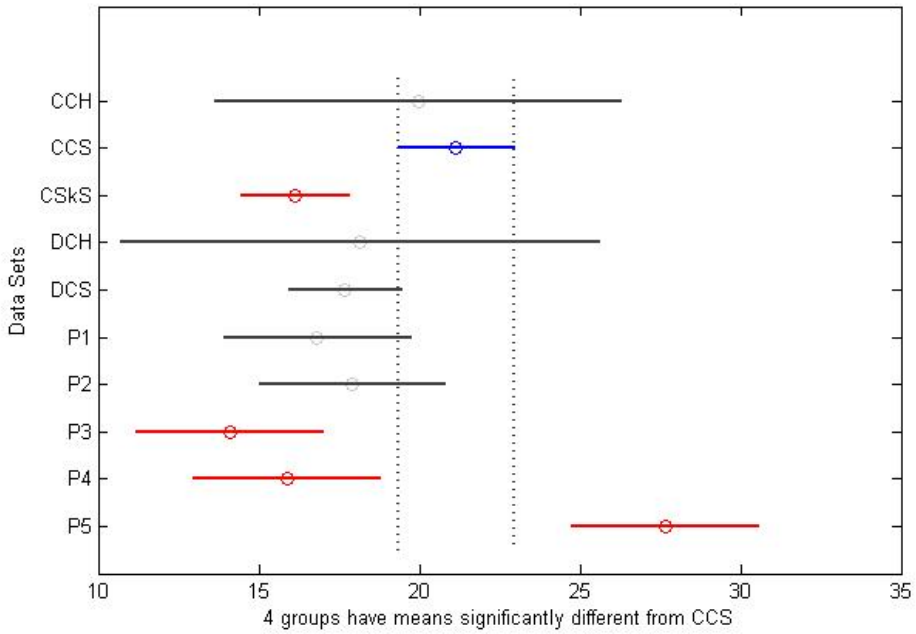

Figure 76 Tukey-Kramer Multiple Comparison of Means for SEM8 (α=0.05)

APPENDIX B: Resulting Images for Skeleton Slopes Method

The following images were processed with the Skeleton Slopes fiber diameter measurement method. The fiber diameters per image can be found in the results section. The following figures, the determined valid edges per image were superimposed over the corresponding original image. Red and blue segments respectively represent the left and right edges of the valid edge pairs found with this method.

CSkS edges superimposed over the narrow distribution simulated images

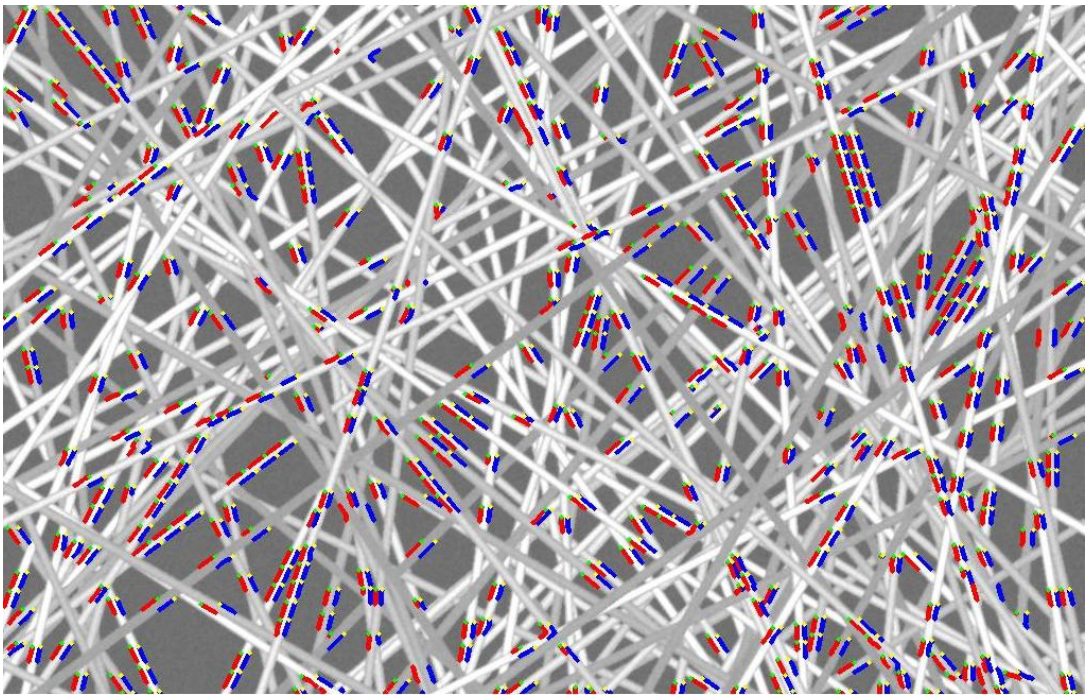

Figure 77 Image narrow10 with CSkS valid edges

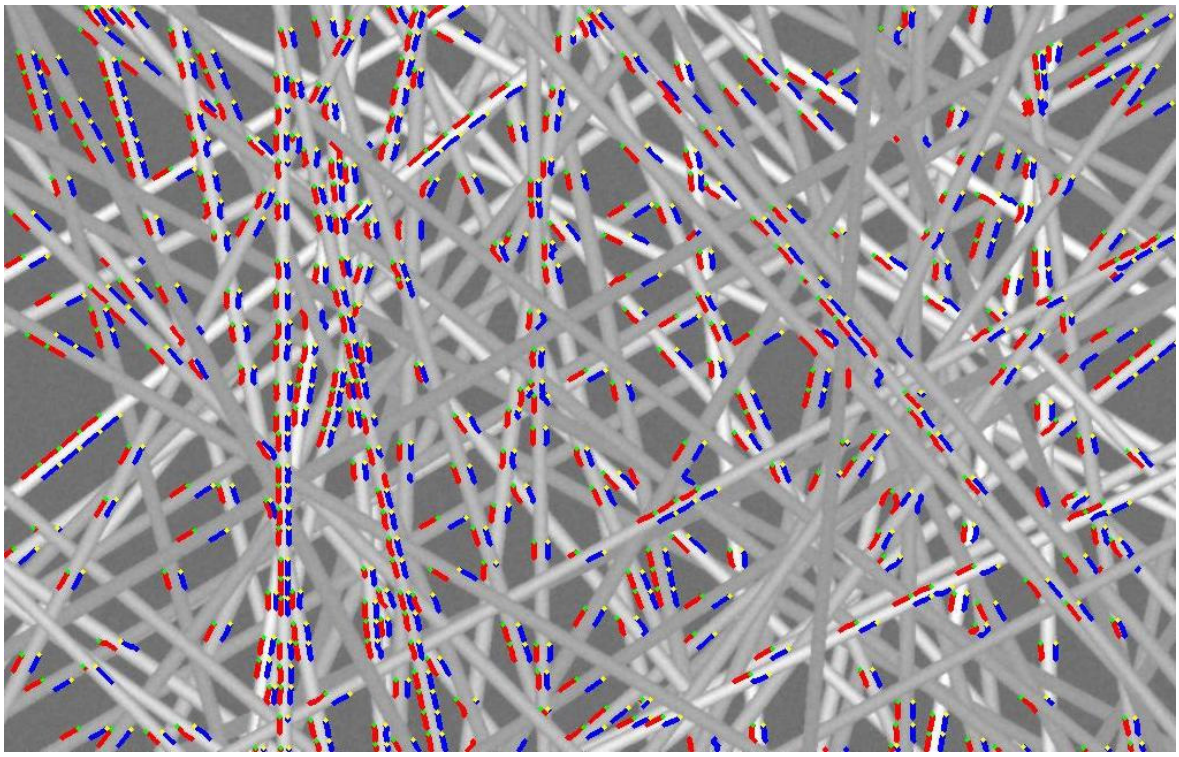

Figure 78 Image narrow15 with CSkS valid edges

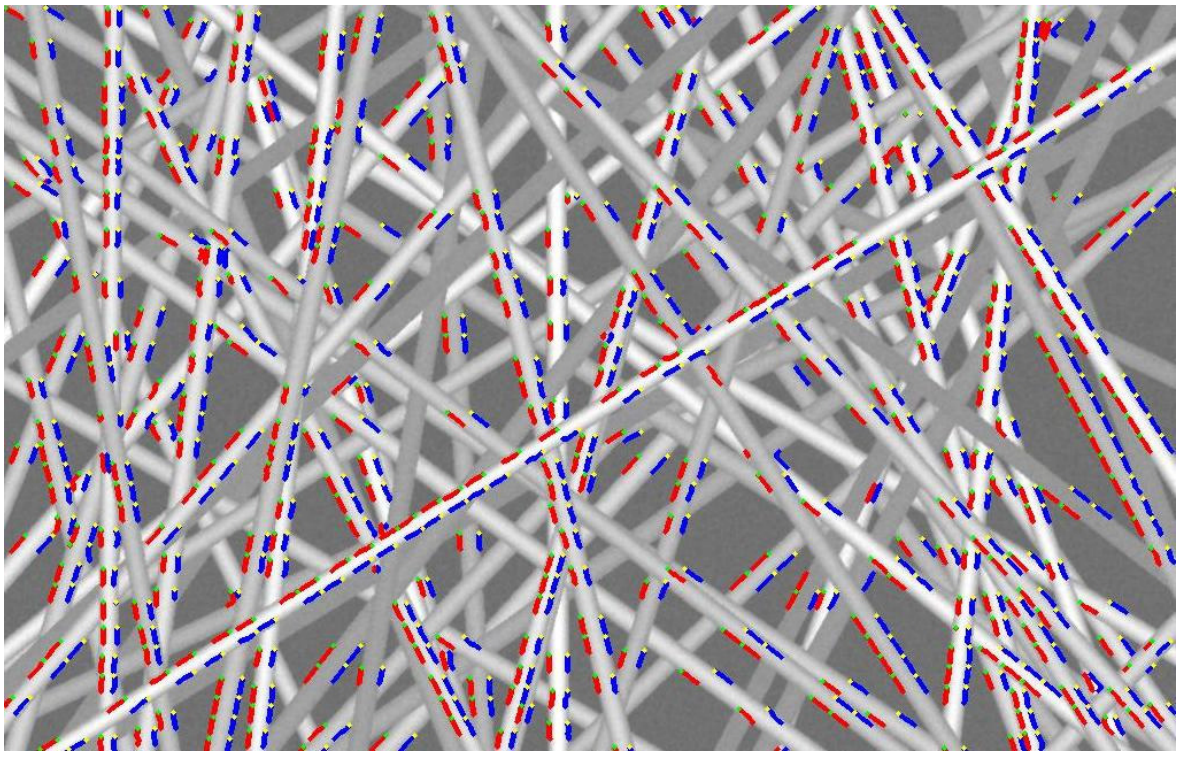

Figure 79 Image narrow20 with CSkS valid edges

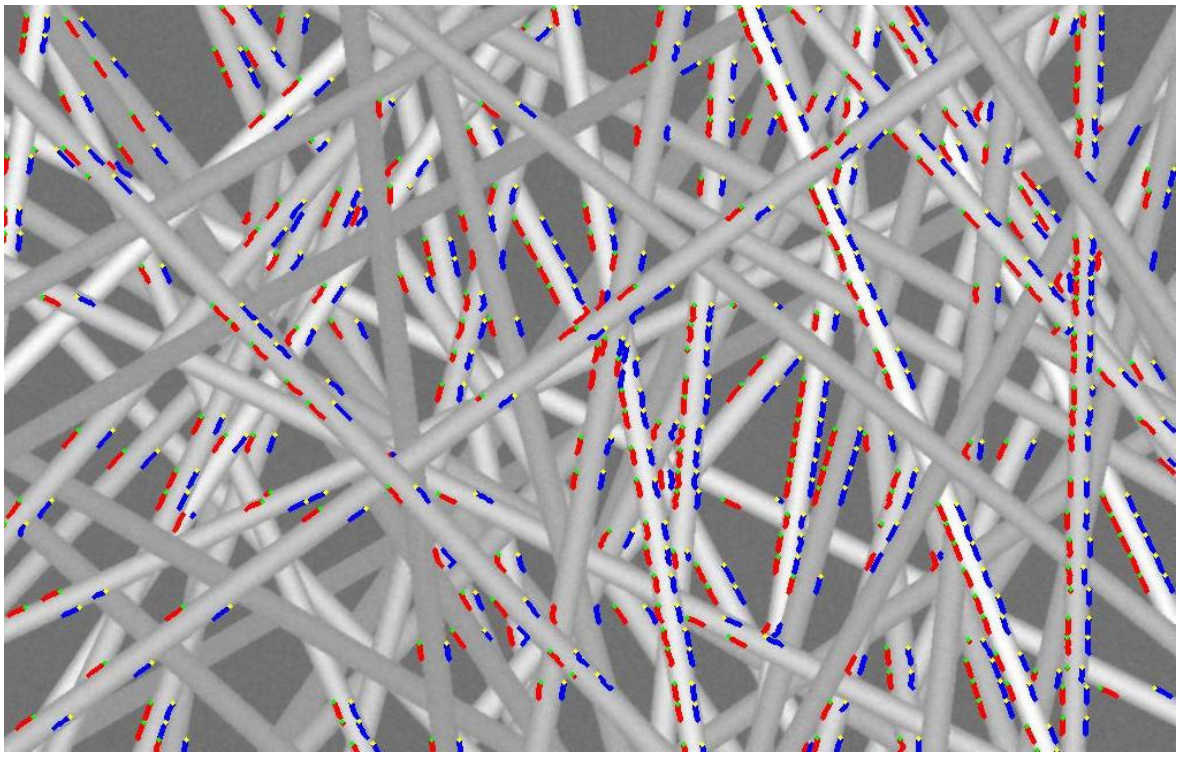

Figure 80 Image narrow25 with CSkS valid edges

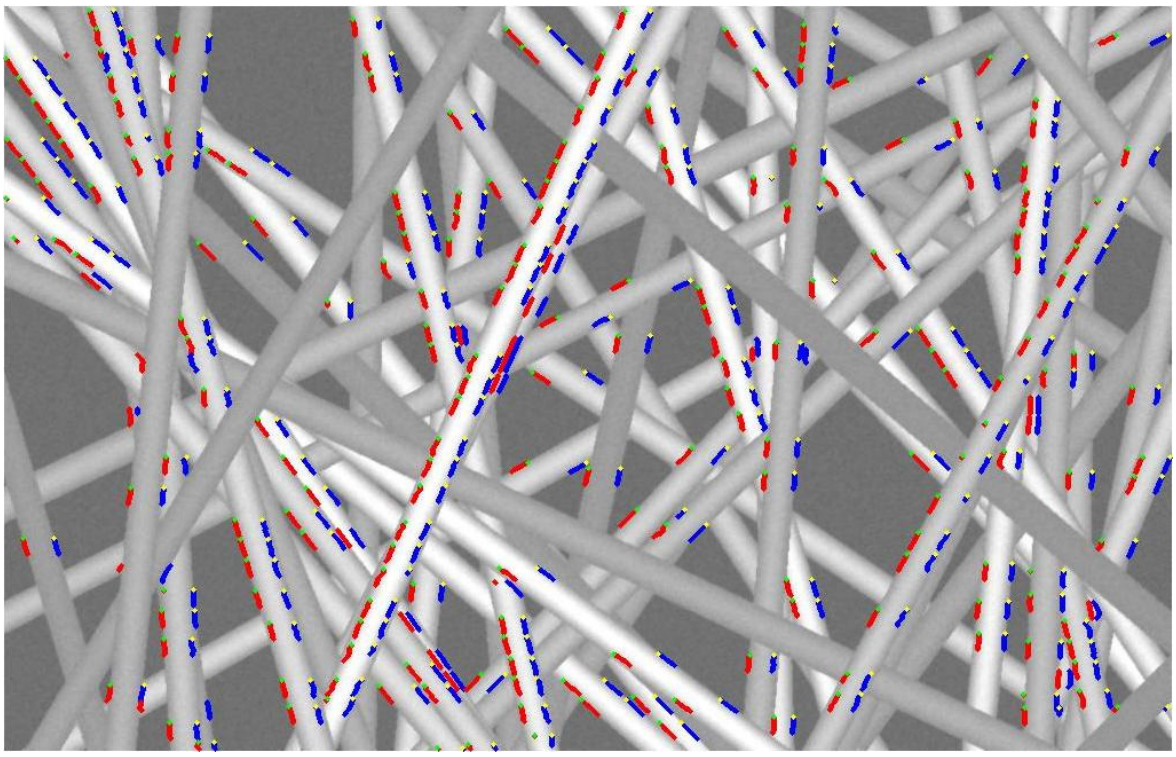

Figure 81 Image narrow30 with CSkS valid edges

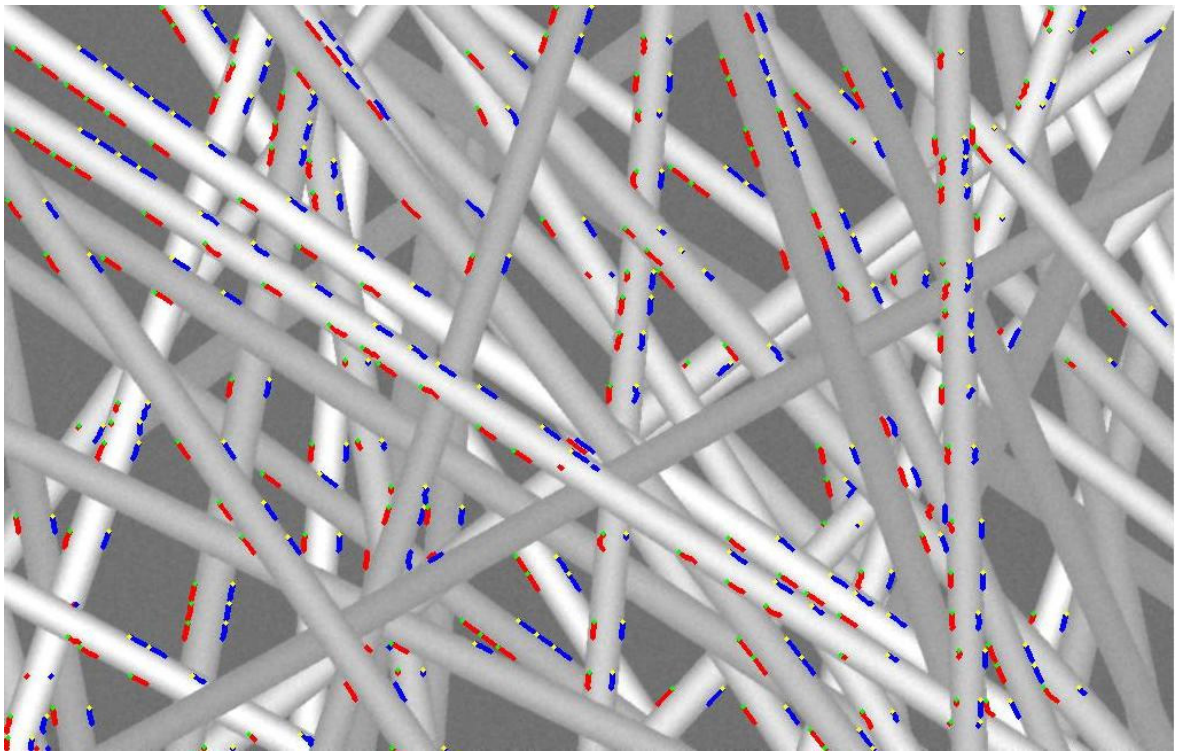

Figure 82 Image narrow35 with CSkS valid edges

CSkS edges superimposed over the wide distribution simulated images

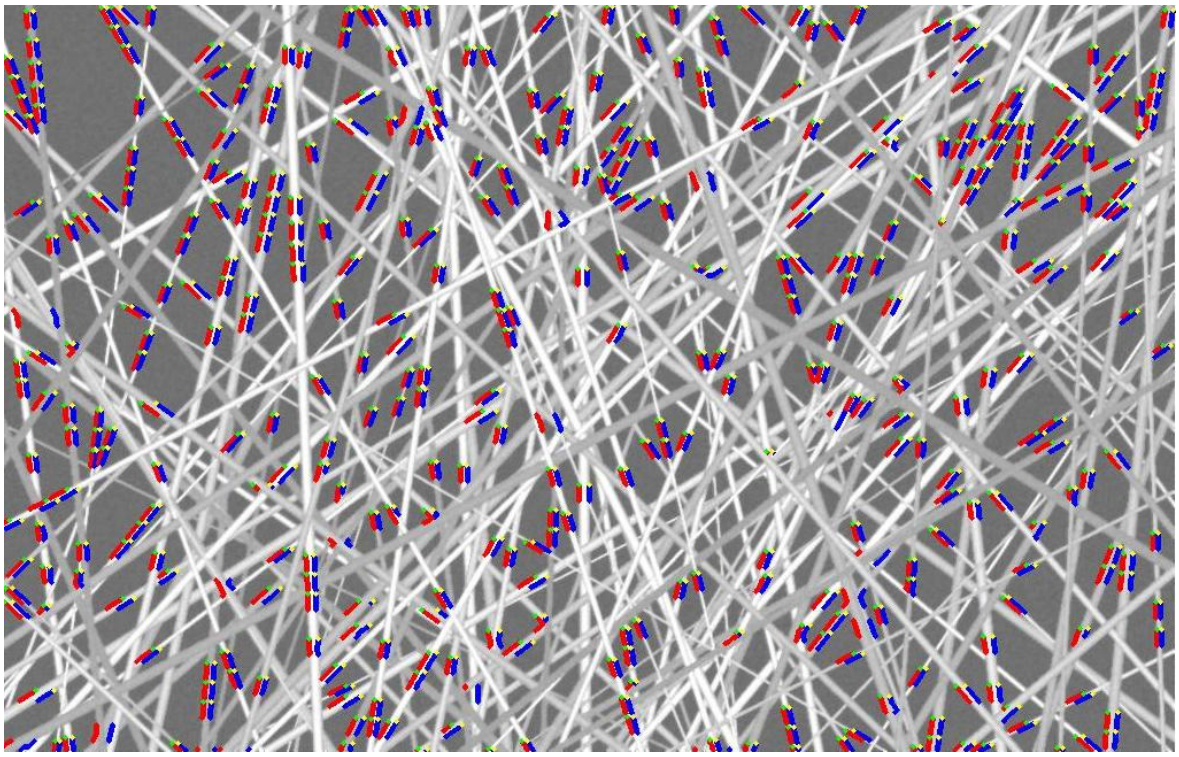

Figure 83 Image wide10 with CSkS valid edges

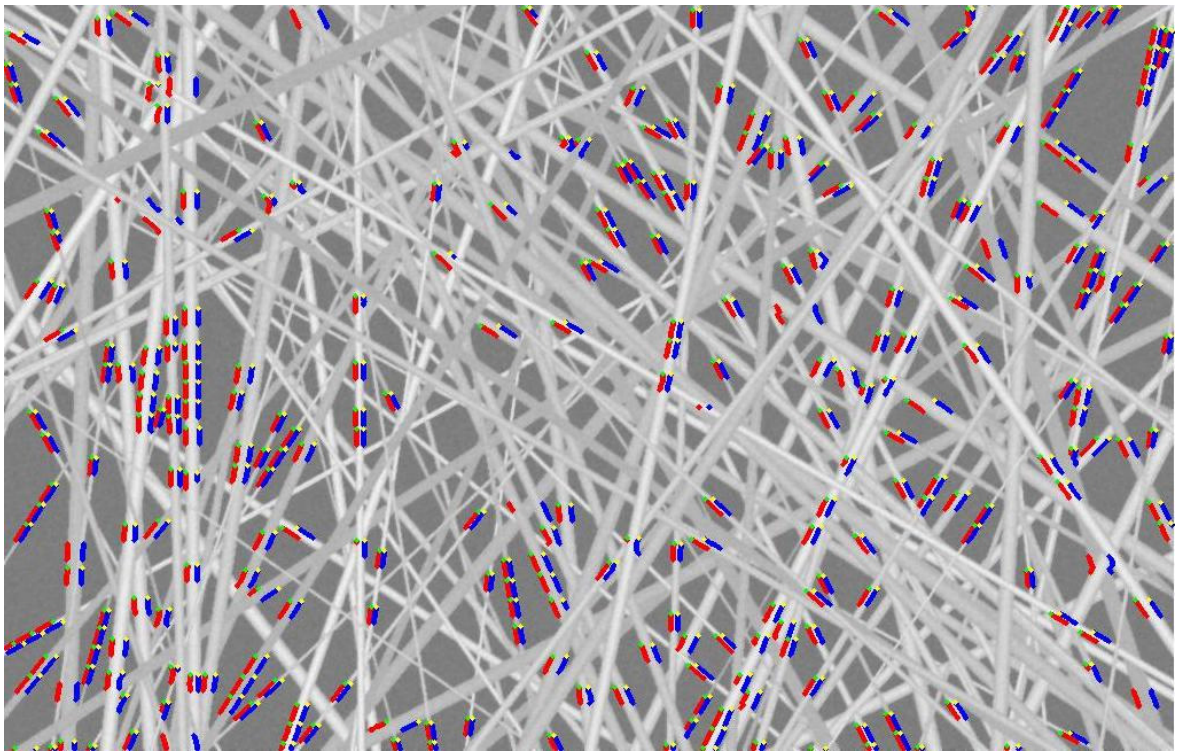

Figure 84 Image wide15 with CSkS valid edges

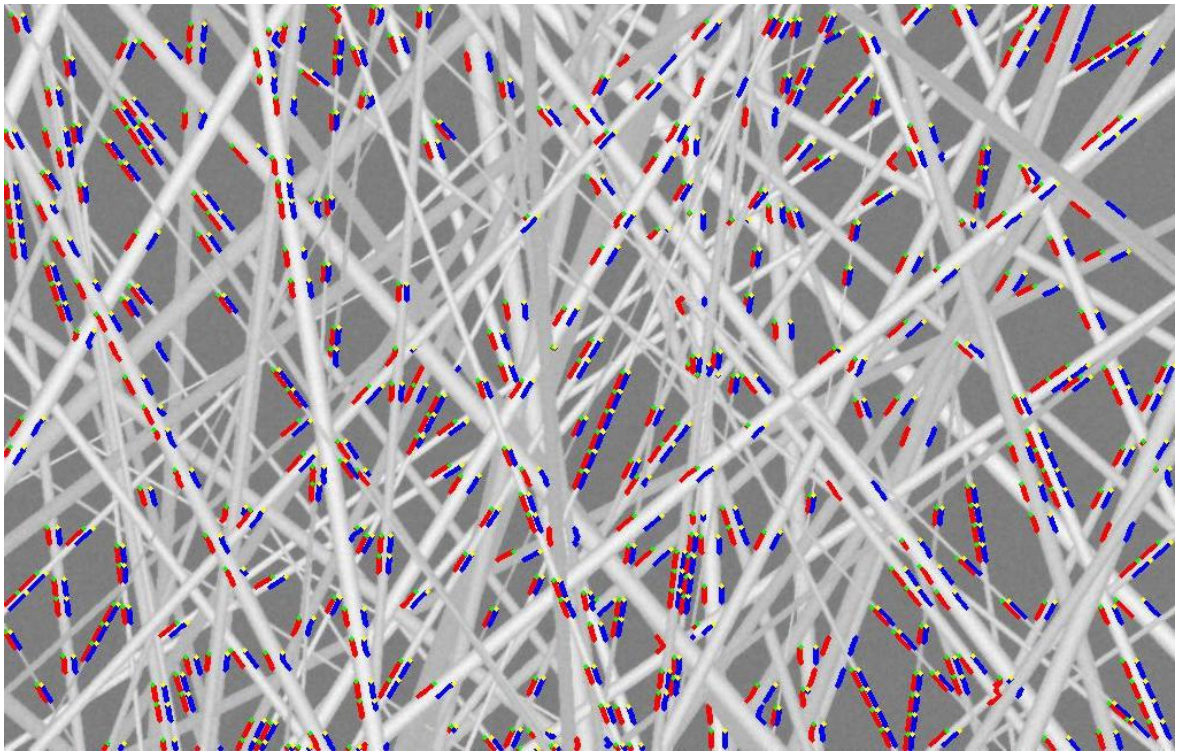

Figure 85 Image wide20 with CSkS valid edges

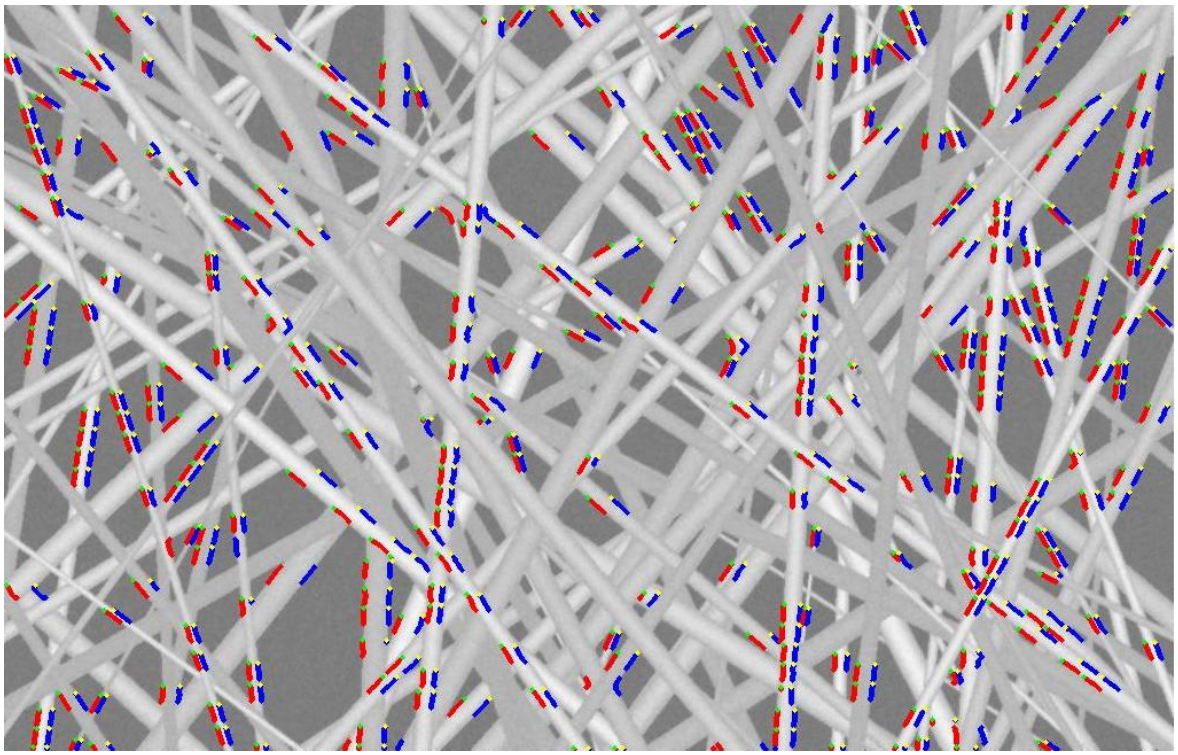

Figure 86 Image wide25 with CSkS valid edges

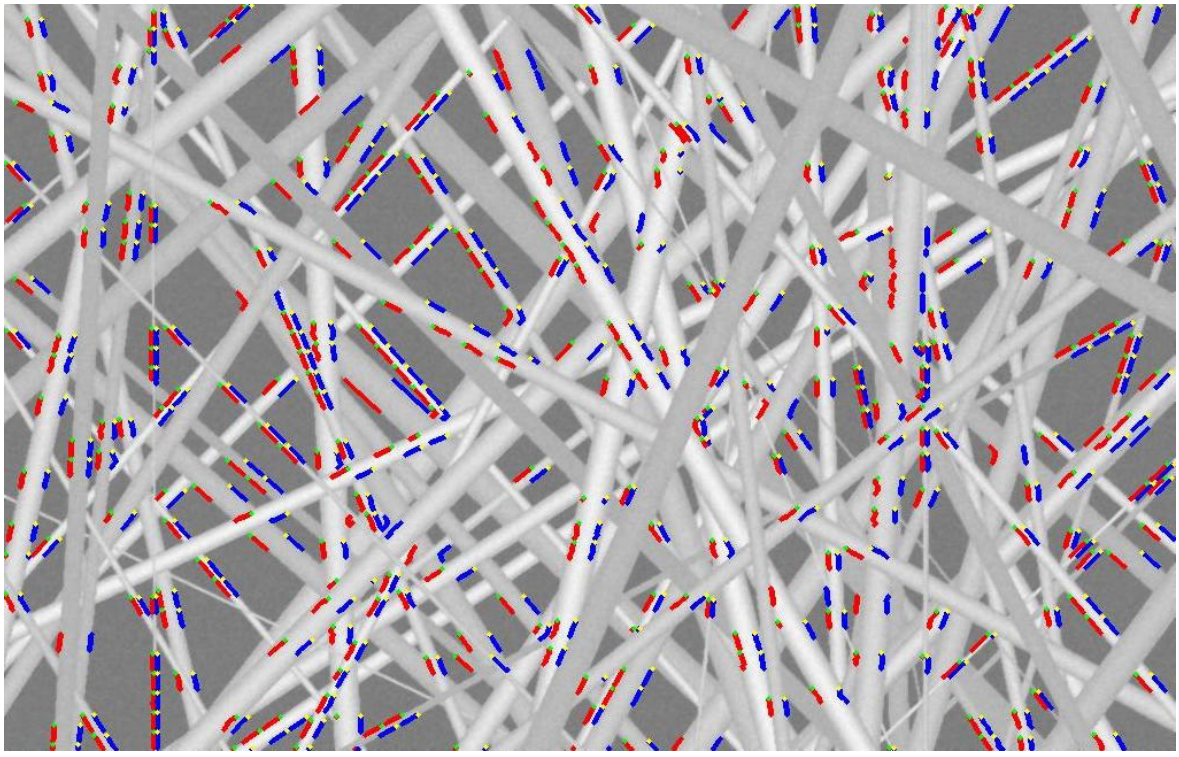

Figure 87 Image wide30 with CSkS valid edges

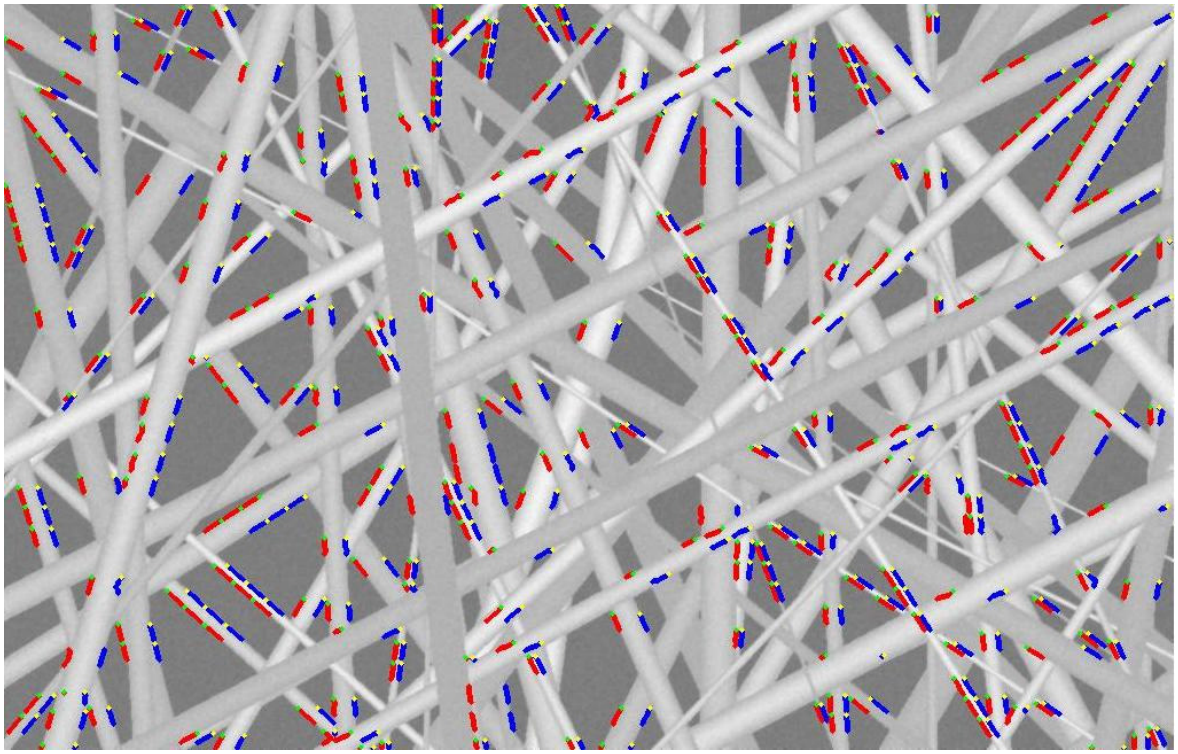

Figure 88 Image wide35 with CSkS valid edges

CSkS edges superimposed over real SEM images

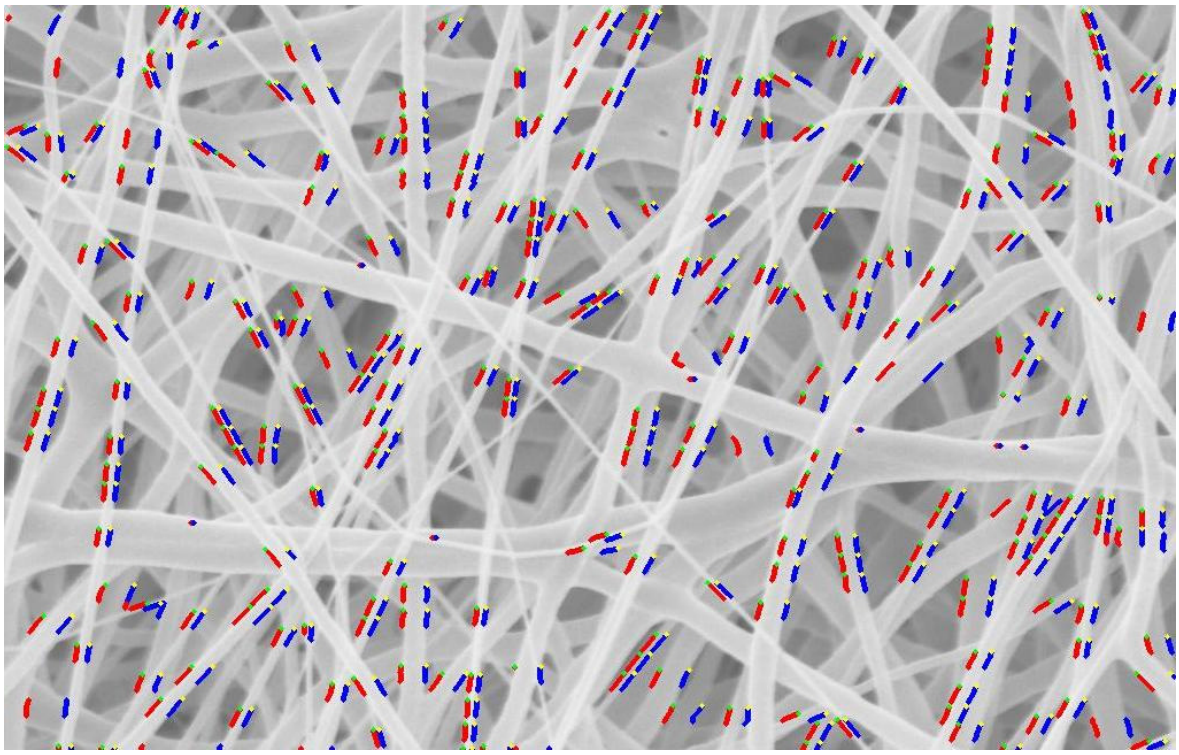

Figure 89 Image SEM1 with CSkS valid edges

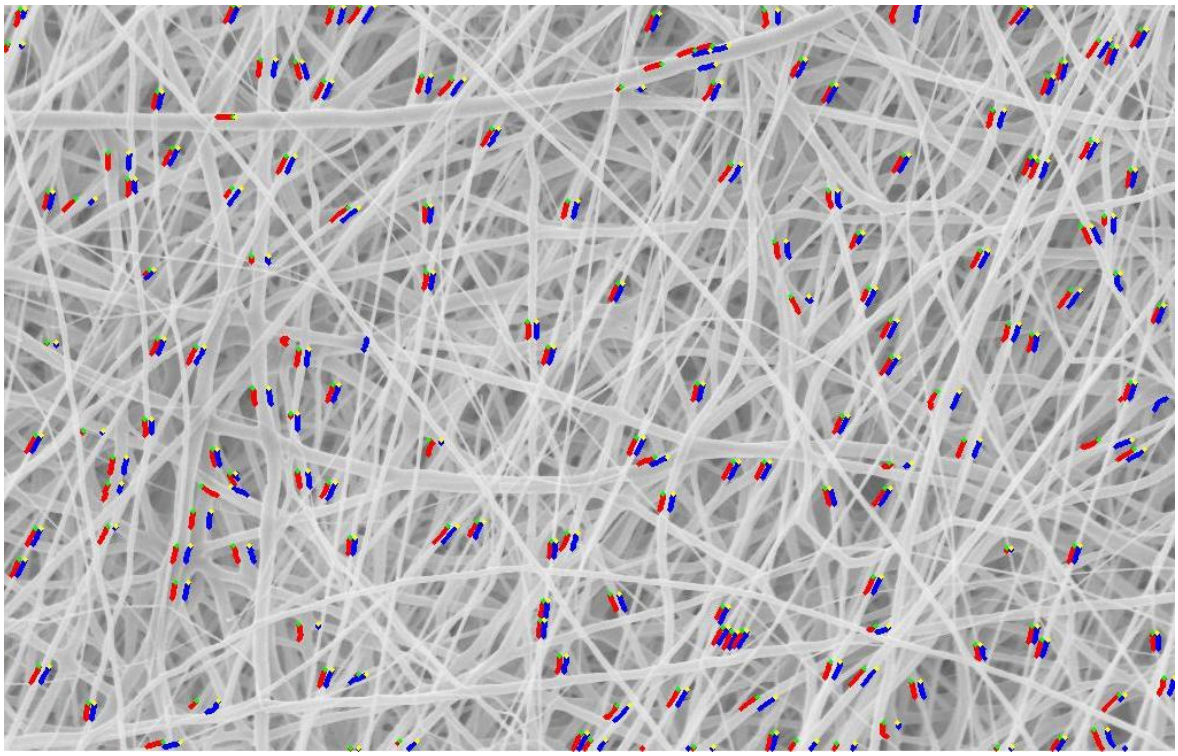

Figure 90 Image SEM2 with CSkS valid edges

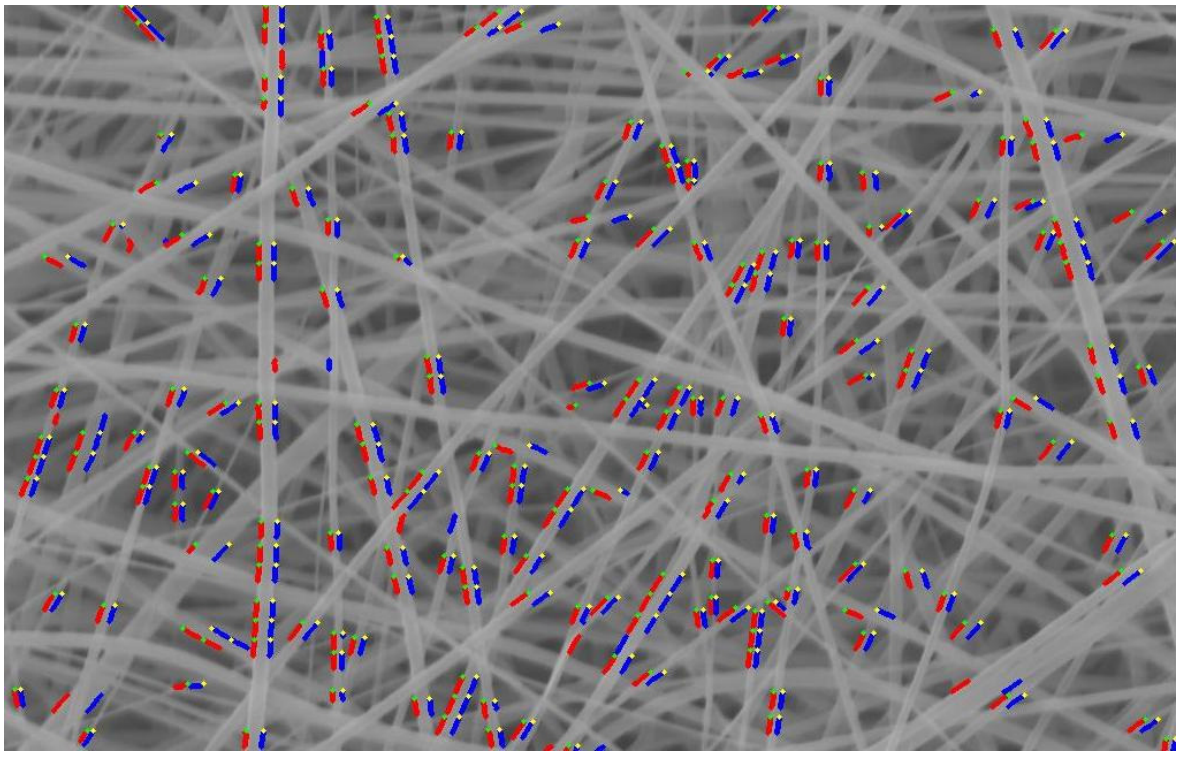

Figure 91 Image SEM3 with CSkS valid edges

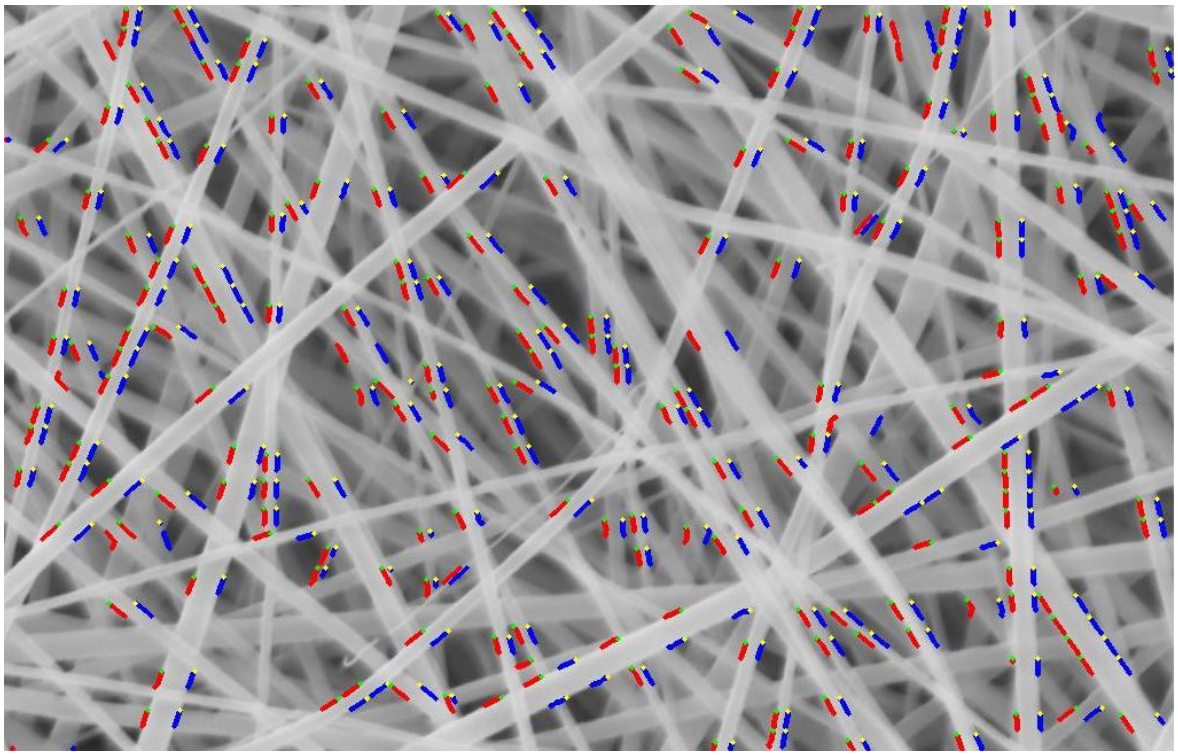

Figure 92 Image SEM4 with CSkS valid edges

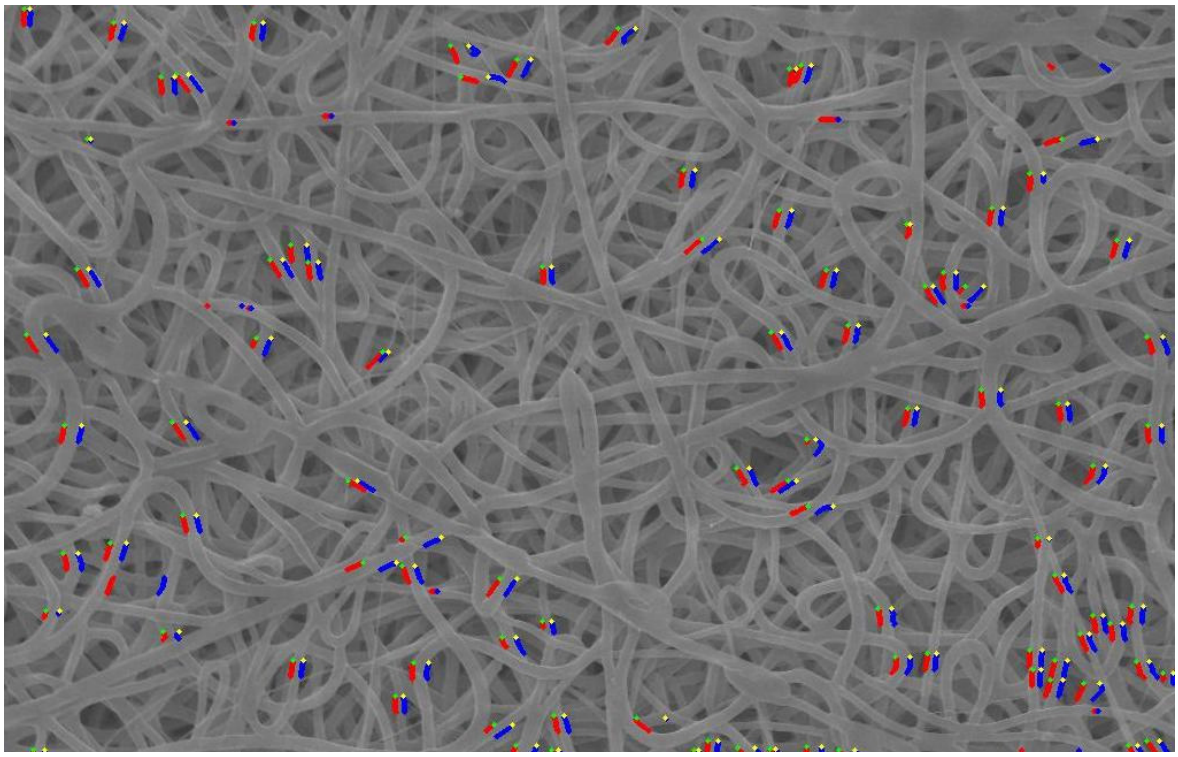

Figure 93 Image SEM5 with CSkS valid edges

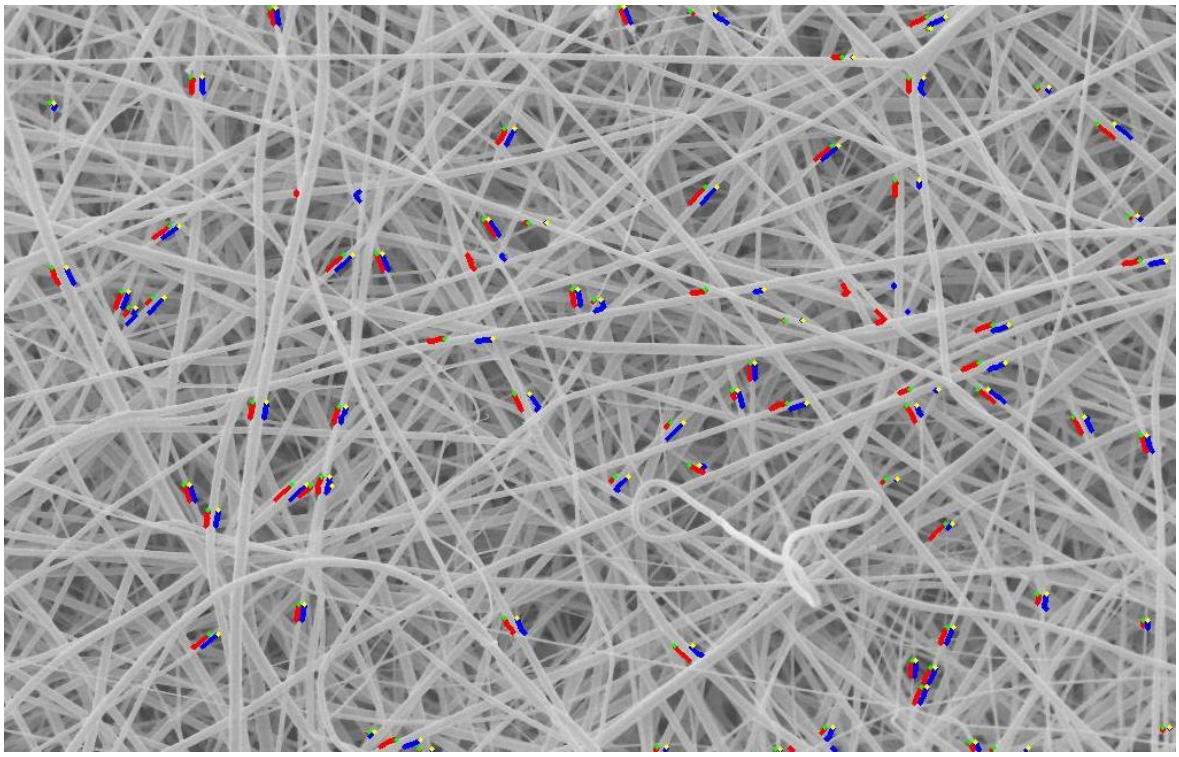

Figure 94 Image SEM6 with CSkS valid edges

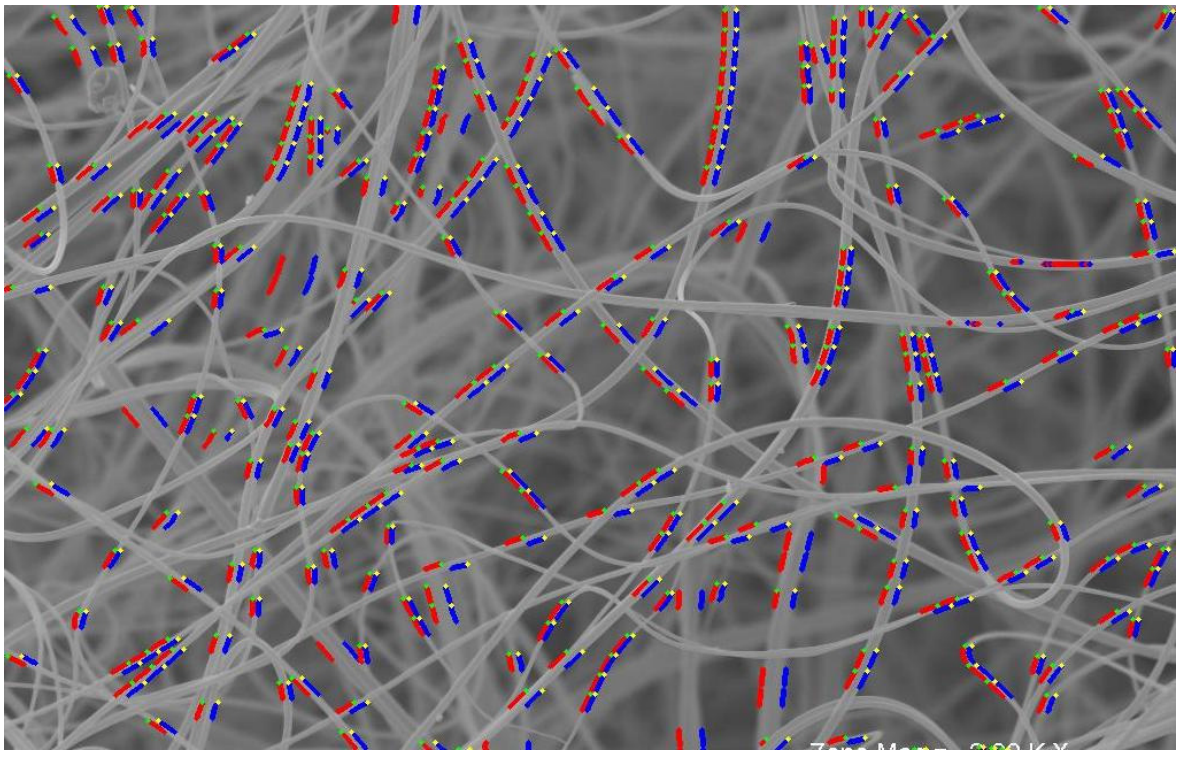

Figure 95 SEM7 with CSkS valid edges

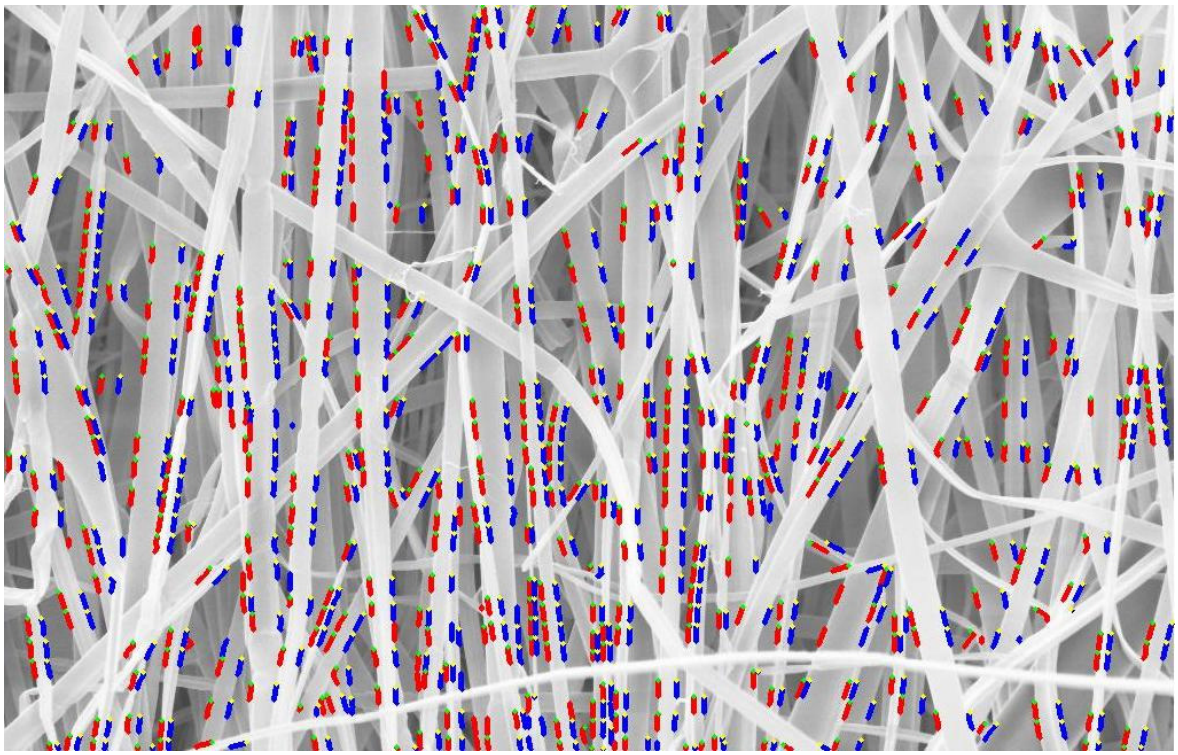

Figure 96 Image SEM8 with CSkS valid edges

APPENDIX C: Resulting Images for Canny Slopes Method

The following images were processed with the Default Canny Slopes fiber diameter measurement method. The fiber diameters per image can be found in the results section. In the following figures, the determined valid edges per image were superimposed over the corresponding original image. Red and blue segments respectively represent the left and right edges of the valid edge pairs found with this method.

DCS edges superimposed over the narrow distribution simulated images

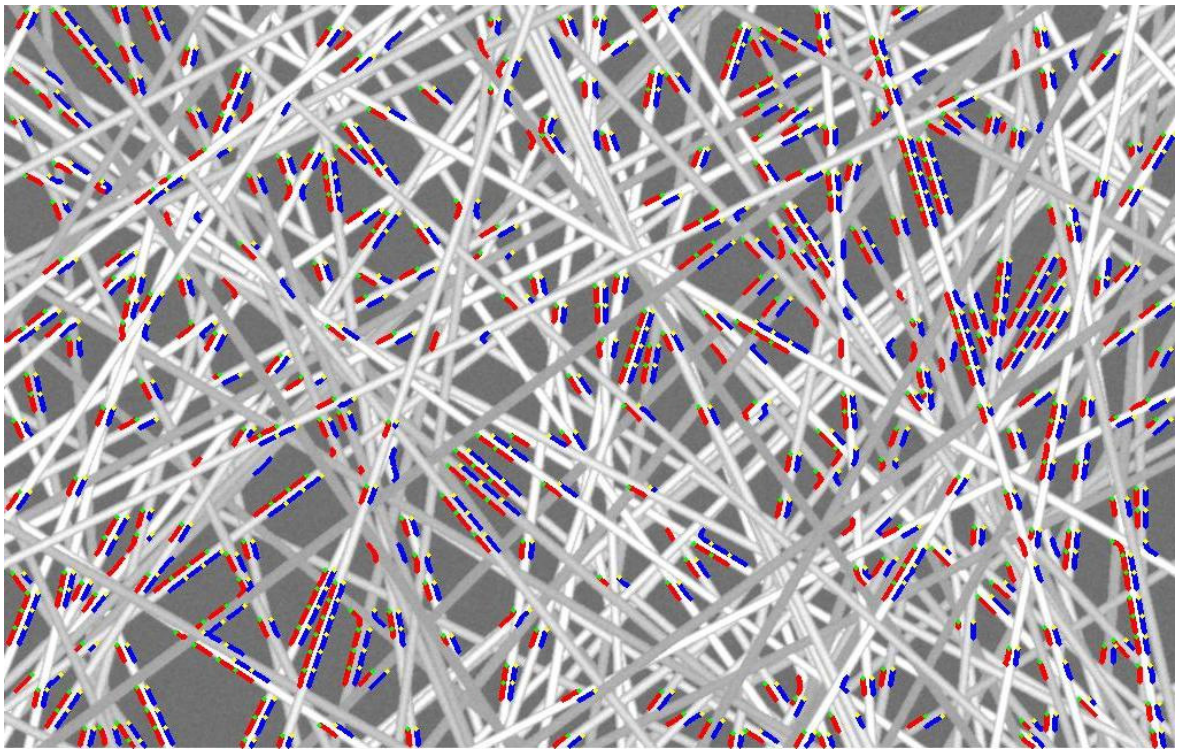

Figure 97 Image narrow10 with DCS valid edges

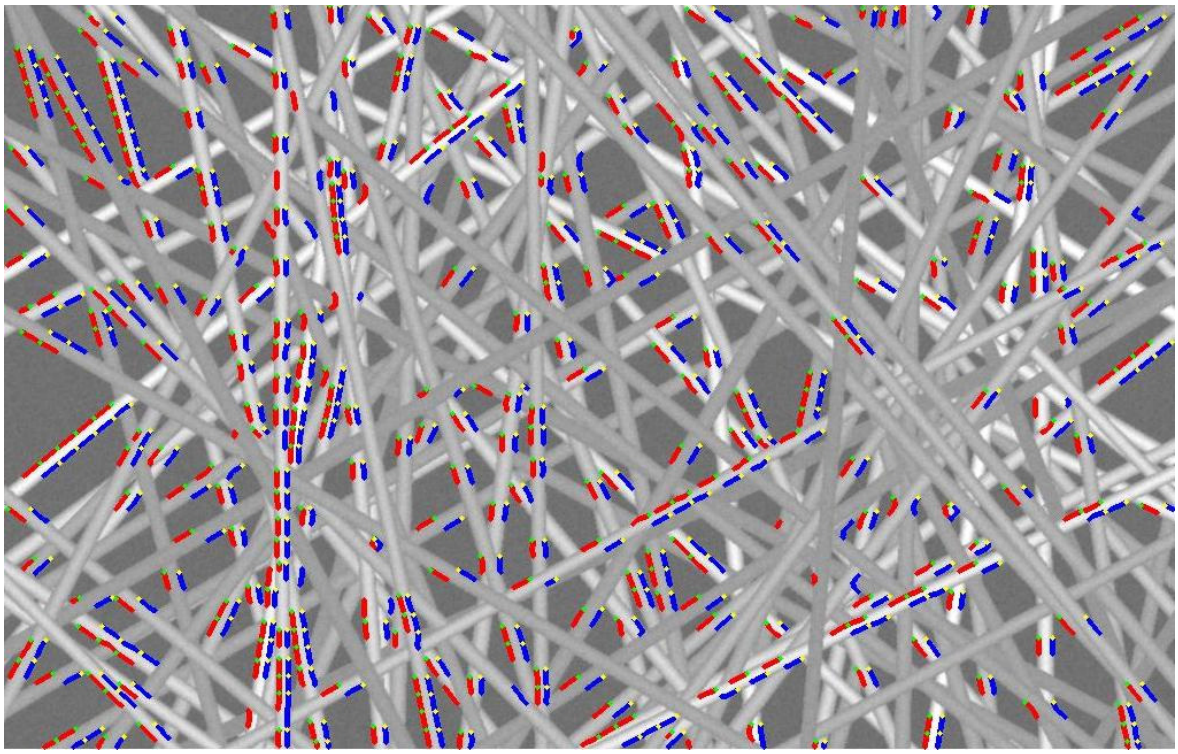

Figure 98 Image narrow15 with DCS valid edges

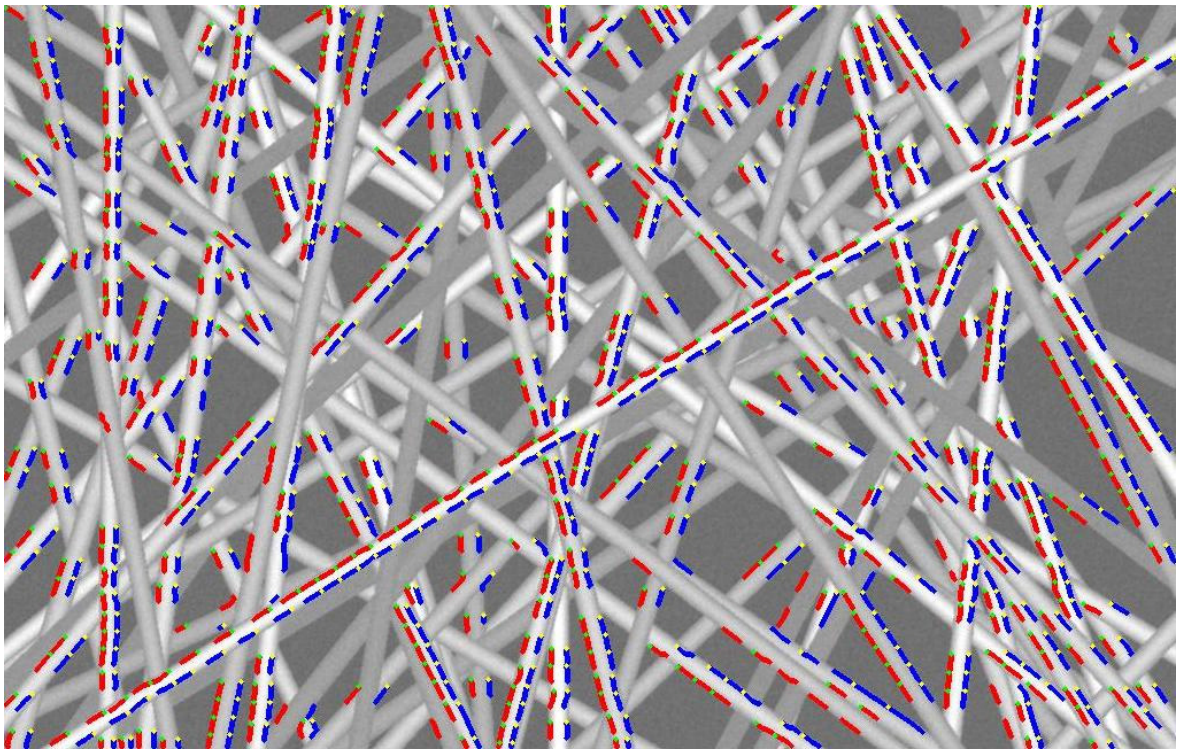

Figure 99 Image narrow20 with DCS valid edges

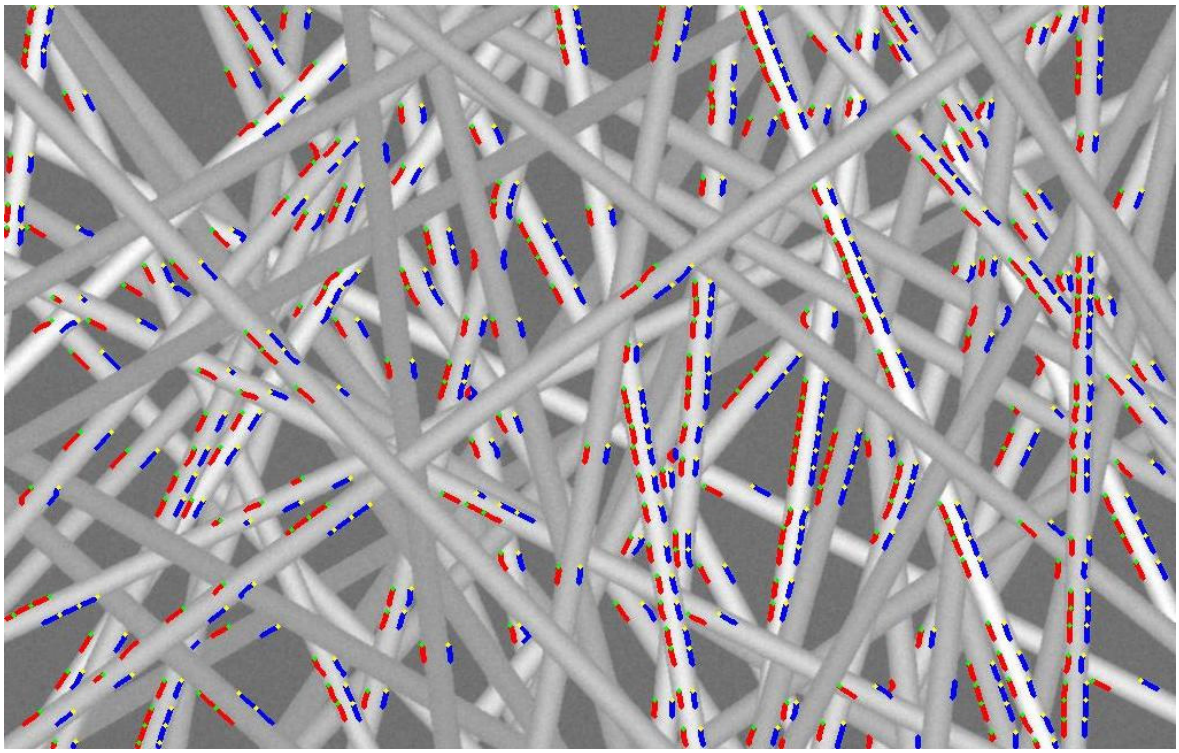

Figure 100 Image narrow25 with DCS valid edges

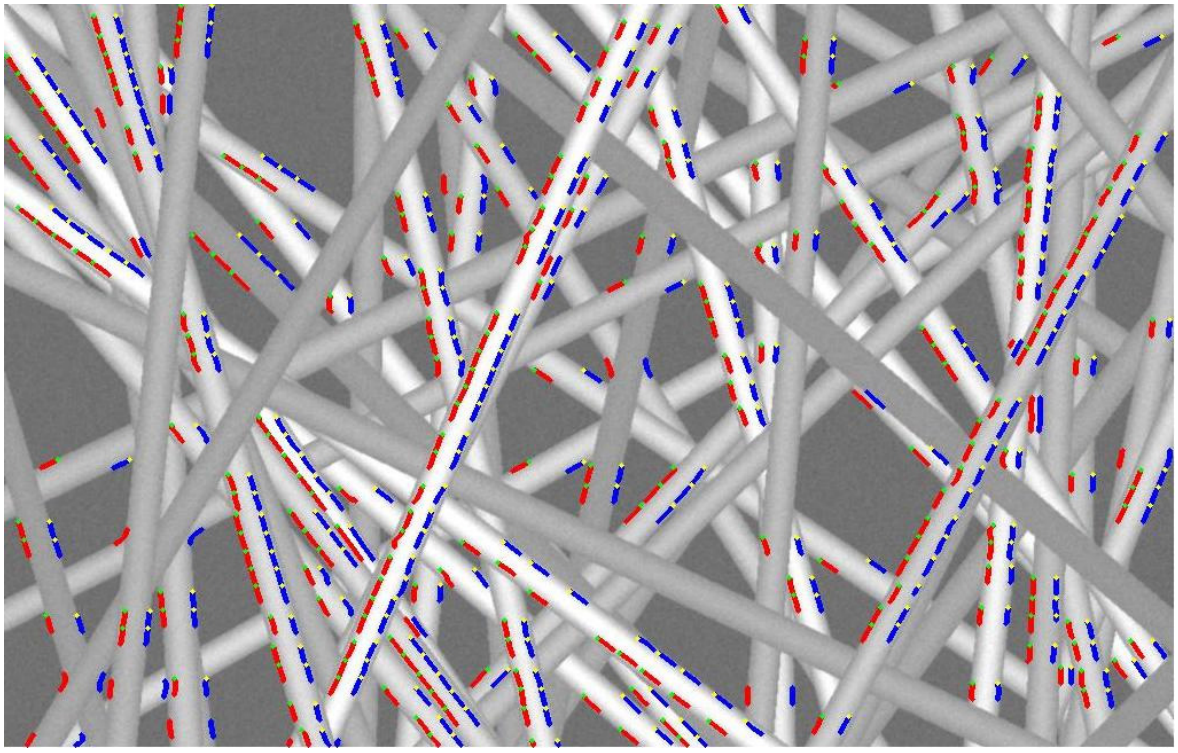

Figure 101 Image narrow30 with DCS valid edges

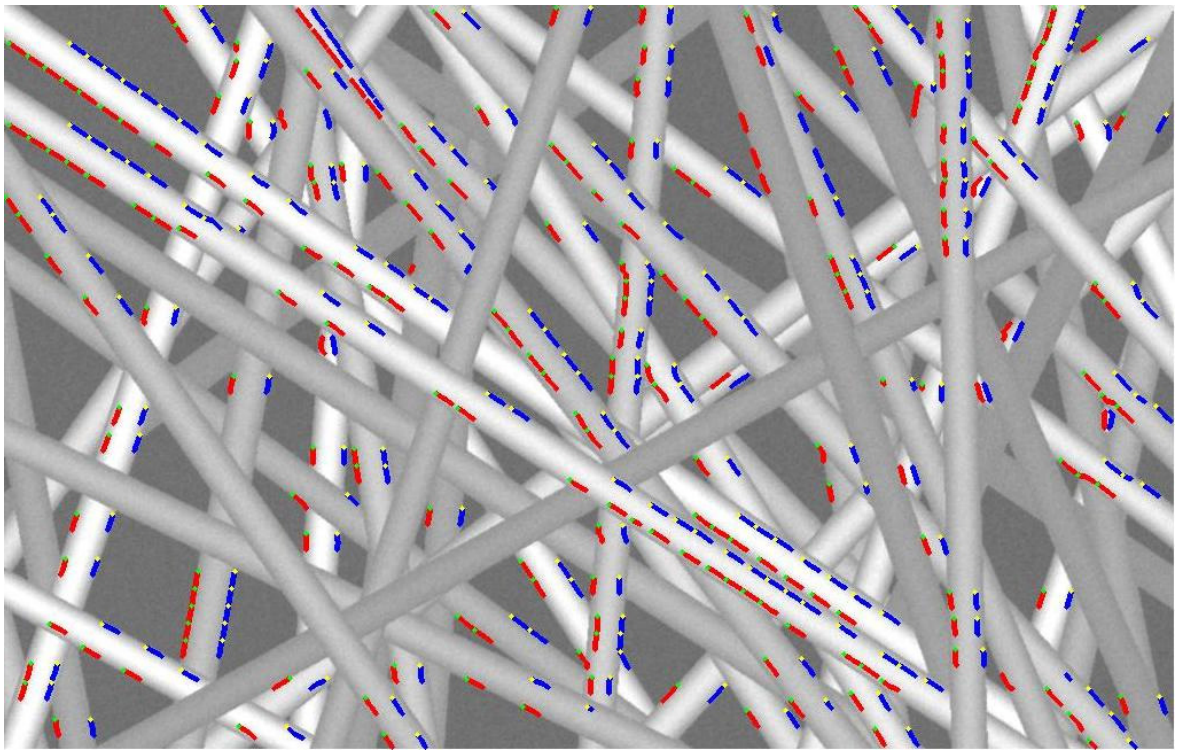

Figure 102 Image narrow35 with DCS valid edges

DCS edges superimposed over the wide distribution simulated images

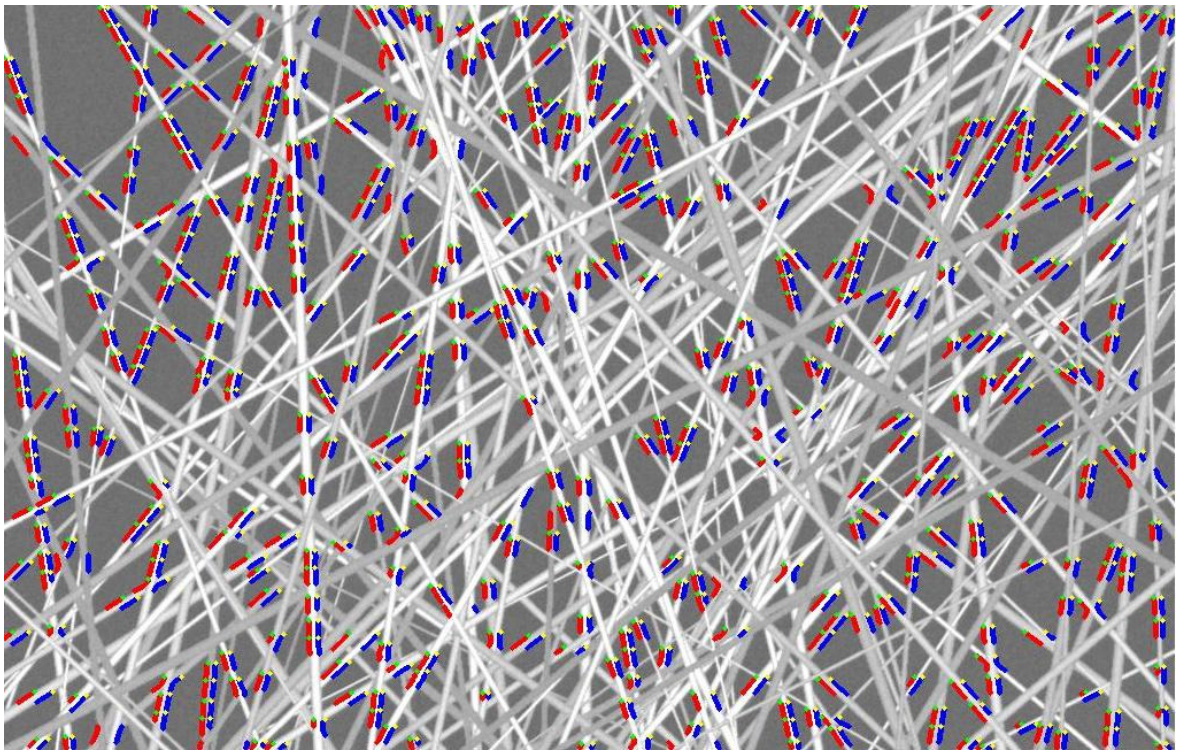

Figure 103 Image wide10 with DCS valid edges

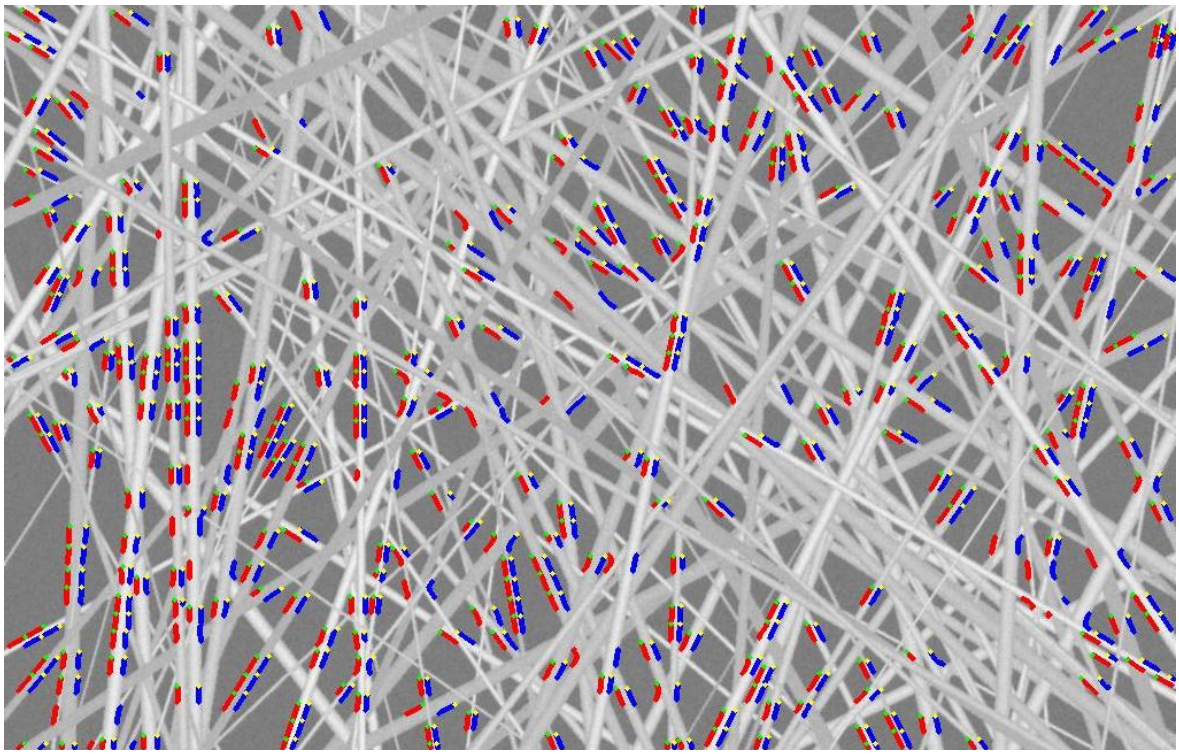

Figure 104 Image wide15 with DCS valid edges

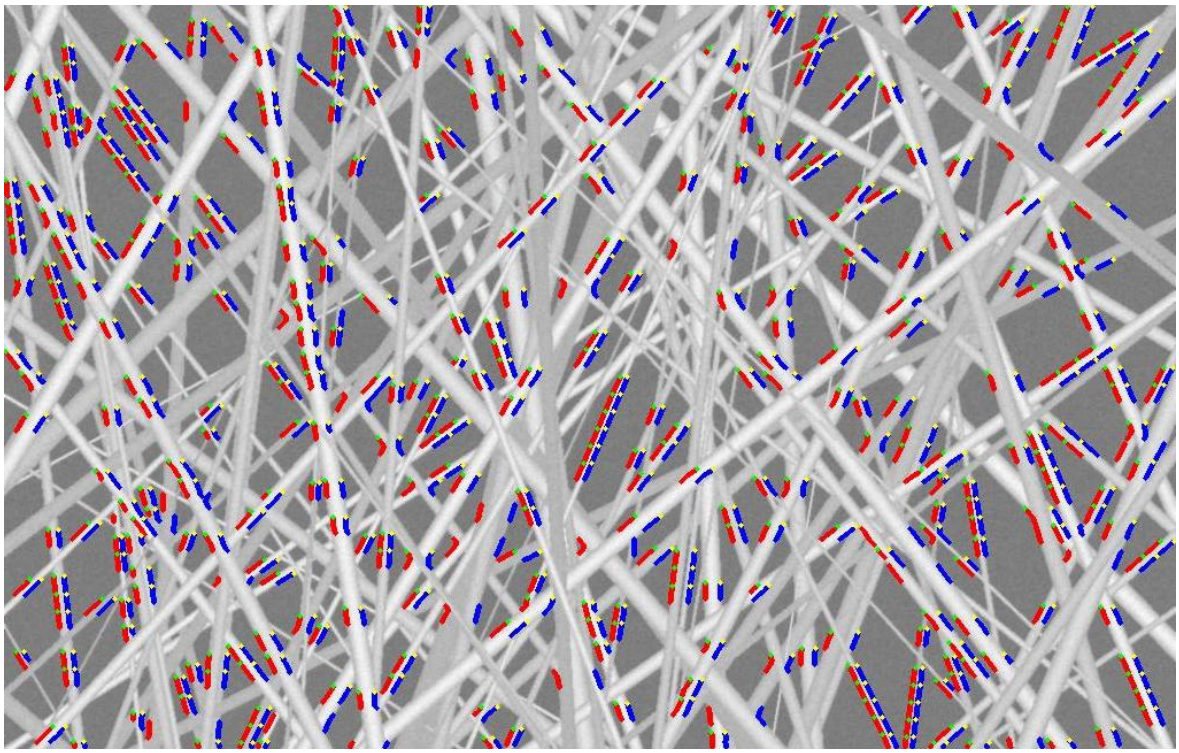

Figure 105 Image wide20 with DCS valid edges

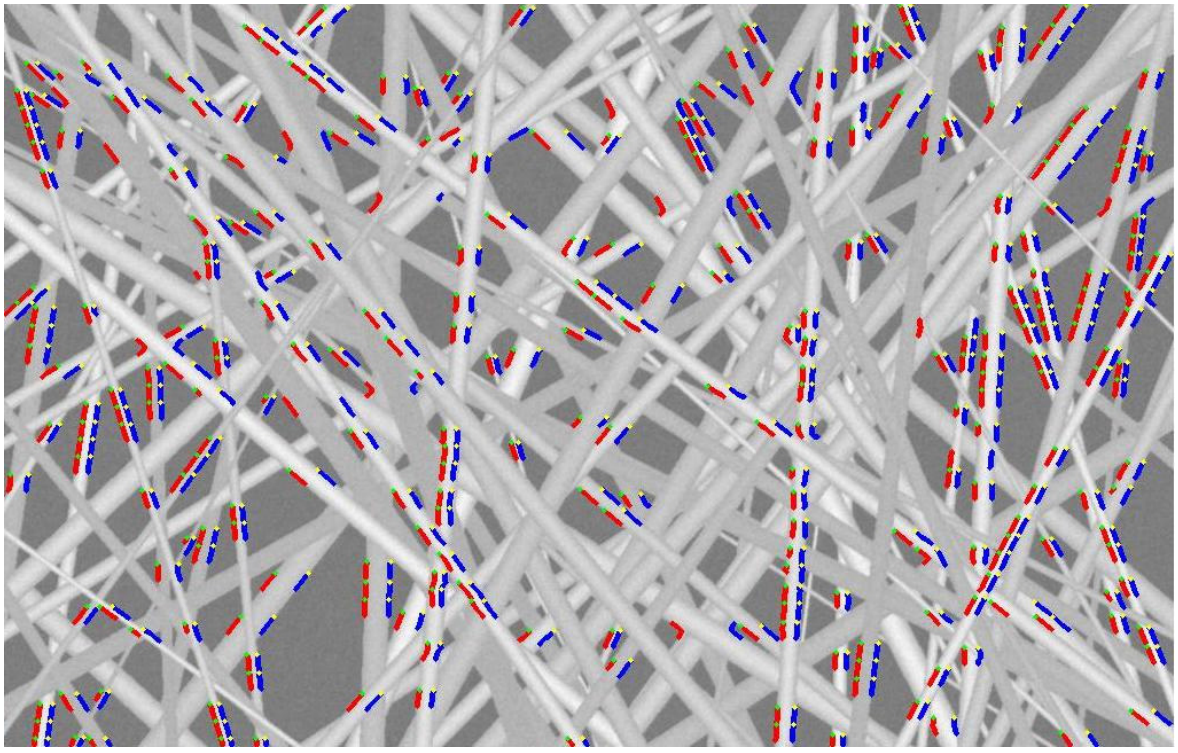

Figure 106 Image wide25 with DCS valid edges

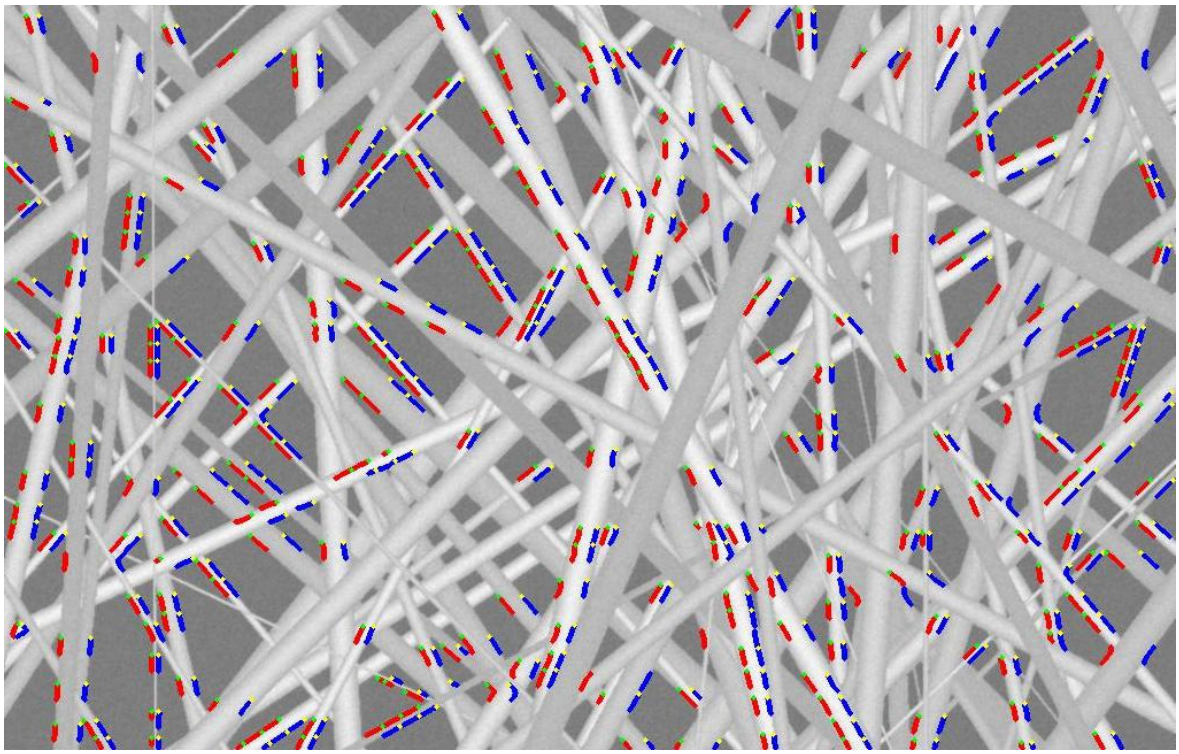

Figure 107 Image wide30 with DCS valid edges

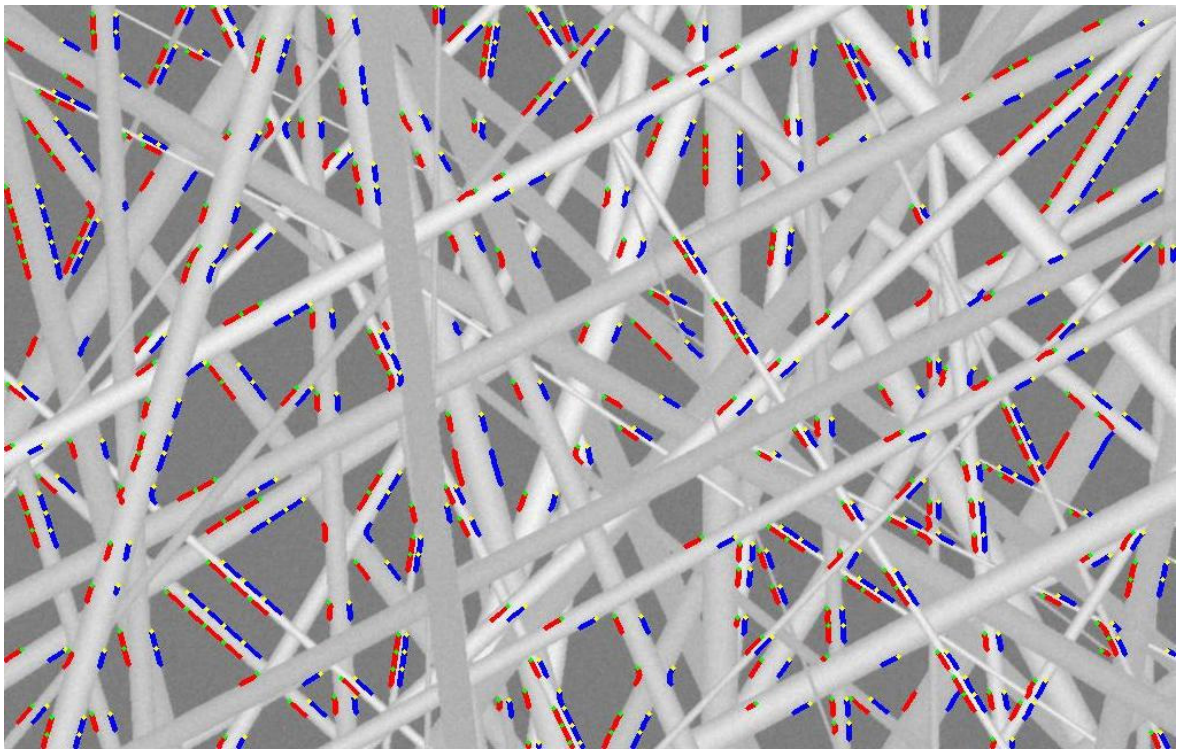

Figure 108 Image wide35 with DCS valid edges

DCS edges superimposed over real SEM images

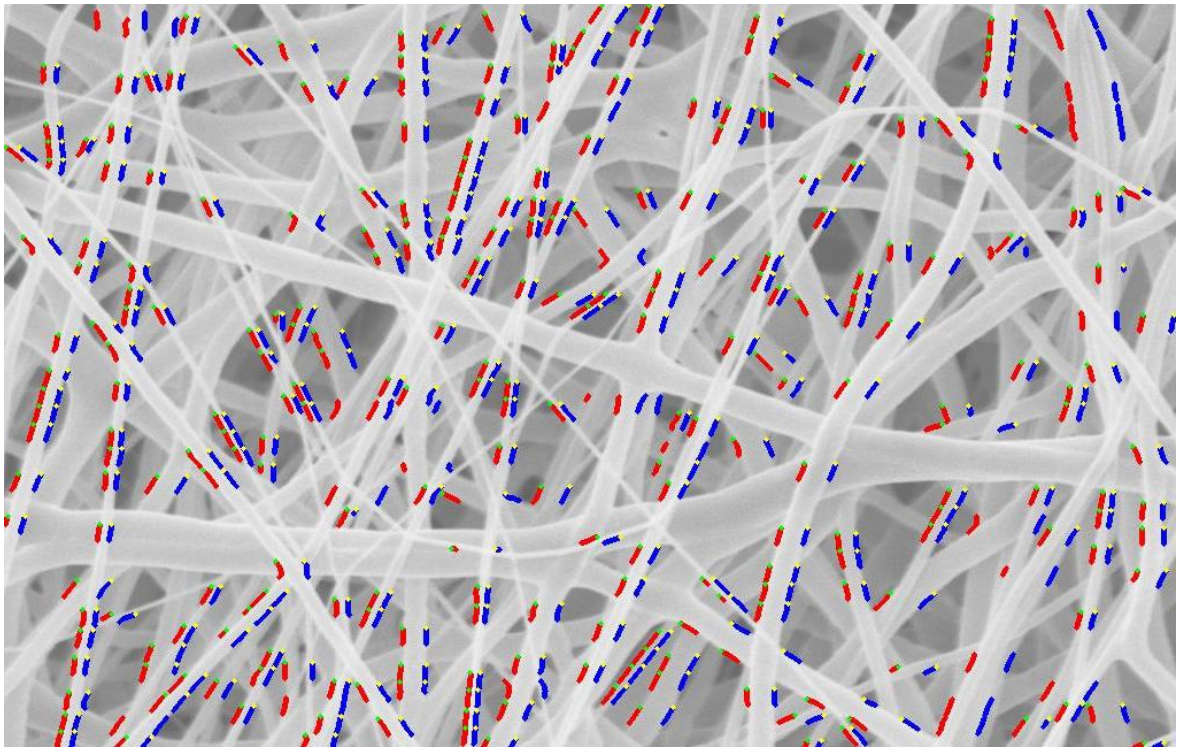

Figure 109 Image SEM1 with DCS valid edges

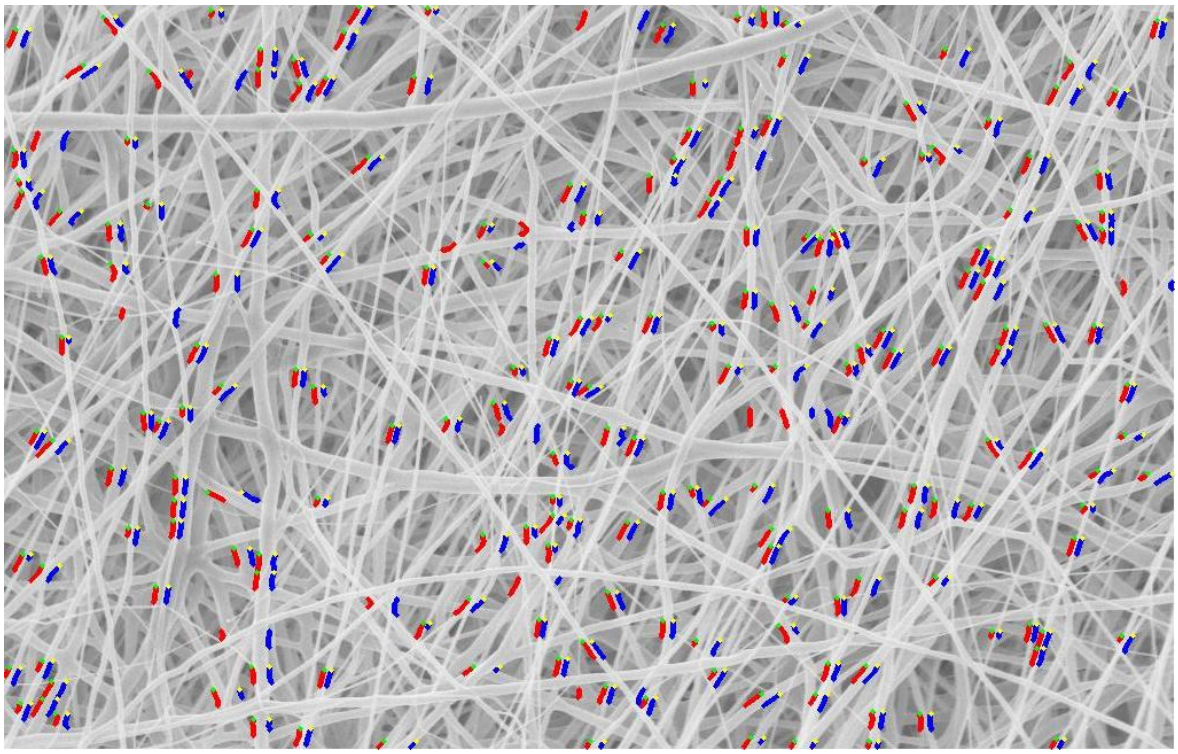

Figure 110 Image SEM2 with DCS valid edges

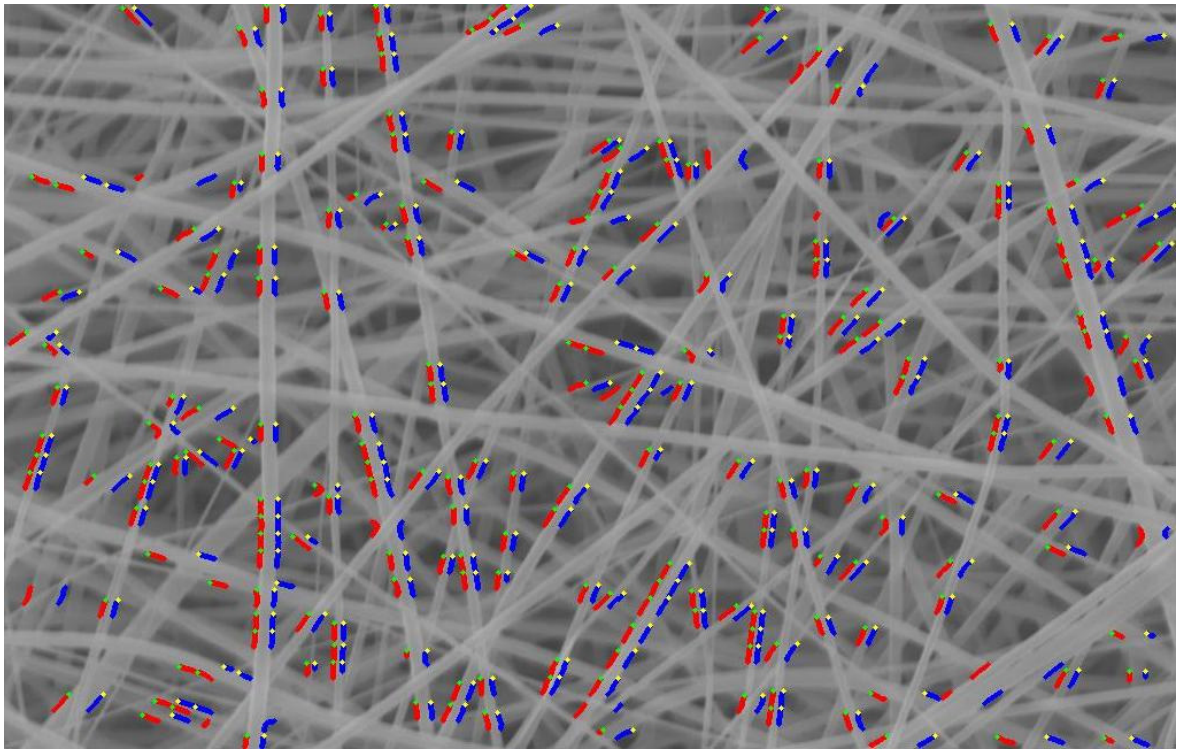

Figure 111 Image SEM3 with DCS valid edges

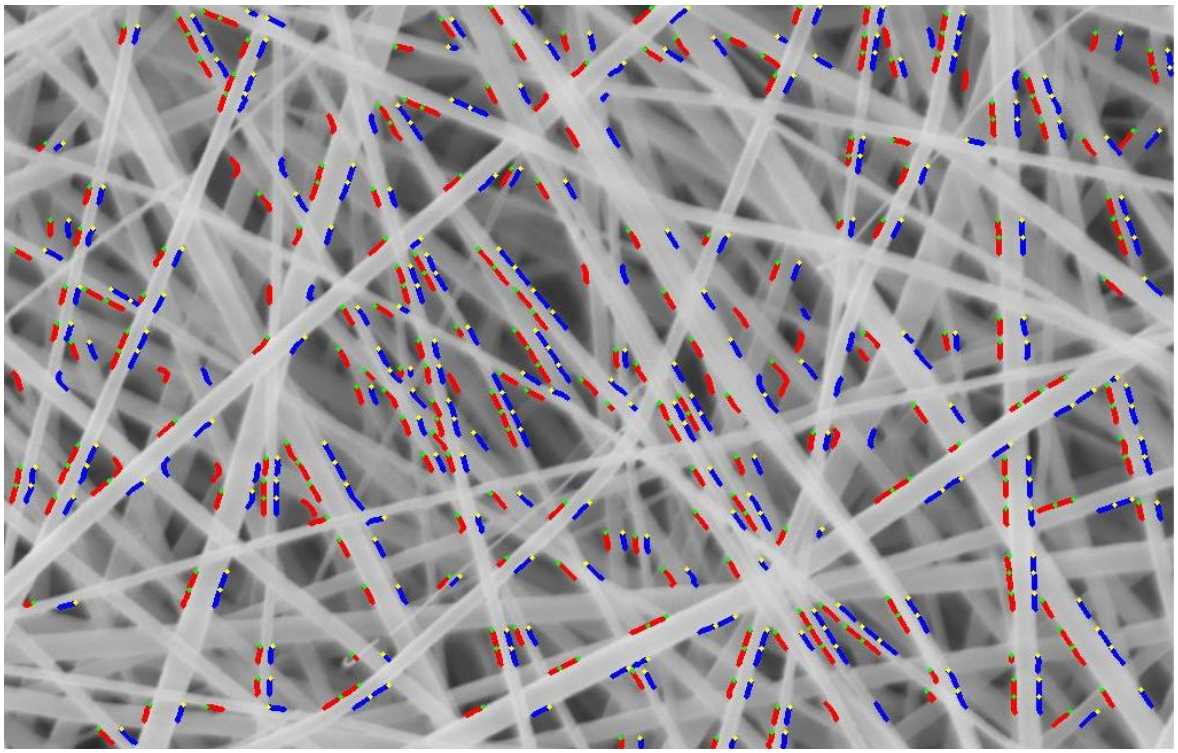

Figure 112 Image SEM4 with DCS valid edges

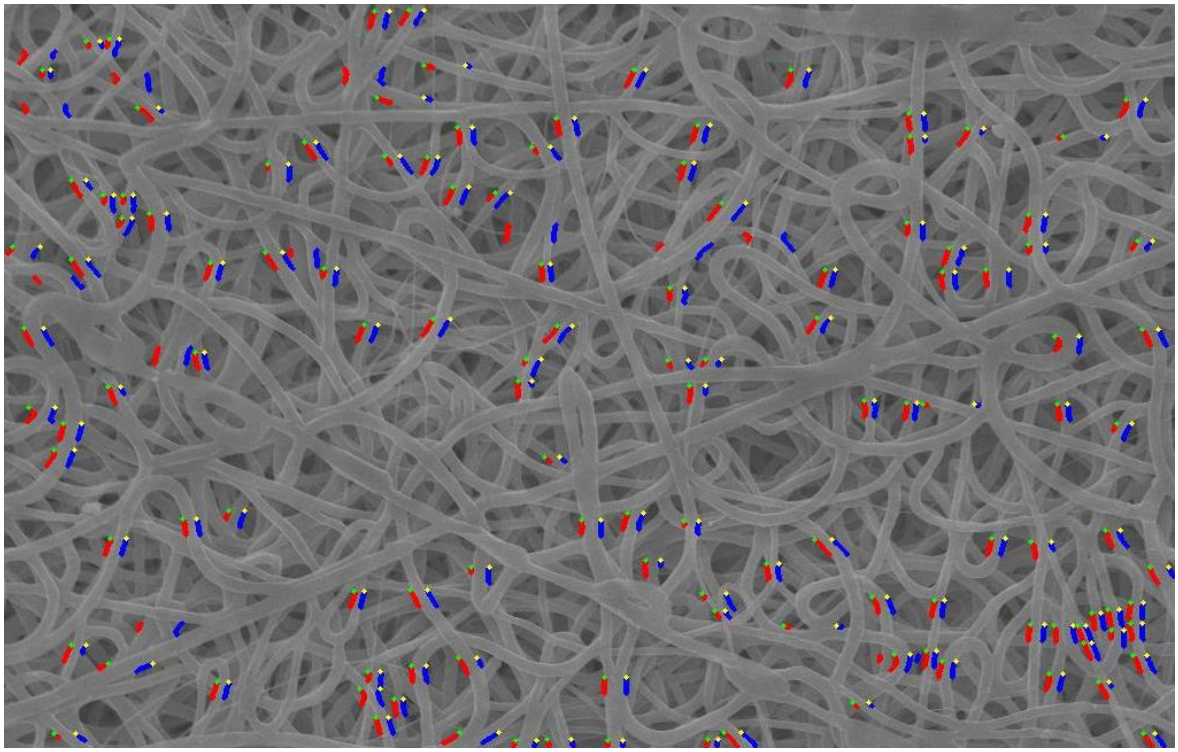

Figure 113 Image SEM5 with DCS valid edges

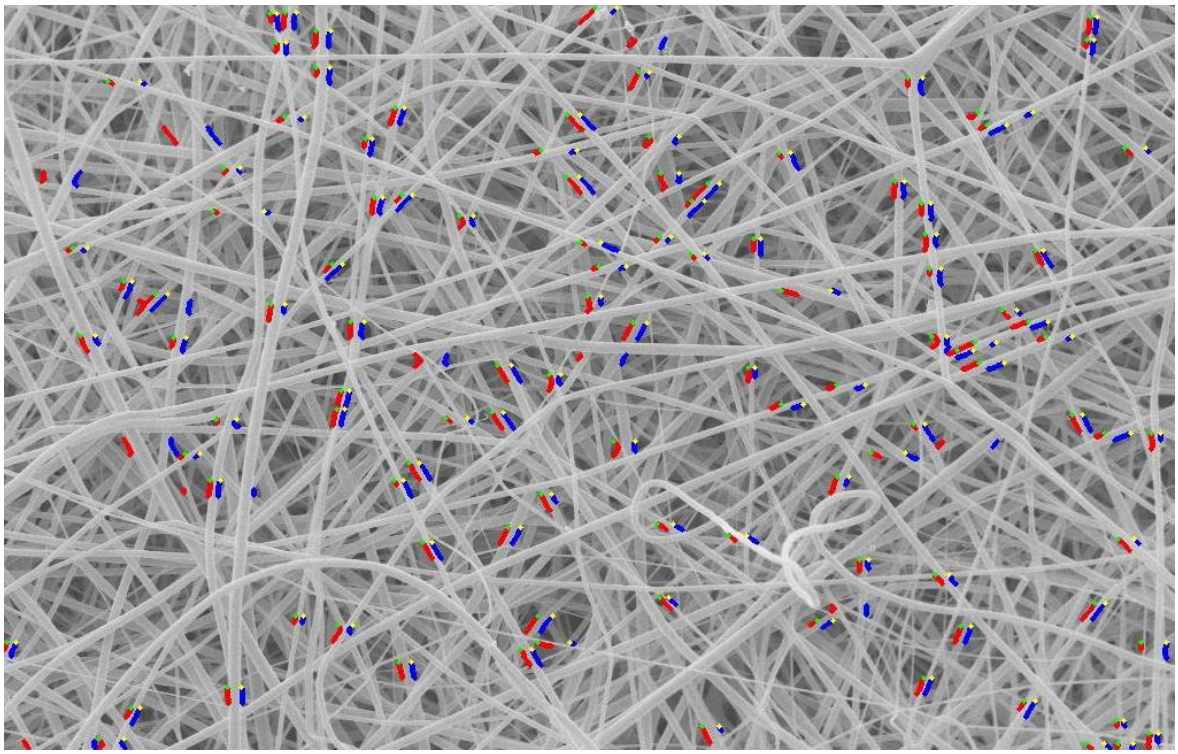

Figure 114 Image SEM6 with DCS valid edges

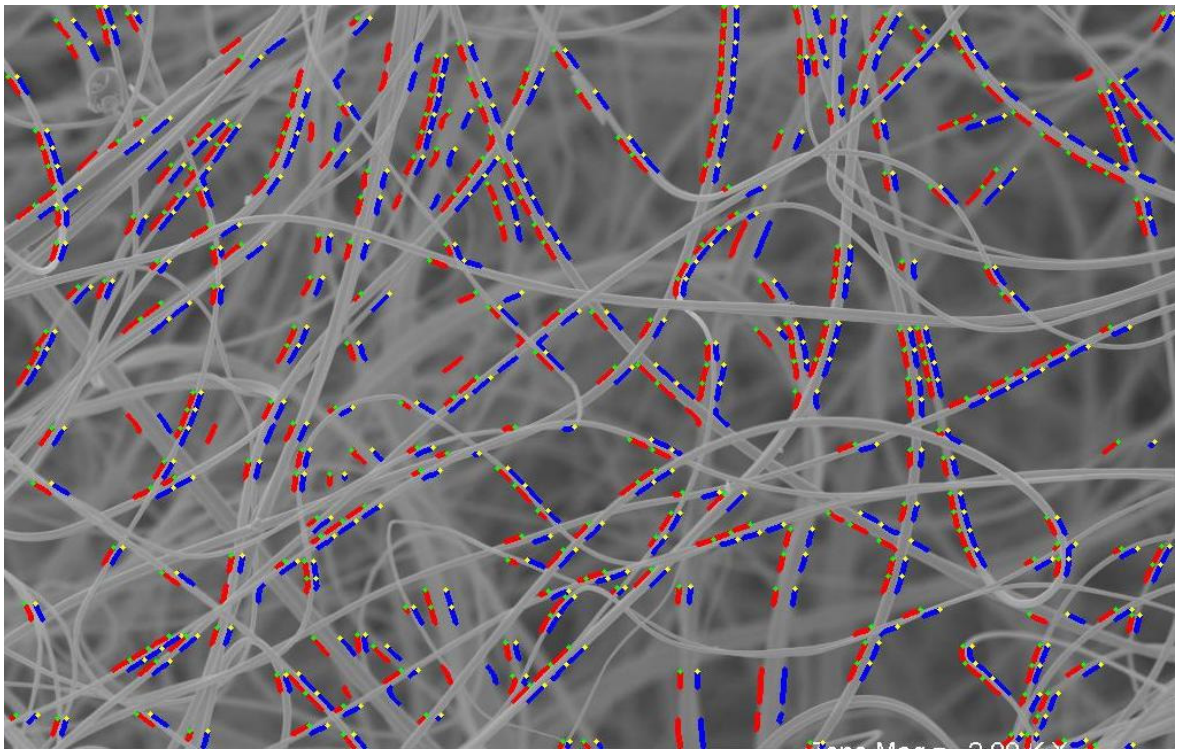

Figure 115 Image SEM7 with DCS valid edges

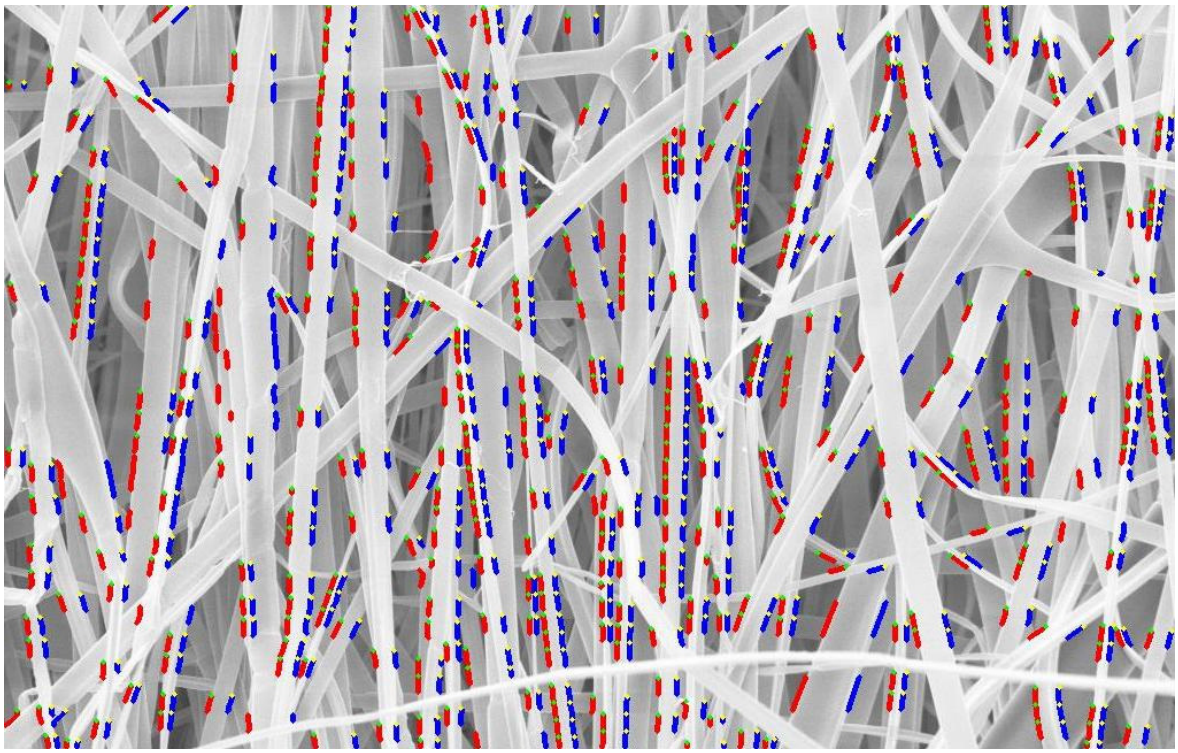

Figure 116 Image SEM8 with DCS valid edges

APPENDIX D: Resulting Images for Canny Hough Method

The following images were processed with the Default Canny Hough fiber diameter measurement method. The fiber diameters per image can be found in the results section. In the following figures, the determined valid edges per image were superimposed over the corresponding original image. Red and blue segments respectively represent the left and right edges of the valid edge pairs found with this method.

DCH edges superimposed over the narrow distribution simulated images

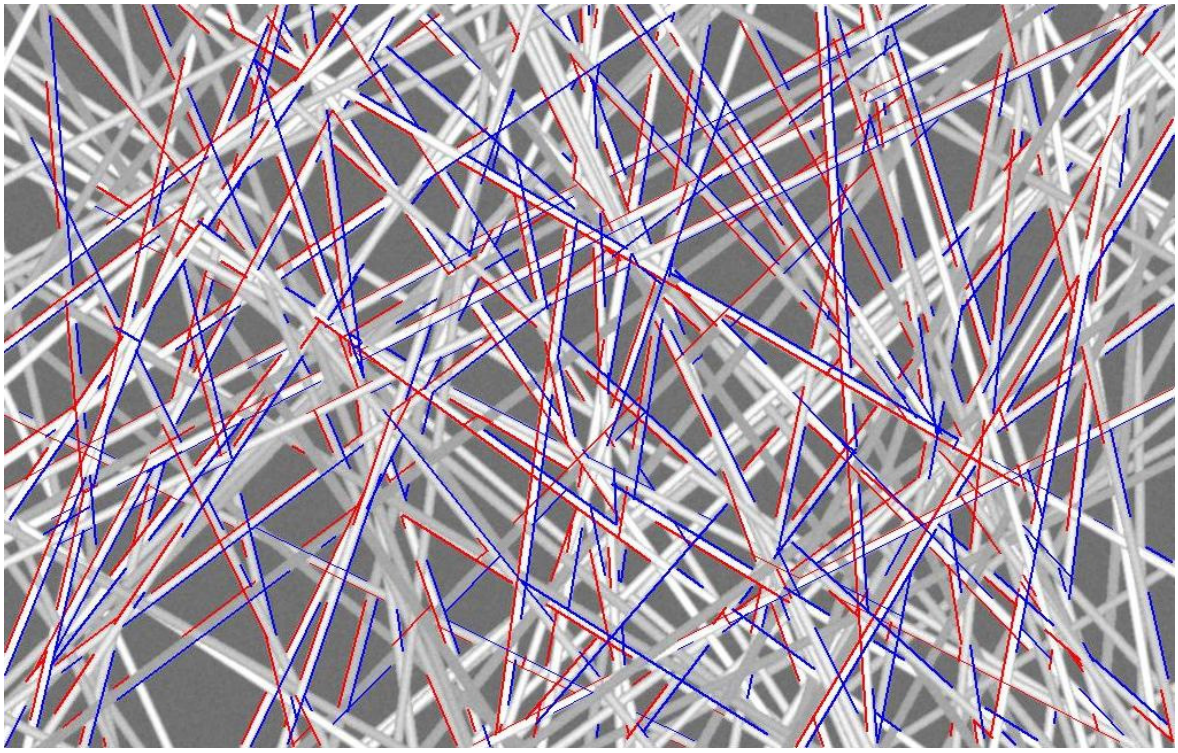

Figure 117 Image narrow10 with DCH valid edges

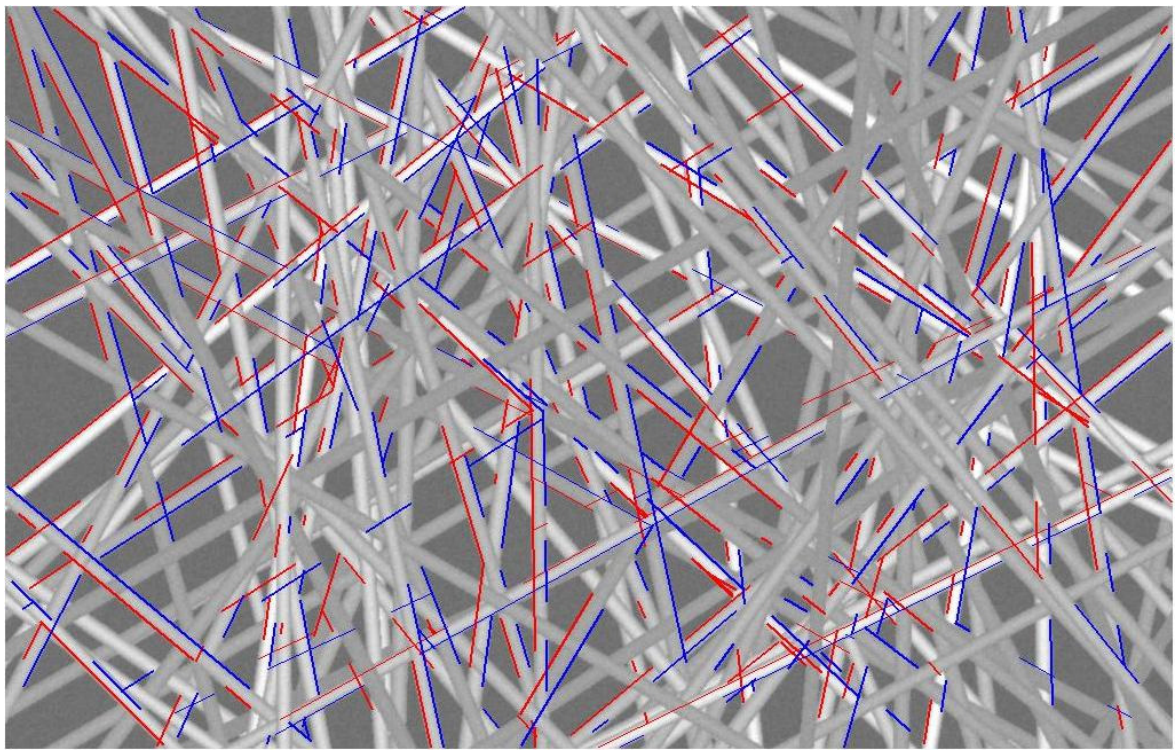

Figure 118 Image narrow15 with DCH valid edges

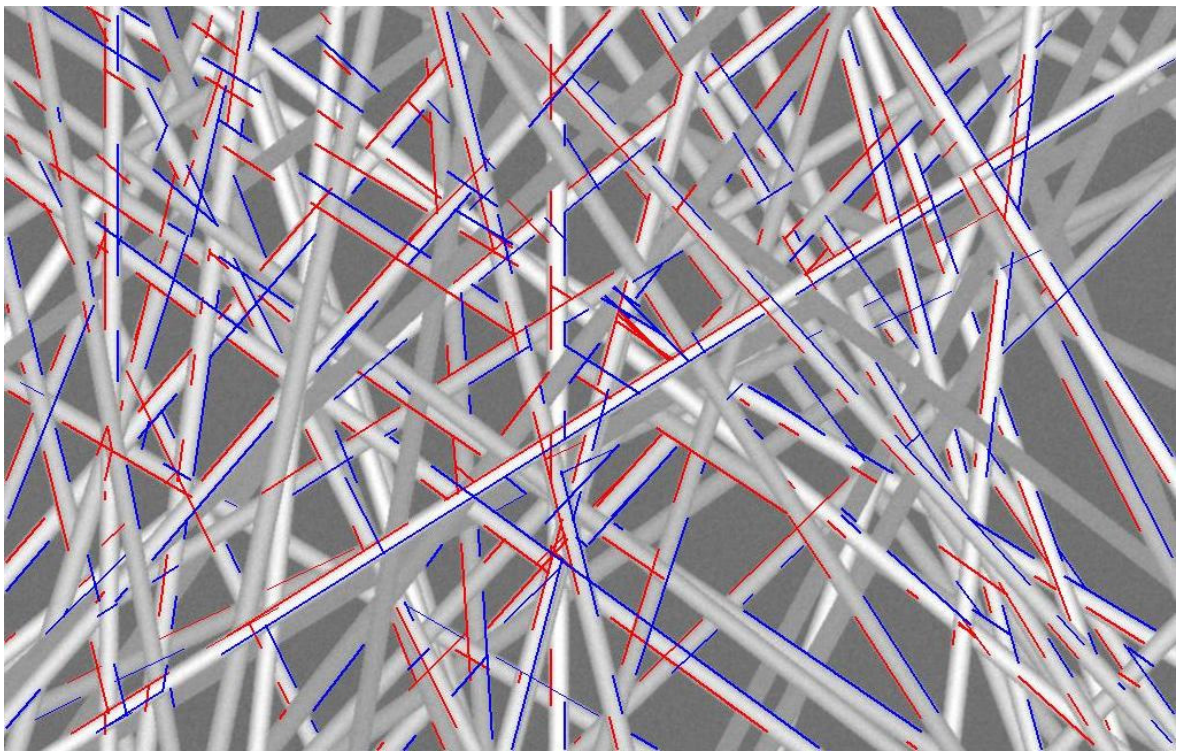

Figure 119 Image narrow20 with DCH valid edges

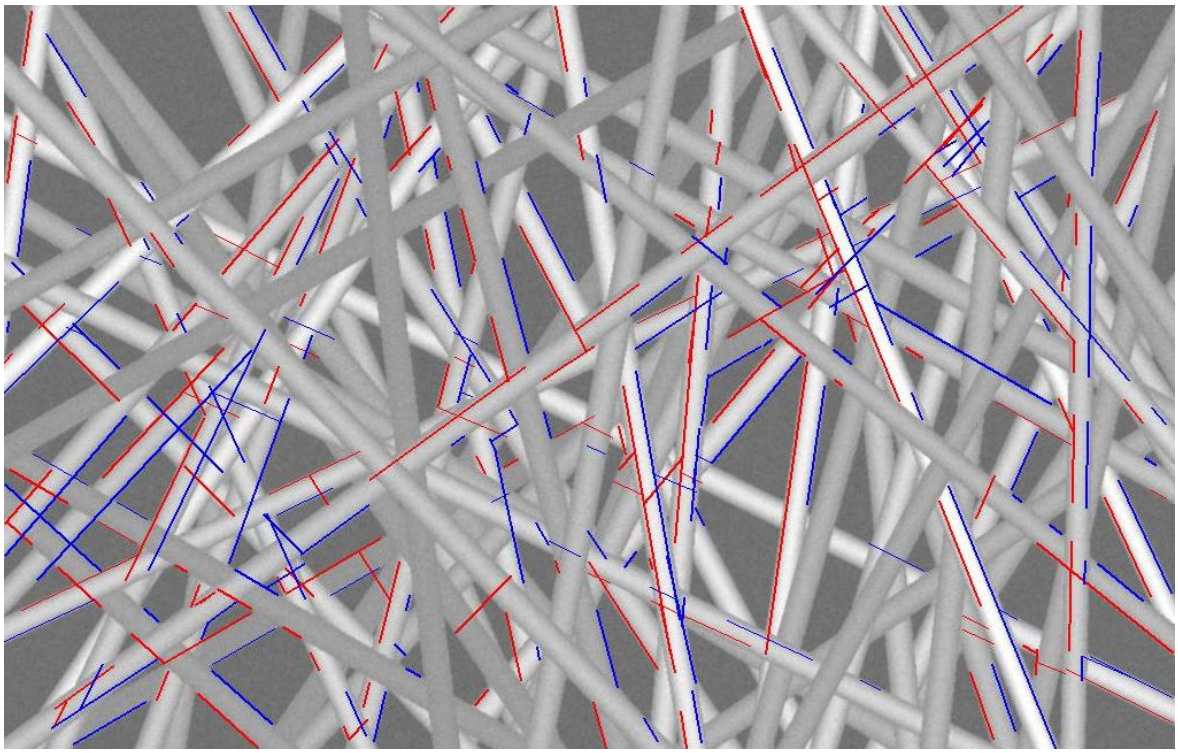

Figure 120 Image narrow25 with DCH valid edges

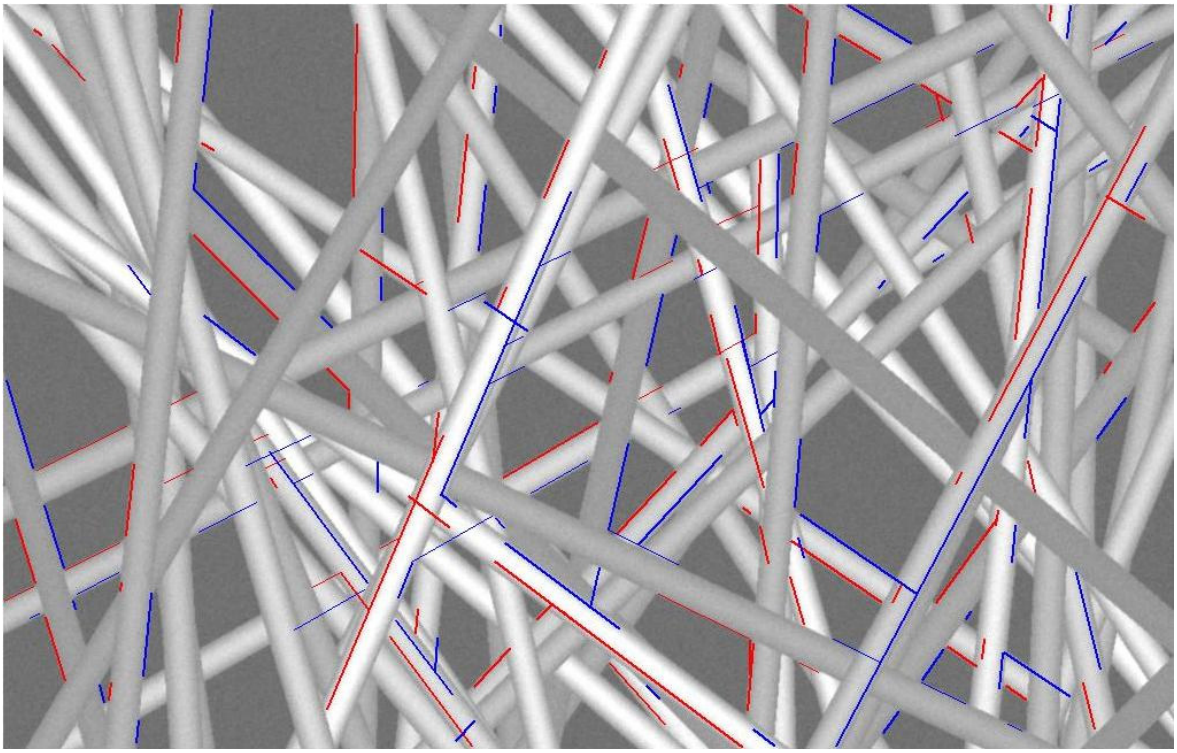

Figure 121 Image narrow30 with DCH valid edges

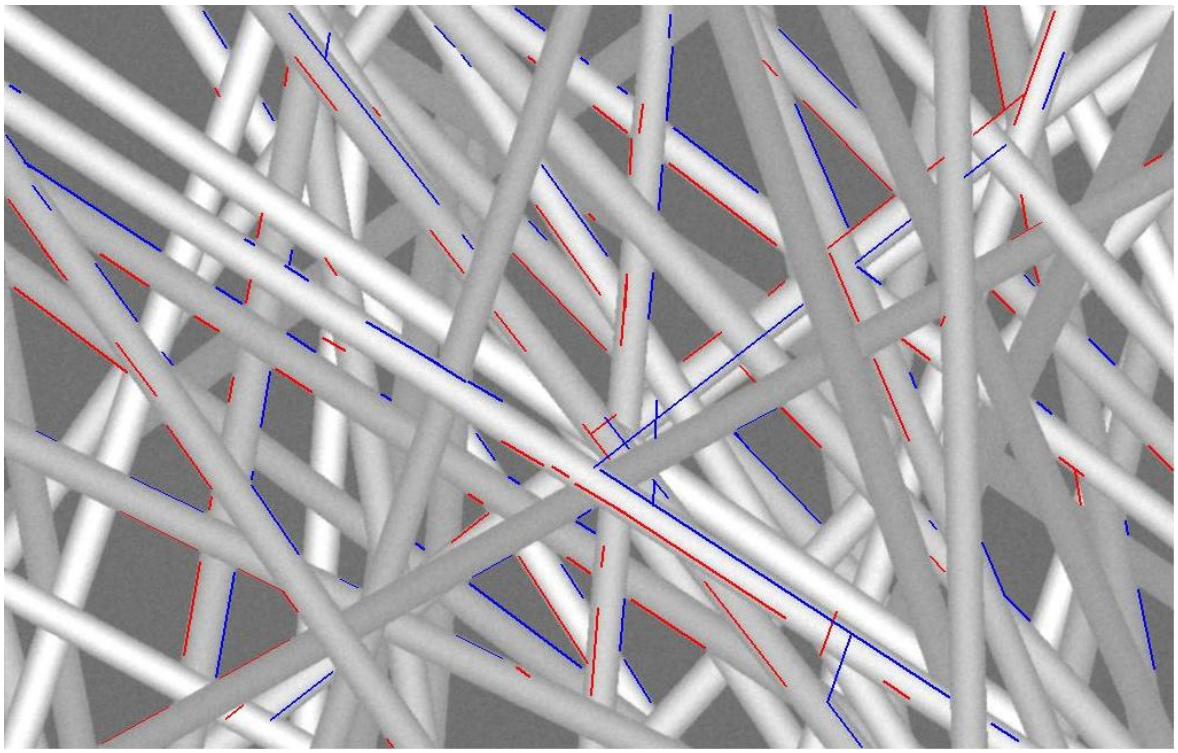

Figure 122 Image narrow35 with DCH valid edges

DCH edges superimposed over the wide distribution simulated images

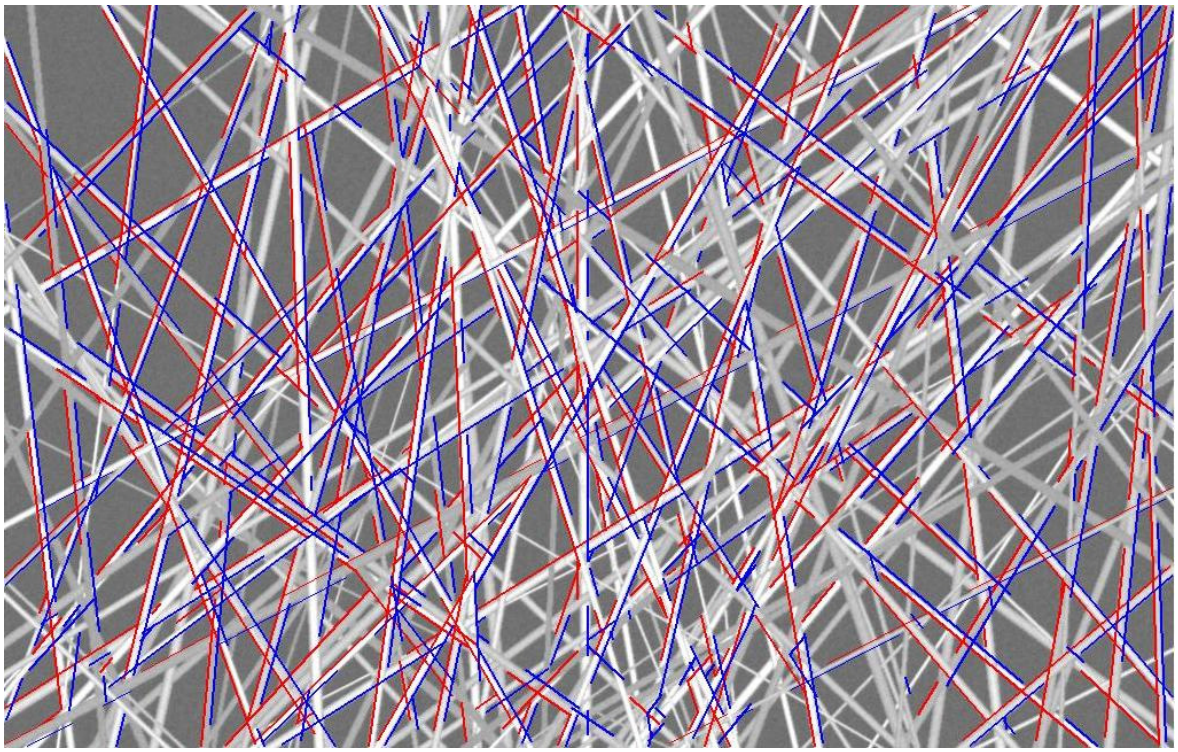

Figure 123 Image wide10 with DCH valid edges

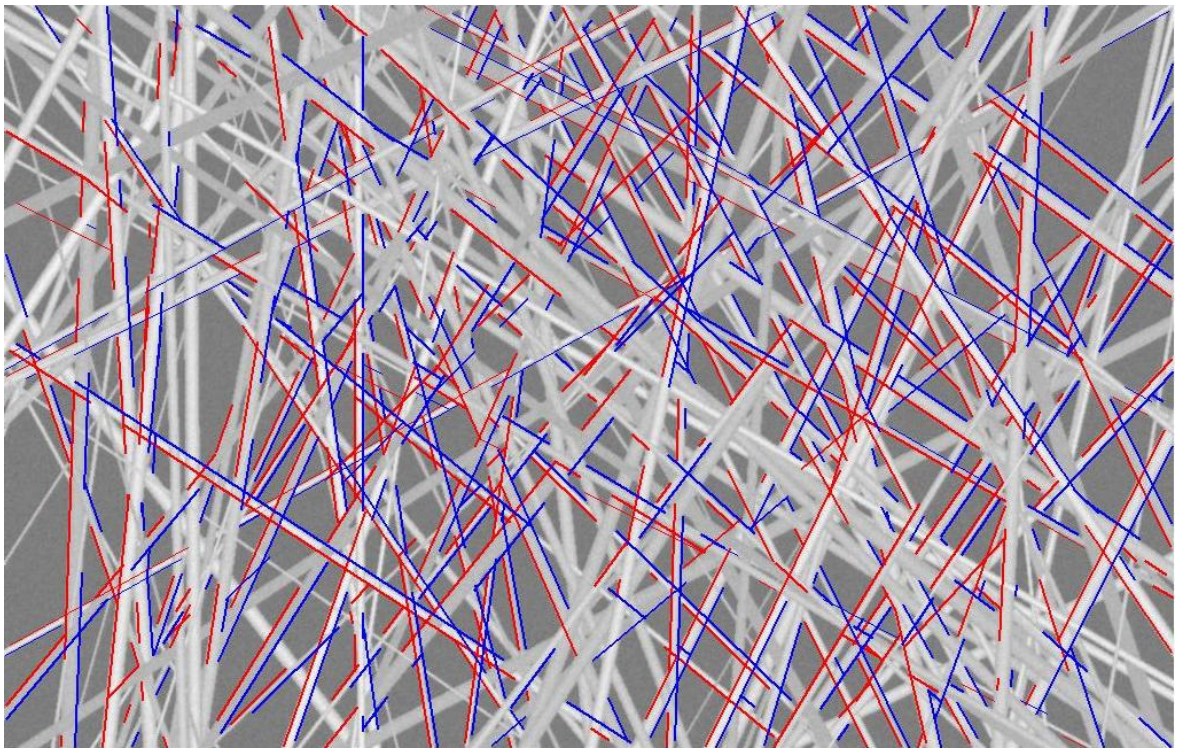

Figure 124 Image wide15 with DCH valid edges

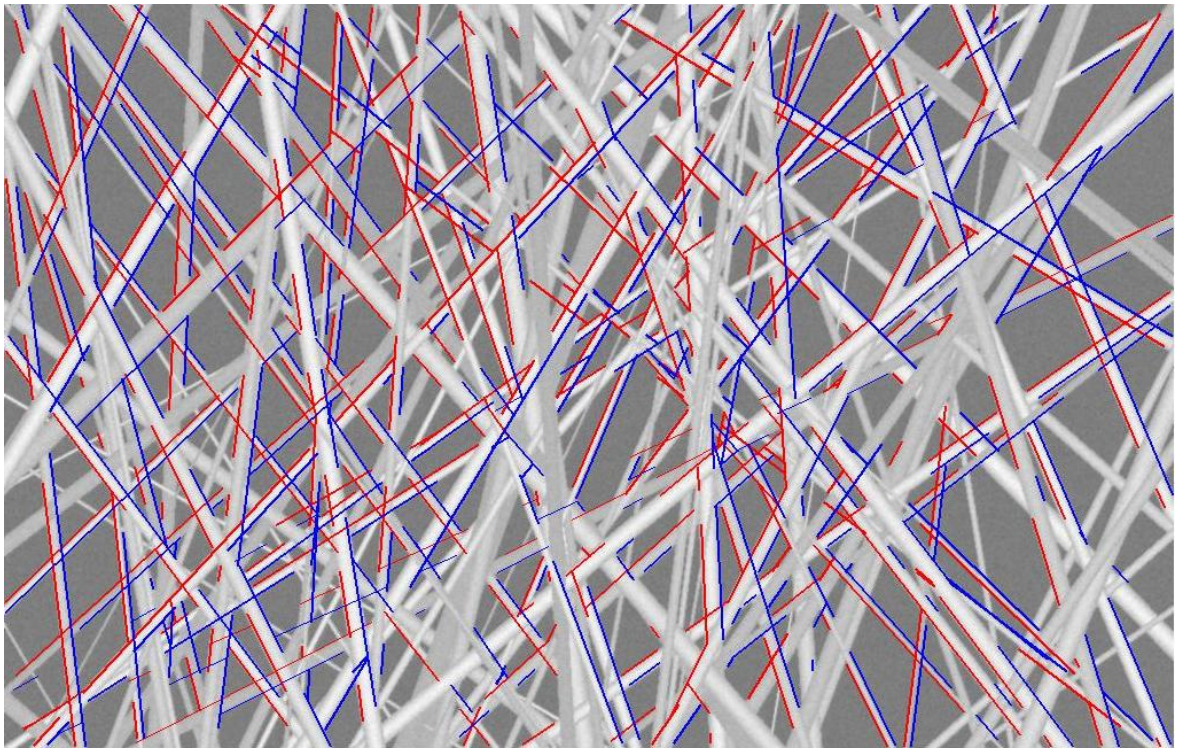

Figure 125 Image wide20 with DCH valid edges

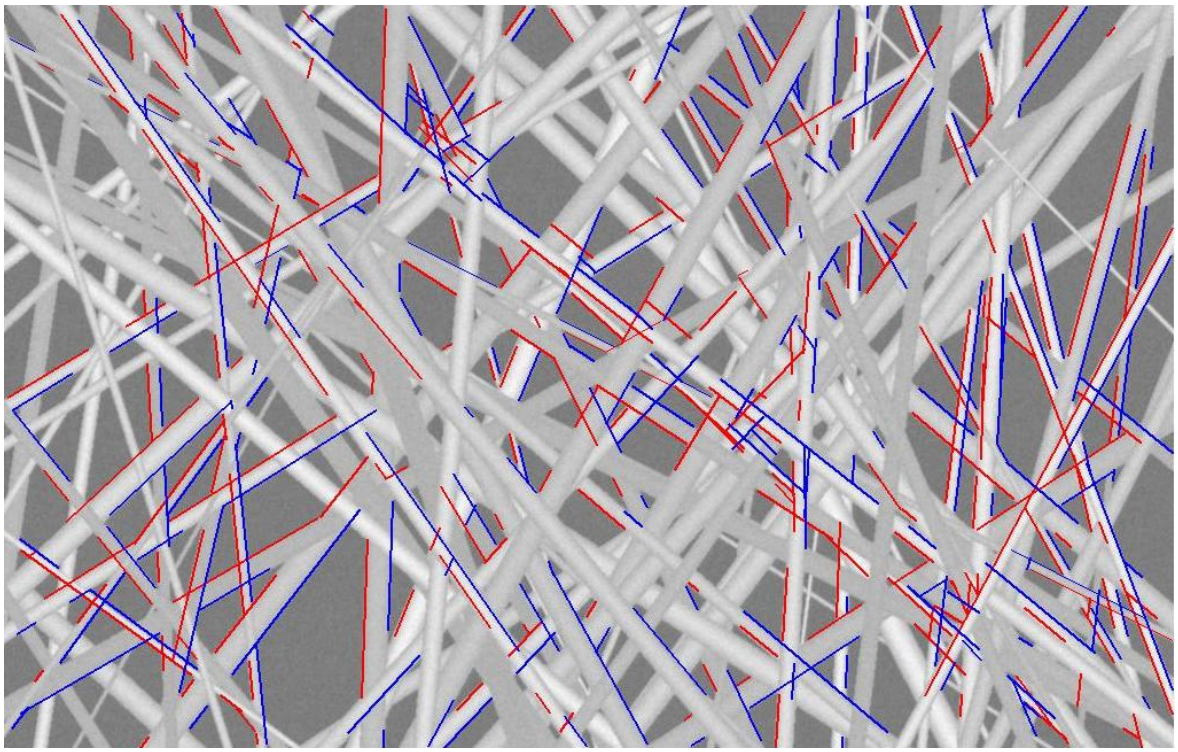

Figure 126 Image wide25 with DCH valid edges

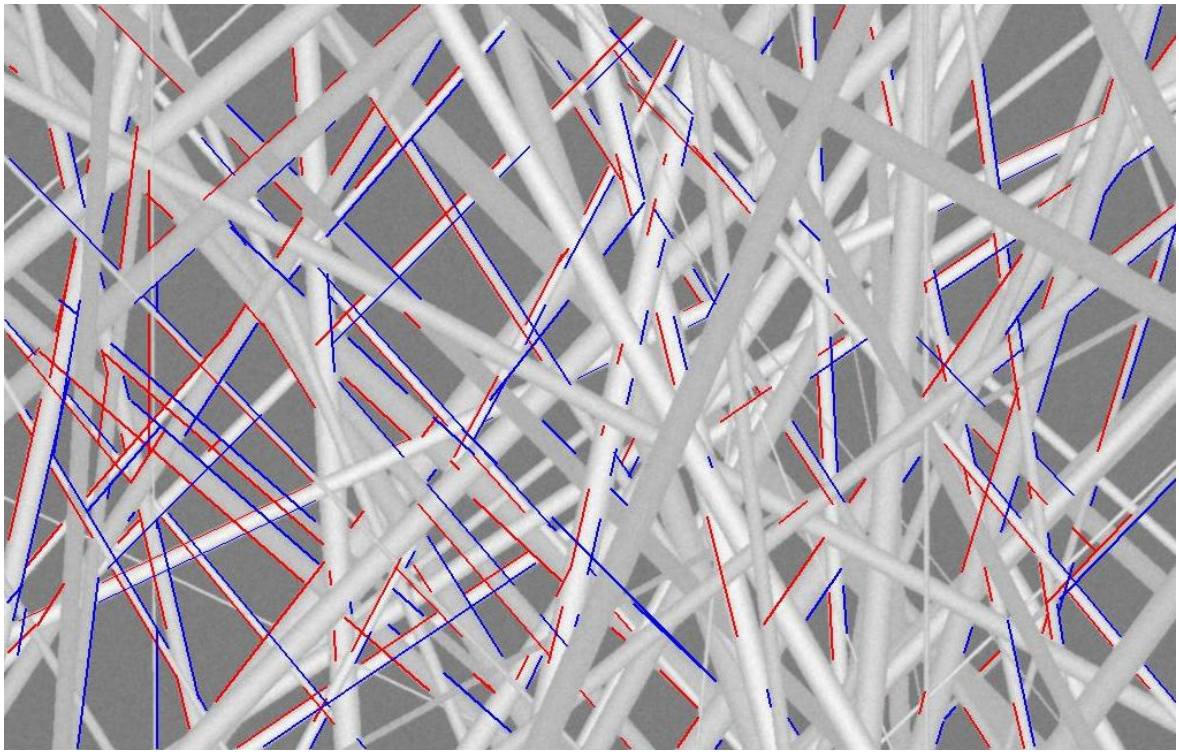

Figure 127 Image wide30 with DCH valid edges

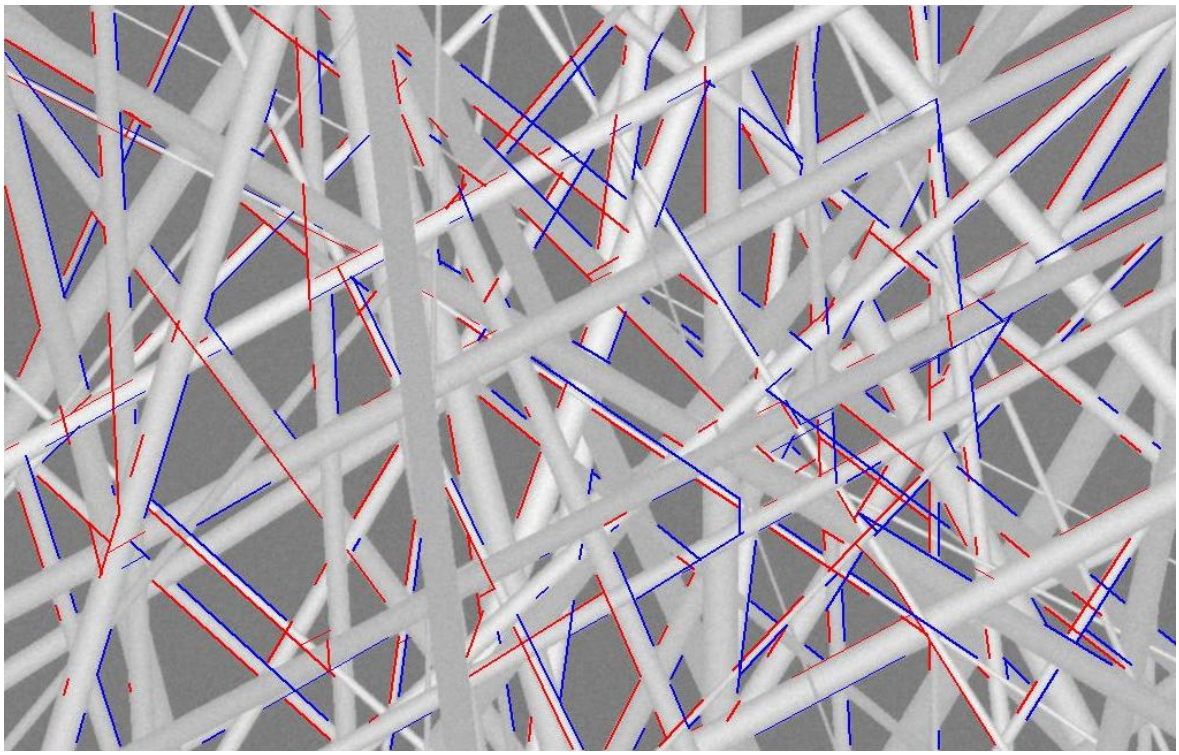

Figure 128 Image wide35 with DCH valid edges

DCH edges superimposed over real SEM images

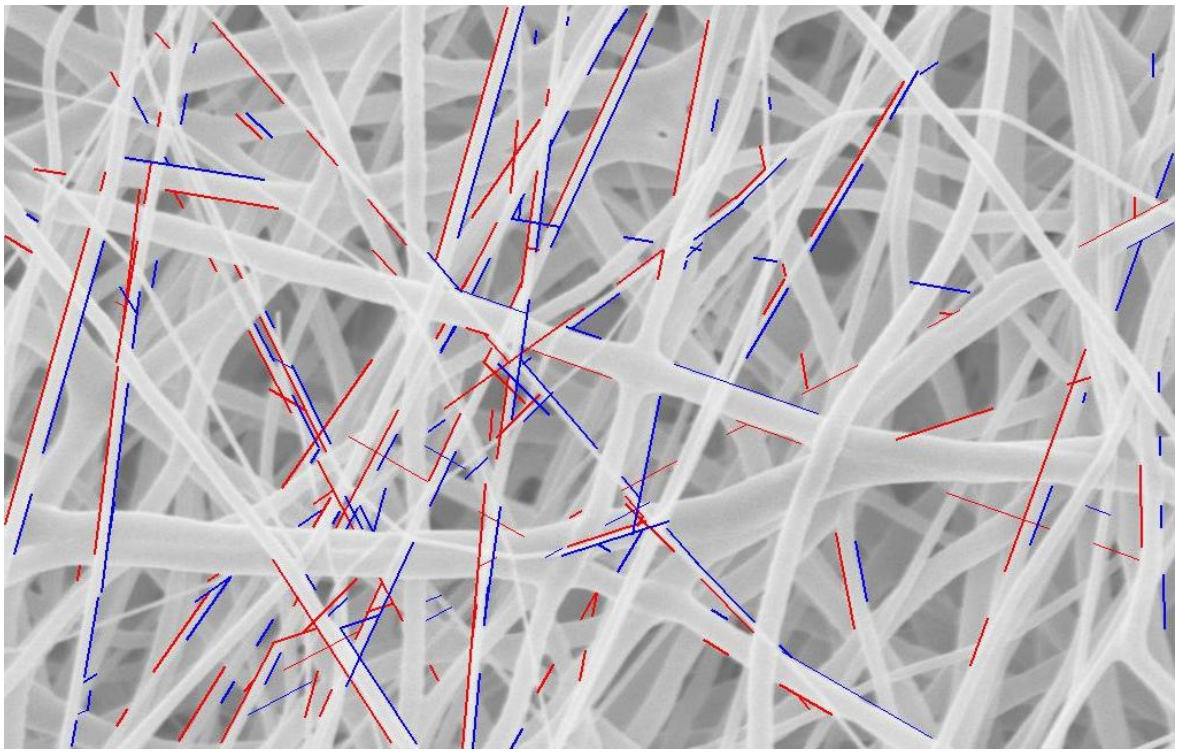

Figure 129 Image SEM1 with DCH valid edges

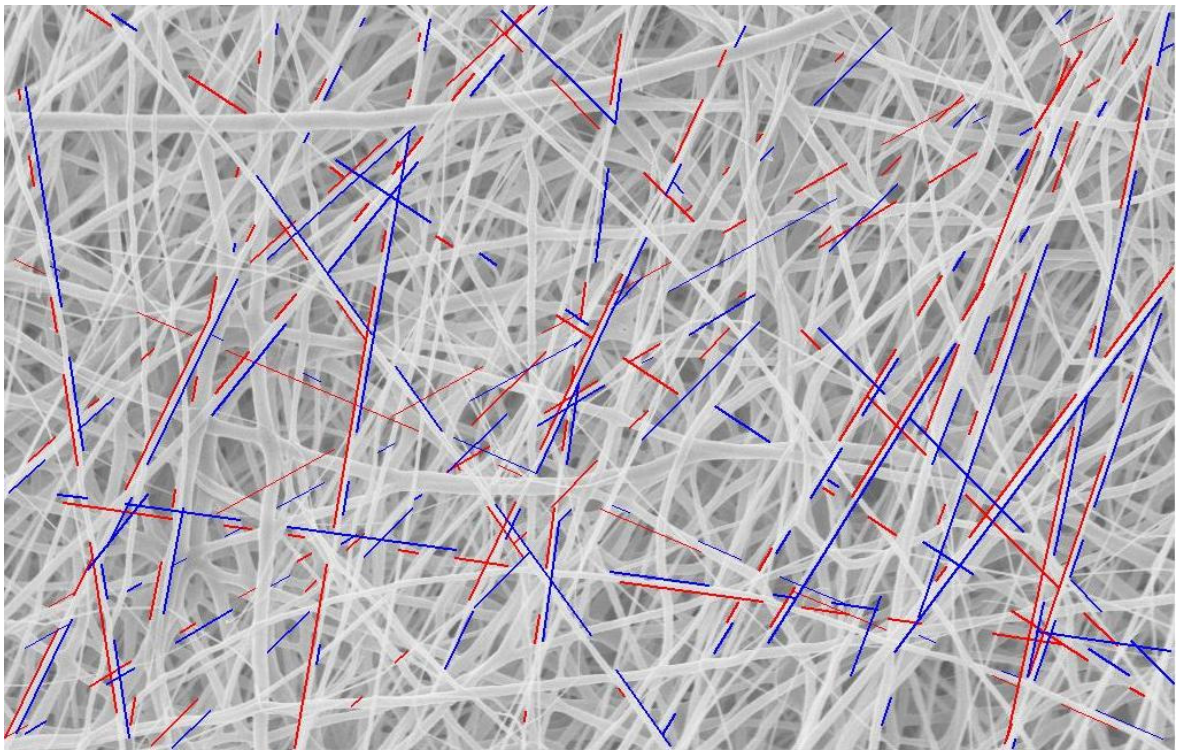

Figure 130 Image SEM2 with DCH valid edges

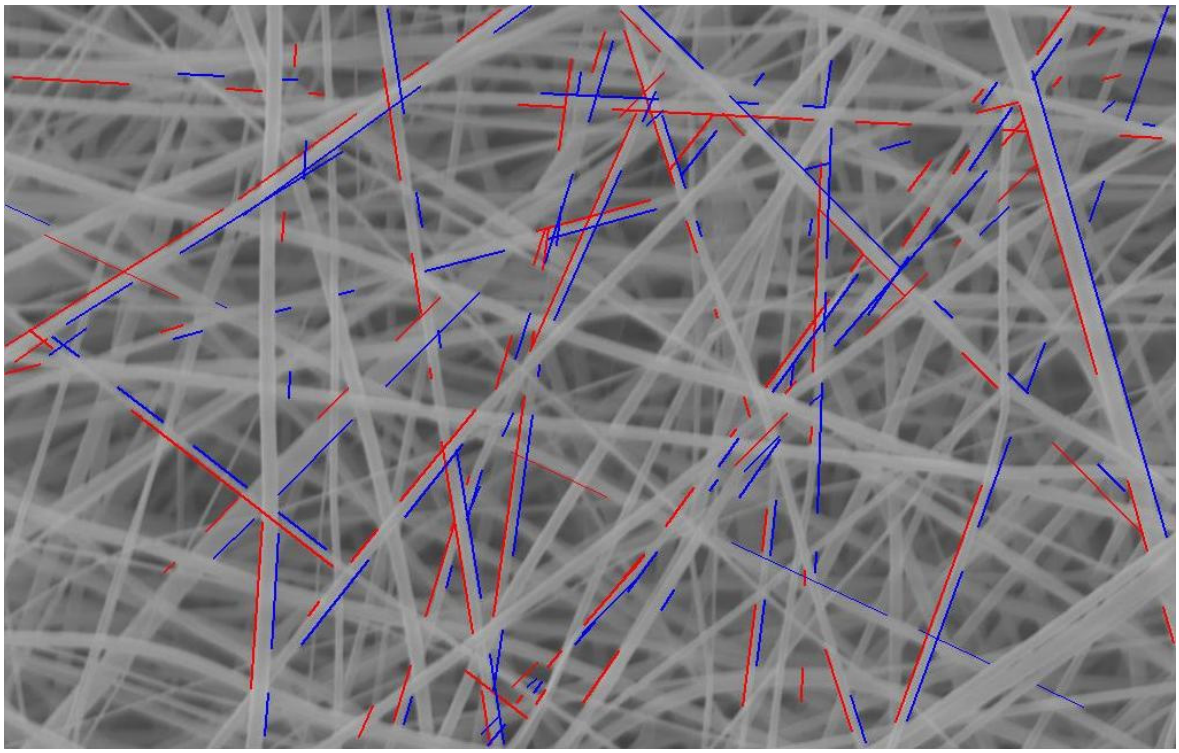

Figure 131 Image SEM3 with DCH valid edges

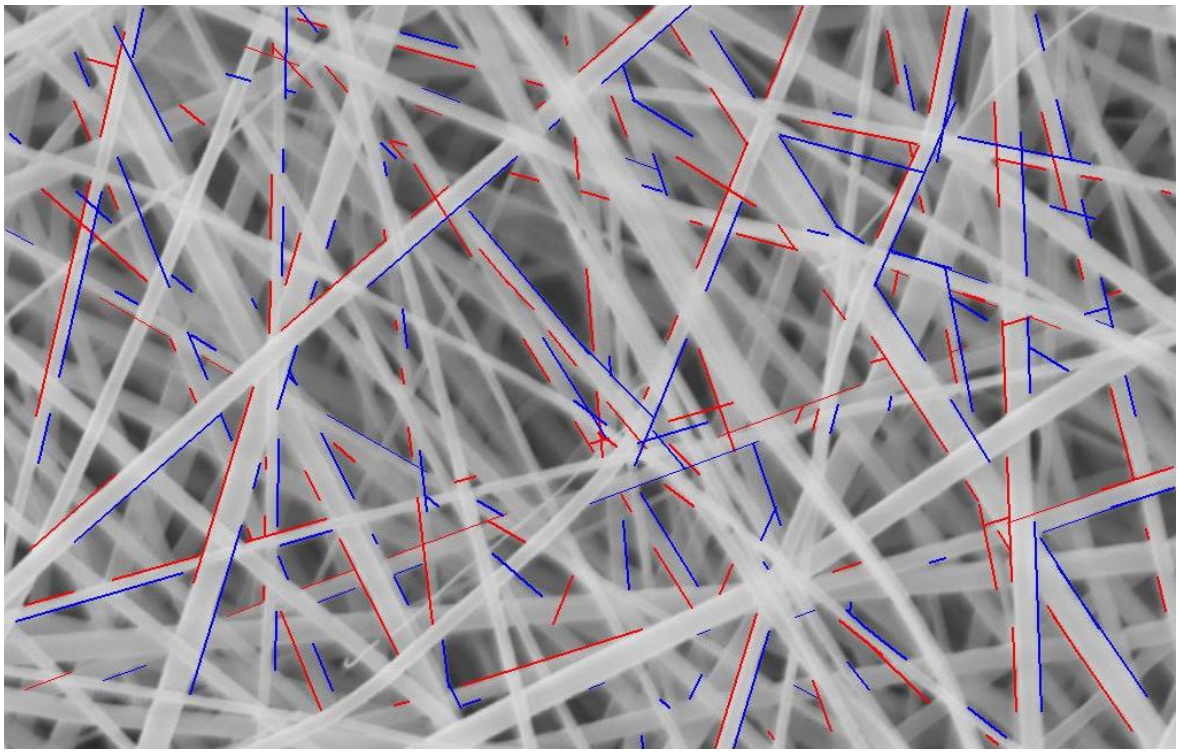

Figure 132 Image SEM4 with DCH valid edges

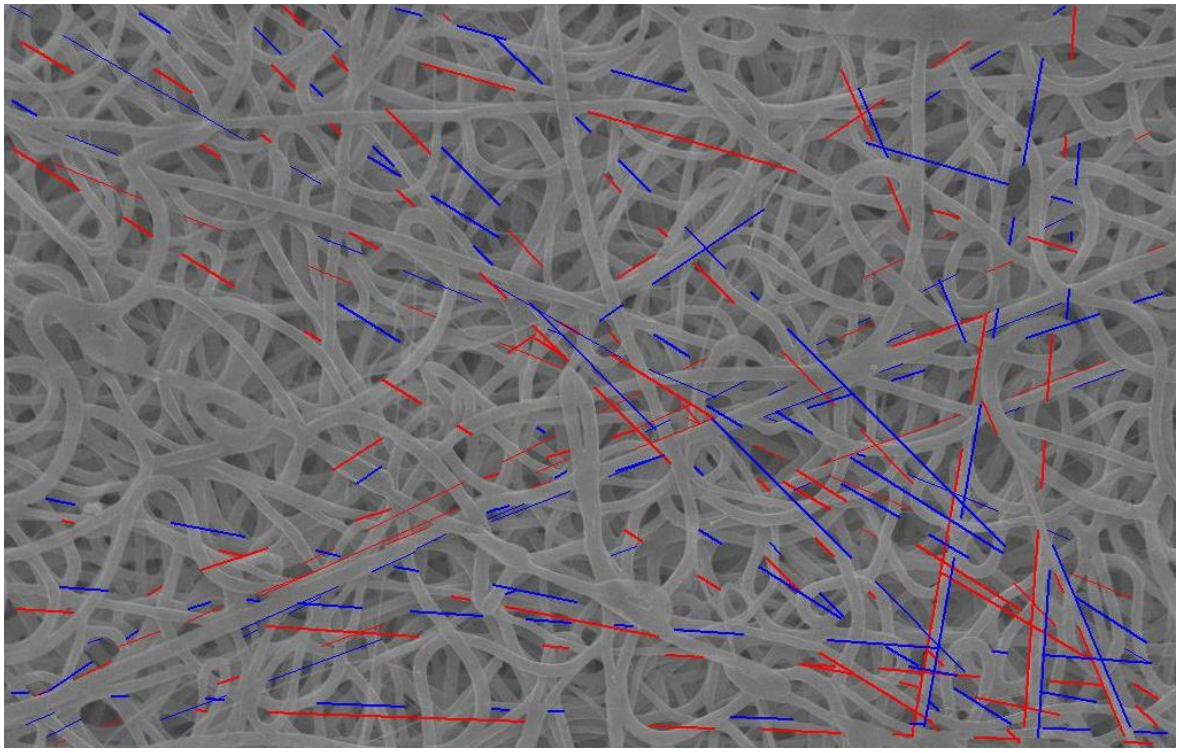

Figure 133 Image SEM5 with DCH valid edges

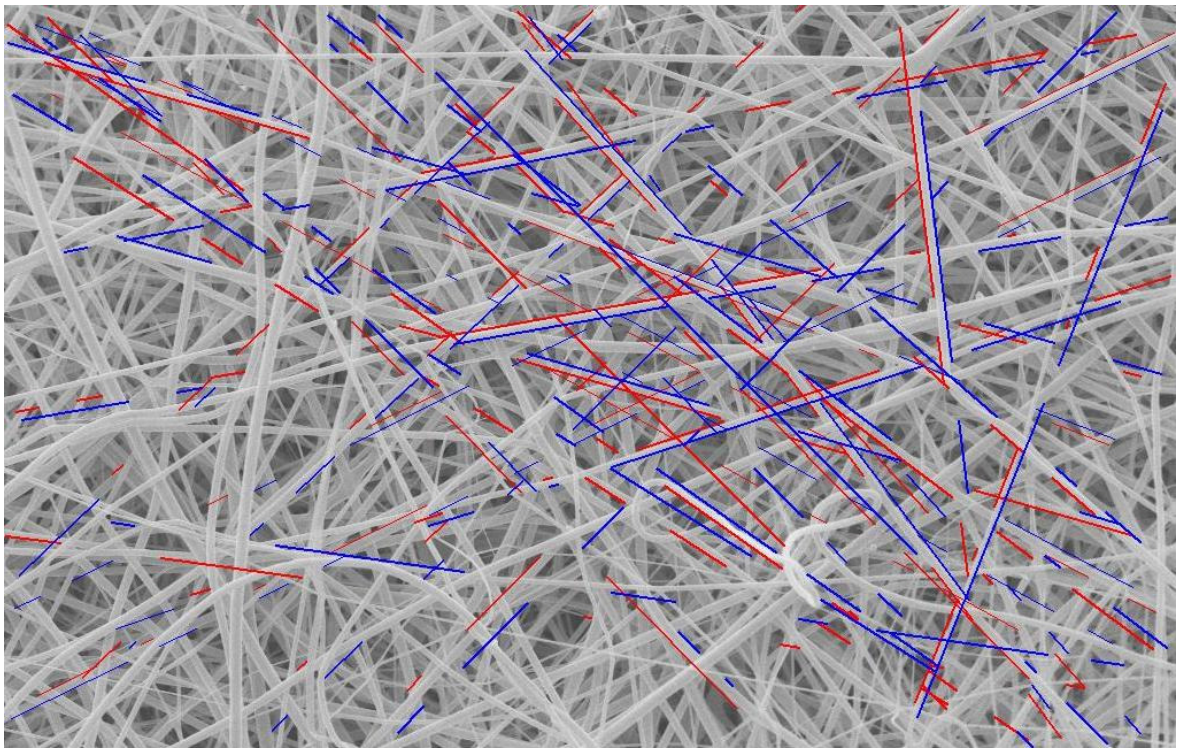

Figure 134 Image SEM6 with DCH valid edges

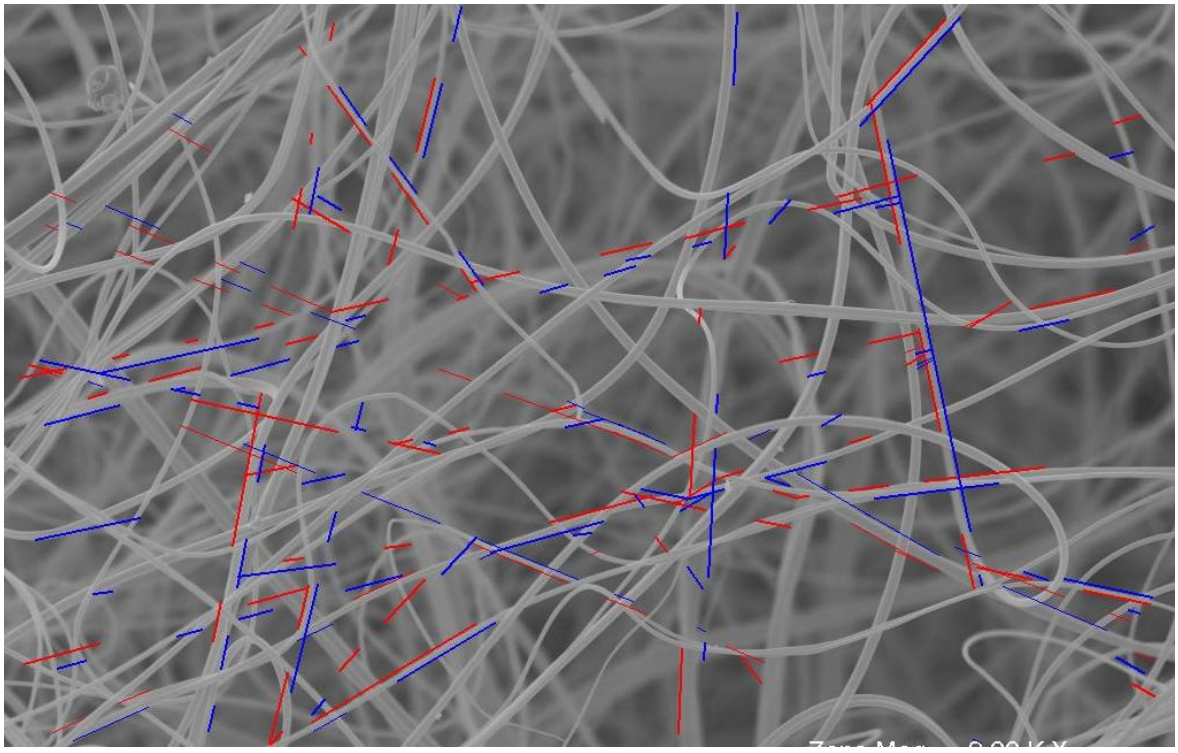

Figure 135 Image SEM7 with DCH valid edges

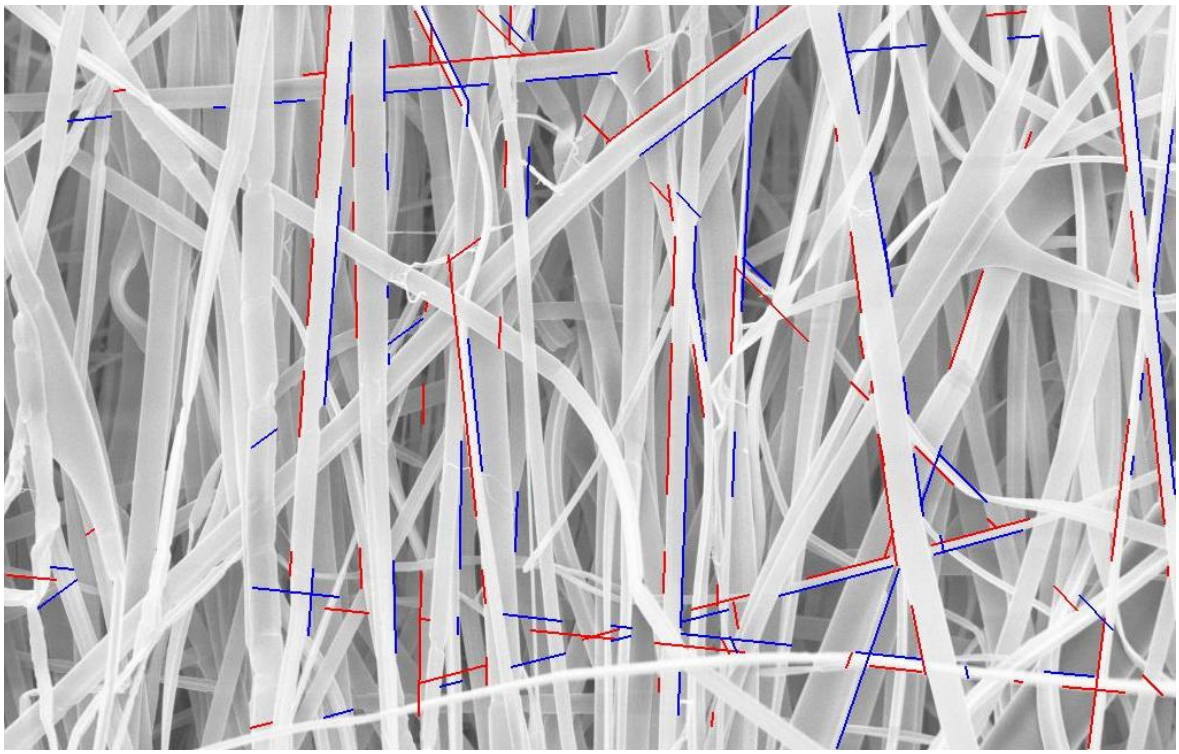

Figure 136 Image SEM8 with DCH valid edges

APPENDIX E: Resulting Images for Custom Canny Slopes Method

The following images were processed with the Custom Canny Slopes fiber diameter measurement method. The fiber diameters per image can be found in the results section. In the following figures, the determined valid edges per image were superimposed over the corresponding original image. Red and blue segments respectively represent the left and right edges of the valid edge pairs found with this method.

CCS edges superimposed over the narrow distribution simulated images

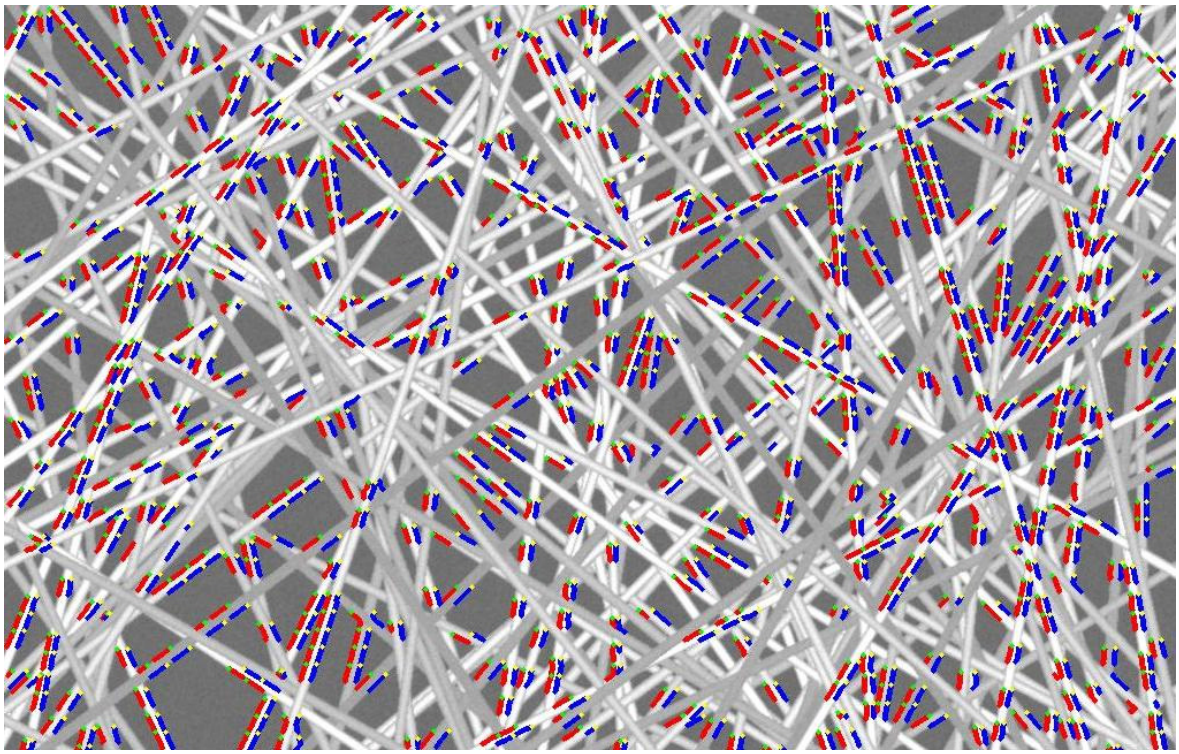

Figure 137 Image narrow10 with CCS valid edges

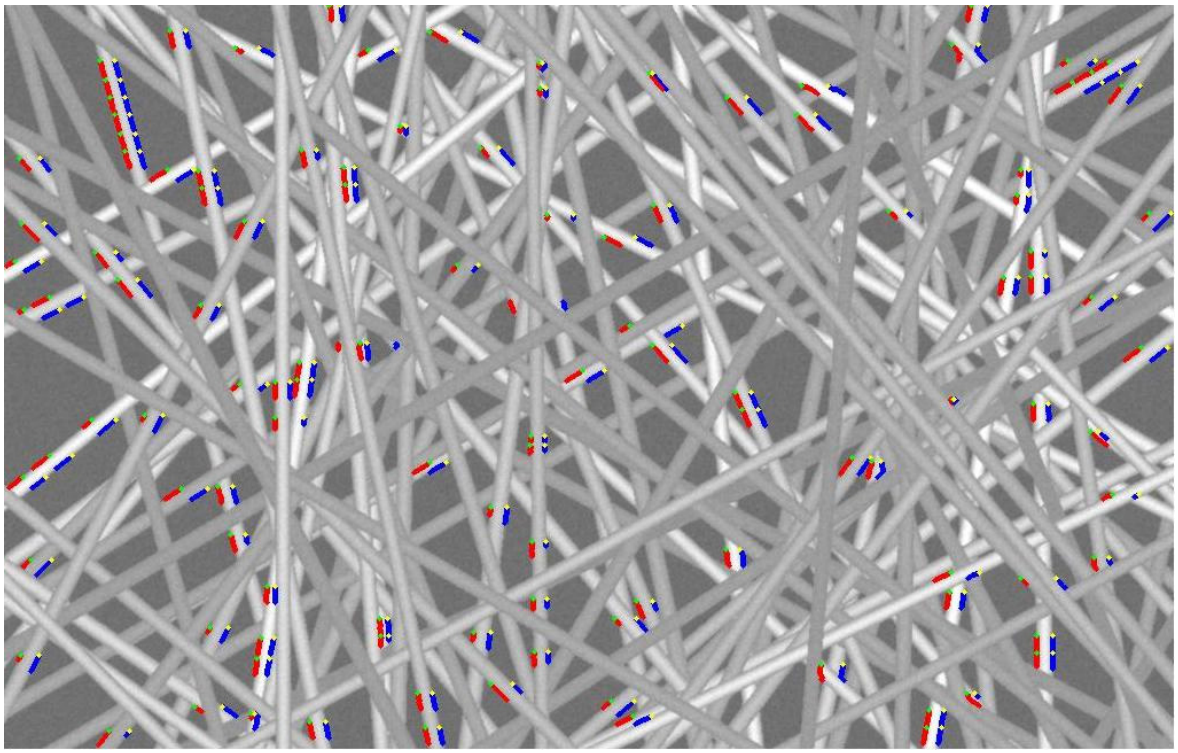

Figure 138 Image narrow15 with CCS valid edges

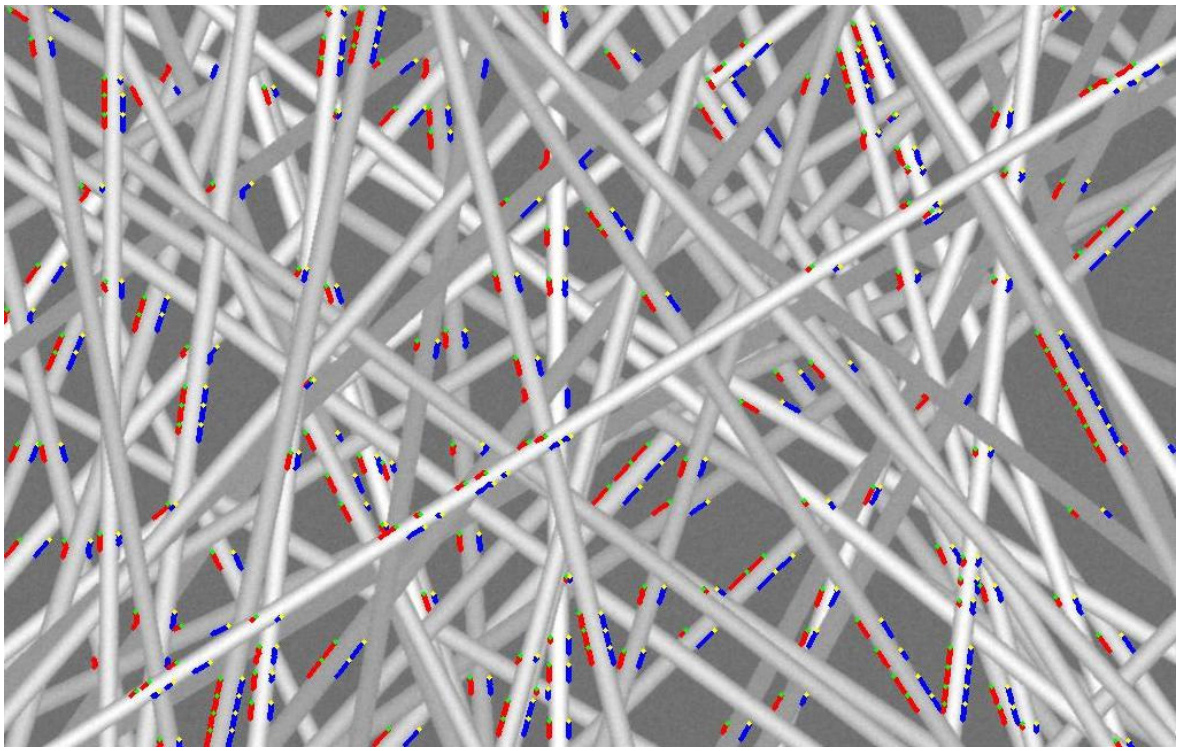

Figure 139 Image narrow20 with CCS valid edges

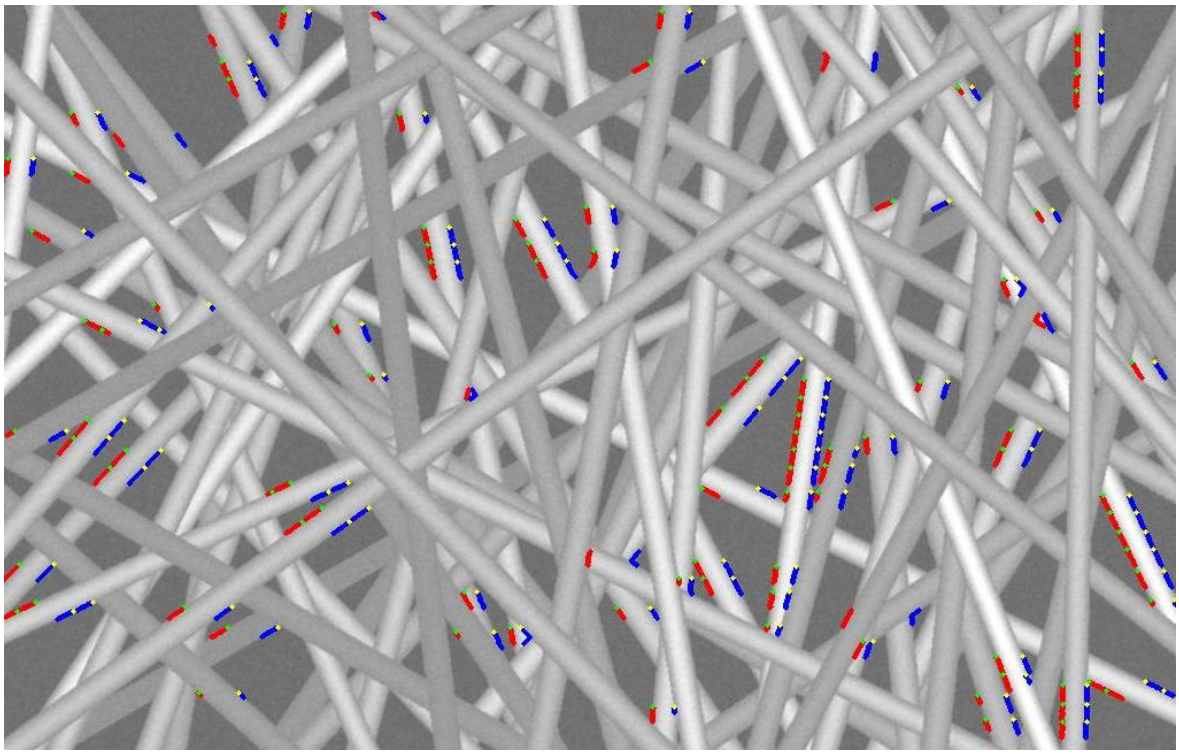

Figure 140 Image narrow25 with CCS valid edges

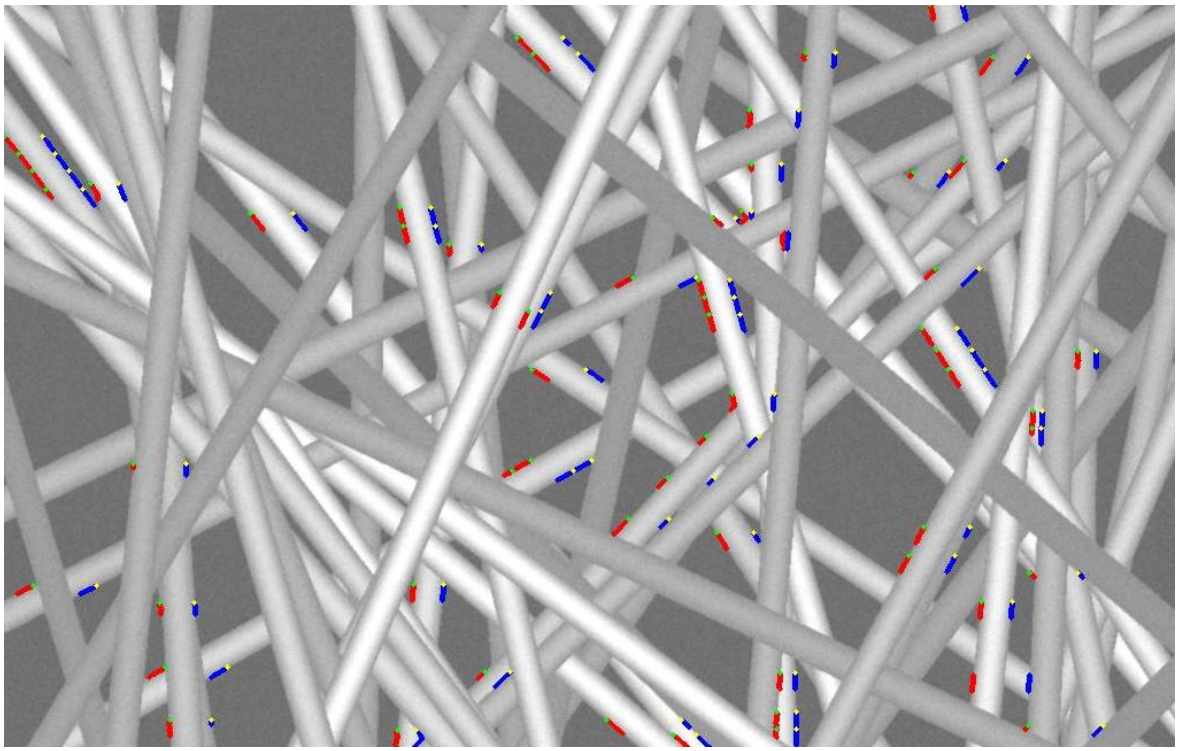

Figure 141 Image narrow30 with CCS valid edges

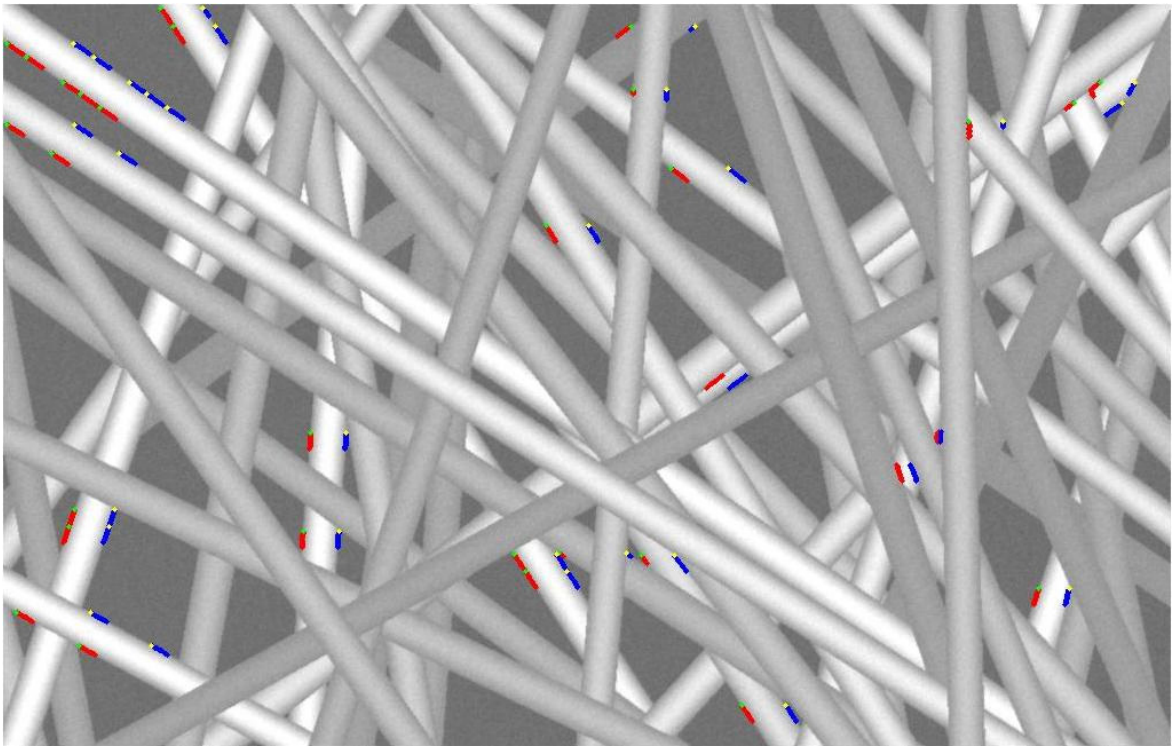

Figure 142 Image narrow35 with CCS valid edges

CCS edges superimposed over the wide distribution simulated images

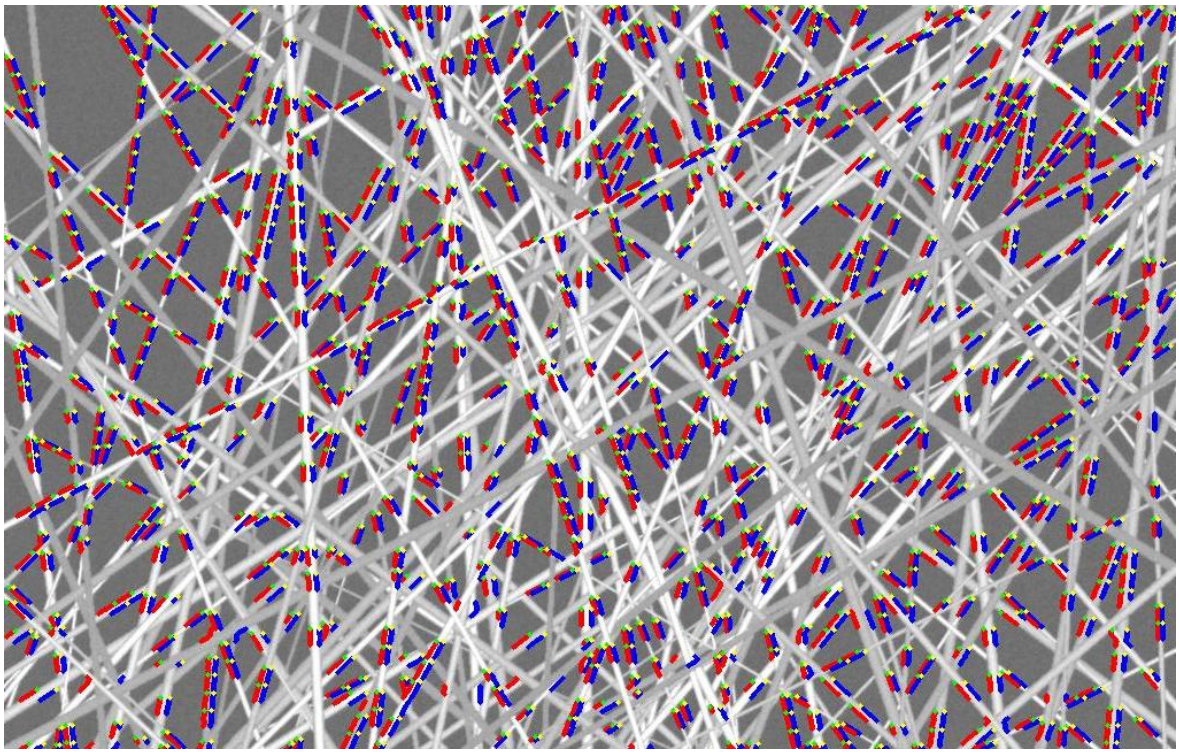

Figure 143 Image wide10 with CCS valid edges

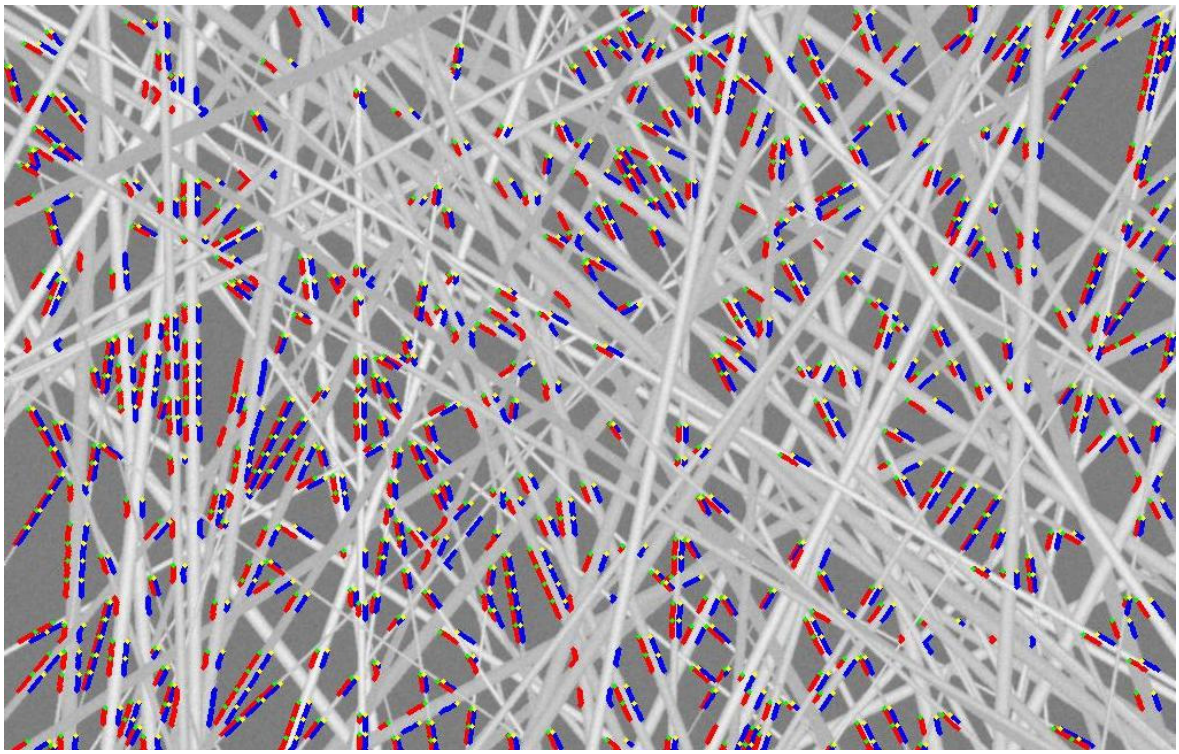

Figure 144 Image wide15 with CCS valid edges

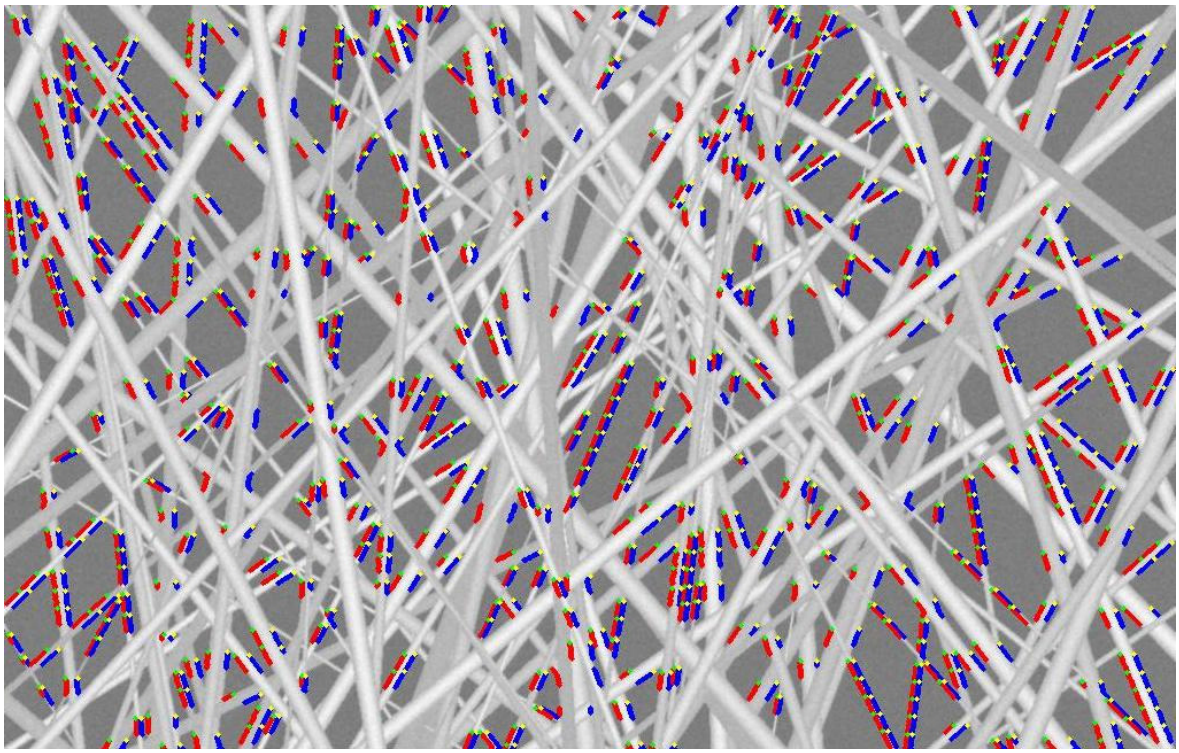

Figure 145 Image wide20 with CCS valid edges

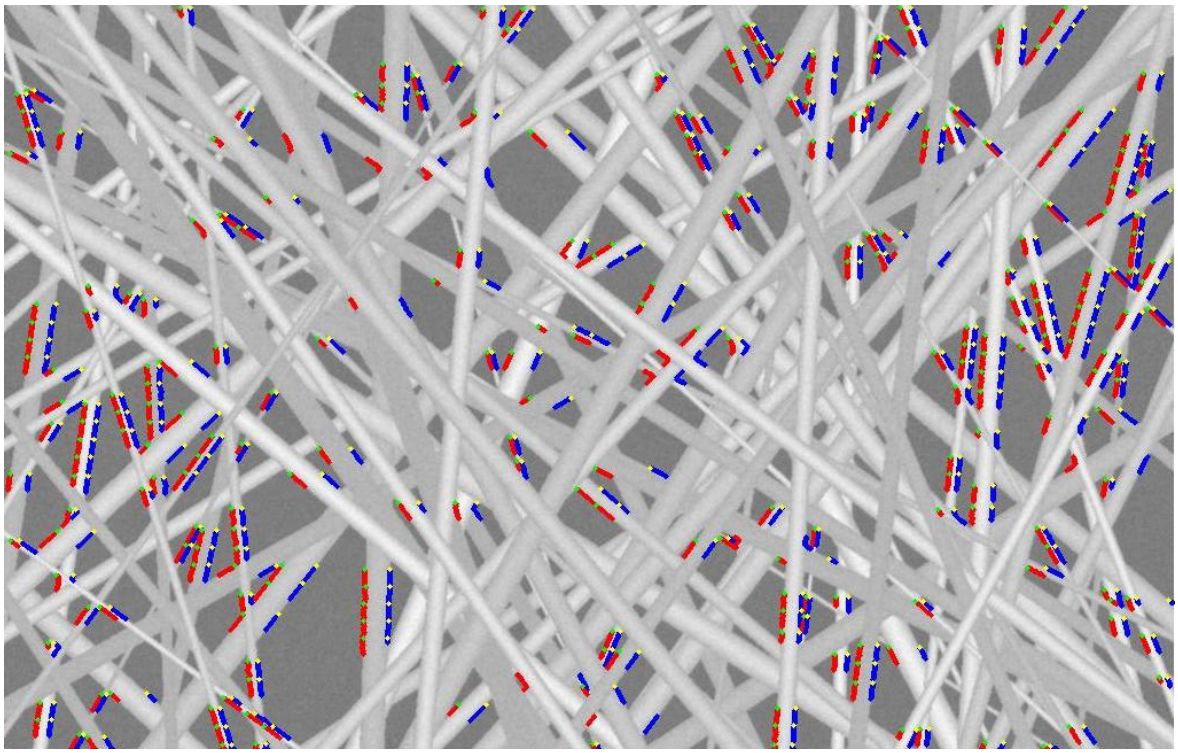

Figure 146 Image wide25 with CCS valid edges

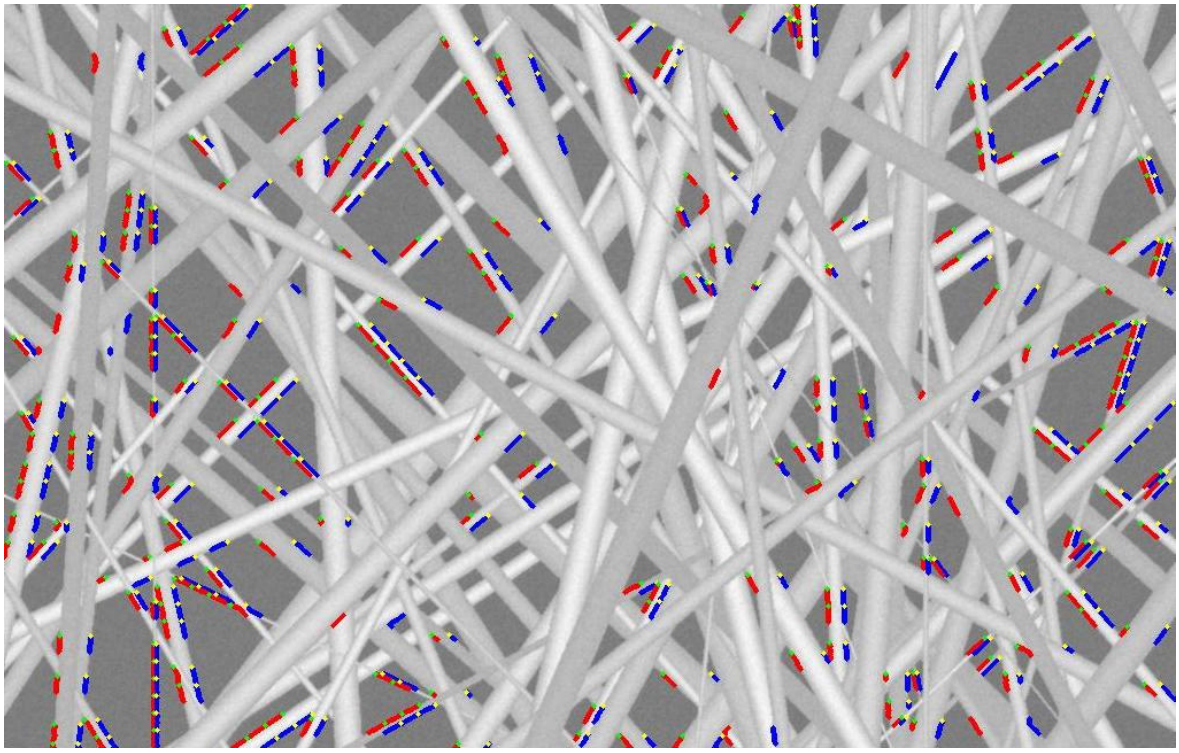

Figure 147 Image wide30 with CCS valid edges

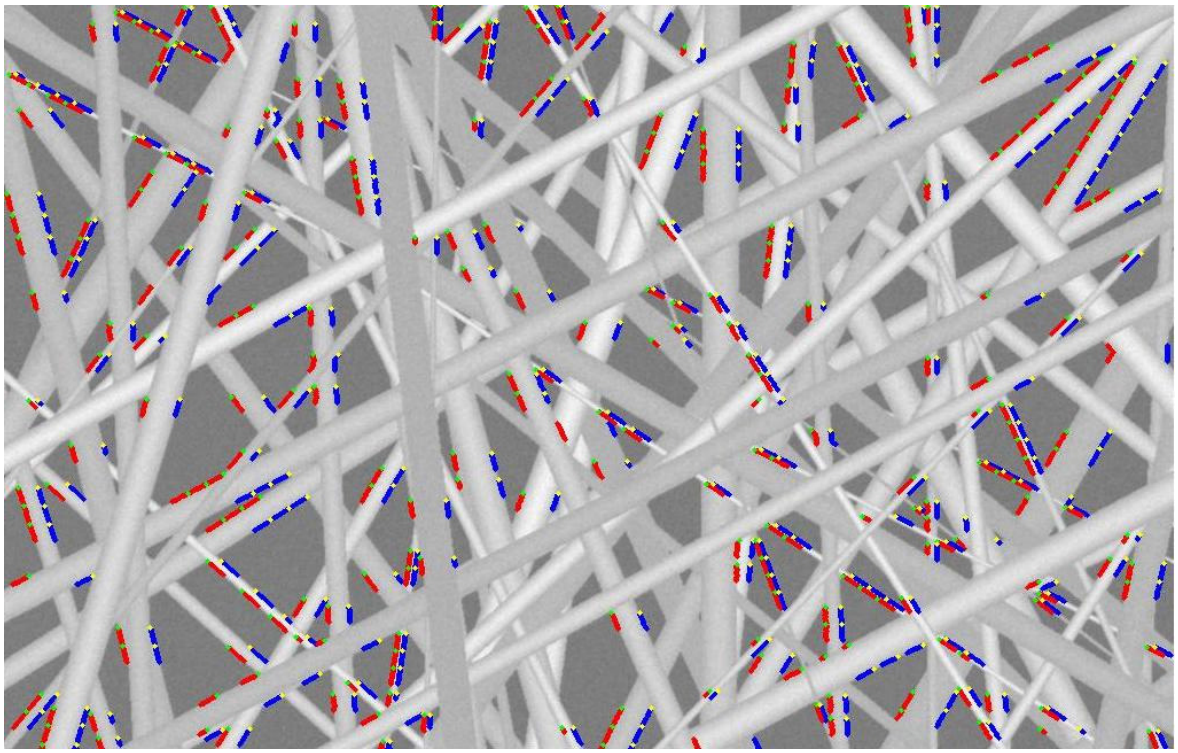

Figure 148 Image wide35 with CCS valid edges

CCS edges superimposed over real SEM images

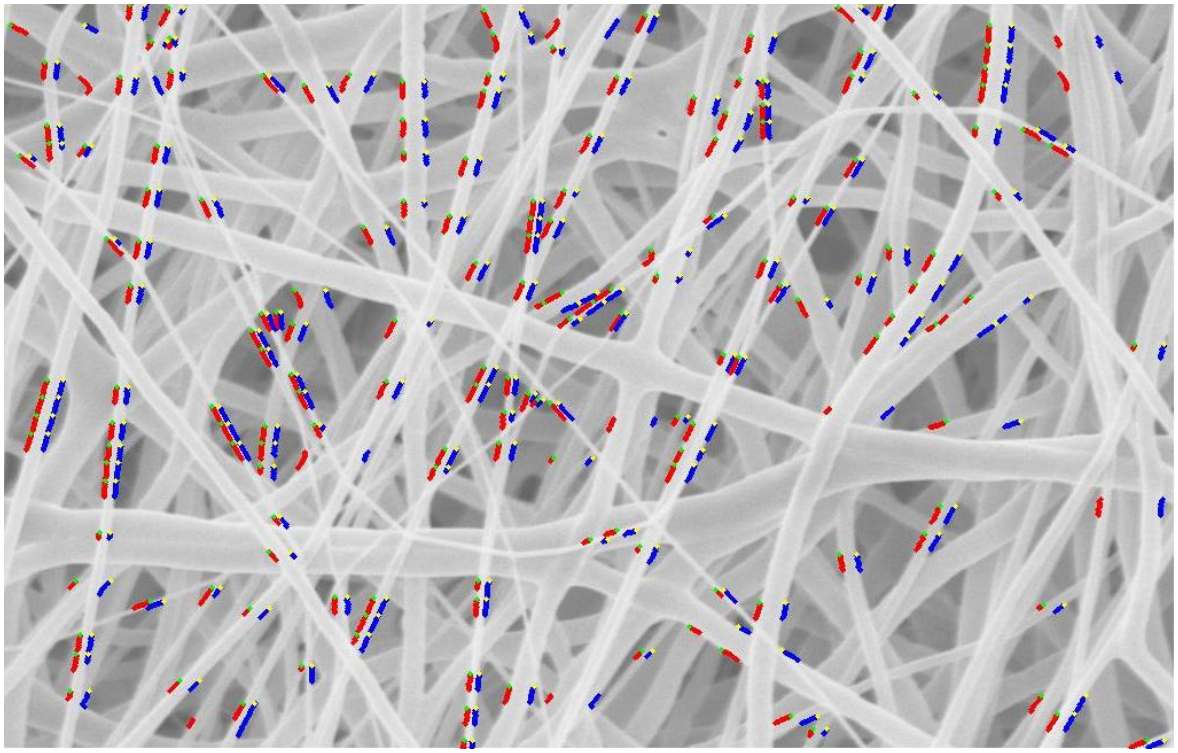

Figure 149 Image SEM1 with CCS valid edges

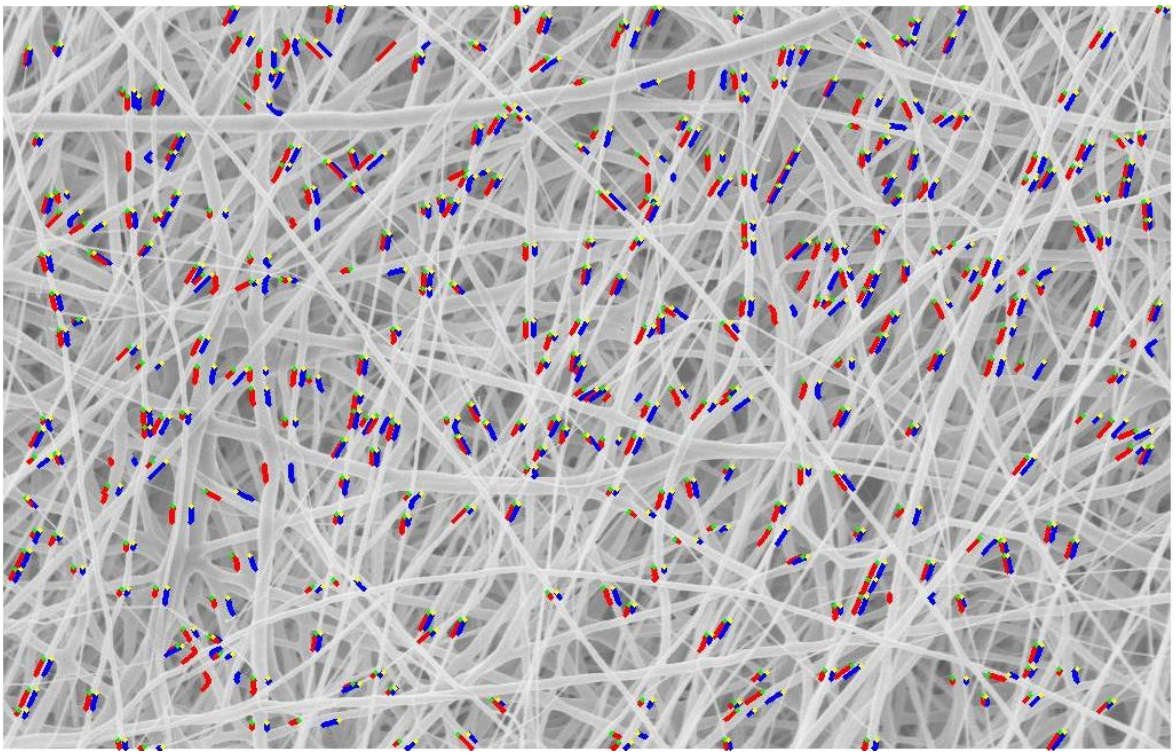

Figure 150 Image SEM2 with CCS valid edges

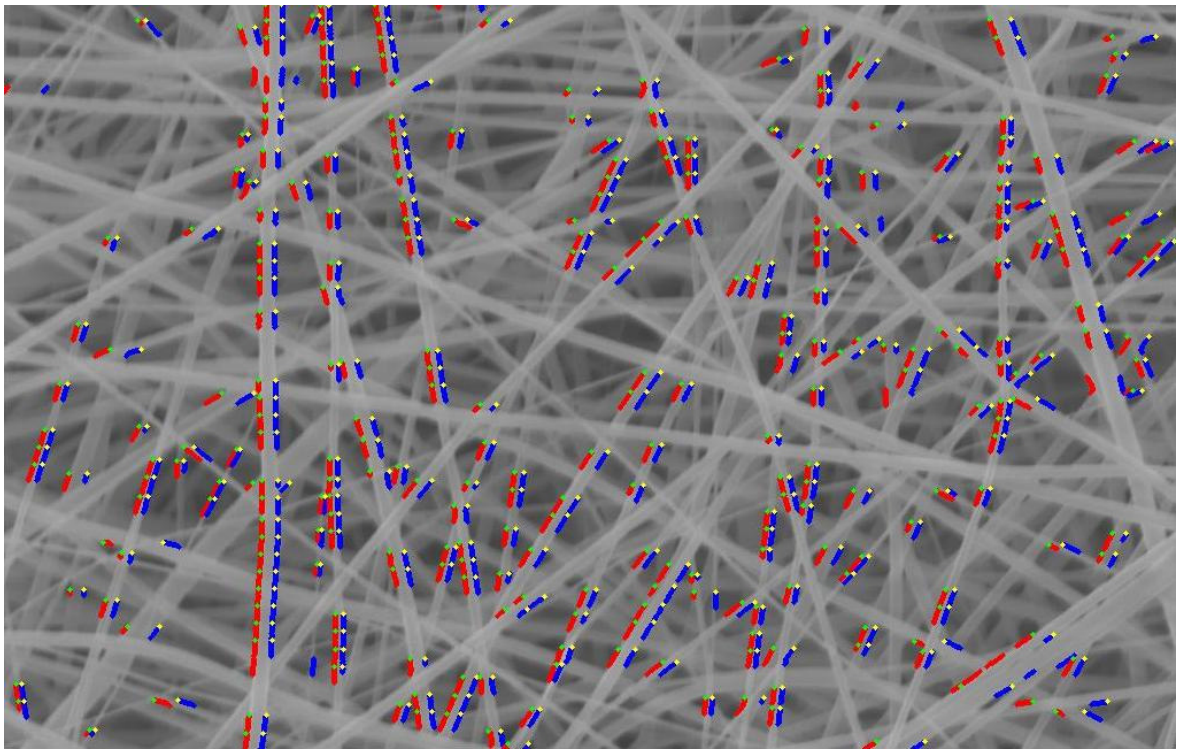

Figure 151 Image SEM3 with CCS valid edges

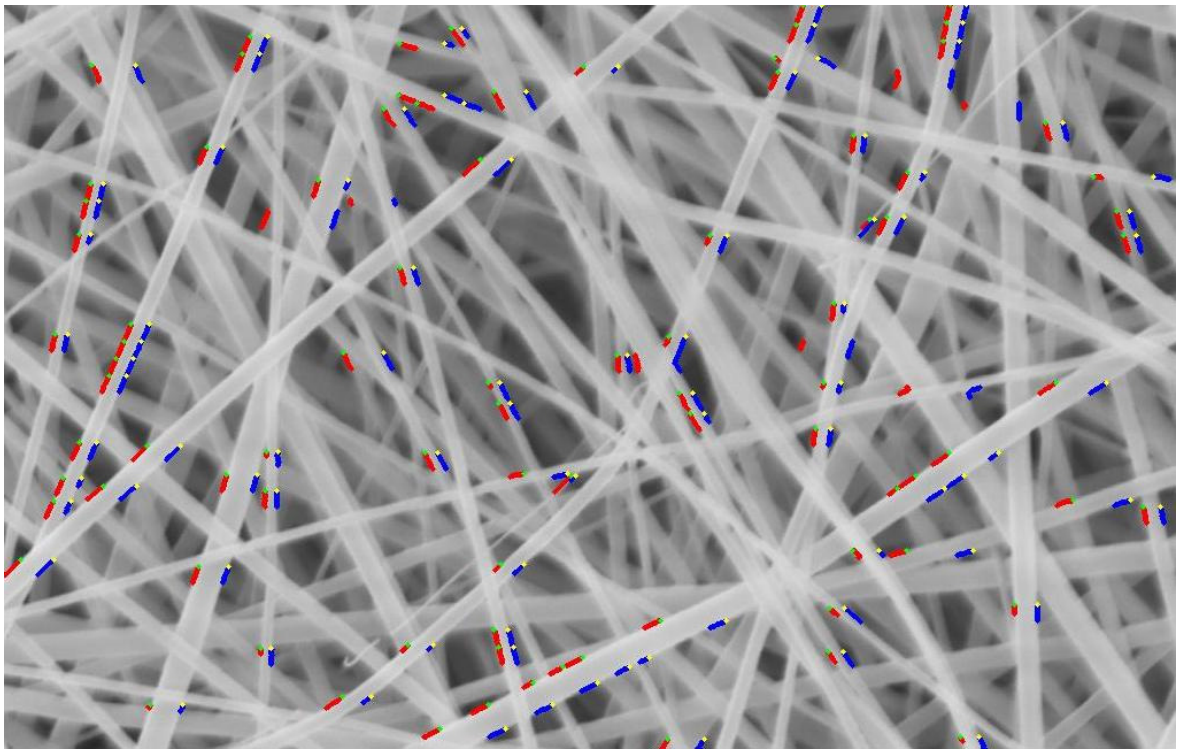

Figure 152 Image SEM4 with CCS valid edges

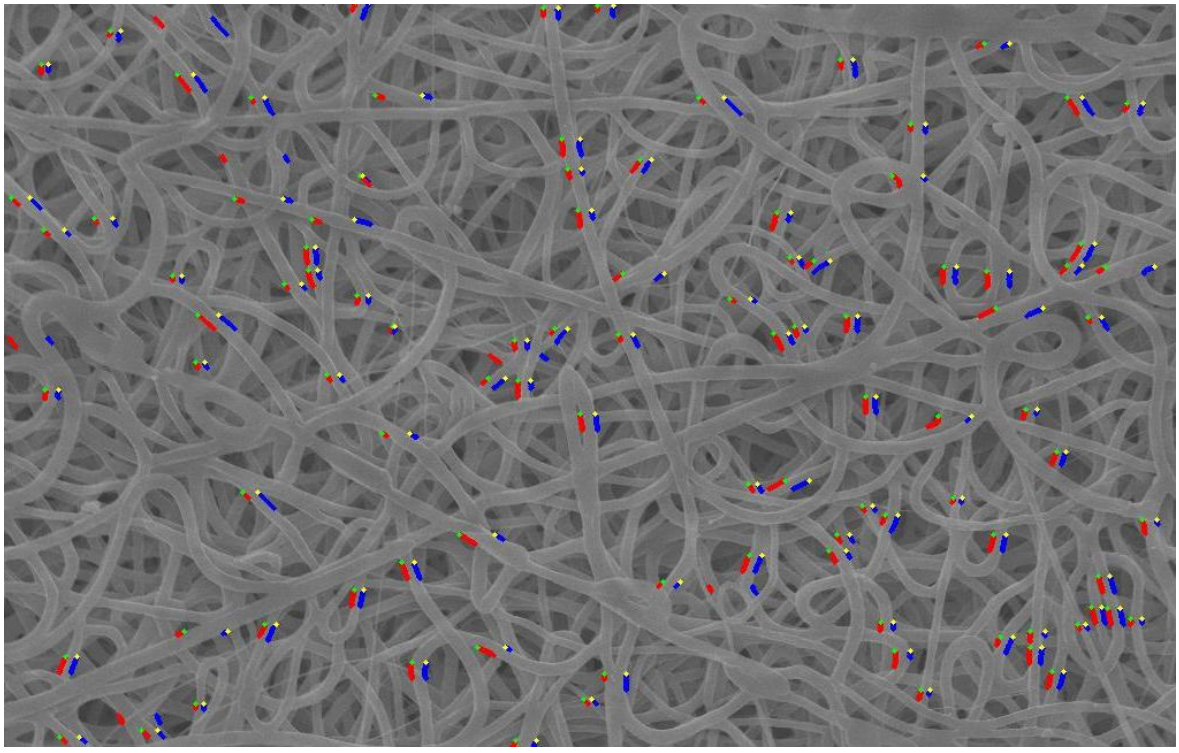

Figure 153 Image SEM5 with CCS valid edges

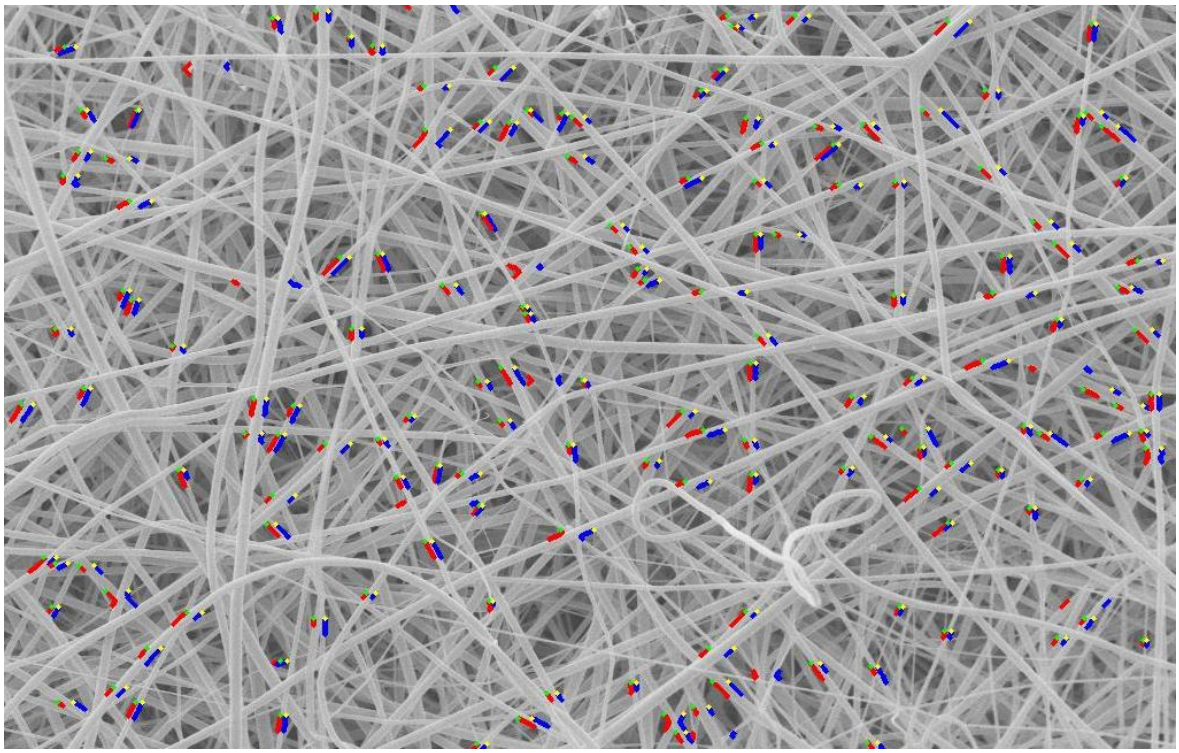

Figure 154 Image SEM6 with CCS valid edges

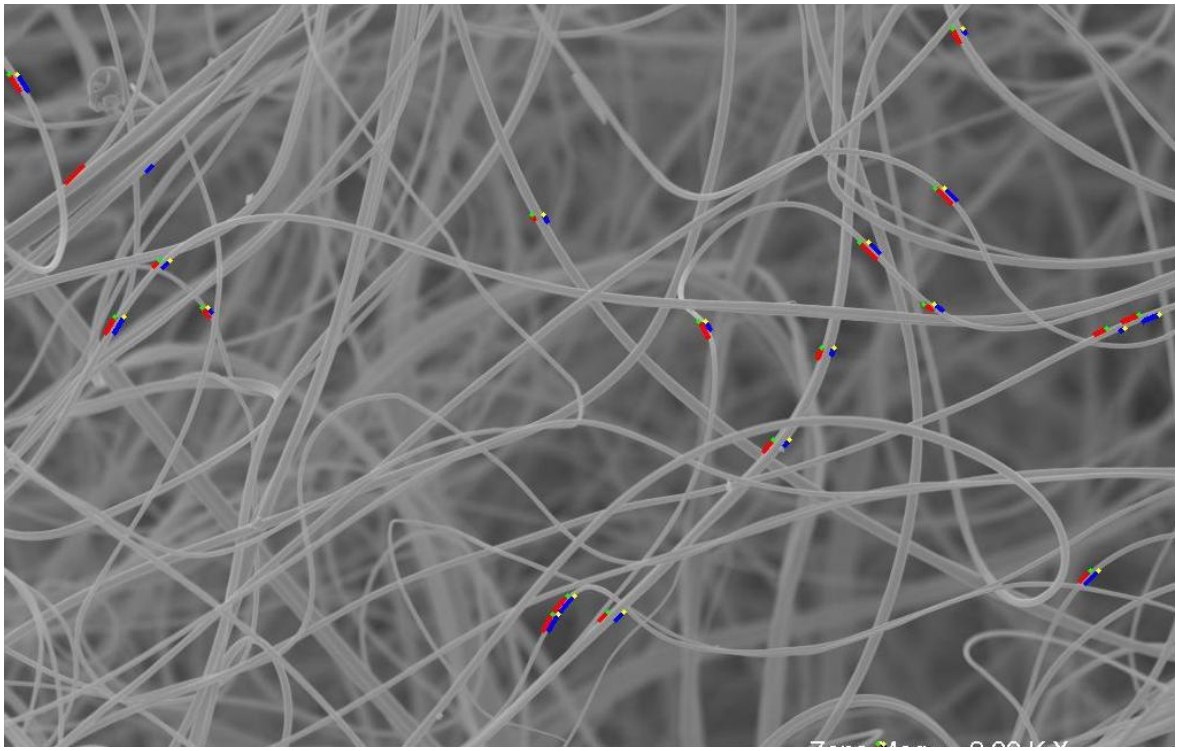

Figure 155 Image SEM7 with CCS valid edges

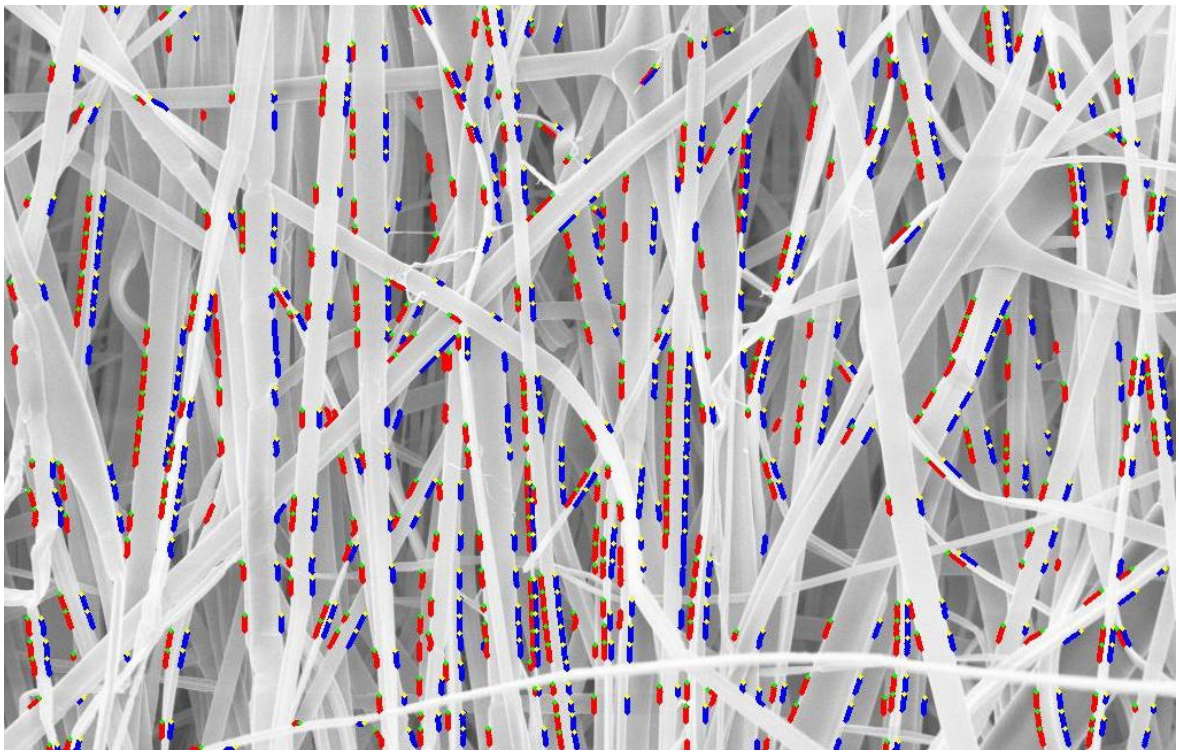

Figure 156 Image SEM8 with CCS valid edges

APPENDIX F: Resulting Images for Custom Canny Hough Method

The following images were processed with the Custom Canny Hough fiber diameter measurement method. The fiber diameters per image can be found in the results section. In the following figures, the determined valid edges per image were superimposed over the corresponding original image. Red and blue segments respectively represent the left and right edges of the valid edge pairs found with this method.

CCH edges superimposed over the narrow distribution simulated images

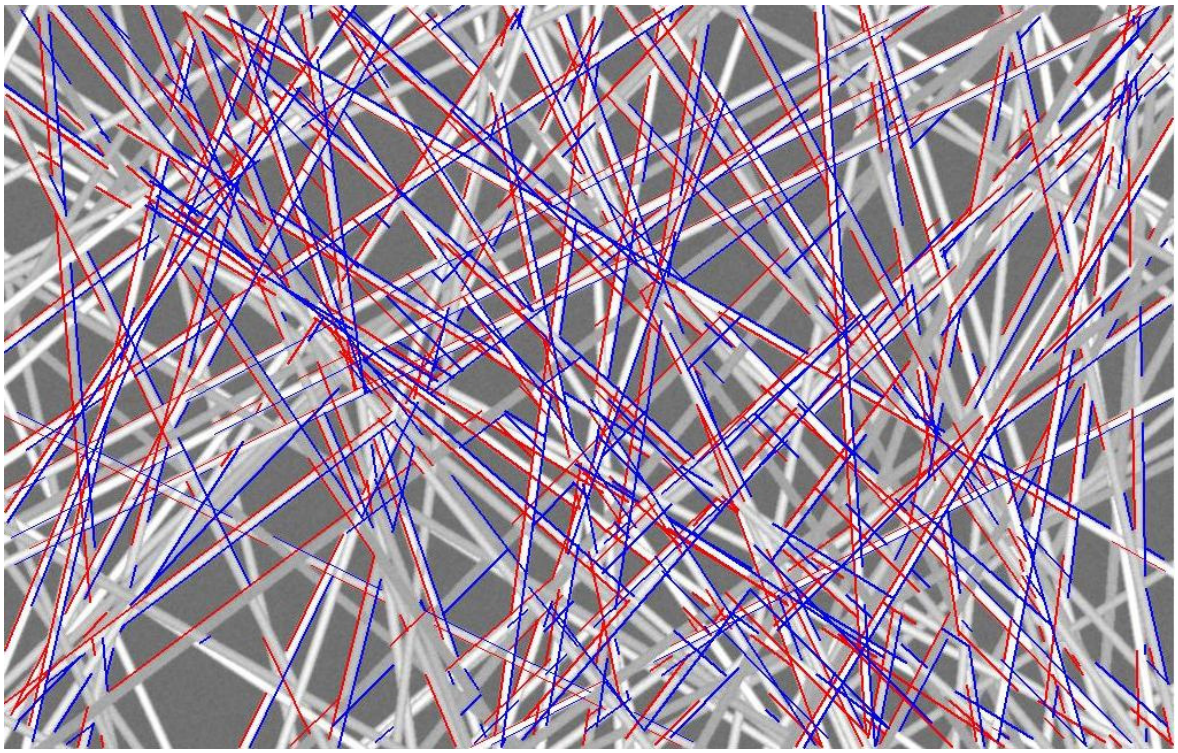

Figure 157 Image narrow10 with CCH valid edges

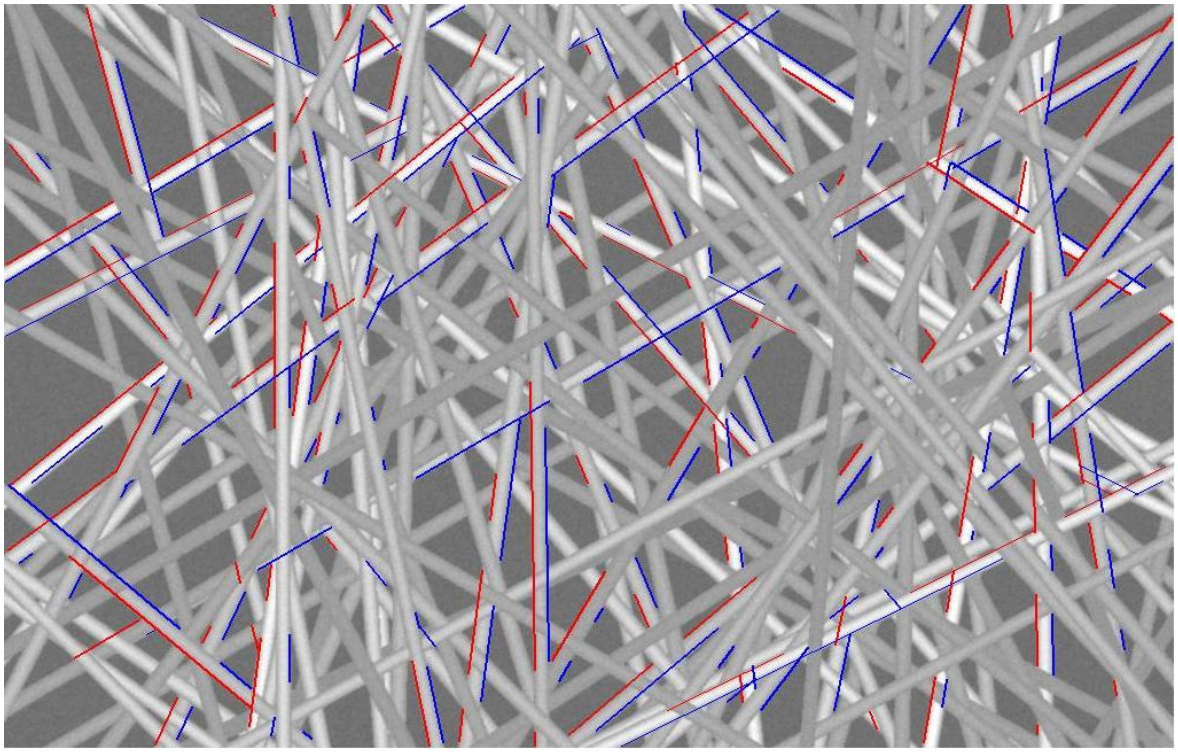

Figure 158 Image narrow15 with CCH valid edges

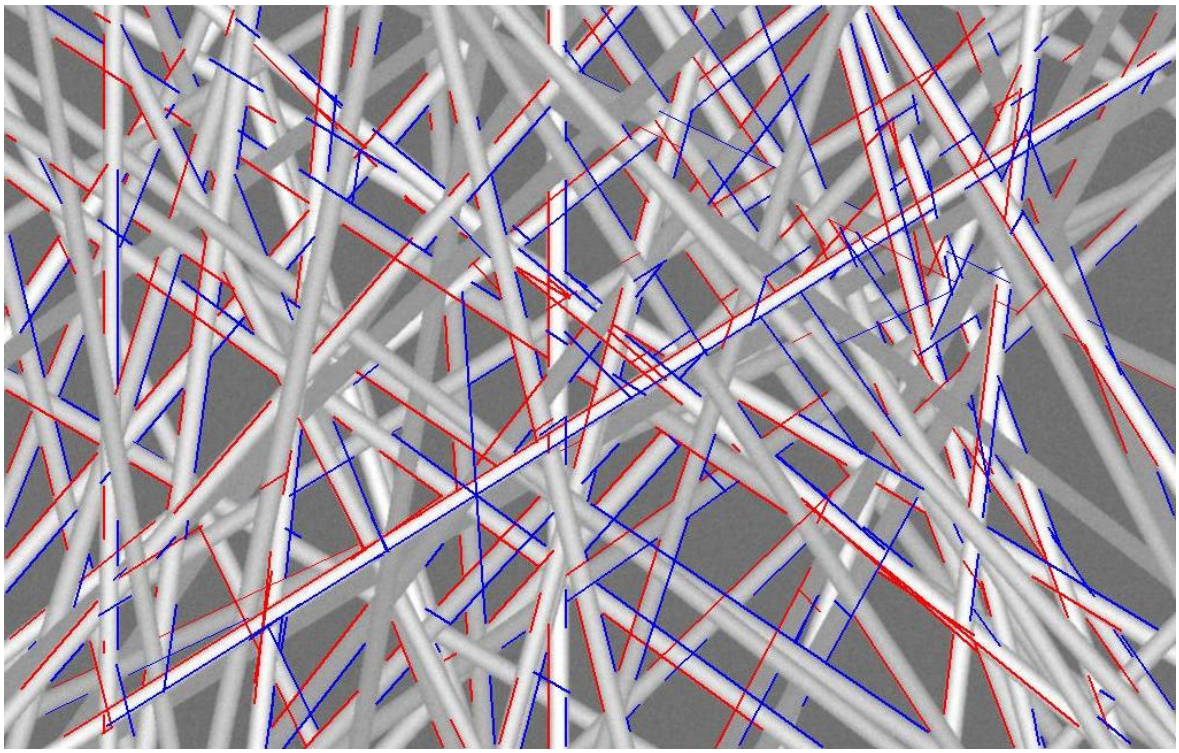

Figure 159 Image narrow20 with CCH valid edges

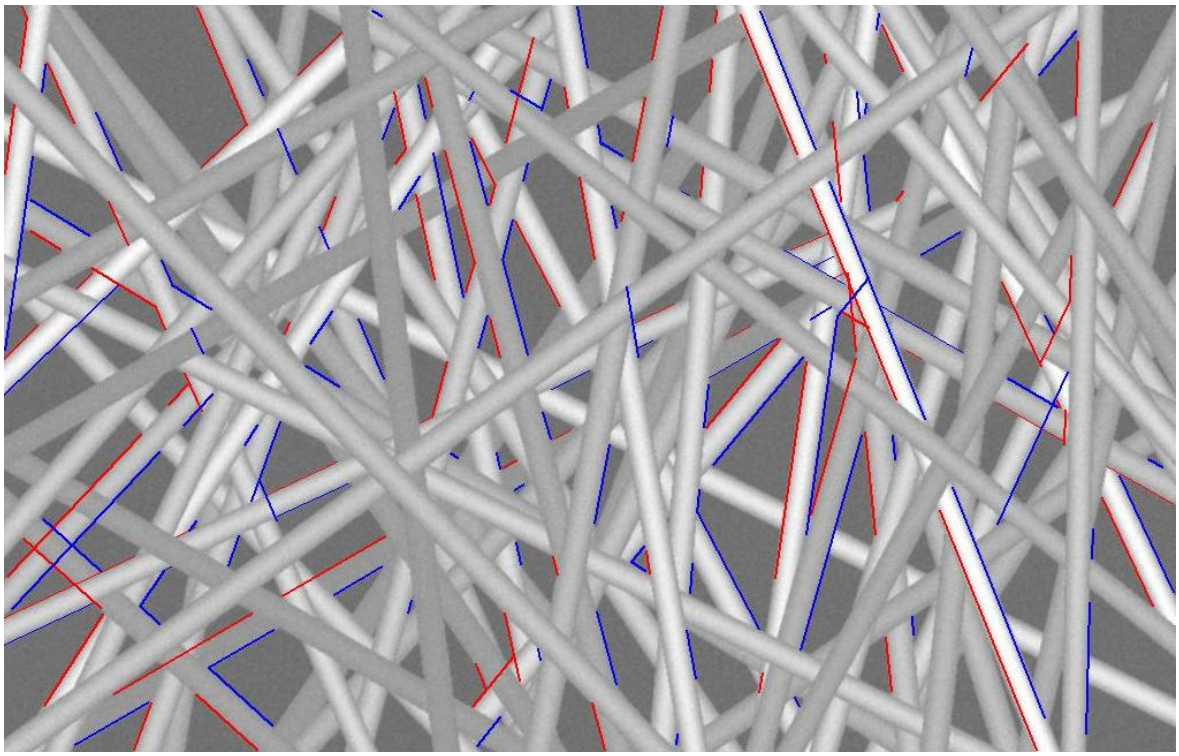

Figure 160 Image narrow25 with CCH valid edges

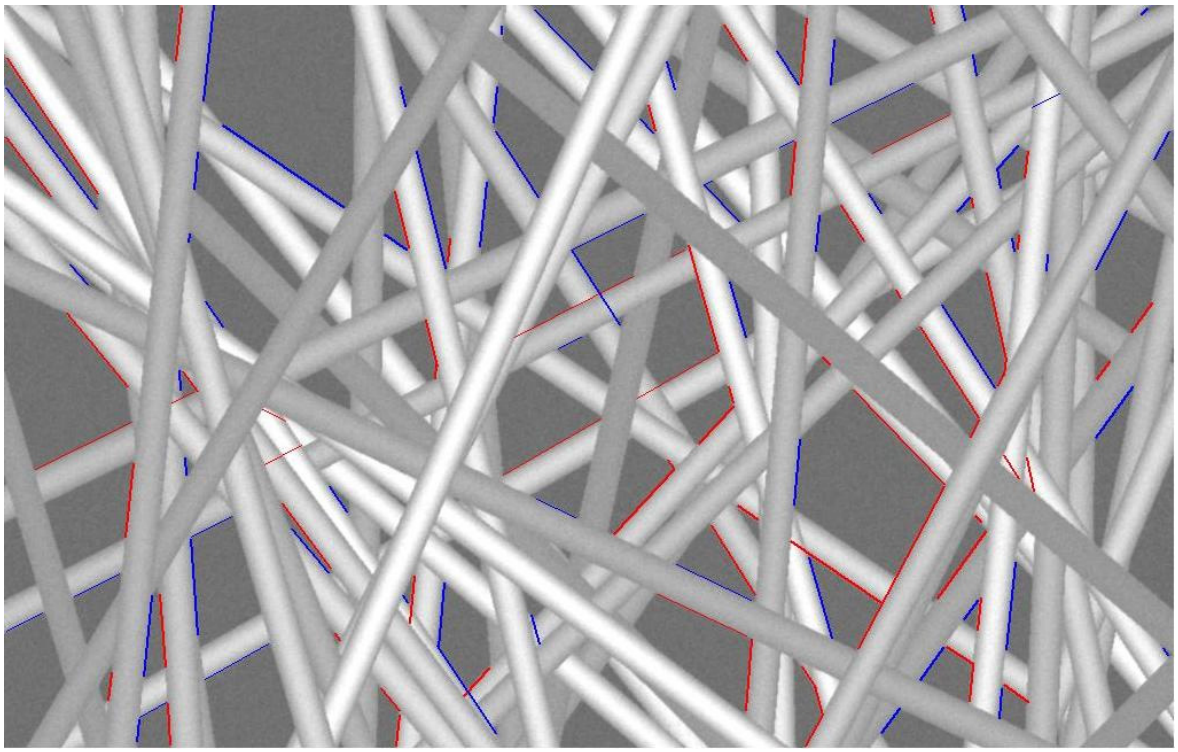

Figure 161 Image narrow30 with CCH valid edges

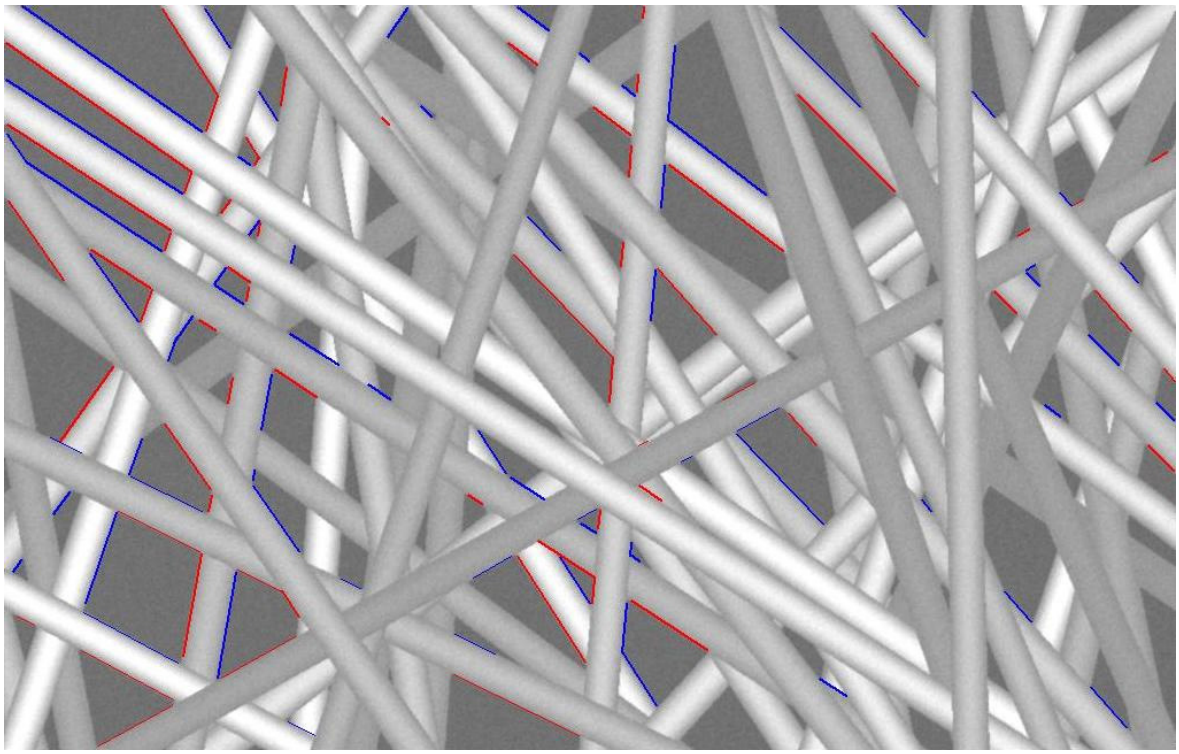

Figure 162 Image narrow35 with CCH valid edges

CCH edges superimposed over the wide distribution simulated images

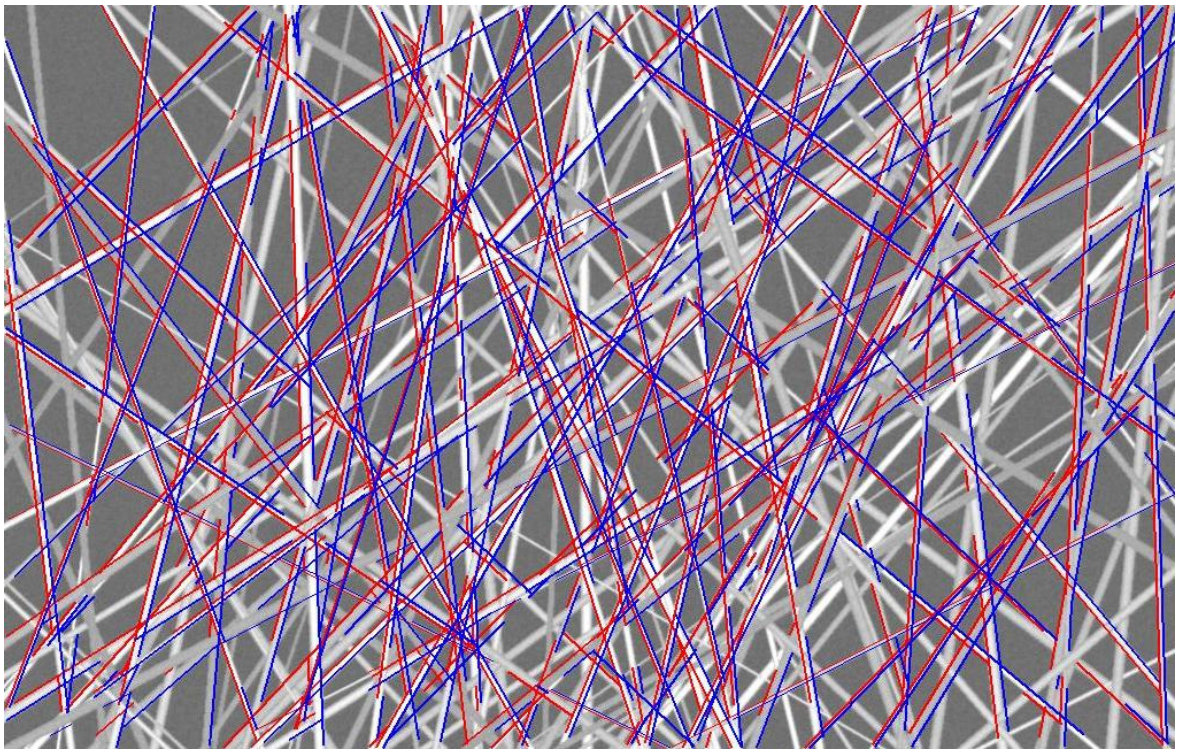

Figure 163 Image wide10 with CCH valid edges

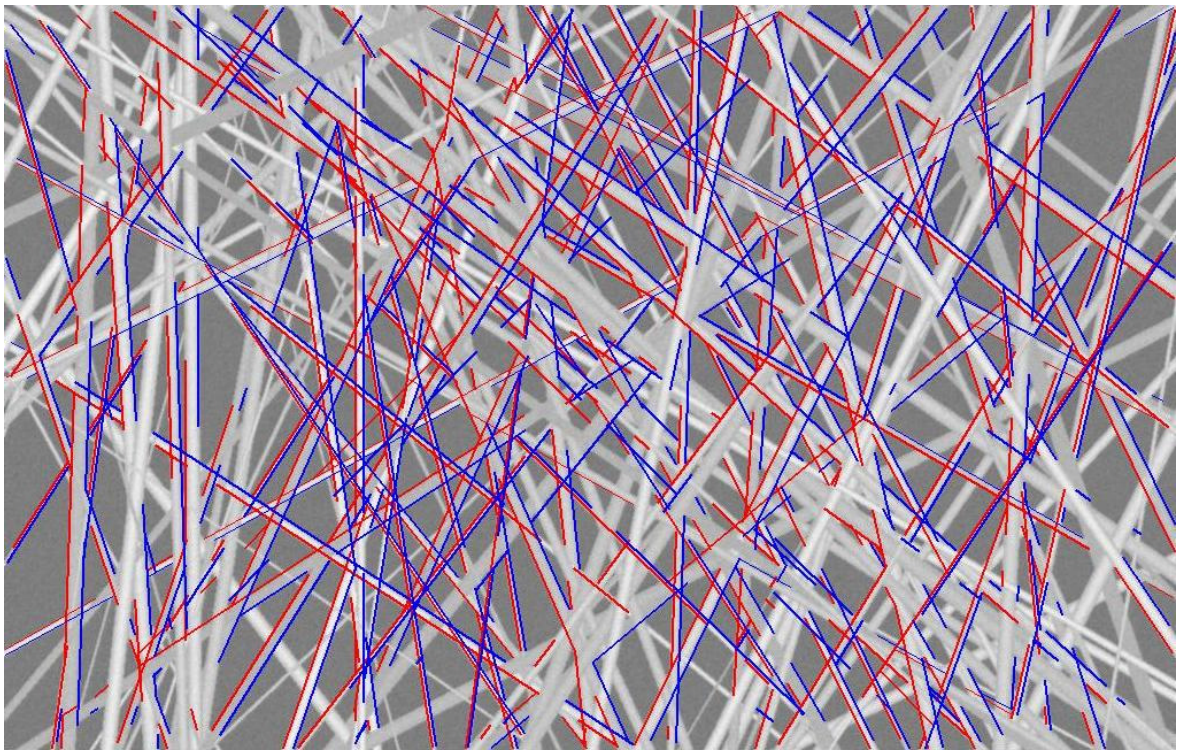

Figure 164 Image wide15 with CCH valid edges

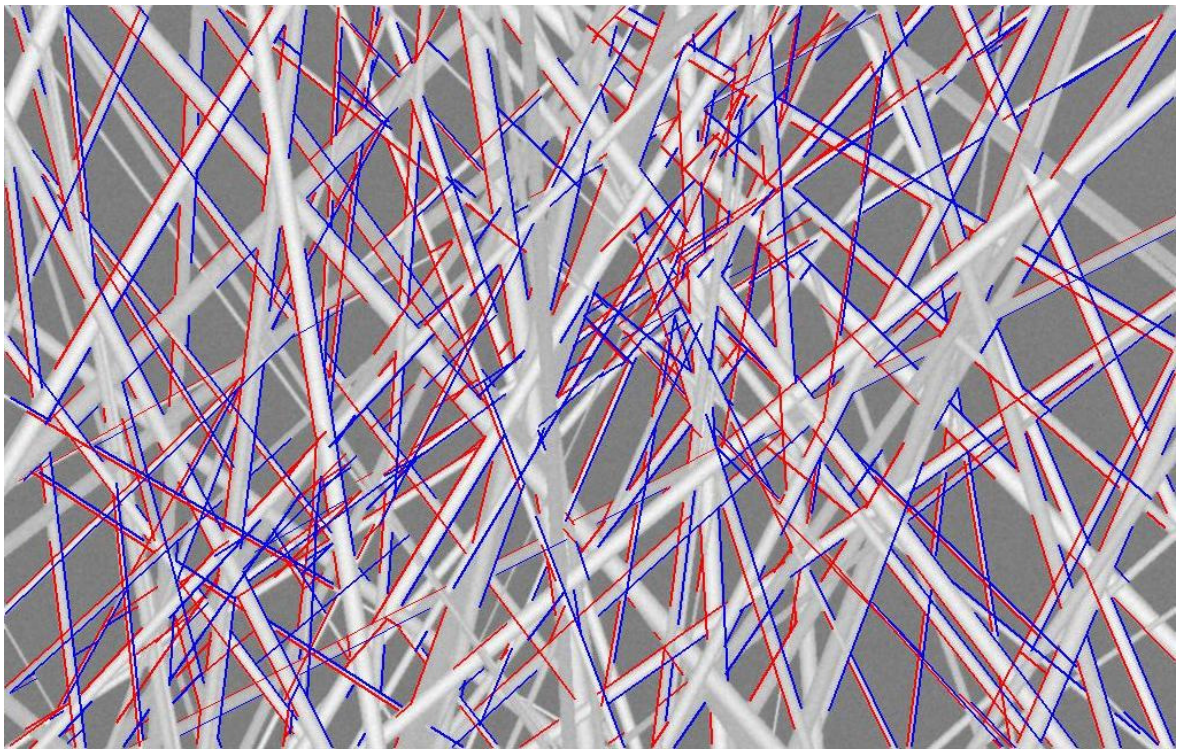

Figure 165 Image wide20 with CCH valid edges

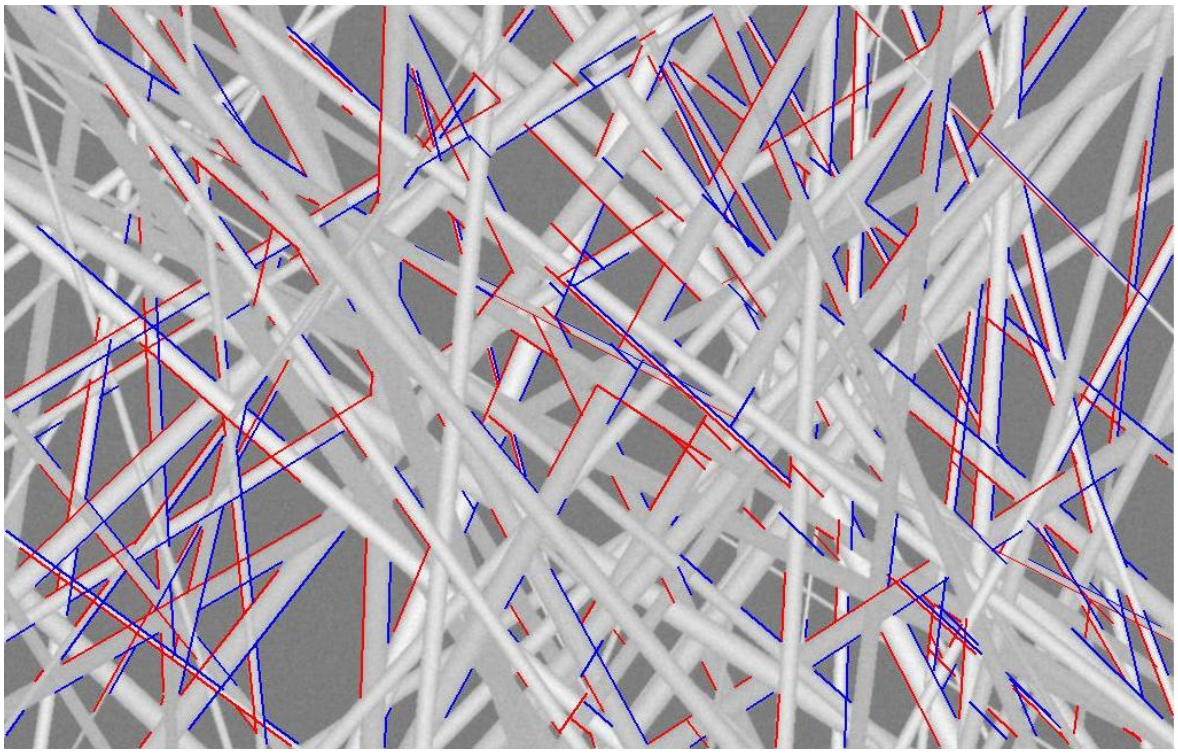

Figure 166 Image wide25 with CCH valid edges

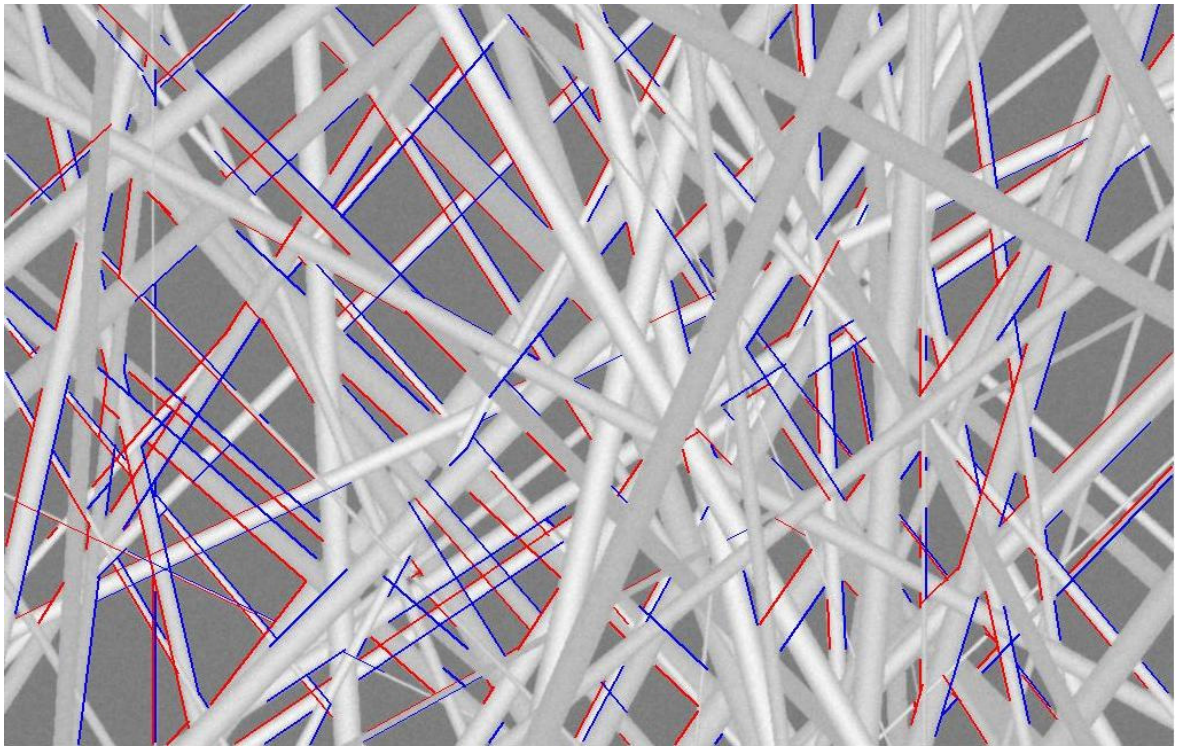

Figure 167 Image wide30 with CCH valid edges

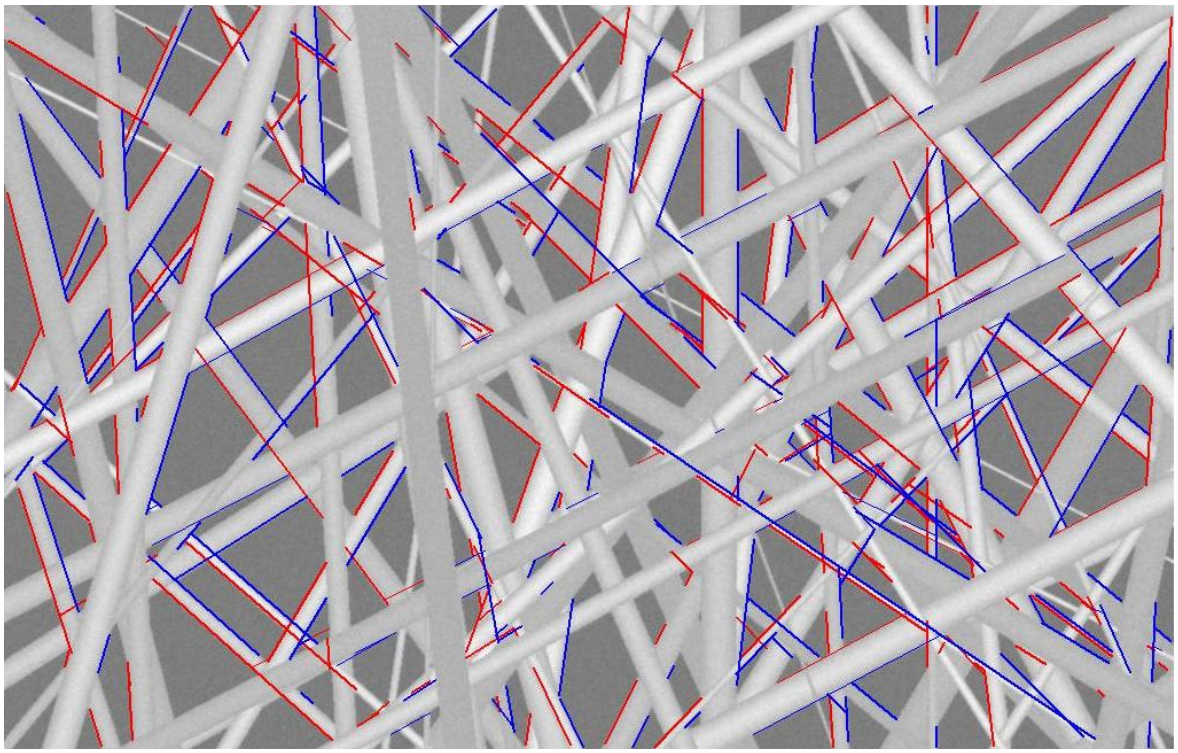

Figure 168 Image wide35 with CCH valid edges

CCH edges superimposed over real SEM images

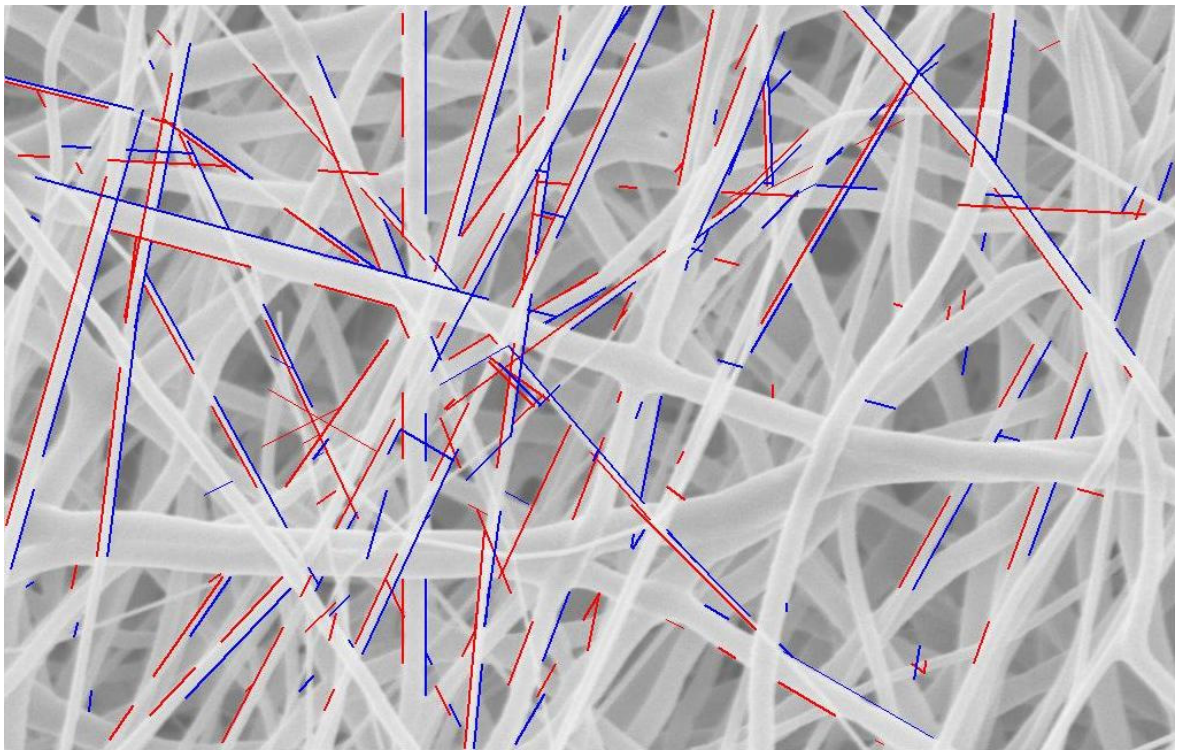

Figure 169 Image SEM1 with CCH valid edges

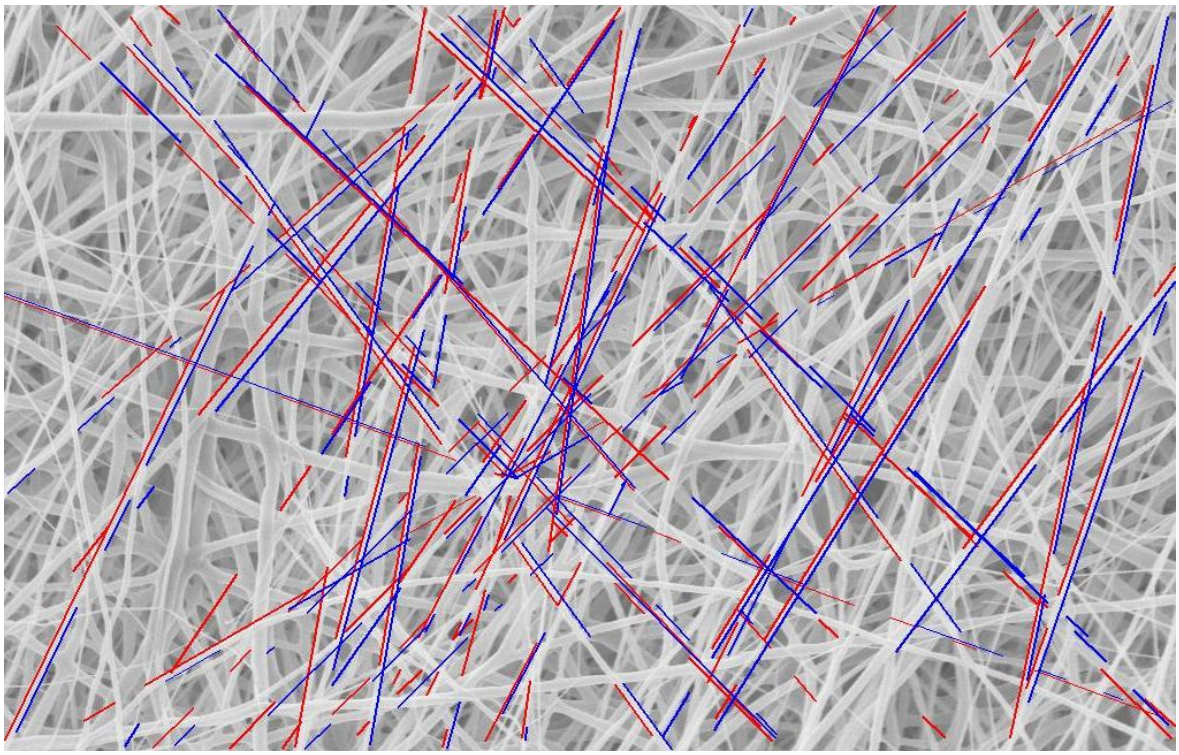

Figure 170 Image SEM2 with CCH valid edges

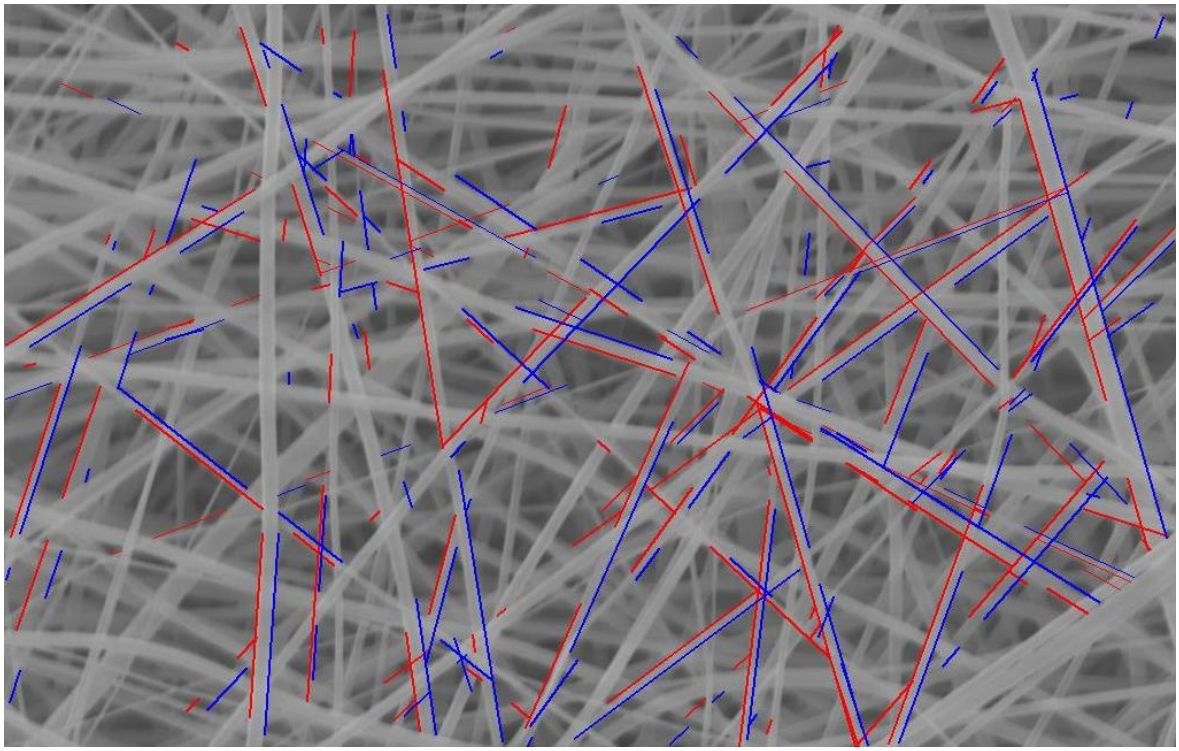

Figure 171 Image SEM3 with CCH valid edges

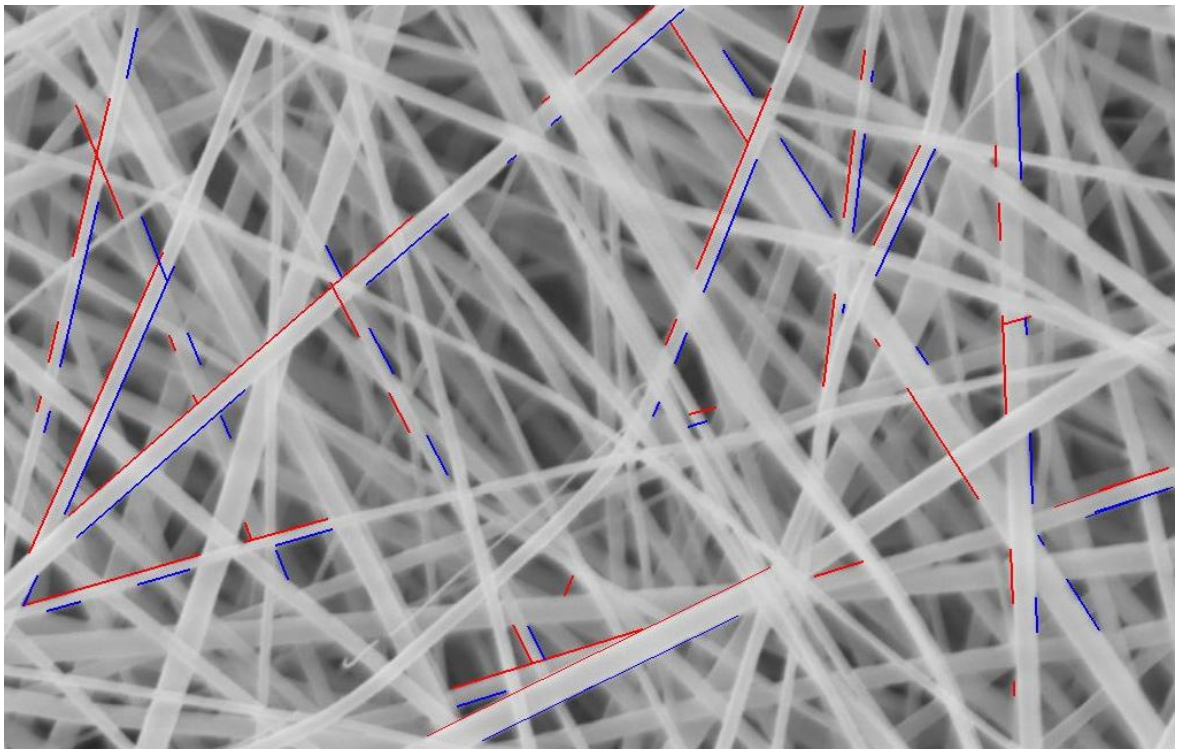

Figure 172 Image SEM4 with CCH valid edges

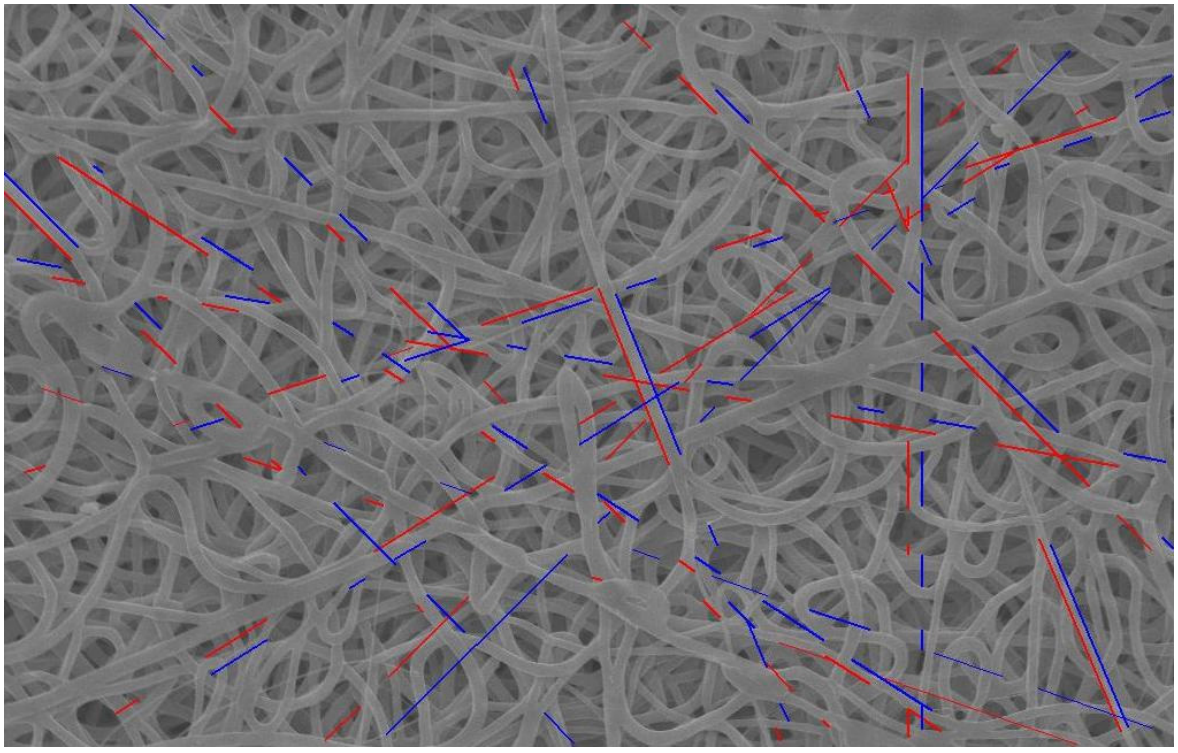

Figure 173 Image SEM5 with CCH valid edges

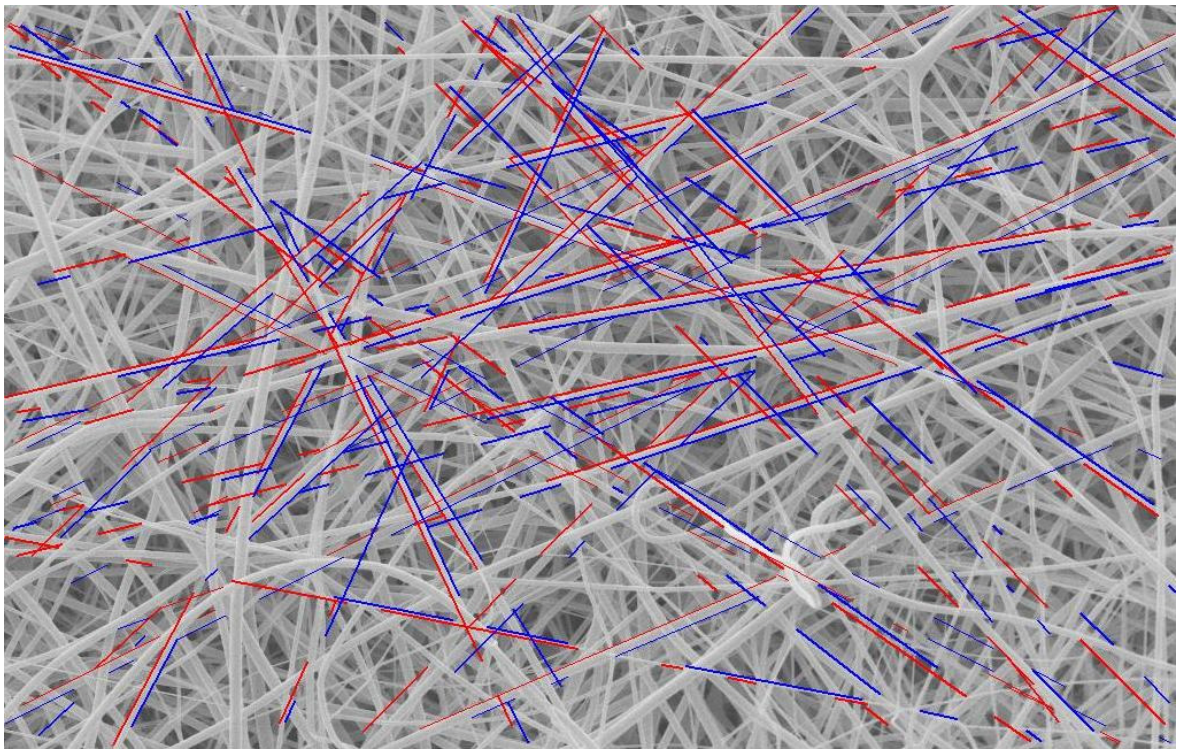

Figure 174 Image SEM6 with CCH valid edges

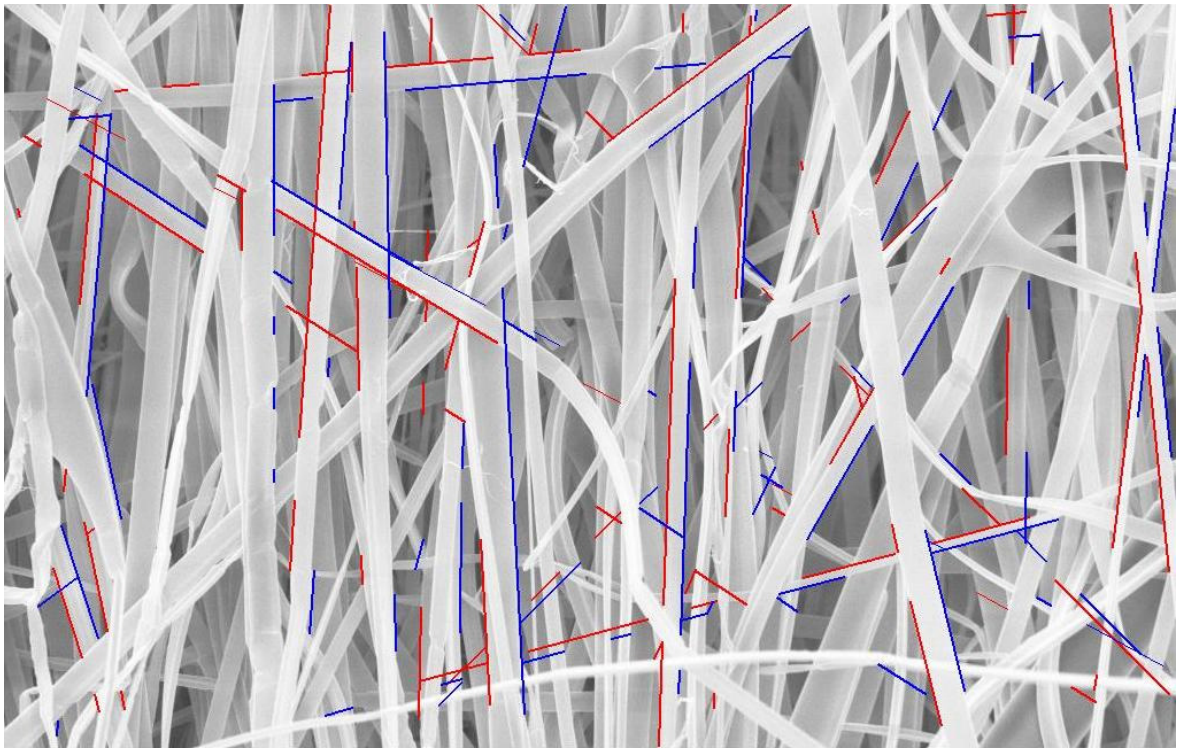

Figure 175 Image SEM8 with CCH valid edges

VITA

Anna Alexandra Bulysheva was born on July11th, 1984 in Novosibirsk, Russia. She moved to Charlotte, NC in her teens and graduated from Charlotte Country Day School in 2002. She attended and graduated in 2006 from the University of North Carolina at Chapel Hill with a Bachelor of Science degree in Biology with a minor in Physics. After graduating with an undergraduate degree, Anna Bulysheva conducted radiofrequency ablation research as a research associate in the Computer Science Department of UNC-Chapel Hill. In 2007 she matriculated at the Virginia Commonwealth University to pursue her graduate education in Biomedical Engineering.